Synthesis, Characterizations and Fluorescence Properties of Chalcones and Heteroaryl Chalcone Derivatives

Thawanrat Kobkeatthawin

A Thesis Submitted in Partial Fulfillment of the Requirements
for the Degree of Master of Science in Inorganic Chemistry
Prince of Songkla University
2011

Thesis Title	Synthesis, Characterizations and Fluorescence Properties of Chalcones and Heteroaryl Chalcone Derivatives
Author	Miss Thawanrat Kobkeatthawin
Major Program	Inorganic Chemistry

Major Advisor:

.....

(Assoc. Prof. Dr. Suchada Chantrapromma)

Co-Advisor:

.....

(Assoc. Prof. Dr. Chatchanok Karalai)

Examining Committee:

.....Chairperson

(Prof. Dr. Supot Hannongbua)

.....

(Assoc. Prof. Dr. Suchada Chantrapromma)

.....

(Assoc. Prof. Dr. Chatchanok Karalai)

.....

(Dr. Chittanon Buranachai)

The Graduate School, Prince of Songkla University, has approved this thesis as partial fulfillment of the requirements for the Master of Science Degree in Inorganic Chemistry

.....

(Prof. Dr. Amornrat Phongdara)

Dean of Graduate School

ชื่อวิทยานิพนธ์	การสังเคราะห์ การหาโครงสร้าง และสมบัติฟลูออเรสเซนซ์ของสารอนุพันธ์ Chalcones และ Heteroaryl Chalcones
ผู้เขียน	นางสาวธวัลรัตน์ กอบเกียรติถวิล
สาขาวิชา	เคมีอนินทรีย์
ปีการศึกษา	2553

บทคัดย่อ

สังเคราะห์สารประกอบอนุพันธ์ chalcones **(TKB1-TKB9)** และ heteroaryl chalcones **(TKD2-TKD21)** จำนวน 18 ชนิด ทำการวิเคราะห์โครงสร้างด้วยเทคนิค FT-IR UV-Vis และ ^{1}H-NMR และศึกษาสมบัติฟลูออเรสเซนซ์ของสารในตัวทำละลายคลอโรฟอร์มที่อุณหภูมิห้อง พบว่า สารประกอบอนุพันธ์ chalcones และ heteroaryl chalcones 14 ชนิด แสดงสมบัติฟลูออเรสเซนซ์ และมีลักษณะของ fluorescence emission คล้ายคลึงกัน เมื่อทำการกระตุ้นด้วยพลังงานที่ความยาวคลื่น 440 นาโนเมตร สำหรับสาร **TKB1-TKB9** พบว่าสารแสดงค่า λ_{em} ในช่วง 450-650 nm สำหรับสาร **TKD2-TKD21** ทำการกระตุ้นพลังงานที่ความยาวคลื่น 310 nm พบว่าสารแสดงค่า λ_{em} ในช่วง 400-600 นาโนเมตร และได้ทำการหาค่า fluorescence quantum yields (Φ_f) ของสาร **TKB1-TKB9** เทียบกับสารมาตรฐาน coumarin 7 ($\Phi_f = 0.49$) ในตัวทำละลายอะซิโตไนไตร พบว่า **TKB7** มีค่า Φ_f มากที่สุดเท่ากับ 0.23 และหาค่า Φ_f ของสาร **TKD2-TKD21** เทียบกับสาร coumarin 1 ($\Phi_f = 0.73$) ในตัวทำละลายเอทานอล พบว่า **TKD19** มีค่า Φ_f มากที่สุดคือ 0.03 นอกจากนี้ได้ทำการหาโครงสร้างด้วยเทคนิคการเลี้ยวเบนของรังสีเอกซ์บนผลึกเดี่ยวของสารประกอบ**TKB3 TKB4 TKD2 TKD6 TKD8** และ **TKD19** พบว่าตกผลึกใน space group $P2_1/c$, $P2_1/c$, $P2_12_12_1$, $P2_12_12_1$, *Pbca* และ *C*2/*c* ตามลำดับ

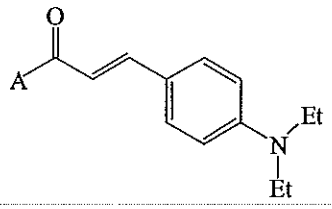

A	Structure	A	Structure	A	Structure
A1	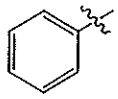 (TKB1)	A2	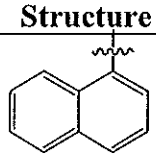 (TKB5)	A3	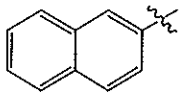 (TKB6)
A4	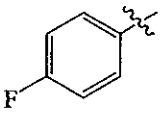 (TKB2)	A5	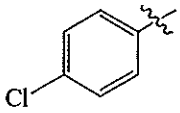 (TKB3)	A6	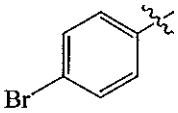 (TKB4)
A7	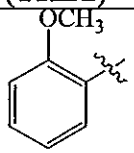 (TKB7)	A8	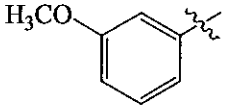 (TKB8)	A9	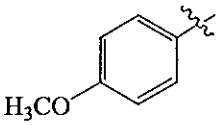 (TKB9)

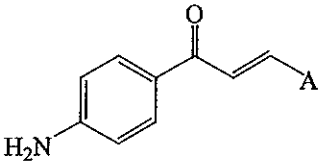

A	Structure	A	Structure	A	Structure
A10	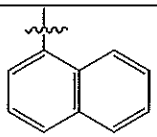 (TKD2)	A11	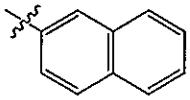 (TKD3)	A12	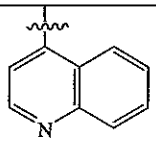 (TKD10)
A13	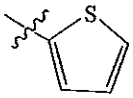 (TKD6)	A14	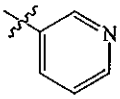 (TKD8)	A15	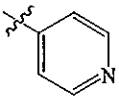 (TKD9)
A16	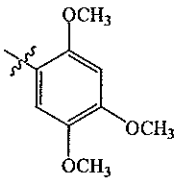 (TKD19)	A17	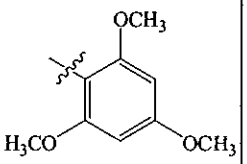 (TKD20)	A18	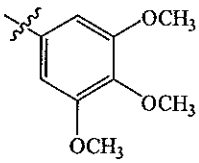 (TKD21)

Thesis Title	Synthesis, Characterizations and Fluorescence Properties of Chalcones and Heteroaryl Chalcone Derivatives
Author	Miss Thawanrat Kobkeatthawin
Major Program	Inorganic Chemistry
Academic Year	2553

Abstract

The eighteen chalcones **(TKB1-TKB9)** and heroaryl chalcone derivatives **(TKD2-TKD21)** were synthesized and characterized by FT-IR, UV-Vis and ^{1}H-NMR spectroscopic method. Their fluorescent properties were studied in chloroform solution at room temperature. It was found that fourteen compounds show fluorescent properties and their emission spectra have similar pattern. Compounds **TKB1-TKB9** present maxima wavelength (λ_{em}) in the range of 450-650 nm when was excited at 440 nm and compounds **TKD2-TKD21** show maxima wavelength (λ_{em}) in the range of 400-600 nm when was excited at 310 nm. The fluorescent quantum yields (Φ_f) of compounds **TKB1-TKB9** were compared with coumarin 7 in acetronitrile (Φ_f = 0.49). It was found that **TKB7** show the highest of fluorescent quantum yield value in chloroform solvent (Φ_f = 0.23). Moreover, the Φ_f values of compounds **TKD2-TKD21** were compared with coumarin 1 in ethanol (Φ_f = 0.73). It was found that **TKD19** show the highest of fluorescent quantum yield value in chloroform solvent (Φ_f = 0.03). In addition, compounds **TKB3, TKB4, TKD3, TKD6, TKD8** and **TKD19** were characterized by single crystal X-ray structure determinations and were found that they crystallized out in space groups $P2_1/c$, $P2_1/c$, $P\,2_1\,2_1\,2_1$, $P\,2_1\,2_1\,2_1$, $Pbca$ and $C2/c$, respectively.

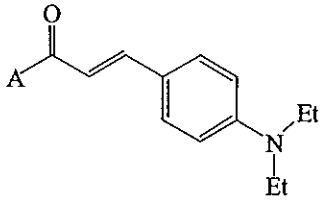

A	Structure	A	Structure	A	Structure
A1	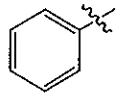 (TKB1)	A2	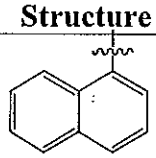 (TKB5)	A3	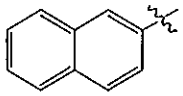 (TKB6)
A4	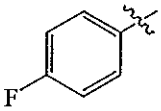 (TKB2)	A5	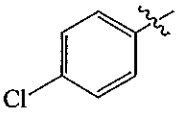 (TKB3)	A6	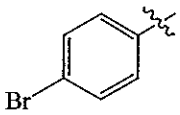 (TKB4)
A7	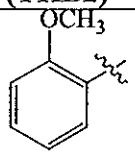 (TKB7)	A8	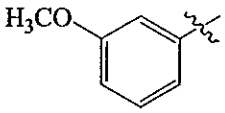 (TKB8)	A9	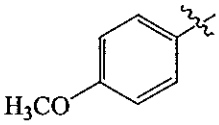 (TKB9)

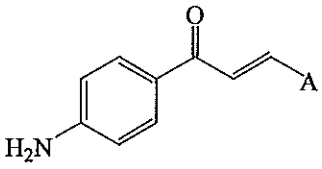

A	Structure	A	Structure	A	Structure
A10	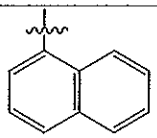 (TKD2)	A11	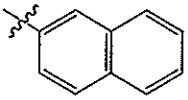 (TKD3)	A12	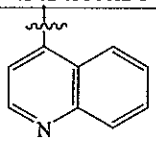 (TKD10)
A13	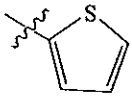 (TKD6)	A14	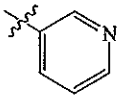 (TKD8)	A15	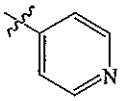 (TKD9)
A16	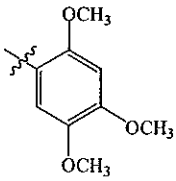 (TKD19)	A17	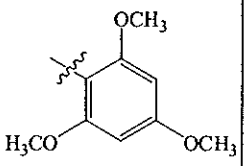 (TKD20)	A18	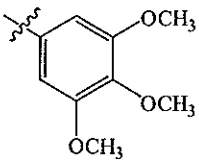 (TKD21)

ACKNOWLEDGEMENT

This thesis could not be successfully completed without the kindness of my major advisor, Associate Professor Dr. Suchada Chantrapromma, Department of Chemistry, Faculty of Science, Prince of Songkla University, who gave good advice and be guidance of this thesis since start until successful. I appreciate in all her contributions of time, ideas, expert and funding to help me accomplished my master degree. Above all, she provide me unflinching encouragement and support in various ways.

My sincere thank is expressed to Associate Professor Dr. Chatchanok Karalai who is my co-advisor for his kind help and suggestions. Special thanks are addressed to Professor Dr. Hoong-Kun Fun, X-ray Crystallography Unit, School of Physics, Universiti Sains Malaysia, Malaysia for X-ray data collections. I also would like to thank Professor Dr. Supot Hannongbua, Department of Chemistry, Faculty of Science, Chulalongkorn University and Dr. Chittanon Buranachai, Department of Physics, Faculty of Science, Prince of Songkla University for the valuable suggestions.

Appreciatory thank to the Center of Excellence for Innovation in Chemistry (PERCH-CIC), Commission on Higher Education, Ministry of Education for financial support. I also thank the Graduate School (PSU) and Prince of Songkla University for financial support through the Crystal Materials Research Unit.

I also would like to thank Department of Chemistry, Faculty of Science, Prince of Songkla University for making available the facilities used in this research. I am also greatly indebted to many staffs here especially Dr. Yaowapa for recording ^{1}H-NMR spectral data

I am very grateful to M.Sc and Ph.D students in the Crystal Materials Research Unit (CMRU) for their kind help and assistance during my study and research activities. Finally, none of this would have been possible without love and encouragement of my family.

Thawanrat Kobkeatthawin

THE RELEVANCE OF THE RESEARCH WORK TO THAILAND

The relevancies of this research are listed below:

1) The eighteen chalcones and heteroaryl chalcones were successfully synthesized, fourteen compounds showed fluorescence properties with the emission wavelength in the range of 400-650 nm in chloroform.

2) Among all the synthesized compounds, (*E*)-3-(4-(diethylamino)-phenyl)-1-(2-methoxyphenyl)prop-2-en-1-one **(TKB7)** shows the highest fluorescent properties with the fluorescent quantum yield value (Φ_f) of 0.23 in chloroform.

3) Six single crystals which are;

- (*E*)-1-(4-chlorophenyl)-3-(4-(diethylamino)phenyl)prop-2-en-1-one **(TKB3)**
- (*E*)-1-(4-bromophenyl)-3-(4-(diethylamino)phenyl)prop-2-en-1-one **(TKB4)**
- (*E*)-1-(4-(aminophenyl)-3-(naphthalen-2-yl)prop-2-en-1-one **TKD3)**
- (*E*)-1-(4-(aminophenyl)-3-(thiophen-2-yl)prop-2-en-1-one **(TKD6)**
- (*E*)-1-(4-(aminophenyl)-3-(pyridin-3-yl)prop-2-en-1-one **(TKD8)**
- (*E*)-1-(4-(aminophenyl)-3-(2,4,5-trimethoxyphenyl)prop-2-en-1-one **(TKD19)**, were successfully growth and determined their structures by single crystal X-ray structure determinations. Their structural data in solid state were obtained and could be benefitted for further investigations.

CONTENTS

CONTENTS (Continued)

CONTENTS (Continued)

CONTENTS (Continued)

CONTENTS (Continued)

CONTENTS (Continued)

CONTENTS (Continued)

LIST OF TABLES

LIST OF TABLES (Continued)

LIST OF ILLUSTRATIONS

LIST OF ILLUSTRATIONS (Continued)

LIST OF ILLUSTRATIONS (Continued)

LIST OF ILLUSTRATIONS (Continued)

LIST OF ILLUSTRATIONS (Continued)

LIST OF ILLUSTRATIONS (Continued)

ABBREVIATIONS AND SYMBOLS

s	=	singlet
d	=	doublet
t	=	triplet
dd	=	doublet of doublet
dt	=	doublet of triplet
g	=	gram
nm	=	nanometer
ml	=	milliliter
mp.	=	melting point
cm^{-1}	=	reciprocal centimeter (wave number)
δ	=	chemical shift relative to TMS
J	=	coupling constant
λ_{max}	=	maximum wavelength
ν	=	absorption frequencies
ε	=	molar extinction frequencies
°C	=	degree celcius
MHz	=	Megahertz
Hz	=	Hertz
ppm	=	part per million
Φ_F	=	fluorescence quantum yield
λ_{ex}	=	excitation wavelength
λ_{em}	=	emission wavelength
Å	=	Angstrom
hr	=	hour
aq	=	aqueous solution
μM	=	micromolar
Trp	=	tryptophan
DTC	=	3,3'-diethylthiacarbocyanine

ABBREVIATIONS AND SYMBOLS (Continued)

LEDs	=	light-emitting diodes
NLO	=	non-linear optic
DMADHC	=	4'-dimethylamino-2,5-dihydroxychalcone
DMC	=	4'-*N,N*-dimethylamino-4-methylacryloylamino chalcone
DMATP	=	3-(4'-dimethylaminophenyl)-1-(2-thienyl)prop-2-en-1-one
DMAFP	=	3-(4'-dimethylaminophenyl)-1-(2-furanyl)prop-2-en-1-one
XRD	=	X-ray diffraction
FT-IR	=	Fourier transform-infrared
UV-Vis	=	Ultraviolet-Visible
NMR	=	Nuclear magnetic resonance
TMS	=	tetramethylsilane
$CDCl_3$	=	deuterochloroform
DMSO-d_6	=	hexadeutero-dimethyl sulphoxide
KBr	=	potassium bromide

CHAPTER 1
INTRODUCTION

1.1 Motivation

Chalcones have been studied for their chemical and biological activities for a long time. They have a wide range of applications such as non-linear optical devices (Venkataraya *et al.*, 2006) and have various biological properties such as anticancer, antityrosinase, antioxidant and antimalarial properties (Aneta *et al.*, 2006; Nishida *et al.*, 2007; Nurettin *et al.*, 2005; Tomar *et al.*, 2010). Some of the synthetic chalcones have also been found to be fluorescent properties (Gaber *et al.*, 2008). These interesting activities have led us to synthesize chalcones and heteroaryl chalcone derivatives in order to study their fluorescence properties. They also have a wide range of applications which can be used in many fields such as fluorescent dyes, liquid crystal display, fluorescent probes and fluorescent sensors (Sabir *et al.*, 2008; Dong *et al.*, 2007) Therefore, in this thesis, the researcher was interested in studying fluorescent property of synthesized chalcones and heteroaryl chalcone derivatives.

1.2 Luminescence

Luminescence is an emission of light from any substance and occurs from electronically excited states. Luminescence is devided into two categories (fluorescence and phosphorescence) depending on the nature of the excited state.

1.2.1 Fluorescence is light emission caused by radiation with light (normally visible or ultraviolet light) and occurring within 10^{-10} to 10^{-8} s after irradiation.

1.2.2 Phosphorescence is a light emission which occur over much longer times after irradiation (10^{-3} to 10^{2} s). It involves storage of energy in metastable states and its release through relatively slow processes. The phenomenon was discovered early on for phosphorus (Valeur *et al.*, 2002).

1.3 Jablonski diagram and electronic transition

The processes which occur between the absorption and emission of light are usually illustrated by the Jablonski diagram (Valeur *et al.*, 2002). The Jablonski diagram is a summary of the radiative and non-radiative transitions

occurring between electronic states in a molecule. The figure below shows the transitions that are common to all systems. The thick, dark lines labeled S_0, S_1 and S_2 correspond to singlet electronic states and those labeled T_1 and T_2 represent triplet electronic states. Vibrational levels are shown with thin lines for each state. The vertical arrows with straight lines represent radiative transitions, while the arrows with wavy lines represent non-radiative transitions.

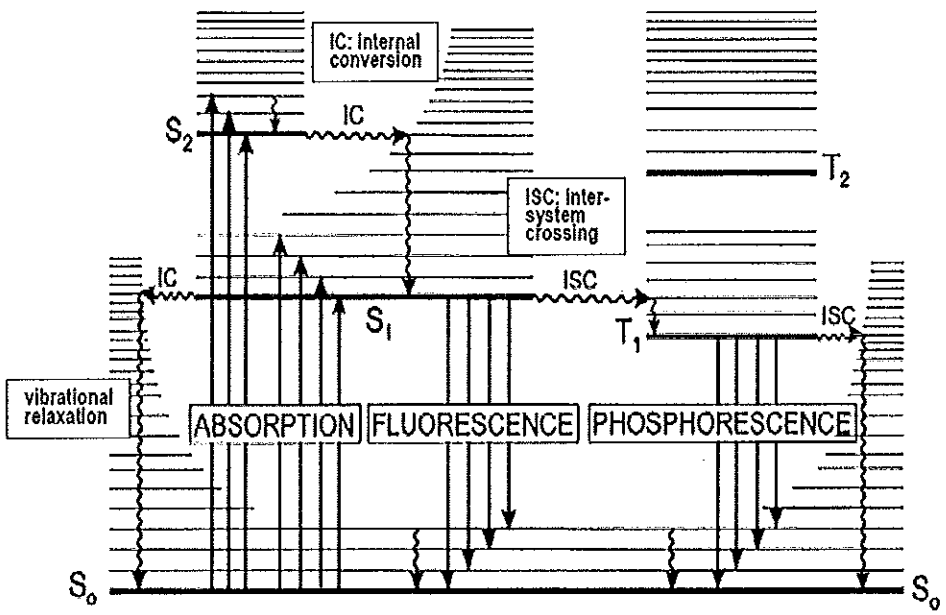

Figure 1 A simplified Jablonski diagram with absorbance, internal conversion, fluorescence, vibrational relaxation, intersystem crossing and phosphorescence.

1.3.1 Absorption (~10^{-15} s)

At room temperature, the vast majority of molecules are in the lowest vibrational level of the ground state. Absorption of a photon of sufficient energy will excite the molecule from the ground state (S_0) to an excited state (S_1, S_2, etc.). Generally, the excitation will be to a higher vibrational level of the excited state.

1.3.2 Vibrational relaxation (~10^{-14} - 10^{-11} s)

This occur within a given electronic state. When a molecule reaches a higher vibrational level of an electronic state, it will quickly relax to the lowest

vibrational level of that state. The energy is released as heat to the surrounding solvent molecules.

1.3.3 Internal conversion (IC, ~10^{-13} to 10^{-9} s)

This is a transition between two electronic states with the same energy (horizontal transition) and the same spin multiplicity (i.e. singlet-singlet or triplet-triplet). The rate will depend on the initial and final states of the transition. (1) A molecule is excited to a higher vibrational level of the state S_2. Vibrational relaxation occurs quickly to the lowest vibrational level of S_2, then it undergoes internal conversion from S_2 to S_1, followed by vibrational relaxation to the lowest vibrational level of S_1. The overall rate is ~10^{-13} to 10^{-11}s. (2) The molecule can transit from the lowest vibrational level of S_1 to a higher vibrational level of S_0. This would be followed by rapid relaxation to the lowest vibrational level of the ground state. This mechanism is one of the non-radiative transitions that can occur during de-excitation. The time scale for S_1 to S_0 internal conversion is ~10^{-11} to 10^{-9} s. The difference in rates for these processes is related to the greater energy difference between the initial and final states (i.e. S_0-S_1 energy difference is greater than S_1-S_2).

1.3.4 Fluorescence (~10^{-10} to 10^{-8} s)

Fluorescence is emission of light from singlet-excited states, in which the electron in the excited orbital is paired (of opposite sign) to the second electron in the ground state orbital. Return to the ground state is spin-allowed and occurs rapidly by emission of a photon. This emission rates of fluorescence are typically 10^{-8}s, so that a typical fluorescence lifetime is near 10 ns. Fluorescence spectral data are generally presented as emission spectra. Emission spectra are dependent on the chemical structure of the fluorophore and the solvent in which it is dissolved.

1.3.5 Intersystem crossing (ISC, ~10^{-10} to 10^{-4} s)

This is a transition between states of different multiplicity (i.e. singlet-triplet or triplet-singlet), but the same energy. It requires an interaction leading to a change of electron spin. This can be achieved through interactions with other

molecules or though spin-orbit coupling within the molecule (e.g. the heavy atom effect). For isolated or shielded molecules, it can lead to phosphorescence emission. For non-protected molecules in solution, it generally leads to non-radiative de-excitation because phosphorescence is very slow process (~10^{-6} to 10^{-2}s), leaving many opportunities for non-radiative decay.

1.3.6 Phosphorescence (~10^{-3} to 10^{2} s)

Phosphorescence is emission of light from triplet-excited states, in which the electron in the excited stated orbital has the same spin orientation as the ground-state electron. Transitions to the ground state are forbidden and the emission rates are slow, so phosphorescence lifetimes are typically milliseconds to seconds. Phosphorescence is usually not seen in fluid solutions at room temperature, but there are many deactivation processes that complete with emission, such as nonradiative decay and quenching processes.

1.3.7 Other processes

In addition, there are other de-excitation processes that are dependent upon the local environment (e.g. interactions with other solute molecules). These include processes such as proton transfer, electron transfer, dynamic quenching, resonance energy transfer, photo-induced chemical reactions, structural changes, excimer and exciplex formation.

1.4 Characteristics of fluorescence emission

1.4.1 Mirror image rule

The emission is the mirror image of the S_0 to S_1 absorption, not of the total absorption spectrum. This is a result of the same transitions being involved in both absorption and emission and the similarities of the vibrational levels of S_0 and S_1. In many molecules these energy levels are not significantly altered by the different electronic distributions of S_0 and S_1. If a particular transition probability between the first and second vibrational levels is largest in absorption, the reciprocal transition is also most probable in emission (Lakowicz *et al.*, 1999). Figure **2** shows an example of this.

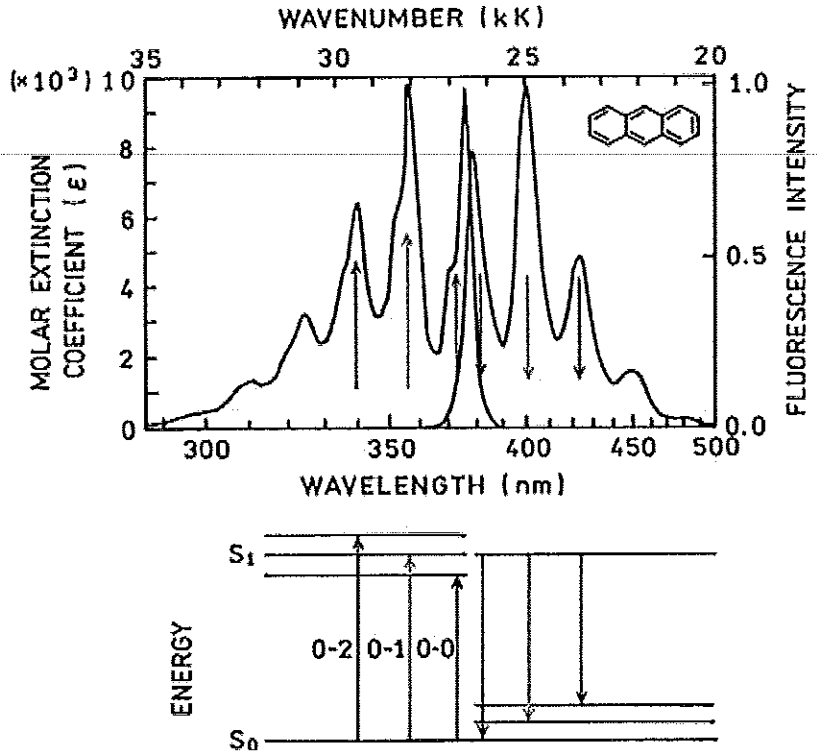

Figure 2 Mirror-image rule and Franck-Condon factors, the absorption and emission spectra are for anthracene. The numbers 0, 1 and 2 refer to vibrational energy levels.

1.4.2 Stokes shift

Stoke shift is the difference (in wavelength or frequency units) between positions of the band maxima of the absorption and emission spectra (fluorescence and Raman being two examples) of the same electronic transition. When a system (be it a molecule or atom) absorbs a photon, it gains energy and enters an excited state. One way for the system to relax is to emit a photon, thus losing its energy (another method would be the loss of heat energy). When the emitted photon has less energy than the absorbed photon, this energy difference is the Stokes shift. If the emitted photon has more energy, the energy difference is called an anti-stokes shift.

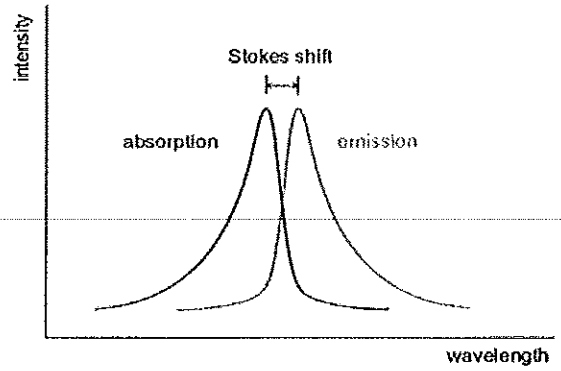

Figure 3 Stokes shift between λ_{max} of absorption and emission spectra

1.5 Fluorophores

A fluorophore is a component of a molecule which causes a molecule to be fluorescent. It is a functional group in a molecule which will absorb energy of a specific wavelength and re-emit energy at a different wavelength. The amount and wavelength of the emitted energy depend on both the fluorophore and the chemical environment of the fluorophore. Each fluorophore has its own specific fluorescence properties. Some typical fluorescent substances (fluorophores) are shown in **Figure 4** (Lakowicz *et al.*, 1999).

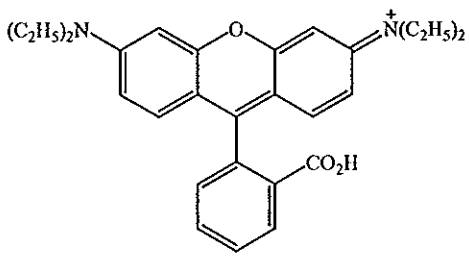

Rhodamine B

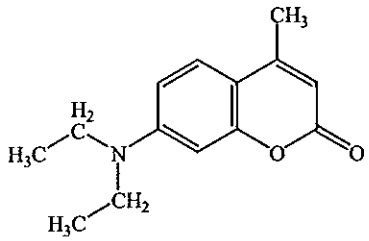

Coumarin1

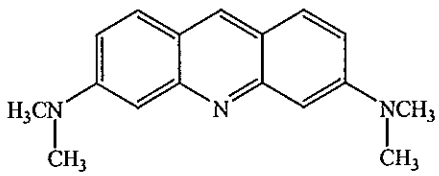

Acridine Orange

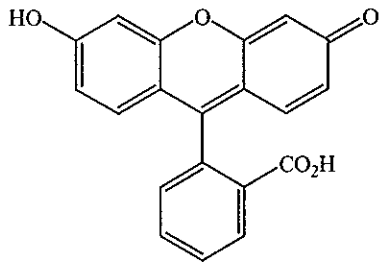

Fluorescein

Figure 4 Structures of typical fluorescent substances

1.6 Lifetime and fluorescence quantum yield

The fluorescence lifetime and quantum yield are important characteristics of a fluorophore. The quantum yield is defined as the number of emitted photons relative to the number of absorbed photons:

$$\Phi = \frac{\Gamma}{\Gamma + k_{nr}} \tag{1}$$

where Γ is the number of photons emitted and k_{nr} is all forms of nonradiative decay from the excited to the ground state. Nonradiative decay is any decay that does not involve the emission of a photon. The quantum yield can be close to unity if the radiationless decay rate is much smaller than the rate of radiative decay, $k_{nr} << \Gamma$.

The lifetime of the excited state is defined by the average time the molecule spends in the excited state prior to return to the ground state. Generally, fluorescence lifetimes are on the order of nanoseconds. The lifetime can be measured by an experiment in which a very short, pulsed excitation is given followed by measurement of the time-dependent intensity. If we let $n(t)$ equal the number of excited molecules at time, t, then the decay in this number is given by:

$$\frac{dn(t)}{dt} = -(\Gamma + k_{nr})n(t) \tag{2}$$

which can also be expressed as:

$$n(t) = n_0 \exp(-t/\tau) \tag{3}$$

The experimentalist actually observes intensity, but this is proportional to the number of photons, and so one can write:

$$I(t) = I_0 \exp(-t/\tau) \tag{4}$$

Thus, the lifetime is calculated from the slope of a plot of log $I(t)$ versus t.

Note that the observed lifetime is the inverse of the total decay rate, $(\Gamma + k_{nr})^{-1}$. The lifetime of the fluorophore in the absence of nonradiative processes is called the intrinsic lifetime and is given by

$$\tau_n = 1/\Gamma \tag{5}$$

Molecules in the fundamental state absorb light with an intensity equal to I and reach an excited state S_n. Then, different competitive processes, including fluorescence, will compete with each other to de-excite the molecule. The rate constant (k) of the excited state is the sum of the kinetic constants of the competitive processes:

$$k = k_r + k_{isc} + k_i \tag{6}$$

The fluorescence quantum yield (Φ_f) is the number of photons emitted by the radiative way over that absorbed by the molecule:

$$\Phi_f = \frac{\text{emitted photons}}{\text{absorbed photons}} = \frac{k_r}{k_r + k_i + k_{isc}} \tag{7}$$

The fluorescence quantum yield of a molecule is obtained by comparing the fluorescence intensity of the molecule with that of a reference molecule with a known quantum yield:

$$\Phi_2 = \frac{OD_1 * \sum F_2}{OD_2 * \sum F_1} \Phi_1 \tag{8}$$

where F_2 is the fluorescence intensity of the molecule of unknown quantum yield Φ_2, and F_1 is the fluorescence intensity of the reference with quantum yield Φ_1.

Therefore, in order to determine fluorophore quantum yield, one needs to measure the optical densities of the fluorophore and of the reference at the excitation wavelength, and to calculate for each of them the sum of their fluorescence intensities along their fluorescence emission spectra.

Finally, one should remember that the standard and the molecule to be analyzed should be studied under the same conditions of temperature and solvent viscosity. Also, it is always better to work at low optical densities in order to avoid corrections for the inner filter effect.

In order to measure quantum yields of an extrinsic fluorophore bound to a protein and which emits at longer wavelengths than in the UV, standards such as 3,3'-diethylthiacarbocyanine iodide (DTC) in methanol (Φ_f = 0.048) and rhodamine 101 in ethanol (Φ_f = 0.92) or any other dyes can be used. Quantum yield is calculated according to this equation:

$$\frac{\Phi_S}{\Phi_R} = \frac{A_S}{A_R} \times \frac{OD_R}{OD_S} \times \frac{n_S^2}{n_R^2} \qquad (9)$$

where, Φ_S and Φ_R are the fluorescence quantum yields of the sample and reference, respectively. A_S and A_R are areas under the fluorescence spectra of the sample and the reference, respectively; $(OD)_S$ and $(OD)_R$ are the respective optical densities (absorbance) of the sample and the reference solution at the excitation wavelength; and n_S and n_R are the values of the refractive index for the respective solvents used for the sample and reference (Barik *et al.*, 2003).

1.7 Fluorescence of organic compound

Fluorescence and absorption spectra of the aromatic hydrocarbons, benzene, naphthalene, anthracene, naphthacene and pentacene exhibit vibrational structure maxima. The wavelengths of the absorption and emission process increase through the series and vary form the ultra-violet region for benzene and naphthalene to the visible region for the higher members. The fluorescence emission (nm) and quantum yields (ϕ) of a few aromatics are given below (West *et al.*, 1956).

Table 1 Fluorescence emission and quantum efficiency

Compound	λ(nm)	Φ_f	Compound	λ(nm)	Φ_f
Benzene	270-310	0.11	Anthracene	370-460	0.46
p-xylene	270-320	0.42	Phenanthrene	280-470	0.27
Hexamethyl benzene	280-330	0.04	Biphenyl	290-360	0.23
Naphthalene	300-360	0.38	Triphenyl-methane	280-340	0.23

The quantum yield of fluorescence in dilute solution increases from a value of about 0.1 for benzene to 0.46 for anthracene and diminishes to a low value for hexamethyl benzene. Fluorescence spectra of annulated condensed ring hydrocarbons are at shorter wavelengths than those of the linear compounds with the same number of rings. Pure phenanthrene, though isomeric with anthracene, fluorescence in the ultra-violet with a quantum yield lower than that of naphthalene whereas anthracene gives blue fluorescence of higher efficiency. Perylene is the only substance among the unsubstituted condensed ring molecule which is noted for powerful fluorescence (Lewis *et al.*, 1939).

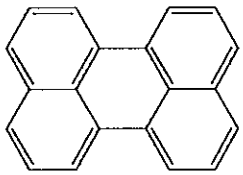

Figure 5 The structure of Perylene

Substitution of aromatic molecules is known to diminish fluorescence. The data on a few substituted benzenes are given below:

Table 2 Fluorescence emission and fluorescence intensity

R	λ emission, (nm)	Fluorescence intensity
H	270-310	10
CH_3	270-320	17
F	270-320	10
Br	290-380	5
I	-	0
OH	285-365	18
NH_2	310-405	20
COOH	310-390	3
CN	280-360	20
NO_2	-	0

F, Br and I atoms diminishes the fluorescence in the order given. In fact, iodobenzene is not fluorescence, because it probably undergoes predissociation. Similarly, the NO_2 group completely eliminates fluorescence by causing a rapid dissipation of the energy of electronic excitation (West *et al.*, 1956).

1.8 Quantum yield, rigid and coplanar structures

Internal rotations are a common deactivation pathway for many chromophores in the excited state. Rotations within the molecule can lead to non-radiative decay through the internal conversion and vibrational relaxation mechanism. This phenomena is shown by the structures of phenolphthalein and fluorescein (Valeur *et al.*, 2002). These molecules differ only by the presence of an additional oxygen atom in fluorescein that bridges two of the aromatic rings in phenolphthalein. Both compounds are good absorbers of visible light, but their fluorescence properties differ markedly. Phenolphthalein is non-fluorescence because its structure has a lot of internal freedom, allowing for rotations within the excited molecule and leading to non-radiative decay. On the other hand, the fluorescein molecule is highly fluorescent

because the additional oxygen atom provides a more rigid structure, suppressing internal rotations.

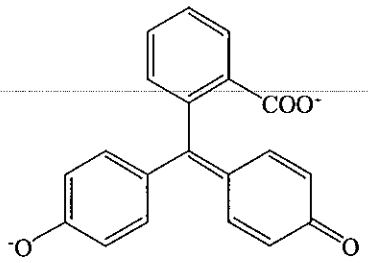

Phenolphthalein (basic form)

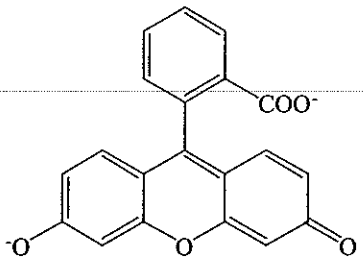

Fluorescein dianion

Figure 6 The structure of phenolphthalein and fluorescein

Another example of the importance of suppressing internal rotations is given by the structures of rhodamine B and rhodamine 101 (Valeur *et al.*, 2002). These molecules are very similar, with the axception that the flexibility of rhodamine 101 is reduced by including the N atoms in ring structures. This modification suppresses internal rotations, giving rhodamine 101 a higher quantum yield (0.92 in ethanol) than rhodamine B (0.54 in ethanol).

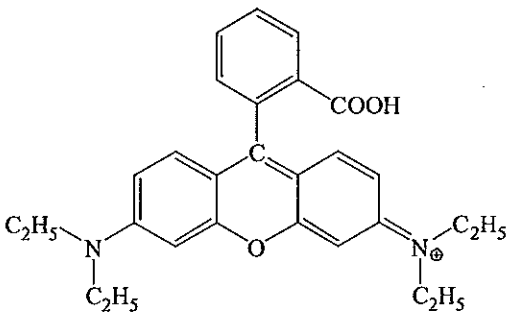

Rhodamine B

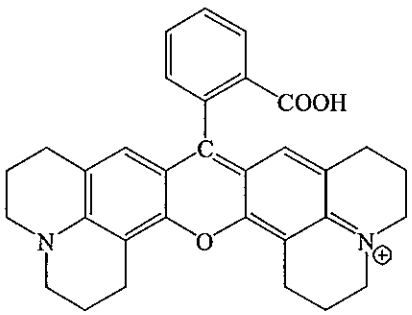

Rhodamine 101

Figure 7 The structure of rhodamine B and rhodamine 101

Thus, a good chromophore has a coplanar structure with a lot of conjugation and has a rigidity in its structure that suppresses internal rotations of the excited molecule.

1.9 Chalcone derivatives

Chalcones or 1,3-diphenyl-2-propene-1-one, in which two aromatic rings are linked by a three carbon α, β-unsaturated carbonyl system. These are well-known precursors of pigments as flavones. Chalcones possess conjugated double bonds and π delocalized electron system on benzene rings which are synthesized by Claisen-Schmidt condensation reaction. They have considerable applications including biological activities such as antibacterial (Prasad *et al.*, 2007), antifungal, antioxidant, anti-inflammatory, non-linear optic (NLO) and electroactive fluorescent materials which are used as fluorescent dyes (Fayed and Awad *et al*, 2004), light-emitting diodes (LEDs) (Sens *et al.*, 1981) and fluorescent sensors (Niu *et al.*, 2006), etc. In general, the compounds which can emit fluorescence light (fluorophore) in visible region under ultraviolet or visible excitation frequently contain mixing structures of aromatic with long π-conjugate system or aliphatic/alicyclic carbonyl corresponding to the structure of chalcone derivatives.

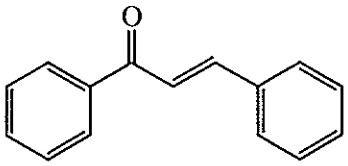

Figure 8 The structure of 1,3-diphenyl-2-propen-1-one

1.10 Review of Literatures

Rurack *et al.*, 2000 synthesized chalcone derivatives and studied for donor-acceptor substitution influent on aromatic ring. Fluorescence properties of chalcones were study in different solvent. In addition, fluorescence quantum yields strongly depends on all three parameter, i.e., the bridging pattern, donor and/or accepter strength, and the solvent polarity.

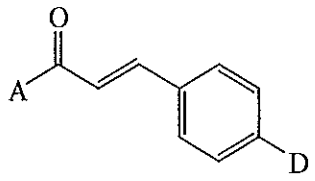

A = acceptor = BT, Ph, Q

D = donor = DMA, H, A15C5, $AT_4$15C5, Jul, OCH_3

A		D	
BT	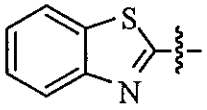	DMA: X = $N(CH_3)_2$ A15C5: X = O $AT_4$15C5: X = S	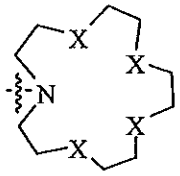
Ph	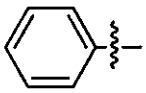	Jul	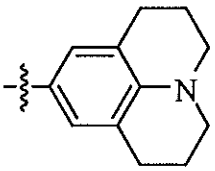
Q	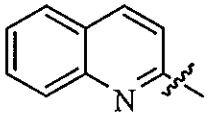		

Rtishchev *et al.*, 2001 studied the relationship between luminescent spectra and luminescent properties of chalcone derivatives for monosubstituted and disubstituted chalcones. The photophysical properties of substituted chalcones are studied as a function of solvent polarity, temperature and metal ion by employing steady-state and time-resolved spectroscopy. Absorption and fluorescence measurement reveal that the strength of the intramolecular charge transfer increase on the order of AT415C5 < A15C5~ DMA <Jul

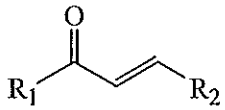

R_1, R_2 = Ph, 4-FC_6H_4, 4-BrC_6H_4, 2-furyl, 2-thienyl, 4-(PhCONH)C_6H_4, 4-$NH_2C_6H_4$, 4-$Me_2NC_6H_4$

Fayed *et al.*, 2004 synthesized chalcone derivatives which was 1-(4'-*R*-phenyl)-5-(4'-N,N-dimethylaminophenyl)-2,4-pentadien-1-one and studied for fluorescent properties. It was found that fluorescence of the compound depends on the nature of substituted group and the polar of solvents.

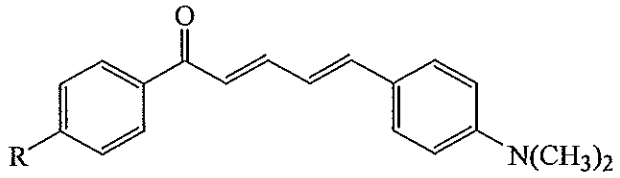

R = H, Cl and OCH_3

Tomečková *et al.*, 2004 synthesized chalcone derivatives which were chalcone (**1**), *E*-2-arylidene-1-tetralones (**2**) and *E*-2-arylidene-1-benzosuberones (**3**) and compared for their reaction rate against mitochondria outer membrane by using fluorescence techniques examine the rate reaction. In addition, it was found that substituted groups on aromatic ring affect to fluorescent properties.

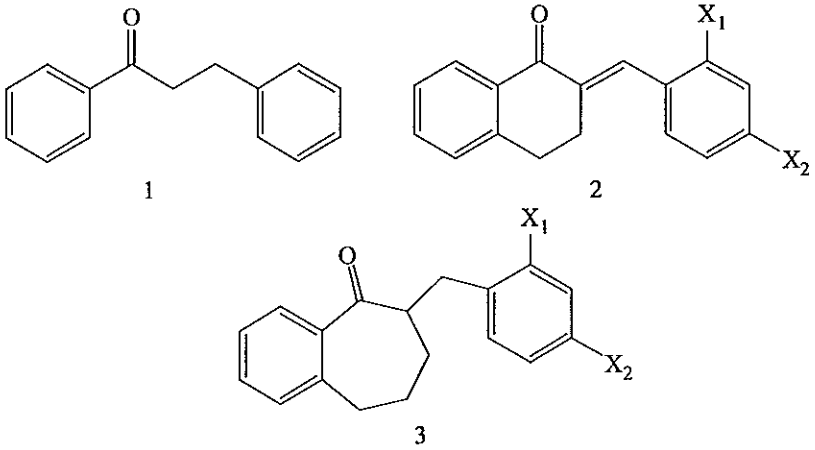

Xu *et al.*, 2005 synthesized 4'-dimethylamino-2,5-dihydroxychalcone (DMADHC) and studied fluorescent properties which may be used as fluorescent probes. The fluorescence behavior is controlled by the mechanism which increase in the fluorescence quantum yield with a suitable enhancement of intramolecular charge transfer: the so-called "negative solvatokinetic effect".

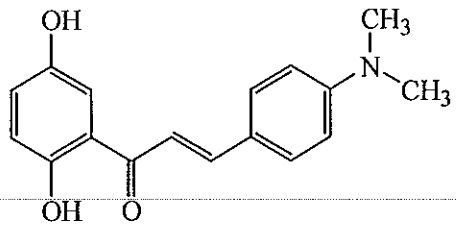

DMADHC

Niu *et al.*, 2006 synthesized chalcone derivatives; 4'-*N,N*-dimethylamino-4-methylacryloylamino chalcone (DMC) for searching for the compound which can use as fluorescent sensor to find water in organic solvent.

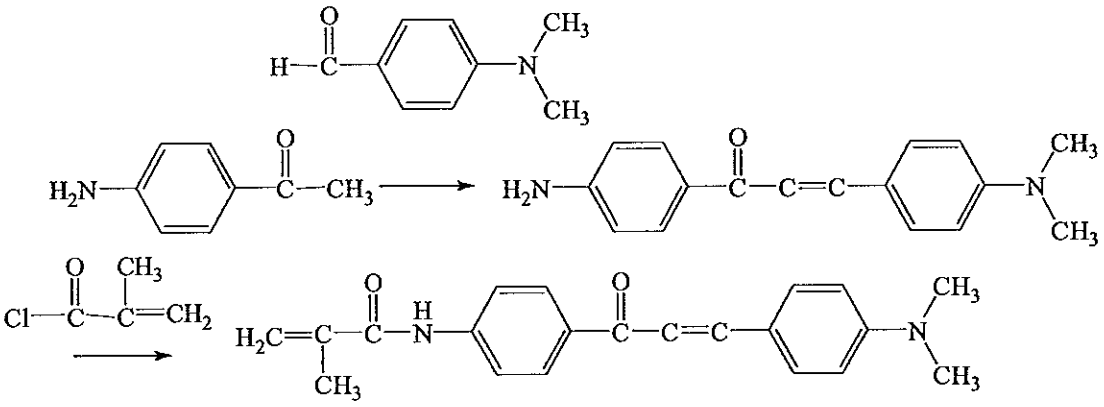

Synthesis diagram of DMC compound

Sun *et al.*, 2008 synthesized coumarin-based derivatives, a chalcone moiety and studied for fluorescent property. Absorption and emission spectra showed red shift according to the strength of the electron-donating moieties and conjugation length. In addition, replacement of carbazolyl donor with triphenylamine group in the chromophore resulted in a strong bathochromic shift.

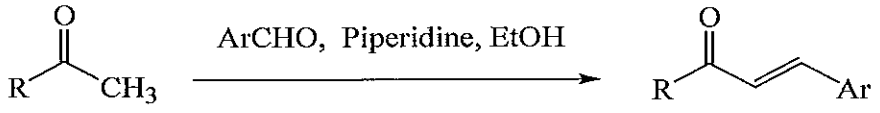

(1A-1E)

1	R
A	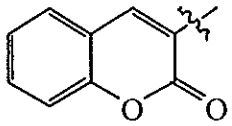
B	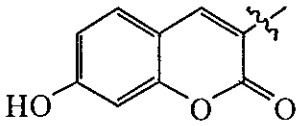
C	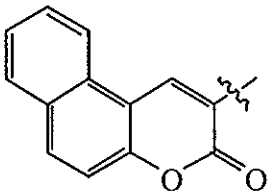
D	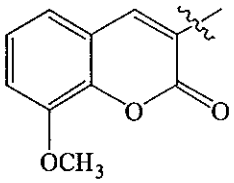
E	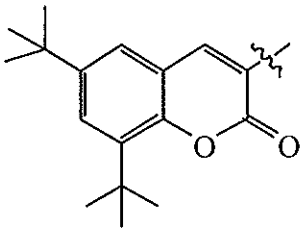

Zhang *et al.*, 2008 synthesized 1-keto-2-(*p*-dimethylaminobenzal)-tetrahydronaphthalene compound and studied for photophysical properties in various solvents in room temperaturethe using absorption and steady-state fluorescence techniques. Its fluorescence spectrum exhibits a large bathochromic shift with an increase in the polarity of solvents. The probe is sensitive to the microenvironment and may be used to probe its microenvironment in biological systems of interest.

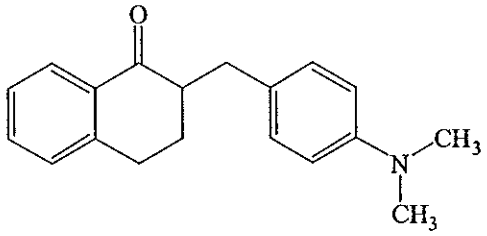

1-keto-2-(*p*-dimethylaminobenzal)-tetrahydronaphthalene

Gaber *et al.*, 2008 synthesized heteroaryl chalcone derivative; 3-(4'-dimethylaminophenyl)-1-(2-thienyl)prop-2-en-1-one (DMATP) and studied for the absorption and fluorescent emission of the compound.

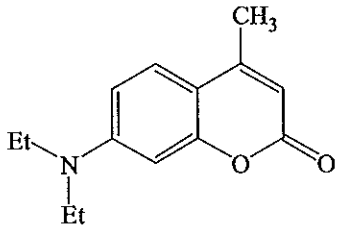

(DMC)

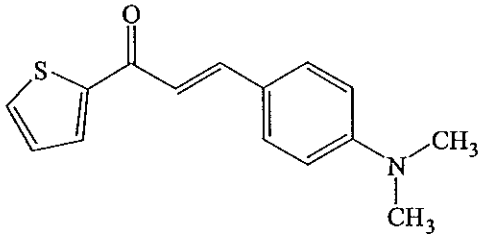

(DMATP)

Gaber *et al.*, 2008 synthesized heteroaryl chalcone derivative; 3-(4'-dimethylaminophenyl)-1-(2-furanyl)prop-2-en-1-one (DMAFP) and studied for the absorption and fluorescent emission of the compound.

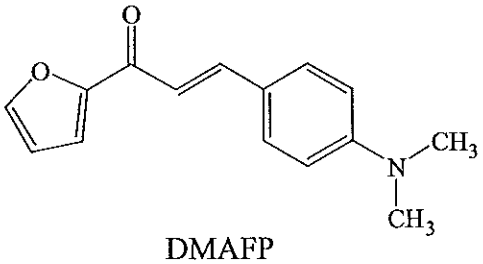

DMAFP

Mashraqui *et al.*, 2008 synthesized a phenothiazine pyridyl chalcone derivative as a new ICT chromophore and studied the effects of various metal ions on its photophysical properties.

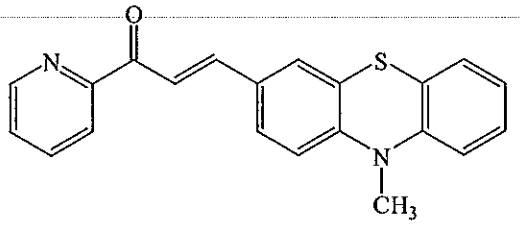

Tomeckova *et al.*, 2009 studied polarity, solubility, colour, absorption and fluorescence quantum yield of dimethylaminochalcone (1) and its cyclic analogues measured in various solvent, which have been studied by absorption and fluorescence spectroscopy. The highest fluorescence and quantum yields have been obtained in DMSO and chloroform.

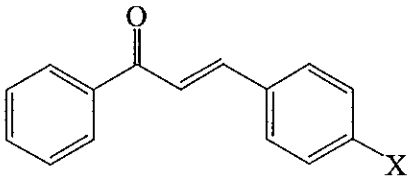

1

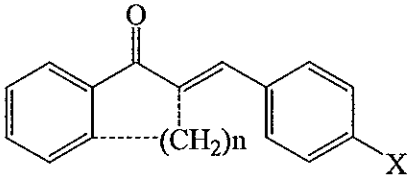

2) n = 1 3) n = 2, 4) n = 3

a) X = H, b) X = $N(CH_3)$

From literatures review, it was found that the structures of the compounds which can show fluorescence properties should have long π conjugated double bonds, aromatic or heterocyclic group, aliphatic/alicyclic carbonyl and donating electron substituent group. From these results, in this study the researcher was interested to synthesize chalcones and heteroaryl chalcone derivatives which contain NH_2 as a donating substituent group (**Figures 9** and **10**).

1.11 Objectives and outline of this study

The objectives of this study are:

1. To synthesize and characterize chalcones and heteroaryl chalcone derivatives by spectroscopic methods.

2. To study their fluorescence properties.

3. To study the crystal structure of the chalcones and heteroaryl chalcone derivatives which their single crystals can be obtained.

4. To study research techniques which can be usefully applied in the future.

In this thesis, the eighteen compounds of chalcones and heteroaryl chalcone derivatives which are expected to exhibit fluorescent property were synthesized. Their structures were characterized by spectroscopy techniques. Single crystal X-ray structure determinations were studied for those compounds which can be crystallized out in order to study for their structures and crystal packings.

The eighteen chalcones and heteroaryl chalcones were designed base on long π conjugated system and different substituted groups in order to obtain fluorophore structures **(Figures 9** and **10)** and studied for their fluorescent properties. The synthesized chalcones in this study are divided into two groups, which are diethylaminobenzaldehyde and aminoacetophenone groups.

In this study, focus was on the effect of different substituted groups of chalcones and heteroaryl chalcone derivatives **(Figures 9** and **10)** which are expected to exhibit fluorescent property along with comparison of their fluorescence properties.

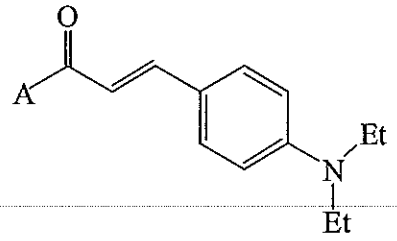

A	Structure	A	Structure	A	Structure
A1	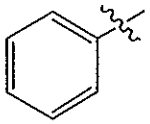 (TKB1)	A2	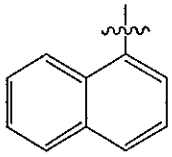 (TKB5)	A3	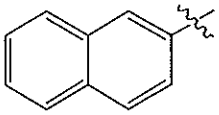 (TKB6)
A4	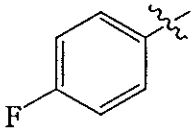 (TKB2)	A5	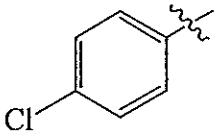 (TKB3)	A6	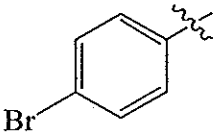 (TKB4)
A7	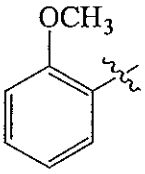 (TKB7)	A8	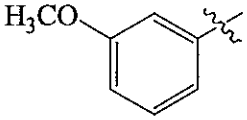 (TKB8)	A9	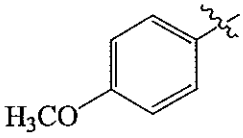 (TKB9)

Figure 9 The structures of the synthesized chalcone derivatives (**TKB1-TKB9**).

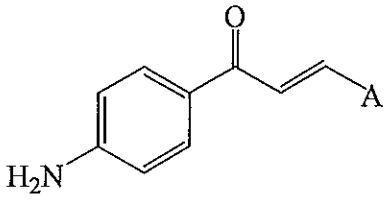

A	Structure	A	Structure	A	Structure
A10	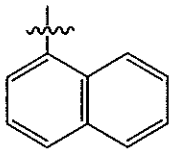 (TKD2)	A11	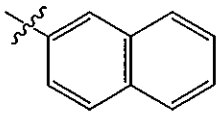 (TKD3)	A12	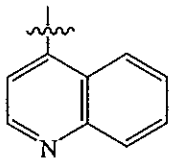 (TKD10)
A13	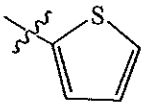 (TKD6)	A14	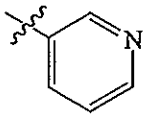 (TKD8)	A15	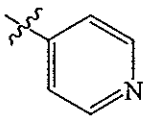 (TKD9)
A16	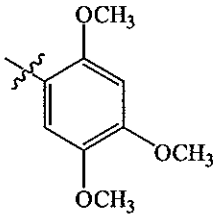 (TKD19)	A17	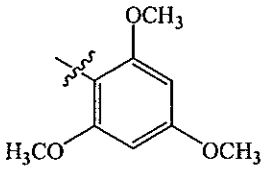 (TKD20)	A18	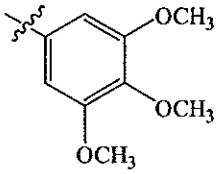 (TKD21)

Figure 10 The structures of the synthesized chalcones and heteroaryl chalcone derivatives (**TKD2-TKD21**).

2. EXPERIMENT

2.1 Instruments and chemicals

2.1.1 Instruments

Proton nuclear magnetic resonance spectra were recorded on FT-NMR Bruker Ultra Shield™ 300 MHz. Spectra were recorded in deuterochloroform mixed with hexadeutero-dimethyl sulphoxide solution and were recorded as δ value in ppm downfield from TMS (internal standard δ 0.00). Infrared spectra were recorded by using FTS 165 FT-IR spectrophotometer. Major bands (ν) were recorded in wave numbers (cm^{-1}). Ultraviolet and visible (UV-Vis) absorption spectra were recorded using a SPECORD S 100 (Analytikjena) and principle bands (λ_{max}) were recorded as wavelengths (nm) and log ε in methanol solution. Melting point was recorded in °C and was measured using an Electrothermal melting point apparatus. Single crystal X-ray diffraction measurements were collected using a Bruker Apex2 CCD diffractometer with a graphite monochromated MoK_{α} radiation. (λ = 0.71073 Å) at a detector distance of 5 cm and with APEX2 software. The collected data were reduced using *SAINT* (Bruker, 2005) program, and the empirical absorption corrections were performed using *SADABS* program. The structures were solved by direct methods and refined by least-squares using the *SHELXTL* (Sheldrick, 2008) software package. Fluorescence excitation and emission spectra were recorded on a Perkin-Elmer LS 55 Luminescence Spectrometer at the ambient temperature.

2.1.2 Chemicals

All chemicals used in this study are AR grade and were used without further purification.

1) Acetophenone from Fluka Chemica, Switzerland
2) 4'-Fluoroacetophenone from Fluka Chemica, China
3) 4'-Chloroacetophenone from Fluka Chemica, Germany
4) 4'-Bromoacetophenone from Fluka Chemica, Germany
5) 1-Acetonaphthone from Fluka Chemica, Switzerland
6) 2-Acetonaphthone from Fluka Chemica, Switzerland

7) 4'-Aminoacetophenone from Merck, Germany
8) 2'–Methoxyacetophenone from Fluka Chemica, Germany
9) 3'–Methoxyacetophenone from Fluka Chemica, Switzerland
10) 4'–Methoxyacetophenone from Sigma-Aldrich, Inc, Switzerland
11) 4–Diethylaminobenzaldehyde from Sigma-Aldrich, Inc, Germany
12) 2–Pyridinecarboxaldehyde from Fluka Chemica, Switzerland
13) 3–Pyridinecarboxaldehyde from Fluka Chemica, Switzerland
14) 4–Pyridinecarboxaldehyde from Fluka Chemica, Switzerland
15) 1–Naphthaldehyde from Fluka Chemica, Switzerland
16) 2 – Naphthaldehyde from Sigma-Aldrich, Inc, Germany
17) 4-quinolinecarboxaldehyde from Sigma-Aldrich, Inc, USA
18) Thiophene-2-carboxaldehyde from Sigma-Aldrich, Inc, USA
19) 2,4,5 - trimethoxybenzaldehyde from Sigma-Aldrich, Inc, UK
20) 2,4,6 - trimethoxybenzaldehyde from Fluka Chemica, USA
21) 3,4,5 - trimethoxybenzaldehyde from Fluka Chemica, China
22) Sodium Hydroxide from Lab-Scan, Ireland
23) Ethanol from Merck, Germany
24) Chloroform from Merck, Germany
25) Acetone from Merck, Germany
26) Coumarin 1 from Sigma-Aldrich, Inc, China
27) Coumarin 7 from Sigma-Aldrich, Inc, USA

2.2 Synthesis of chalcones and heteroaryl chalcone derivatives

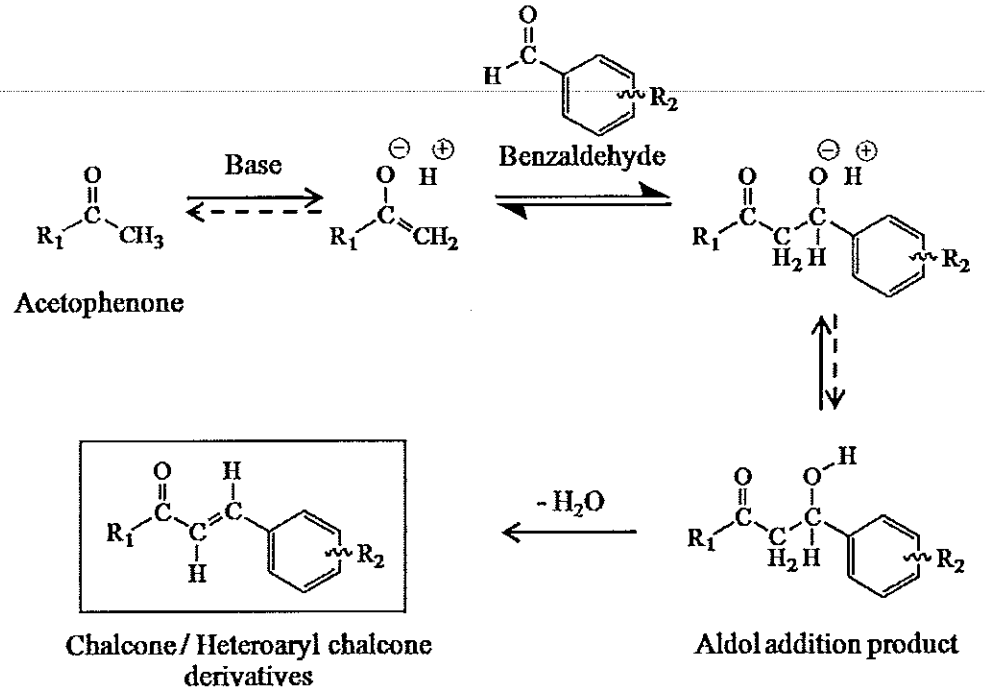

Figure 11 Synthesis of chalcones and heteroaryl chalcone derivatives.

All compounds were synthesized by base catalyzed Aldol condensation reaction using the ratio of ketone:aldehyde of 1:1 (Patil *et al.*, 2009). A straightforward approach to synthesize the series of chalcones and heteroaryl chalcone derivative is summarized in **Figure 11.**

2.3 Synthesis and characterization of chalcones and heteroaryl chalcone derivatives

2.3.1 (*E*)-3-(4-diethylaminophenyl)-1-phenylprop-2-en-1-one (TKB1)

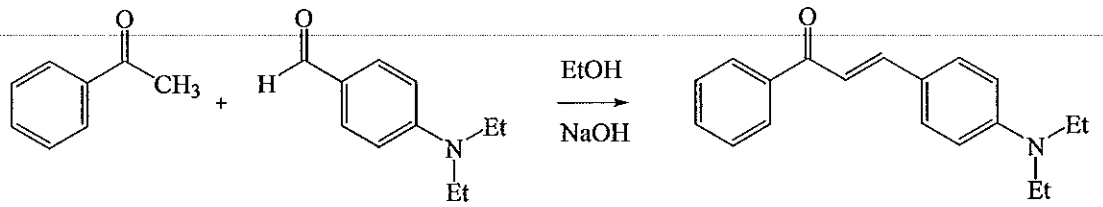

acetophenone **4-(diethylamino)benzaldehyde** **(TKB1)**

The solution of 2 mmol (0.23 ml) of acetophenone in ethanol 20 ml, the solution of 2 mmol (0.35 g) of 4'-diethylaminobenzaldehyde in ethanol 20 ml and 20% NaOH (aq) 5 ml were mixed and stirred at 5 °C for 4 hrs, the solid was then appeared. The resulting solid was collected by filtration, washed with diethylether, dried and the residue was purified by column chromatography (chloroform-hexane, 5:5 v/v) to afford **TKB1** as a yellow viscous oil.

Yellow viscous oil was obtained in ca. 32% yield. UV-Vis ($CHCl_3$) λ_{max} (nm) (ε x10^4): 258.71 (2.58), 424.40 (2.93). FT-IR (neat) ν (cm^{-1}): 2971 (sp^2 C-H aromatic stretching), 1683 (C=O stretching), 1520 (C=C aromatic stretching), 1187 (C-N stretching). ^{1}H NMR (see **Table 3**)

2.3.2 (*E*)-1-(4-fluorophenyl)-3-(4-(diethylamino)phenyl)prop-2-en-1-one (TKB2)

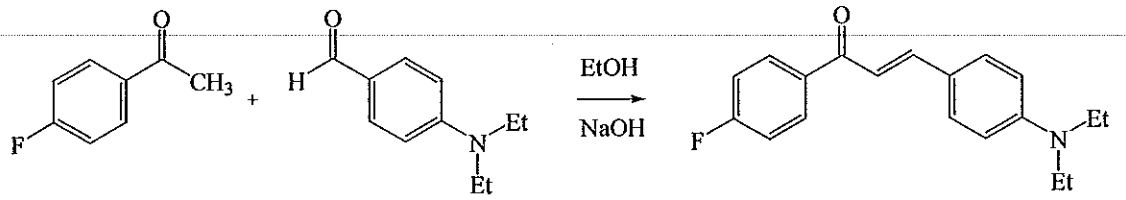

4-fluoro-acetophenone **4-(diethylamino)-benzaldehyde** **(TKB2)**

The solution of 2 mmol (0.24 ml) of 4-fluoroacetophenone in ethanol 15 ml, the solution of 2 mmol (0.35 g) of 4'-diethylaminobenzaldehyde in ethanol 20 ml and 30% NaOH (aq) 5 ml were mixed and stirred at 5 °C for 4 hrs, the solid was then obtained. The resulting solid was collected by filtration, washed with diethylether, dried and the residue was purified by column chromatography (hexane-dichlorometane, 4:6 v/v) to afford **TKB2** as an orange viscous oil.

Orange viscous oil was obtained in ca. 24% yield. UV-Vis ($CHCl_3$) λ_{max} (nm) (ε x10^4): 264.68 (10.8), 417.82 (1.02). FT-IR (neat) ν (cm^{-1}): 2926 (sp^2 C-H aromatic stretching), 1672 (C=O stretching), 1596 (C=C aromatic stretching), 811 (C-F stretching), 1153 (C-N stretching). ^{1}H NMR (see **Table 4**)

2.3.3 (*E*)-1-(4-chlorophenyl)-3-(4-(diethylamino)phenyl)prop-2-en-1-one (TKB3)

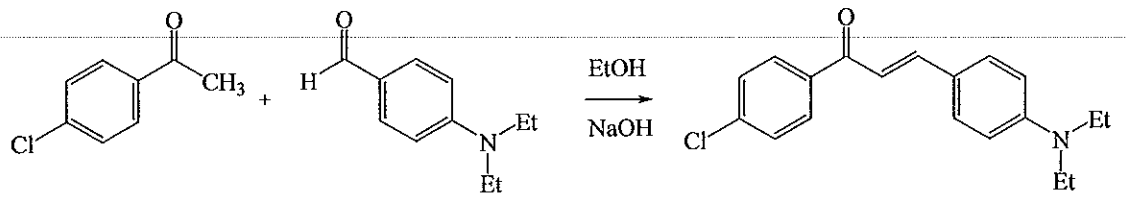

4-chloro-acetophenone **4-(diethylamino)-benzaldehyde** **(TKB3)**

The solution of 2 mmol (0.26 ml) of 4-chloroacetophenone in ethanol 20 ml, the solution of 2 mmol (0.35 g) of 4'-diethylaminobenzaldehyde in ethanol 20 ml and 20% NaOH (aq) 5 ml were mixed and stirred at 5 °C for 2 hrs, the solid was then obtained. The resulting solid was collected by filtration, washed with diethylether, dried and purified by repeated recrystallization from methanol.

Pale yellow powder was obtained in ca. 86% yield (m.p.101-102 °C). UV-Vis ($CHCl_3$) λ_{max} (nm) (ε x10^4): 272.88 (14.8), 424.40 (3.06). FT-IR (neat) ν (cm^{-1}): 2970 (sp^2 C-H aromatic stretching), 1576 (C=O stretching), 1521 (C=C aromatic stretching), 808 (C-Cl stretching), 1186 (C-N stretching). ^{1}H NMR (see **Table 5**)

2.3.4 (*E*)-1-(4-bromophenyl)-3-(4-(diethylamino)phenyl)prop-2-en-1-one (TKB4)

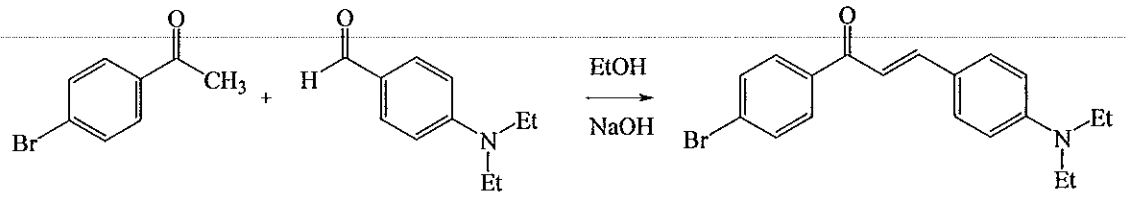

4-bromo-acetophenone **4-(diethylamino)-benzaldehyde** **(TKB4)**

The solution of 2 mmol (0.39 g) of 4-bromoacetophenone in ethanol 25 ml, the solution of 2 mmol (0.35 g) of 4'-diethylaminobenzaldehyde in ethanol 20 ml and 20% NaOH (aq) 5 ml were mixed and stirred at 5 °C for 3 hrs, the solid was then appeared. The resulting solid was collected by filtration, washed with diethyl ether, dried and purified by repeated recrystallization from methanol.

Yellow powder was obtained in ca. 75% yield (m.p.119-120 °C). UV-Vis ($CHCl_3$) λ_{max} (nm) (ε x10^4): 272.88 (11.6), 424.40(1.16). FT-IR (neat) ν (cm^{-1}): 2361 (sp^2 C-H aromatic stretching), 1572 (C=O stretching), 1520 (C=C aromatic stretching), 807 (C-Br stretching), 1186 (C-N stretching). ^{1}H NMR (see **Table 9**)

2.3.5 (*E*)-3-(4-(diethylamino)phenyl)-1-(naphthalen-1-yl)prop-2-en-1-one (TKB5)

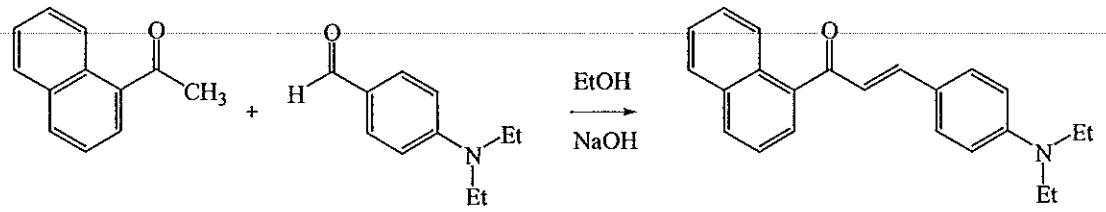

1-acetonaphthone **4-(diethylamino)-benzaldehyde** **(TKB5)**

The solution of 2 mmol (0.30 ml) of 1-acetonaphthone in ethanol 15 ml, the solution of 2 mmol (0.35 g) of 4'-diethylaminobenzaldehyde in ethanol 20 ml and 40% NaOH (aq) 5 ml were mixed and stirred at 5 °C for 6 hrs, the solid was then appeared. The resulting solid was collected by filtration, washed with diethylether, dried and the residue was purified by column chromatography (dichloromethane-hexane-ethylacetate, 5:4.5:0.5 v/v) to afford **TKB5** as an orange viscous oil.

Orange viscous oil was obtained in ca. 38% yield. UV-Vis ($CHCl_3$) λ_{max} (nm) (ε x10^4): 254.20 (5.21), 406.55 (9.70). FT-IR (neat) ν (cm^{-1}): 2972 (sp^2 C-H aromatic stretching), 1591 (C=O stretching), 1521 (C=C aromatic stretching), 1183 (C-N stretching). ^{1}H NMR (see **Table 13**)

2.3.6 (*E*)-3-(4-(diethylamino)phenyl)-1-(naphthalen-2-yl)prop-2-en-1-one (TKB6)

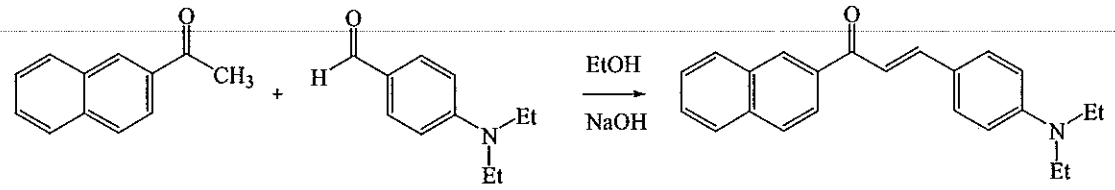

2-acetonaphthone **4-(diethylamino)-benzaldehyde** **(TKB6)**

The solution of 2 mmol (0.27 ml) of 2-acetonaphthone in ethanol 15 ml, the solution of 2 mmol (0.35 g) of 4'-diethylaminobenzaldehyde in ethanol 20 ml and 20% NaOH (aq) 5 ml were mixed and stirred at 5 °C for 8 hrs, the solid was then obtained. The resulting solid was collected by filtration, washed with diethylether, dried and the residue was purified by column chromatography (chloroform-hexane, 6:4 v/v) to afford **(TKB6)** as a viscous oil.

Yellow viscous oil was obtained in ca. 27% yield. UV-Vis ($CHCl_3$) λ_{max} (nm) (ε x10^4): 249.58 (3.81), 424.40 (4.05), FT-IR (neat) ν (cm^{-1}): 2969 (sp^2 C-H aromatic stretching), 1682 (C=O stretching), 1597 (C=C aromatic stretching), 1230 (C-N stretching). ^{1}H NMR (see **Table 14**)

2.3.7 (*E*)-3-(4-(diethylamino)phenyl)-1-(2-methoxyphenyl)prop-2-en-1-one (TKB7)

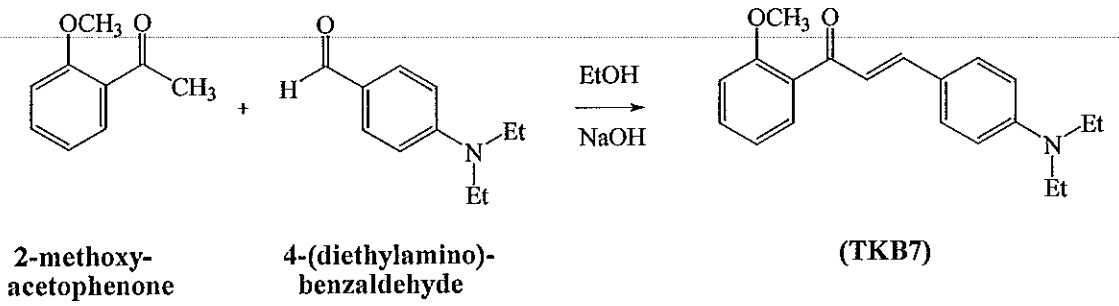

The solution of 2 mmol (0.30 g) of 2-methoxyacetophenone in ethanol 25 ml, the solution of 2 mmol (0.35 g) of 4'-diethylaminobenzaldehyde in ethanol 20 ml and 20% NaOH (aq) 5 ml were mixed and stirred at room temperature for 9 hrs, the solid was the obtained. The resulting solid was collected by filtration, washed with diethylether, dried and the residue was purified by column chromatography (ethylacetate-hexane, 2:8 v/v) to afford **TKB7** as an orange viscous oil.

Orange viscous oil was obtained in ca. 33% yield. UV-Vis ($CHCl_3$) λ_{max} (nm) (ε x10^4): 278.70 (21.7), 425.23 (18.5), FT-IR (neat) ν (cm^{-1}): 2970 (sp^2 C-H aromatic stretching), 1566 (C=O stretching), 1520 (C=C aromatic stretching), 1184 (C-N stretching). ^{1}H NMR (see **Table 16**)

2.3.8 (*E*)-3-(4-(diethylamino)phenyl)-1-(3-methoxyphenyl)prop-2-en-1-one (TKB8)

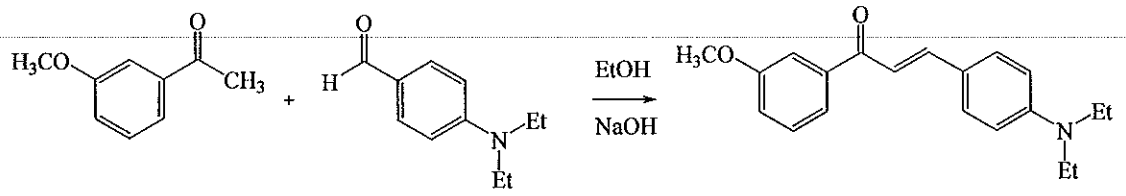

3-methoxy-acetophenone **4-(diethylamino)-benzaldehyde** **(TKB8)**

The solution of 2 mmol (0.30 g) of 4-methoxyacetophenone in ethanol 25 ml, the solution of 2 mmol (0.35 g) of 4'-diethylaminobenzaldehyde in ethanol 20 ml and 40% NaOH (aq) 5 ml were mixed and stirred at 5 °C for 8 hrs, the solid was then appeared. The resulting solid was collected by filtration, washed with diethylether, dried and the residue was purified by column chromatography (ethylacetate-hexane, 2:8 v/v) to afford **TKB8** as an orange viscous oil.

Orange viscous oil was obtained in ca. 30% yield. UV-Vis ($CHCl_3$) λ_{max} (nm) (ε x10^4): 281.19 (30.9), 422.75 (11.9), FT-IR (neat) ν (cm^{-1}): 2971 (sp^2 C-H aromatic stretching), 1599 (C=O stretching), 1521 (C=C aromatic stretching), 1169 (C-N stretching). ^{1}H NMR (see **Table 17**)

2.3.9 (*E*)-3-(4-(diethylamino)phenyl)-1-(4-methoxyphenyl)prop-2-en-1-one (TKB9)

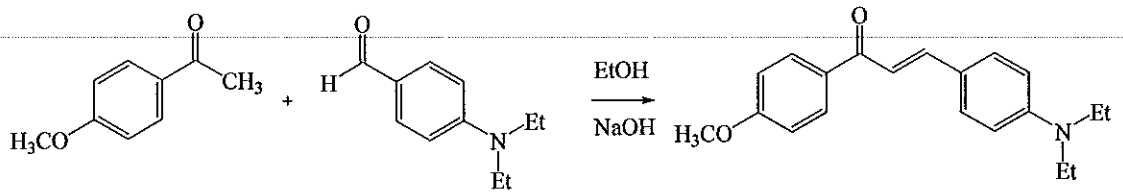

4-methoxy-acetophenone **4-(diethylamino)-benzaldehyde** **(TKB9)**

The solution of 2 mmol (0.27 ml) of 2-methoxyacetophenone in ethanol 15 ml, the solution of 2 mmol (0.35 g) of 4'-diethylaminobenzaldehyde in ethanol 20 ml and 20% NaOH (aq) 5 ml were mixed and stirred at room temperature for 9 hrs, the solid was then appeared. The resulting solid was collected by filtration, washed with diethylether, dried and purified by repeated recrystallization from acetone.

Yellow powder was obtained in ca. 82% yield (m.p.103-104 °C). UV-Vis ($CHCl_3$) λ_{max} (nm) (ε x10^4): 276.21 (1.79), 407.08 (2.45), FT-IR (neat) ν (cm^{-1}): 2968 (sp^2 C-H aromatic stretching), 1595 (C=O stretching), 1520 (C=C aromatic stretching), 1184 (C-N stretching). ^{1}H NMR (see **Table 15**)

2.3.10 (*E*)-1-(4-(aminophenyl)-3-(naphthalen-1-yl)prop-2-en-1-one (TKD2)

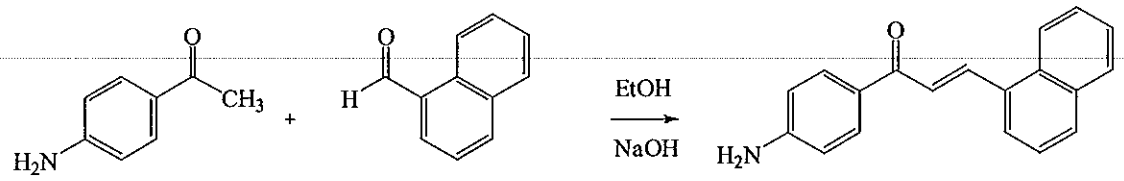

4-amino-acetophenone **1-naphthaldehyde** **(TKD2)**

The solution of 3 mmol (0.46 g) of 4-aminoacetophenone in ethanol 20 ml, the solution of 3 mmol (0.40 g) of 1-naphthaldehyde in ethanol 15 ml and 20% NaOH (aq) 5 ml were mixed and stirred at room temperature for 1 hr, the solid was then appeared. The resulting solid was collected by filtration, washed with diethylether, dried and purified by repeated recrystallization from acetone. The purity of the compound was confirmed by thin-layer chromatography.

Yellow powder was obtained in ca. 73% yield (m.p.197-198 °C). UV-Vis ($CHCl_3$) λ_{max} (nm) (ε x10^4): 252.91 (1.98), 358.33 (2.57), FT-IR (KBr) ν (cm^{-1}): 3327 (N-H stretching), 2487 (sp^2 C-H aromatic stretching), 1581 (C=O stretching), 1400 (C=C aromatic stretching). ^{1}H NMR (see **Table 18**)

2.3.11 (*E*)-1-(4-(aminophenyl)-3-(naphthalen-2-yl) prop-2-en-1-one (TKD3)

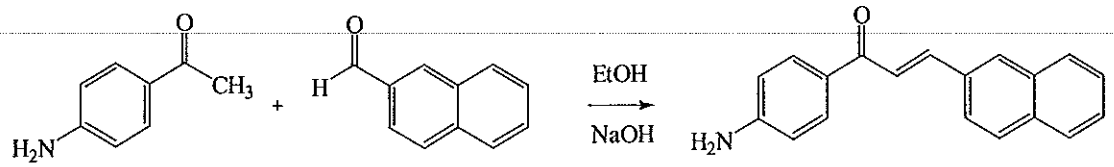

4-amino-acetophenone **2-naphthaldehyde** **(TKD3)**

The solution of 3 mmol (0.40 g) of 4-aminoacetophenone in ethanol 20 ml, the solution of 3 mmol (0.46 g) of 2-naphthaldehyde in ethanol 25 ml and 20% NaOH (aq) 5 ml were mixed and stirred at room temperature for 6 hrs, the solid was then obtained. The resulting solid was collected by filtration, washed with diethylether, dried and purified by repeated recrystallization from acetone. The purity of the compound was confirmed by thin-layer chromatography.

Pale yellow powder was obtained in ca. 79% yield (m.p.143-144 °C). UV-Vis ($CHCl_3$) λ_{max} (nm) (ε x10^4): 246.25 (2.98), 285.35 (2.14), 340.94 (3.00), FT-IR (KBr) ν (cm^{-1}): 3339 (N-H stretching), 2400 (sp^2 C-H aromatic stretching), 1602 (C=O stretching), 1298 (C=C aromatic stretching). ^{1}H NMR (see **Table 19**)

2.3.12 (*E*)-1-(4-(aminophenyl)-3-(thiophen-2-yl) prop-2-en-1-one (TKD6)

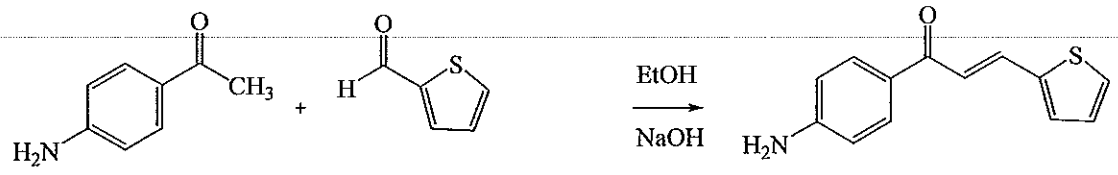

4-amino-acetophenone **thiophene benzaldehyde** **(TKD6)**

The solution of 3 mmol (0.40 g) of 4-aminoacetophenone in ethanol 20 ml, the solution of 3 mmol (0.33 ml) of thiophene-2-carboxaldehyde in ethanol 15 ml and 10% NaOH (aq) 5 ml were mixed and stirred at room temperature for 2 hrs, the solid was then appeared. The resulting solid was collected by filtration, washed with diethylether, dried and purified by repeated recrystallization from acetone. The purity of the compound was confirmed by thin-layer chromatography.

Yellow powder was obtained in ca. 84% yield (m.p.105-106 °C). UV-Vis ($CHCl_3$) λ_{max} (nm) (ε x10^4): 244.58 (1.18), 360.81 (2.69). FT-IR (KBr) ν (cm^{-1}): 3342 (N-H stretching), 2400 (sp^2 C-H aromatic stretching), 1597 (C=O stretching), 1437 (C=C aromatic stretching). ^{1}H NMR (see **Table 23**)

2.3.13 (*E*)-1-(4-(aminophenyl)-3-(pyridin-3-yl)prop-2-en-1-one (TKD8)

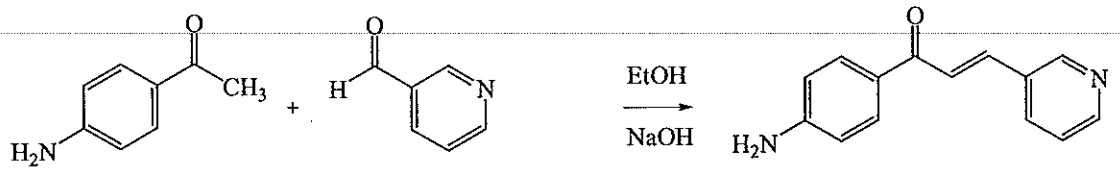

4-amino-acetophenone **3-pyridine benzaldehyde** **(TKD8)**

The solution of 3 mmol (0.40 g) of 4-aminoacetophenone in ethanol 20 ml, the solution of 3 mmol (0.18 ml) of 3-pyridinecarboxaldehyde in ethanol 15 ml and 10% NaOH (aq) 5 ml were mixed and stirred at room temperature for 1 hr, the solid was then appeared. The resulting solid was collected by filtration, washed with diethylether, dried and purified by repeated recrystallization from acetone. The purity of the compound was confirmed by thin-layer chromatography.

Yellow powder was obtained in ca. 68% yield (m.p.180-181 °C). UV-Vis ($CHCl_3$) λ_{max} (nm) (ε x10^4): 244.58 (1.36), 335.97 (1.79), FT-IR (KBr) ν (cm^{-1}): 3345 (N-H stretching), 2367 (sp^2 C-H aromatic stretching), 1605 (C=O stretching), 1416 (C=N stretching) and 1235 (C=C aromatic stretching). ^{1}H NMR (see **Table 27**)

2.3.14 (*E*)-1-(4-(aminophenyl)-3-(pyridin-4-yl)prop-2-en-1-one (TKD9)

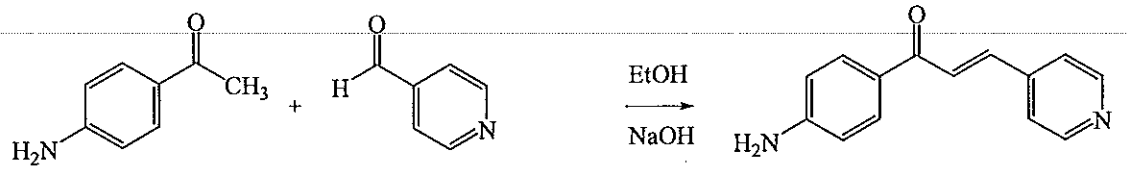

4-amino-acetophenone **4-pyridine benzaldehyde** **(TKD9)**

The solution of 3 mmol (0.40 g) of 4-aminoacetophenone in ethanol 20 ml, the solution of 3 mmol (0.32 ml) of 4-pyridinecarboxaldehyde in ethanol 15 ml and 10% NaOH (aq) 5 ml were mixed and stirred at room temperature for 5 hrs, the solid was then appeared. The resulting solid was collected by filtration, washed with diethylether, dried and purified by repeated recrystallization from acetone. The purity of the compound was confirmed by thin-layer chromatography.

Yellow powder was obtained in ca. 70% yield (m.p.213-214 °C). UV-Vis ($CHCl_3$) λ_{max} (nm) (ε x10^4): 262.90 (1.17), 340.94 (0.87), FT-IR (KBr) ν (cm^{-1}): 3152 (N-H stretching), 2400 (sp^2 C-H aromatic stretching), 1588 (C=O stretching), 1346 (C=C aromatic stretching). ^{1}H NMR (see **Table 31**)

2.3.15 (*E*)-1-(4-(aminophenyl)-3-(quinolin-4-yl)prop-2-en-1-one (TKD10)

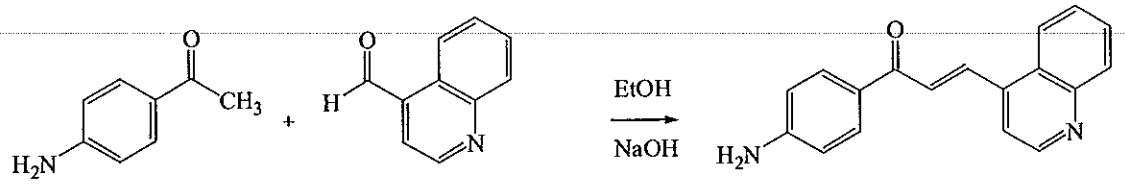

4-amino-acetophenone **4-quinoline benzaldehyde** **(TKD10)**

The solution of 2 mmol (0.27 g) of 4-aminoacetophenone in ethanol 20 ml, the solution of 2 mmol (0.18 ml) of 4-quinolinecarboxaldehyde in ethanol 15 ml and 20% NaOH (aq) 5 ml were mixed and stirred at 5 °C for 5 hrs, the solid was then obtained. The resulting solid was collected by filtration, washed with diethyl ether, dried and purified by repeated recrystallization from acetone. The purity of the compound was confirmed by thin-layer chromatography.

Orange powder was obtained in ca. 59% yield (m.p.235-236 °C). UV-Vis ($CHCl_3$) λ_{max} (nm) (ε x10^4): 244.58 (0.04), 331.00 (0.20), FT-IR (KBr) ν (cm^{-1}): 3394 (N-H stretching), 2363 (sp^2 C-H aromatic stretching), 1572 (C=O stretching), 1340 (C=C aromatic stretching). ^{1}H NMR (see **Table 32**)

2.3.16 (*E*)-1-(4-(aminophenyl)-3-(2,4,5-trimethoxyphenyl)prop-2-en-1-one (TKD19)

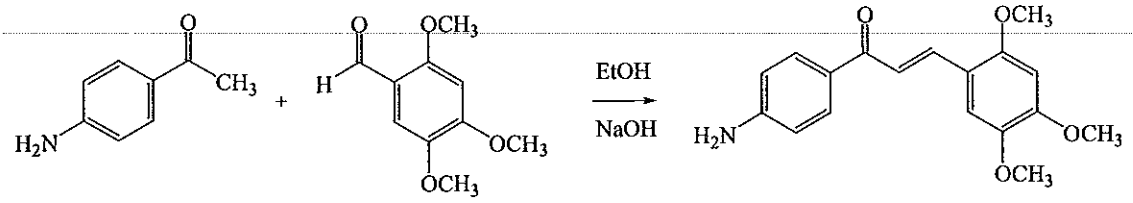

4-amino-acetophenone **2,4,5-trimethoxy-benzaldehyde** **(TKD19)**

The solution of 2 mmol (0.27 g) of 4-aminoacetophenone in ethanol 20 ml, the solution of 2 mmol (0.39 g) of 2,4,5-trimethoxybenzaldehyde in ethanol 20 ml and 40% NaOH (aq) 5 ml were mixed and stirred at room temperature for 4 hrs, the solid was then obtained. The resulting solid was collected by filtration, washed with diethylether, dried and purified by repeated recrystallization from acetone. The purity of the compound was confirmed by thin-layer chromatography.

Orange powder was obtained in ca. 63% yield (m.p.207-208 °C). UV-Vis ($CHCl_3$) λ_{max} (nm) (ε x10^4): 244.58 (2.08), 322.71 (2.18), 379.83 (2.20), FT-IR (KBr) ν (cm^{-1}): 3350 (N-H stretching), 2366 (*sp*^{2} C-H aromatic stretching), 1600 (C=O stretching), 1209 (C=C aromatic stretching), 1026 (C-O stretching). ^{1}H NMR (see **Table 33**)

2.3.17 (*E*)-1-(4-(aminophenyl)-3-(2,4,6-trimethoxyphenyl)prop-2-en-1-one (TKD20)

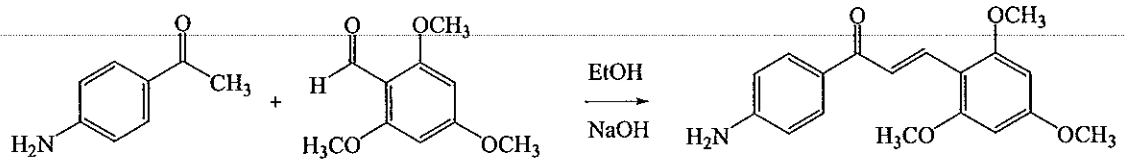

4-amino-acetophenone **2,4,6-trimethoxy-benzaldehyde** **(TKD20)**

The solution of 3 mmol (0.40 g) of 4-aminoacetophenone in ethanol 20 ml, the solution of 3 mmol (0.58 g) of 2,4,6-trimethoxybenzaldehyde in ethanol 15 ml and 20% NaOH (aq) 5 ml were mixed and stirred at room temperature for 4 hrs, the solid was then appeared. The resulting solid was collected by filtration, washed with diethylether, dried and purified by repeated recrystallization from acetone. The purity of the compound was confirmed by thin-layer chromatography.

Yellow powder was obtained in ca. 79% yield (m.p.228-229 °C). UV-Vis ($CHCl_3$) λ_{max} (nm) (ε x10^4): 253.74 (2.27), 356.67 (2.93), FT-IR (KBr) ν (cm^{-1}): 3361 (N-H stretching), 2486 (sp^2 C-H aromatic stretching), 1584 (C=O stretching), 1520, 1282 (C=C aromatic stretching), 1020 (C-O stretching). ^{1}H NMR (see **Table 37**)

2.3.18 (*E*)-1-(4-(aminophenyl)-3-(3,4,5-trimethoxyphenyl)prop-2-en-1-one (TKD21)

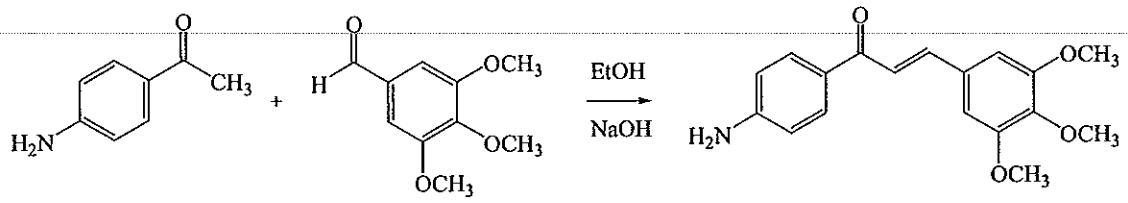

4-amino-acetophenone **3,4,5-trimethoxy-benzaldehyde** **(TKD21)**

The solution of 2 mmol (0.27 g) of 4-aminoacetophenone in ethanol 20 ml, the solution of 2 mmol (0.39 g) of 3,4,5-trimethoxybenzaldehyde in ethanol 25 ml and 40% NaOH (aq) 5 ml were mixed and stirred at room temperature for 6 hrs, the solid was the appeared. The resulting solid was collected by filtration, washed with diethylether, dried and purified by repeated recrystallization from acetone. The purity of the compound was confirmed by thin-layer chromatography.

Pale yellow powder was obtained in ca. 67% yield (m.p.240-241 °C). UV-Vis ($CHCl_3$) λ_{max} (nm) (ε x10^4): 253.78 (2.29), 354.67 (2.90) FT-IR (KBr) ν (cm^{-1}): 3358 (N-H stretching), 2939 (sp^2 C-H aromatic stretching), 1584 (C=O stretching), 1503 (C=C aromatic stretching), 1028 (C-O stretching) ^{1}H NMR (see **Table 38**)

2.4 Absorption, excitation and emission spectral properties

2.4.1 UV-Vis spectral of chalcones and heteroaryl chalcone derivatives

The UV-Vis absorbtion spectral data of all chalcones and heteroaryl chalcone derivatives were collected in the range of 200-800 nm at room temperature. The concentrations of all compounds were prepared at 2.5 μM in chloroform solution.

2.4.2 Excitation and emission spectral of chalcones and heteroaryl chalcone derivatives

The fluorescence spectrum of all chalcones and heteroaryl chalcone derivatives were recorded in chloroform solution at room temperature. The concentrations of all compounds were prepared at 2.5 μM in chloroform solution. For the emission spectra of the compounds, the excitation wavelength was fixed at 440 nm for **TKB1-TKB9** and 310 nm for **TKD2-TKD21**, which are the values in the range of maxima excitation wavelength for comparison of their emission. Their excitation spectra were studied by fixing the emission wavelength at 520 nm for **TKB1-TKB9** and 430 nm for **TKD2-TKD21**, which are the values in range of maxima emission wavelength.

2.5 Fluorescent quantum yield of chalcones and heteroaryl chalcone derivatives

The fluorescence quantum yield (Φ_f) is the ratio of photons absorbed to photons emitted through fluorescence. In other words the quantum yield gives the probability of the excited state being deactivated by fluorescence rather than by another, non-radiative mechanism. Essentially, solutions of the standard and test samples with identical absorbance at the same excitation wavelength can be assumed to be absorbing the same number of photons. Hence, a simple ratio of the integrated fluorescence intensities of the two solutions (recorded under identical conditions) will yield the ratio of the quantum yield values. Since Φ_f for the standard sample is known, it is trivial to calculate the Φ_f for the test sample. The determination for fluorescent quantum yields of chalcones and heteroaryl chalcones derivatives were carried out following the literature methods (Williams *et al.*, 1983; Dhami *et al.*, 1995)

2.5.1 General experimental considerations

Standard samples; should be chosen to ensure they absorb at the excitation wavelength of choice for the test sample, and, if possible, emit in a similar region to the test sample. The standard samples must be well characterized and suitable for such use.

Cuvettes; standard 10 mm path length fluorescence cuvettes are sufficient for running the fluorescence measurements. In order to minimise errors in calculating the absorbance of each solution, it is advisable to use absorption cuvettes with extended path lengths.

Concentration range; in order to minimize re-absorption effects absorbances in the 10 mm fluorescence cuvette should never exceed 0.1 at and above the excitation wavelength. Above this level, non-linear effects may be observed due to inner filter effects, and the resulting quantum yield values may be perturbed. Remember that this maximum allowable value of the recorded absorbance must be adjusted depending upon the path length of the absorption cuvette being used.

Sample preparation; It is vital that all glassware is kept scrupulously clean, and solvents must be of spectroscopic grade and checked for background fluorescence.

2.5.2 The procedure for measurement the fluorescent quantum yield

2.5.2.1 Record the UV-Vis absorbance spectrum of the solvent background for the chosen sample. Note down the absorbance at the excitation wavelength to be used.

2.5.2.2 Record the fluorescence spectrum of the same solution in the 10 mm fluorescence cuvette. Calculate and note down the integrated fluorescence intensity from the fully corrected fluorescence spectrum.

2.5.2.3 Repeat steps 1. and 2. for five solutions with increasing concentrations of the chosen sample. There will be six solutions in all, corresponding to absorbances at the excitation wavelength.

2.5.2.4 Plot a graph between integrated fluorescence intensity and absorbance. The result should be a straight line with gradient m, and intercept = 0.

2.5.2.5 Repeat steps 2.5.2.1 to 2.5.2.4 for the remaining samples.

2.5.3 Calculation of fluorescence quantum yields from acquired data

The gradients of the graphs obtained above are proportional to the quantum yield of the different samples. Absolute values are calculated using the standard samples which have a fixed and known fluorescence quantum yield value, according to the following equation:

$$\Phi_X = \Phi_{ST}\left(\frac{Grad_X}{Grad_{ST}}\right)\left(\frac{n_X^{\ 2}}{n_{ST}^{\ 2}}\right) \qquad (10)$$

where the subscripts ST and X denote standard and test respectively, Φ is the fluorescence quantum yield, *Grad* is the gradient from the plot of integrated fluorescence between intensity and absorbance, and n the refractive index of the solvent.

2.5.4 Standard for fluorescence quantum yields measurements and the condition used in fluorescence studies

Fluorescence quantum yields were measured by comparison with the integrated fluorescence from Coumarin standards. As standard, Coumarin 7 (Φ = 0.49) in acetronitrile was used to compare for compounds **TKB1-TKB9** and Coumarin1 (Φ= 0.73) in ethanol for **TKD2-TKD21.**

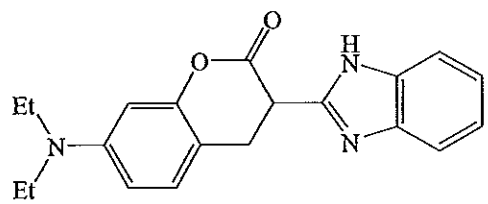

Figure 12 The structure of coumarin 7

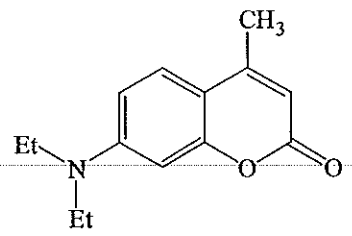

Figure13 The structure of coumarin 1

For chalcones and heteroaryl chalcone derivatives, the fluorescent quantum yields were measured in $CHCl_3$ solution in six concentrations (0, 0.5, 1.0, 1.5, 2.0, 2.5 μM). The integrated fluorescence intensity (peak of fluorescence emission) and absorbance of the sample solution were plotted to find the gradient.

CHAPTER 3

RESULTS AND DISCUSSION

3.1 Structural elucidations of chalcones

3.1.1 (*E*)-3-(4-diethylamino) phenyl)-1-phenylprop-2-en-1-one (TKB1)

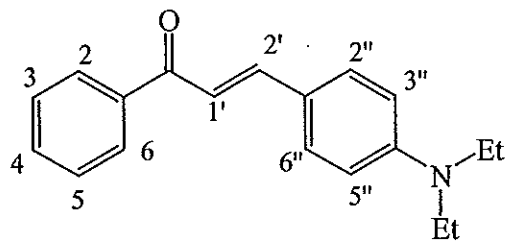

(TKB1)

A yellow viscous oil of compound **TKB1** was obtained in 32% yield, The UV-Vis absorption bands **(Figure 51)** were shown at 258.71 and 424.40 nm. The FT-IR spectrum of **TKB1 (Figure 50)** revealed the stretching vibration of aromatic C-H at 2971 cm^{-1}. The strong peak of C=O stretching vibration was observed at 1683 cm^{-1} and C=C stretching vibration in aromatic ring at 1520 cm^{-1}. The C-N stretching vibration was observed at 1187 cm^{-1}.

The ^{1}H NMR spectrum of **TKB1 (Figure 49**, see **Table 3)** showed two *doublet* signals of equivalent protons H-2, H-6 and H-3, H-5 at δ8.00 (2H, *d*, *J* = 7.2 Hz) and δ7.49 (2H, *d*, *J* = 7.2 Hz), respectively. Signal of *trans* protons H-1' and H-2' appeared at δ7.31 (1H, *d*, *J* = 15.3 Hz) and δ7.78 (1H, *d*, *J* = 15.3 Hz), respectively. The *triplet* signals at δ7.43-7.56 were assigned to H-4. Two *doublet* signals of equivalent protons H-2", H-6" and H-3", H-5" appeared at δ7.54 (2H, *d*, *J* = 9.0 Hz) and δ6.68 (2H, *d*, *J* = 9.0 Hz), respectively. The *triplet* signal of CH_3 and the *quartet* signal of CH_2 were observed at δ1.16 (3H, *t*, *J* = 6.9 Hz) and δ3.37 (2H, *q*, *J* = 6.9 Hz), respectively. These spectroscopic data confirmed that **TKB1** is (*E*)-3-(4-diethylamino) phenyl)-1-phenylprop-2-en-1-one.

Table 3 ^{1}H NMR of compound **TKB1**

Position	**δ_H (ppm), *mult*, *J* (Hz)**
CH_3	1.21, *t*, 6.9 Hz
CH_2	3.42, *q*, 6.9 Hz
2, 6	8.00, *d*, 7.2 Hz
3, 5	7.49, *d*, 7.2 Hz
4	7.43 – 7.56, *m*
1'	7.31, *d*, 15.3 Hz
2'	7.78, *d*, 15.3 Hz
2'', 6''	7.54, *d*, 9.0 Hz
3'', 5''	6.68, *d*, 9.0 Hz

3.1.2 (*E*)-1-(4-fluorophenyl)-3-(4-(diethylamino)phenyl)prop-2-en-1-one (TKB2)

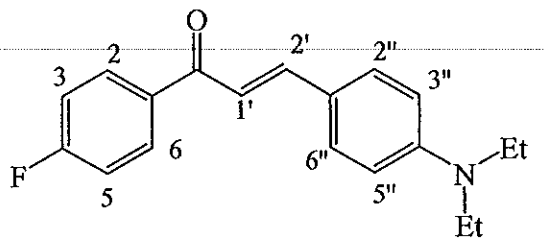

(TKB2)

Compound **TKB2** was obtained as an orange viscous oil (24% yield). The UV-Vis absorption bands **(Figure 54)** were shown at 264.68 and 417.82 nm. The FT-IR spectrum of **TKB2** **(Figure 53)** revealed the stretching vibration of aromatic C-H at 2926 cm^{-1}. The strong peak of C=O stretching vibration was observed at 1672 cm^{-1} and C=C stretching vibration in aromatic ring at 1596 cm^{-1}. The C-F stretching was observed at 811 $cm^{-1}$and C-N stretching was observed at 1153 cm^{-1}.

The ^{1}H NMR spectrum of **TKB2** **(Figure 52**, see **Table 4)** showed two *doublet* signals of equivalent protons H-2, H-6 and H-3, H-5 at δ7.73 (2H, *d*, J = 7.2 Hz) and δ6.68 (2H, *d*, J = 7.2), respectively. Signal of *trans* protons H-1' and H-2' appeared at δ7.28 (1H, *d*, J = 15.3 Hz) and δ7.80 (1H, *d*, J = 15.3 Hz), respectively. Two *doublet* signals of equivalent protons H-2", H-6" and H-3", H-5" appeared at δ7.54 (2H, *d*, J = 8.1 Hz) and δ7.14 (2H, *d*, J = 8.1 Hz), respectively. The *triplet* signal of CH_3 and the *quartet* signal of CH_2 were observed at δ1.30 (3H, *t*, J = 6.9 Hz) and δ3.44 (2H, *q*, J = 6.9 Hz), respectively. These spectroscopic data confirmed that **TKB2** is (*E*)-1-(4-fluorophenyl)-3-(4-(diethylamino)phenyl)prop-2-en-1-one.

Table 4 ^{1}H NMR of compound **TKB2**

Position	δ_H (ppm), *mult*, *J* (Hz)
CH_3	1.30, *t*, 6.9 Hz
CH_2	3.44, *q*, 6.9 Hz
2, 6	7.73, *d*, 7.2 Hz
3, 5	7.14, *d*, 7.2 Hz
1'	7.28, *d*, 15.3 Hz
2'	7.80, *d*, 15.3 Hz
2", 6"	7.54, *d*, 8.1 Hz
3", 5"	6.68, *d*, 8.1 Hz

3.13 (*E*)-1-(4-chlorophenyl)-3-(4-(diethylamino)phenyl)prop-2-en-1-one (TKB3)

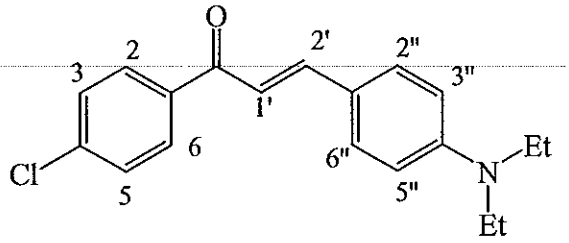

(TKB3)

Compound **TKB3** was obtained as a yellow solid (86% yield), mp. 101-102 °C. The UV-Vis absorption bands **(Figure 57)** were shown at 272.88 and 424.40 nm. The FT-IR spectrum of **TKB3** **(Figure 56)** revealed the stretching vibration of aromatic C-H at 2970 cm^{-1}. The strong peak of C=O stretching vibration was observed at 1576 $cm^{-1}$and C=C stretching vibration in aromatic ring at 1521 cm^{-1}. The C-F stretching was observed at 808 $cm^{-1}$and C-N stretching was observed at 1186 cm^{-1}.

The ^{1}H NMR spectrum of **TKB3** **(Figure 55**, see **Table 5)** showed two *doublet* signals of equivalent protons H-2, H-6 and H-3, H-5 at δ8.04 (2H, *d*, *J* = 6.9 Hz) and δ7.52 (2H, *d*, *J* = 6.9 Hz), respectively. Signal of *trans* protons H-1' and H-2' appeared at δ7.43 (1H, *d*, *J* = 15.3 Hz) and δ7.68 (1H, *d*, *J* = 15.3 Hz), respectively. In addition, two *doublet* signals of equivalent protons H-2", H-6" and H-3", H-5" appeared at δ7.59 (2H, *d*, *J* = 9.0 Hz) and δ6.68 (2H, *d*, *J* = *9.0* Hz), respectively. The *triplet* signal of CH_3 and the *quartet* signal of CH_2 were observed at δ1.16 (3H, *t*, *J* = 6.9 Hz) and δ3.37 (2H, *q*, *J* = 6.9 Hz), respectively. These spectroscopic data confirmed that **TKB3** is (*E*)-1-(4-chlorophenyl)-3-(4-(diethylamino)phenyl)prop-2-en-1-one.

Table 5 ^{1}H NMR of compound **TKB3**

Position	δ_H (ppm), *mult*, *J* (Hz)
CH_3	1.16, *t*, 6.9 Hz
CH_2	3.37, *q*, 6.9 Hz
2, 6	8.04, *d*, 6.9 Hz
3, 5	7.52, *d*, 10.8 Hz
1'	7.43, *d*, 15.3 Hz
2'	7.68, *d*, 15.3 Hz
2", 6"	7.59, *d*, 9.0 Hz
3", 5"	6.68, *d*, 9.0 Hz

The crystal structure and packing of **TKB3** is illustrated in **Figures 14** and **15**. The crystal and experiment data are given in **Table 6**. Bond lengths and angles are shown in **Table 7**. Hydrogen-bond geometry is shown in **Table 8**. The X-ray study shows that the **TKB3** crystallized out in centrosymmetric space group P21/c.

The asymmetric unit of **TKB3** contains two molecules, *A* and *B*, which differ in conformation of the ethyl groups of the diethylamino substituents. In molecule *A*, two ethyl groups are on the same side of the molecular plane, while they are on opposite sides in molecule *B* (**Figure 14**). The bond lengths and bond angles in the two molecules are also slightly different. The molecules of **TKB3** exist in an *E* configuration with respect to the C8=C9 double bond [1.349 (2) Å in molecule *A* and 1.341 (2) Å in molecule B] and the torsion angle C7–C8–C9–C10 is -178.39 (14)° in molecule *A* and 176.11 (4)° in molecule *B*. Two benzene rings are twisted at 16.27 (7)° in molecule *A* [16.99 (7) ° in molecule *B*]. The prop-2-en-1-one unit (C7-C9/O1) is planar with the rms 0.0066 (2) Å for molecule *A* [0.0116 (2) Å for molecule *B*]. The mean plane through the pro-2-en-1-one unit makes the dihedral angles of 19.02 (10) and 3.43 (10)° with the C1-C6 and C10-C15 benzene rings, respectively in molecule

A [the corresponding values are 9.94 (10) and 7.31 (10)° in molecule B]. Two ethyl groups of the diethylamino substituent in molecule A are on the same side with the torsion angles C13A-N1A-C16A-C17A = -78.38 (18)° and C13A–N1A–C18A–C19A = 81.27 (18)° indicating the (-)-syn-clinal and (+)-syn-clinal conformations, respectively; whereas in molecule *B*, the two ethyl groups are on the opposite sides with the torsion angles C13B–N1B–C16B–C17B = 99.04 (17)° and C13B–N1B–C18B–C19B = 84.38 (17)° indicating the (+)-anti-clinal and (+)-syn-clinal conformations, respectively. Weak intramolecular C9A—H9AA···O1A, C5B—H5BA···O1B and C9B—H9BA···O1B hydrogen bonds generate S(5) ring motifs (Bernstein *et al.*, 1995). The bond distances in **TKB3** are of normal values (Allen *et al.*, 1987) and are comparable with those in the related structure (Chantrapromma *et al.*, 2009). In the crystal **(Figure 14)**, the 4-chlorophenyl and the pro-2-en-1-one units of the molecules are linked by weak intermolecular C—H···O hydrogen bonds **(Table 8)** resulting in the molecules being connected into ribbons propagating along the *b* direction.

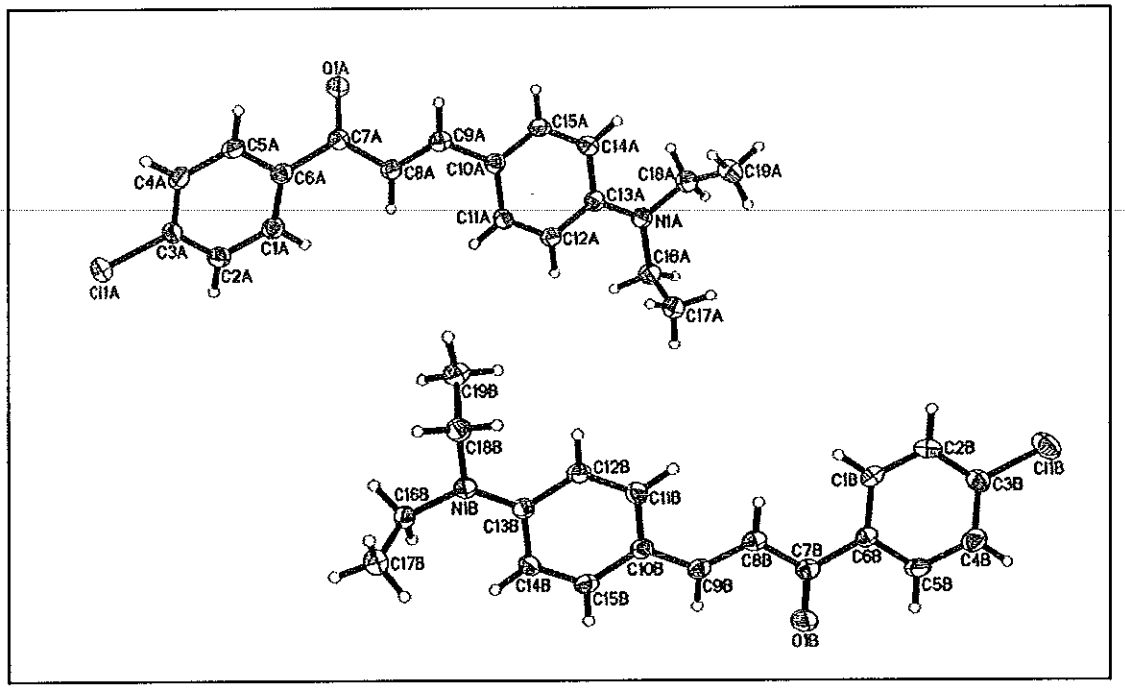

Figure 14 X-ray ORTEP diagram of the compound **TKB3**

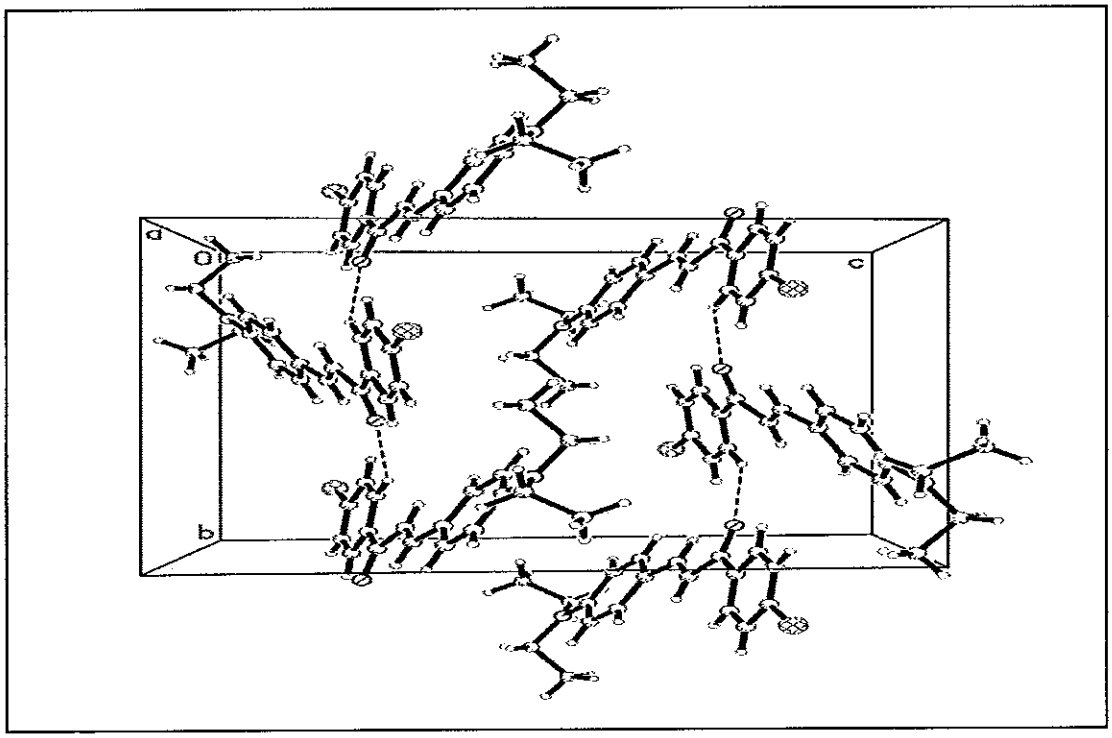

Figure 15 Packing diagram of **TKB3** viewed down the *a* axis with H-bonds shown as dashed lines.

Table 6 Crystal data and structure refinement for **TKB3**

Identification code	**TKB3**
Empirical formula	$C_{19}H_{20}ClNO$
Formula weight	313.81
Temperature	100.0 K
Wavelength	0.71073 Å
Crystal system, space group	Monoclinic, $P2_1/c$
Unit cell dimensions	a = 17.2073(2) Å α = (90)° b = 11.9467(1) Å β = 97.2680(10)° c = 15.7996(2) Å γ = (90)°
Volume	3221.84(6) $Å^3$
Z, Calculated density	8, 1.294 Mg/m^3
Absorption coefficient	0.239 mm^{-1}
F(000)	1328
Crystal size	0.33 x 0.23 x 0.10 mm
Theta range for data collection	1.19 to 30.00 deg.
Limiting indices	-23<=h<=24, -12<=k<=16, -21<=l<=22
Reflections collected / unique	47596 / 9400 [R(int) = 0.0407]
Completeness to theta = 30.00	100.0 %
Max. and min. transmission	0.9765 and 0.9252
Refinement method	Full-matrix least-squares on F^2
Data / restraints / parameters	9400 / 0 / 401
Goodness-of-fit on F^2	1.098
Final R indices [I>2σ(I)]	R1 = 0.0479, wR2 = 0.1021
R indices (all data)	R1 = 0.0834, wR2 = 0.1220
Largest diff. peak and hole	0.318, -0.346 $e.A^{-3}$

Table 7 Bond lengths [Å] and angles [°] for **TKB3**

O1A-C7A	1.2326(18)	N1A-C13A	1.3741(19)
N1A-C16A	1.458(2)	N1A-C18A	1.459(2)
C1A-C2A	1.389(2)	C1A-C6A	1.394(2)
C1A-H1AA	0.9300	C2A-C3A	1.384(2)
C2A-H2AA	0.9300	C3A-C4A	1.389(2)
C4A-C5A	1.381(2)	C4A-H4AA	0.9300
C5A-C6A	1.399(2)	C5A-H5AA	0.9300
C6A-C7A	1.501(2)	C7A-C8A	1.469(2)
C8A-C9A	1.349(2)	C8A-H8AA	0.9300
C9A-C10A	1.449(2)	C9A-H9AA	0.9300
C10A-C15A	1.404(2)	C10A-C11A	1.404(2)
C11A-C12A	1.373(2)	C11A-H11A	0.9300
C12A-C13A	1.417(2)	C12A-H12A	0.9300
C13A-C14A	1.414(2)	C14A-C15A	1.381(2)
C14A-H14A	0.9300	C15A-H15A	0.9300
C16A-C17A	1.524(2)	C16A-H16A	0.9700
C16A-H16B	0.9700	C17A-H17A	0.9600
C17A-H17B	0.9600	C17A-H17C	0.9600
C18A-C19A	1.524(2)	C18A-H18A	0.9700
C18A-H18B	0.9700	C19A-H19A	0.9600
C19A-H19B	0.9600	C19A-H19C	0.9600
Cl1B-C3B	1.7405(16)	O1B-C7B	1.2320(18)
N1B-C13B	1.3687(19)	N1B-C18B	1.460(2)
N1B-C16B	1.4610(19)	C1B-C2B	1.388(2)
C1B-C6B	1.399(2)	C1B-H1BA	0.9300
C2B-C3B	1.379(2)	C2B-H2BA	0.9300
C3B-C4B	1.387(2)	C4B-C5B	1.383(2)
C4B-H4BA	0.9300	C5B-C6B	1.394(2)
C5B-H5BA	0.9300	C6B-C7B	1.495(2)
C7B-C8B	1.465(2)	C8B-C9B	1.341(2)

Table 7 Bond lengths [Å] and angles [°] for **TKB3** (Continued)

C8B-H8BA	0.9300	C9B-C10B	1.448(2)
C9B-H9BA	0.9300	C10B-C11B	1.403(2)
C10B-C15B	1.403(2)	C11B-C12B	1.375(2)
C11B-H11B	0.9300	C12B-C13B	1.418(2)
C12B-H12B	0.9300	C13B-C14B	1.413(2)
C14B-C15B	1.382(2)	C14B-H14B	0.9300
C15B-H15B	0.9300	C16B-C17B	1.520(2)
C16B-H16C	0.9700	C16B-H16D	0.9700
C17B-H17D	0.9600	C17B-H17E	0.9600
C17B-H17F	0.9600	C18B-C19B	1.522(2)
C18B-H18C	0.9700	C18B-H18D	0.9700
C19B-H19D	0.9600	C19B-H19E	0.9600
C19B-H19F	0.9600	C13A-N1A-C16A	121.13(13)
C13A-N1A-C18A	121.34(13)	C16A-N1A-C18A	117.10(12)
C2A-C1A-C6A	121.02(14)	C2A-C1A-H1AA	119.5
C6A-C1A-H1AA	119.5	C3A-C2A-C1A	119.04(15)
C3A-C2A-H2AA	120.5	C1A-C2A-H2AA	120.5
C2A-C3A-C4A	121.26(14)	C2A-C3A-Cl1A	118.93(12)
C4A-C3A-Cl1A	119.81(12)	C5A-C4A-C3A	118.98(15)
C5A-C4A-H4AA	120.5	C3A-C4A-H4AA	120.5
C4A-C5A-C6A	121.24(15)	C4A-C5A-H5AA	119.4
C6A-C5A-H5AA	119.4	C1A-C6A-C5A	118.40(14)
C1A-C6A-C7A	123.13(14)	C5A-C6A-C7A	118.47(14)
O1A-C7A-C8A	122.12(14)	O1A-C7A-C6A	119.20(14)
C8A-C7A-C6A	118.68(14)	C9A-C8A-C7A	120.77(15)
C9A-C8A-H8AA	119.6	C7A-C8A-H8AA	119.6
C8A-C9A-C10A	128.20(15)	C8A-C9A-H9AA	115.9
C10A-C9A-H9AA	115.9	C15A-C10A-C11A	116.37(14)
C15A-C10A-C9A	119.98(14)	C11A-C10A-C9A	123.63(14)
C12A-C11A-C10A	122.00(14)	C12A-C11A-H11A	119.0

Table 7 Bond lengths [Å] and angles [°] for **TKB3** (Continued)

C10A-C11A-H11A	119.0	C11A-C12A-C13A	121.81(15)
C15A-C10A-C9A	119.98(14)	C11A-C10A-C9A	123.63(14)
C12A-C11A-C10A	122.00(14)	C12A-C11A-H11A	119.0
C10A-C11A-H11A	119.0	C11A-C12A-C13A	121.81(15)
C11A-C12A-H12A	119.1	C13A-C12A-H12A	119.1
N1A-C13A-C14A	122.01(14)	N1A-C13A-C12A	121.73(14)
C14A-C13A-C12A	116.25(14)	C15A-C14A-C13A	121.14(14)
C15A-C14A-H14A	119.4	C13A-C14A-H14A	119.4
C14A-C15A-C10A	122.38(15)	C14A-C15A-H15A	118.8
C10A-C15A-H15A	118.8	N1A-C16A-C17A	114.24(13)
N1A-C16A-H16A	108.7	C17A-C16A-H16A	108.7
N1A-C16A-H16B	108.7	C17A-C16A-H16B	108.7
H16A-C16A-H16B	107.6	C16A-C17A-H17A	109.5
C16A-C17A-H17B	109.5	H17A-C17A-H17B	109.5
C16A-C17A-H17C	109.5	H17A-C17A-H17C	109.5
H17B-C17A-H17C	109.5	N1A-C18A-C19A	114.14(13)
N1A-C18A-H18A	108.7	C19A-C18A-H18A	108.7
N1A-C18A-H18B	108.7	C19A-C18A-H18B	108.7
H18A-C18A-H18B	107.6	C18A-C19A-H19A	109.5
C18A-C19A-H19B	109.5	H19A-C19A-H19B	109.5
C18A-C19A-H19C	109.5	H19A-C19A-H19C	109.5
H19B-C19A-H19C	109.5	C13B-N1B-C18B	121.49(12)
C13B-N1B-C16B	122.73(13)	C18B-N1B-C16B	115.52(12)
C2B-C1B-C6B	120.35(14)	C2B-C1B-H1BA	119.8
C6B-C1B-H1BA	119.8	C3B-C2B-C1B	119.53(15)
C3B-C2B-H2BA	120.2	C1B-C2B-H2BA	120.2
C2B-C3B-C4B	121.31(15)	C2B-C3B-Cl1B	119.26(13)
C4B-C3B-Cl1B	119.42(12)	C5B-C4B-C3B	118.81(15)
C5B-C4B-H4BA	120.6	C3B-C4B-H4BA	120.6
C4B-C5B-C6B	121.27(15)	C4B-C5B-H5BA	119.4

Table 7 Bond lengths [Å] and angles [°] for **TKB3** (Continued)

C6B-C5B-H5BA	119.4	C5B-C6B-C1B	118.71(14)
C5B-C6B-C7B	118.04(14)	C1B-C6B-C7B	123.26(14)
O1B-C7B-C8B	121.12(14)	O1B-C7B-C6B	119.33(14)
C8B-C7B-C6B	119.54(14)	C9B-C8B-C7B	120.80(15)
C9B-C8B-H8BA	119.6	C7B-C8B-H8BA	119.6
C8B-C9B-C10B	128.56(15)	C8B-C9B-H9BA	115.7
C10B-C9B-H9BA	115.7	C11B-C10B-C15B	116.32(14)
C11B-C10B-C9B	123.19(14)	C15B-C10B-C9B	120.48(14)
C12B-C11B-C10B	122.45(14)	C12B-C11B-H11B	118.8
C10B-C11B-H11B	118.8	C11B-C12B-C13B	121.00(14)
C11B-C12B-H12B	119.5	C13B-C12B-H12B	119.5
N1B-C13B-C14B	121.71(14)	N1B-C13B-C12B	121.35(14)
C14B-C13B-C12B	116.93(14)	C15B-C14B-C13B	120.84(14)
C15B-C14B-H14B	119.6	C13B-C14B-H14B	119.6
C14B-C15B-C10B	122.41(14)	C14B-C15B-H15B	118.8
C10B-C15B-H15B	118.8	N1B-C16B-C17B	113.25(13)
N1B-C16B-H16C	108.9	C17B-C16B-H16C	108.9
N1B-C16B-H16D	108.9	C17B-C16B-H16D	108.9
H16C-C16B-H16D	107.7	C16B-C17B-H17D	109.5
C16B-C17B-H17E	109.5	H17D-C17B-H17E	109.5
C16B-C17B-H17F	109.5	H17D-C17B-H17F	109.5
H17E-C17B-H17F	109.5	N1B-C18B-C19B	112.83(13)
N1B-C18B-H18C	109.0	C19B-C18B-H18C	109.0
N1B-C18B-H18D	109.0	C19B-C18B-H18D	109.0
H18C-C18B-H18D	107.8	C18B-C19B-H19D	109.5
C18B-C19B-H19E	109.5	H19D-C19B-H19E	109.5
C18B-C19B-H19F	109.5	H19D-C19B-H19F	109.5
H19E-C19B-H19F	109.5		

Table 8 Hydrogen-bond geometry (Å,°)

D—H···*A*	D—H	H···*A*	D···*A*	D—H···*A*
C1B—H1BA··· O1B^{i}	0.93	2.47	3.2746 (19)	145
C16B—H16C··· O1A^{ii}	0.97	2.42	3.3749 (19)	168
C2A—H2AA··· Cg1^{iii}	0.93	2.60	3.3377 (17)	137
Symmetry codes: (i) x+1, y−1, z; (ii) x, y+1, z; (iii) −x, −y+1, −z+2.				

3.1.4 (*E*)-1-(4-bromophenyl)-3-(4-(diethylamino)phenyl)prop-2-en-1-one (TKB4)

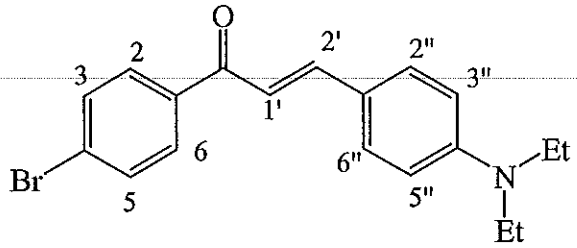

(TKB4)

Compound **TKB4** was obtained as a yellow solid (75% yield), mp. 119-120 °C. The UV-Vis absorption bands **(Figure 60)** were shown at 272.88 and 424.40 nm. The FT-IR spectrum of **TKB4 (Figure 59)** revealed the stretching vibration of aromatic C-H at 2361 cm^{-1}. The strong peak of C=O stretching vibration was observed at 1602 $cm^{-1}$and C=C stretching vibration in aromatic ring at 1520 cm^{-1}. The C-Br stretching was observed at 807 $cm^{-1}$and C-N stretching was observed at 1186 cm^{-1}.

The ^{1}H NMR spectrum of **TKB4 (Figure 58**, see **Table 9)** showed two *doublet* signals of equivalent protons H-2, H-6 and H-3, H-5 at δ7.90 (2H, *d*, *J* = 8.4 Hz) and δ7.53 (2H, *d*, *J* = 8.4 Hz), respectively. Signal of *trans* protons H-1' and H-2' appeared at δ7.30 (1H, *d*, *J* = 15.3 Hz) and δ7.73 (1H, *d*, *J* = 15.3 Hz), respectively. In addition, two *doublet* signals of equivalent protons H-2", H-6" and H-3", H-5" appeared at δ7.64 (2H, *d*, *J* = 9.0 Hz) and δ6.67 (2H, *d*, *J* = *9.0* Hz), respectively. The *triplet* signal of CH_3 and the *quartet* signal of CH_2 were observed at δ1.21 (3H, *t*, *J* = 6.9 Hz) and δ3.42 (2H, *q*, *J* = 6.9 Hz), respectively. These spectroscopic data confirmed that **TKB4** is (*E*)-1-(4-bromophenyl)-3-(4-(diethylamino)phenyl)prop-2-en-1-one.

Table 9 ^{1}H NMR of compound **TKB4**

Position	δ_H **(ppm),** ***mult,*** ***J*** **(Hz)**
CH_3	1.21, *t*, 6.9 Hz
CH_2	3.42, *q*, 6.6 Hz
2, 6	7.90, *d*, 8.4 Hz
3, 5	7.53, *d*, 8.4 Hz
1'	7.30, *d*, 15.3 Hz
2'	7.73, *d*, 15.3 Hz
2'', 6''	7.64, *d*, 9.0 Hz
3'', 5''	6.67, *d*, 9.0 Hz

The crystal structure and packing of **TKB4** is illustrated in **Figures 16** and **17**. The crystal and experiment data are given in **Table 10**. Bond lengths and angles were shown in **Table 11**.

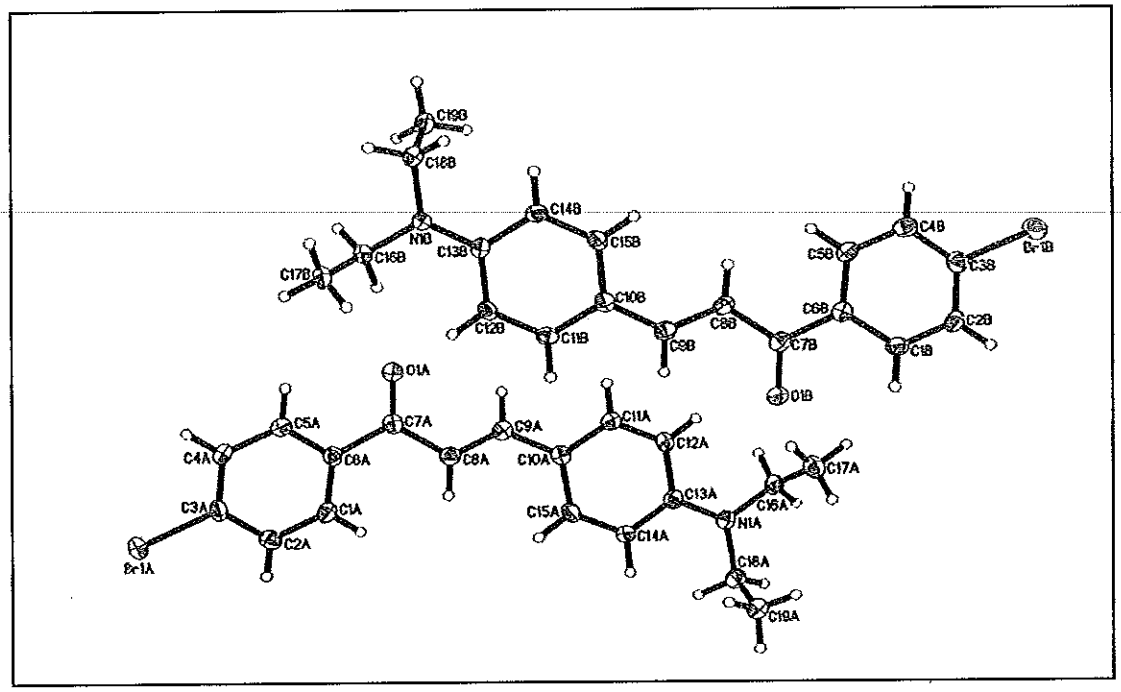

Figure 16 X-ray ORTEP diagram of the compound **TKB4**

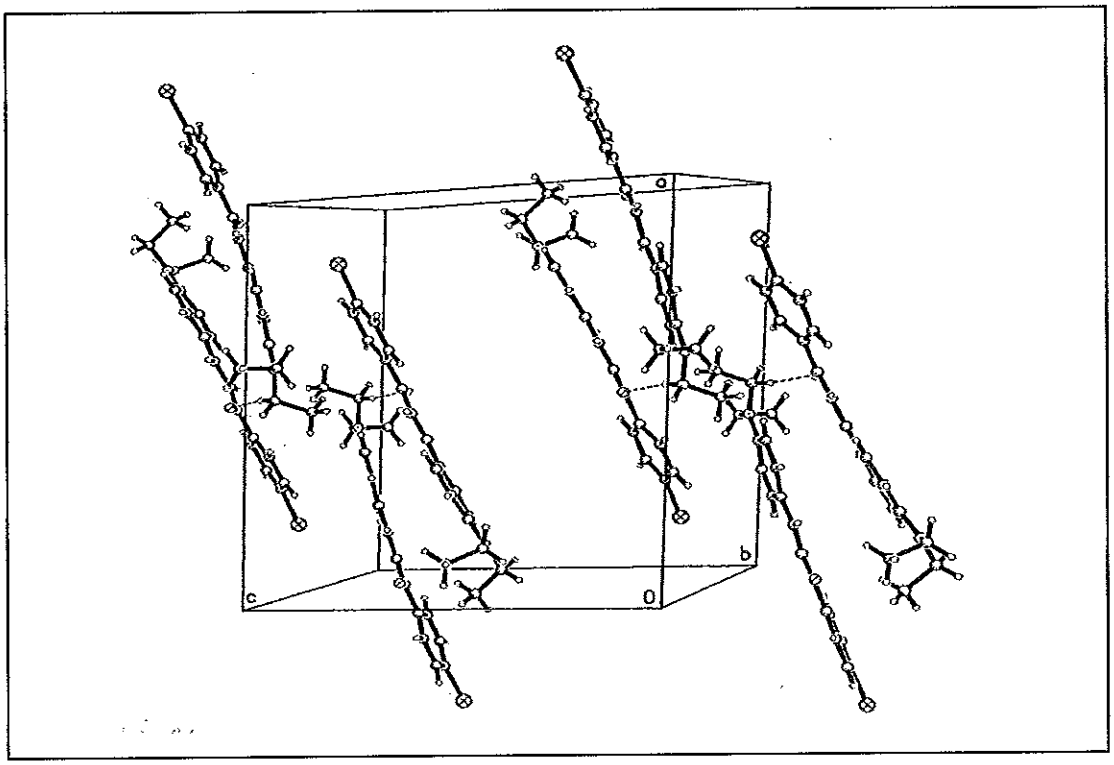

Figure 17 Packing diagram of **TKB4** viewed down the *a* axis with H-bonds shown as dashed lines.

Table 10 Crystal data and structure refinement for **TKB4**.

Identification code	**TKB4**
Empirical formula	$C_{19}H_{20}BrNO$
Formula weight	358.26
Temperature	100.0(1) K
Wavelength	0.71073 Å
Crystal system, space group	Monoclinic, $P2_1/c$
Unit cell dimensions	a = 17.0560 (4) Å α = (90)° b = 12.0631(3) Å β = 94.6960(10) ° c = 15.9001(4) Å γ = (90)°
Volume	3260.44(14) $Å^3$
Z, Calculated density	8, 1.460 Mg/m^3
Absorption coefficient	2.523 mm^{-1}
F(000)	1472
Crystal size	0.58 x 0.16 x 0.09 mm
Theta range for data collection	1.20 to 27.50 deg.
Limiting indices	-22<=h<=22, -15<=k<=15, -20<=l<=19
Reflections collected / unique	32053 / 7452 [R(int) = 0.0518]
Completeness to theta = 30.00	99.6 %
Max. and min. transmission	0.8048 and 0.3224
Refinement method	Full-matrix least-squares on F^2
Data / restraints / parameters	7452 / 0 / 401
Goodness-of-fit on F^2	1.050
Final R indices [I>2σ(I)]	R1 = 0.0361, wR2 = 0.0765
R indices (all data)	R1 = 0.0648, wR2 = 0.0904
Largest diff. peak and hole	0.907, -0.299 $e.A^{-3}$

Table 11 Bond lengths [Å] and angles [°] for **TKB4**

Br1A-C3A	1.906(2)	O1A-C7A	1.230(3)
N1A-C13A	1.370(3)	N1A-C16A	1.460(3)
N1A-C18A	1.462(3)	C1A-C2A	1.387(4)
C1A-C6A	1.390(4)	C1A-H1AA	0.9300
C2A-C3A	1.381(4)	C2A-H2AA	0.9300
C3A-C4A	1.382(4)	C4A-C5A	1.385(4)
C4A-H4AA	0.9300	C5A-C6A	1.395(4)
C5A-H5AA	0.9300	C6A-C7A	1.507(3)
C7A-C8A	1.467(4)	C8A-C9A	1.348(3)
C8A-H8AA	0.9300	C9A-C10A	1.441(4)
C9A-H9AA	0.9300	C10A-C11A	1.405(3)
C10A-C15A	1.408(4)	C11A-C12A	1.381(3)

3.1.5 (*E*)-3-(4-(diethylamino)phenyl)-1-(naphthalen-1-yl)prop-2-en-1-one (TKB5)

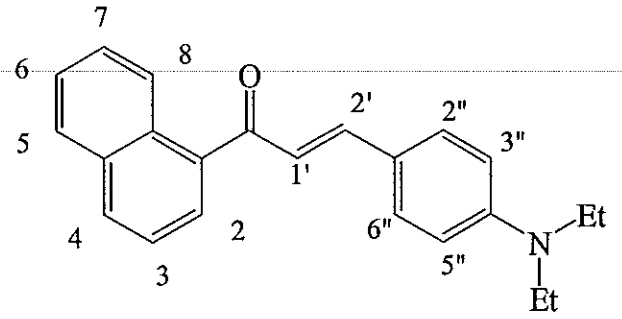

(TKB5)

Compound **TKB5** was obtained as an orange viscous oil (38% yield). The UV-Vis absorption bands **(Figure 63)** were shown at 254.20 and 406.5 nm. The FT-IR spectrum of **TKB5 (Figure 62)** revealed the stretching vibration of aromatic C-H at 2972 cm^{-1}. The strong peak of C=O stretching vibration was observed at 1591 $cm^{-1}$and C=C stretching vibration in aromatic ring at 1521 cm^{-1}. The C-N stretching was observed at 1183 cm^{-1}.

The ^{1}H NMR spectrum of **TKB5 (Figure 61**, see **Table 12)** showed two *doublet* signals of equivalent protons H-2", H-6" and H-3", H-5" at δ7.43 (2H, *d*, *J* = 8.7 Hz) and δ6.63 (2H, *d*, *J* = 8.7 Hz), respectively. Signal of *trans* protons H-1' and H-2' appeared at δ7.05 (1H, *d*, *J* = 15.9 Hz) and δ7.45-7.55 (1H, *m*), respectively. Resonances of aromatic protons of naphthalenyl part H-2 to H-8 were shown at δ7.90 (1H, *d*, *J* = 8.1 Hz), δ7.55 (1H, *t*, *J* = 8.1 Hz), δ7.95 (1H, *d*, *J* = 8.1 Hz), δ7.70 (1H, *d*, *J* = 8.7 Hz), δ7.45-7.55 (1H, *m*), δ7.45-7.55 (1H, *m*) and δ8.25 (1H, *dd* , *J* = 2.3 Hz), respectively. The *triplet* signal of CH_3 and the *quartet* signal of CH_2 were observed at δ1.20 (3H, *t*, *J* = 7.2 Hz) and δ3.40 (2H, *q*, *J* = 10.8 Hz), respectively. These spectroscopic data confirmed that **TKB5** is (*E*)-3-(4-(diethylamino)phenyl)-1-(naphthalen-1-yl)prop-2-en-1-one.

Table 12 ^{1}H NMR of compound **TKB5**

Position	**δ_H (ppm), *mult*, *J* (Hz)**
CH_3	1.20, *t*, 7.2 Hz
CH_2	3.40, *q*, 10.8 Hz
2	7.90, *d*, 8.1Hz
3	7.55, *t*, 8.1 Hz
4	7.95, *d*, 8.1 Hz
5	7.70, *d*, 8.7 Hz
6	7.45-7.55, *m*
7	7.45-7.55, *m*
8	8.25, *d*, 8.7 Hz
1'	7.05, *d*, 15.9 Hz
2'	7.45-7.55, *m*
2", 6"	7.43, *d*, 8.7 Hz
3", 5"	6.63, *d*, 8.7 Hz

3.1.6 (*E*)-3-(4-(diethylamino)phenyl)-1-(naphthalen-2-yl)prop-2-en-1-one (TKB6)

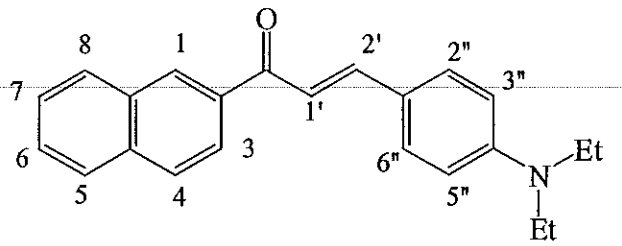

(TKB6)

Compound **TKB6** was obtained as a yellow viscous oil (27% yield). The UV-Vis absorption bands **(Figure 66)** were shown at 249.58 and 424.40 nm. The FT-IR spectrum of **TKB6 (Figure 65)** revealed the stretching vibration of aromatic C-H at 2969 cm^{-1}. The strong peak of C=O stretching vibration was observed at 1682 cm^{-1} and C=C stretching vibration in aromatic ring at 1597 cm^{-1}. The C-N stretching was observed at 1230 cm^{-1}.

The ^{1}H NMR spectrum of **TKB6 (Figure 64**, see **Table 13)** showed two *doublet* signals of equivalent protons H-2", H-6" and H-3", H-5" at δ7.62 (2H, *d*, J = 8.7 Hz) and δ6.72 (2H, *d*, J = 8.7 Hz), respectively. Signal of *trans* protons H-1' and H-2' appeared at δ7.50 (1H, *d*, J = 15.6 Hz) and δ7.88 (1H, *d*, J = 15.6 Hz), respectively. Resonances of aromatic protons of naphthalenyl part H-1 to H-8 were shown at δ8.55 (1H, *s*), δ7.96 (1H, *d*, J = 9.0 Hz), δ7.94 (1H, *bd*, J = 9.0 Hz), δ8.03 (1H, *dd*, J = 9.0, 3.0 Hz), δ7.63-7.00, *m*, H-6, H-7 and δ8.13 (1H, *dd*, J = 9.0, 3.0 Hz), respectively. The *triplet* signal of CH_3 and the *quartet* signal of CH_2 were observed at δ1.26 (3H, *t*, J = 7.2 Hz) and δ3.49 (2H, *q*, J = 10.8 Hz), respectively. These spectroscopic data confirmed that **TKB6** is (*E*)-3-(4-(diethylamino)phenyl)-1-(naphthalen-2-yl)prop-2-en-1-one.

Table 13 ^{1}H NMR of compound **TKB6**

Position	δ_H **(ppm),** ***mult,*** ***J*** **(Hz)**
CH_3	1.26, *t*, 7.2 Hz
CH_2	3.49, *q*, 7.2 Hz
1	8.55, *s*
3	7.96, *d*, 9.0 Hz
4	7.94, *bd,* 9.0 Hz
5	8.03, *dd,* 9.0, 3.0 Hz
6	(7.63-7.00), *m*
7	(7.63-7.00), *m*
8	8.13, *dd*, 9.0, 3.0 Hz
1'	7.50, *d*, 15.6 Hz
2'	7.88, *d*, 15.6 Hz
2", 6"	7.62, *d*, 8.7 Hz
3", 5"	6.72, *d*, 8.7 Hz

3.1.7 (*E*)-3-(4-(diethylamino)phenyl)-1-(2-methoxyphenyl)prop-2-en-1-one (TKB7)

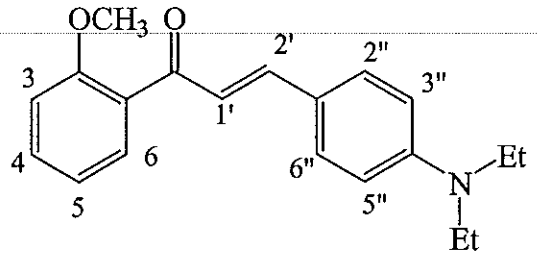

(TKB7)

Compound **TKB7** was obtained as an orange viscous oil (33% yield). The UV-Vis absorption bands **(Figure 69)** were shown at 278.70 and 425.23 nm. The FT-IR spectrum of **TKB7 (Figure 68)** revealed the stretching vibration of aromatic C-H at 2970 cm^{-1}. The strong peak of C=O stretching vibration was observed at 1566 $cm^{-1}$and C=C stretching vibration in aromatic ring at 1520 cm^{-1}. The C-N stretching was observed at 1184 cm^{-1}.

The ^{1}H NMR spectrum of **TKB7 (Figure 67**, see **Table 14)** showed two *doublet* signals of equivalent protons H-2", H-6" and H-3", H-5" at δ7.46 (2H, *d*, J = 8.4 Hz) and δ6.65 (2H, *d*, J = 8.4 Hz), respectively. Signal of *trans* protons H-1' and H-2' appeared at δ7.10 (1H, *d*, J = 15.9 Hz) and δ7.55 (1H, *d*, J = 15.9 Hz), respectively. The *doublet* signal of H-3 was observed at δ6.99 (1H, *d*, J = 8.1 Hz). The *triplet* signal of H-5 was observed at δ7.04 (1H, *t*, J = 7.5 Hz). Two *multiplet* signals at δ 7.53 to 7.59 were assigned to H-4 and H-6, respectively. Methoxy proton showed the *singlet* signal at δ 3.90 (3H, *s*). In addition, the *triplet* signal of CH_3 and the *quartet* signal of CH_2 were observed at δ1.20 (3H, *t*, J = 6.9 Hz) and δ3.42 (2H, *q*, J = 6.9 Hz), respectively. These spectroscopic data confirmed that **TKB7** is (*E*)-3-(4-(diethylamino)phenyl)-1-(2-methoxyphenyl)prop-2-en-1-one

Table 14 ^{1}H NMR of compound **TKB7**

Position	**δ_H (ppm), *mult*, *J* (Hz)**
CH_3	1.20, *t*, 6.9 Hz
CH_2	3.44, *q*, 7.2 Hz
OCH_3	3.90, *s*
3	6.99, *d*, 8.1 Hz
4	7.53 – 7.59, *m*
5	7.04, *t*, 7.5 Hz
6	7.53 – 7.59, *m*
1'	7.10, *d*, 15.9 Hz
2'	7.55, *d*, 15.9 Hz
2", 6"	7.46, *d*, 8.4 Hz
3", 5"	6.65, *d*, 8.4 Hz

3.1.8 (*E*)-3-(4-(diethylamino)phenyl)-1-(3-methoxyphenyl)prop-2-en-1-one (TKB8)

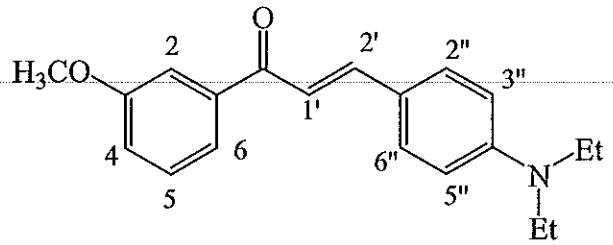

(TKB8)

Compound **TKB8** was obtained as an orange viscous oil (30% yield). The UV-Vis absorption bands **(Figure 72)** were shown at 281.19 and 422.75 nm. The FT-IR spectrum of **TKB8 (Figure 71)** revealed the stretching vibration of aromatic C-H at 2971 cm^{-1}. The strong peak of C=O stretching vibration was observed at 1599 cm^{-1} and C=C stretching vibration in aromatic ring at 1521 cm^{-1}. The C-N stretching was observed at 1169 cm^{-1}.

The ^{1}H NMR spectrum of **TKB8 (Figure 70**, see **Table 15)** showed two *doublet* signals of equivalent protons H-2", H-6" and H-3", H-5" at δ7.55 (2H, *d*, J = 8.4 Hz) and δ6.69 (2H, *d*, J = 8.4 Hz), respectively. Signal of *trans* protons H-1' and H-2' appeared at δ7.32 (1H, *d*, J = 15.6 Hz) and δ7.82 (1H, *d*, J = 15.6 Hz), respectively. The aromatic protons of H-2 to H-6 were shown at δ7.29 (1H, *s*), δ7.12 (1H, *dd*, J = 7.5, 2.3 Hz), δ7.42 (1H, *t*, J = 7.5 Hz) and δ7.61 (1H, *bd*, J = 1.0 Hz), respectively. Methoxy proton showed the *singlet* signal at δ 3.86 (3H, *s*). In addition, the *triplet* signal of CH_3 and the *quartet* signal of CH_2 were observed at δ1.23 (3H, *t*, J = 6.9 Hz) and δ3.44 (2H, *q*, J = 7.2 Hz), respectively. These spectroscopic data confirmed that **TKB7** is (*E*)-3-(4-(diethylamino)phenyl)-1-(3-methoxyphenyl)prop-2-en-1-one

Table 15 ^{1}H NMR of compound **TKB8**

Position	**δ_H (ppm), *mult*, *J* (Hz)**
CH_3	1.23, *t*, 6.9 Hz
CH_2	3.44, *q*, 7.2 Hz
OCH_3	3.86, *s*
2	7.29, *s*
4	7.12, *dd*, 7.5, 2.3 Hz
5	7.42, *t*, 7.5 Hz
6	7.61, *bd*, 1.0 Hz
1'	7.32, *d*, 15.6 Hz
2'	7.82, *d*, 15.6 Hz
2", 6"	7.55, *d*, 8.4 Hz
3", 5"	6.69, *d*, 8.4 Hz

3.1.9 (*E*)-3-(4-(diethylamino)phenyl)-1-(4-methoxyphenyl)prop-2-en-1-one (TKB9)

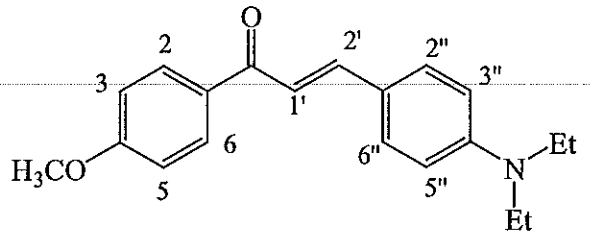

(TKB9)

Compound **TKB9** was obtained as an yellow solidl (82% yield), mp.103-104 °C. The UV-Vis absorption bands **(Figure 75)** were shown at 276.21 and 407.08 nm. The FT-IR spectrum of **TKB9** **(Figure 74)** revealed the stretching vibration of aromatic C-H at 2968 cm^{-1}. The strong peak of C=O stretching vibration was observed at 1595 cm^{-1} and C=C stretching vibration in aromatic ring at 1520cm^{-1}. The C-N stretching was observed at 1184 cm^{-1}.

The ^{1}H NMR spectrum of **TKB9** **(Figure 73**, see **Table 16)** showed two *doublet* signals of equivalent protons H-2", H-6" and H-3", H-5" at δ7.65 (2H, *d*, *J* = 8.1 Hz) and δ6.69 (2H, *d*, *J* = 8.1 Hz), respectively. Signal of *trans* protons H-1' and H-2' appeared at δ7.30 (1H, *d*, *J* = 15.9 Hz) and δ7.78 (1H, *d*, *J* = 15.9 Hz), respectively. The *doublet* signals of equivalent protons H-2, H-6 and H-3, H-5 at δ8.09 (2H, *d*, *J* = 7.2 Hz) and δ7.05 (2H, *d*, *J* = 7.2 Hz), respectively. In addition, the *triplet* signal of CH_3 and the *quartet* signal of CH_2 were observed at δ1.10 (3H, *t*, *J* = 7.2 Hz) and δ3.40 (2H, *q*, *J* = 6.3 Hz), respectively. These spectroscopic data confirmed that **TKB9** is (*E*)-3-(4-(diethylamino) phenyl)-1-(4-methoxyphenyl)prop-2-en-1-one

Table 16 ^{1}H NMR of compound **TKB9**

Position	δ_H **(ppm),** ***mult*****,** ***J*** **(Hz)**
CH_3	1.10, *t*, 7.2 Hz
CH_2	3.40, *q*, 6.3 Hz
OCH_3	3.80, *s*
2, 6	8.09, *d*, 7.2 Hz
3, 5	7.05, *d*, 7.2 Hz
1'	7.30, *d*, 15.3 Hz
2'	7.78, *d*, 15.3 Hz
2", 6"	7.55, *d*, 8.1 Hz
3", 5"	6.69, *d*, 8.1 Hz

3.1.10 (*E*)-1-(4-(aminophenyl)-3-(naphthalen-1-yl)prop-2-en-1-one (TKD2)

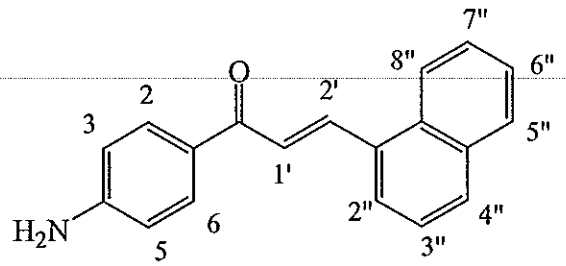

(TKD2)

Compound **TKD2** was obtained as a yellow solid (73% yield), mp. 197-198 °C. The UV-Vis absorption bands **(Figure 78)** were shown at 252.91 and 358.33 nm. The FT-IR spectrum of **TKD2** **(Figure 77)** revealed the stretching vibration of aromatic C-H at 2487 cm^{-1}. The strong peak of C=O stretching vibration was observed at 1581 $cm^{-1}$and C=C stretching vibration in aromatic ring at 1400 cm^{-1}. The N-H stretching vibration was observed at 3327 cm^{-1}.

The ^{1}H NMR spectrum of **TKD2** **(Figure 76, see Table 17)** showed two *doublet* signals of equivalent protons H-2, H-6 and H-3, H-5 at δ8.27 (2H, *d*, *J* = 8.4 Hz) and δ6.64 (2H, *d*, *J* = 8.4 Hz), respectively. Signal of *trans* protons H-1' and H-2' appeared at δ7.93 (1H, *d*, *J* = 15.3 Hz) and δ8.45 (1H, *d*, *J* = 15.3 Hz), respectively. Resonances of aromatic protons of naphthalenyl part H-2" to H-8" were shown at δ7.66 (1H, *d*, *J* = 7.2 Hz), δ7.56 (1H, *t*, *J* = 7.2 Hz), δ8.04 (1H, *d*, *J* = 7.2 Hz), δ7.99 (1H, *d*, *J* = 7.2 Hz), δ7.60 (1H, *t*, *J* = 7.2 Hz), δ7.63 (1H, *t*, *J* = 7.2 Hz) and δ8.18 (1H, *d*, *J* = 7.2 Hz), respectively. The singlet signals at δ6.19 (2H) was assigned as NH_2. These spectroscopic data confirmed that **TKD2** is (*E*)-1-(4-(aminophenyl)-3-(naphthalen-1-yl)prop-2-en-1-one.

Table 17 ^{1}H NMR of compound **TKD2**

Position	δ_H (ppm), *mult*, *J* (Hz)
NH_2	6.19, *s*
2, 6	8.27, *d*, 8.4 Hz
3, 5	6.64, *d*, 8.4 Hz
1'	7.93, *d*, 15.3 Hz
2'	8.45, *d*, 15.3 Hz
2"	7.55-7.68, *m*
3"	8.02, *t*, 7.2 Hz
4"	7.55-7.68, *m*
5"	7.98, *d*, 7.2 Hz
6"	7.55-7.68, *m*
7"	7.55-7.68, *m*
8"	8.18, *d*, 7.2 Hz

3.1.11 (*E*)-1-(4-(aminophenyl)-3-(naphthalen-2-yl)prop-2-en-1-one (TKD3)

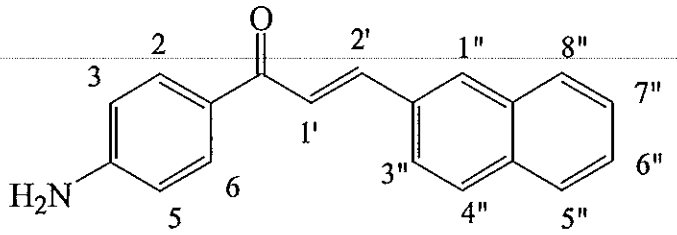

(TKD3)

Compound **TKD3** was obtained as a yellow solid (79% yield), mp. 143-144 °C. The UV-Vis absorption bands **(Figure 81)** were shown at 246.25, 285.35 and 340.94 nm. The FT-IR spectrum of **TKD3** **(Figure 80)** revealed the stretching vibration of aromatic C-H at 2400 cm^{-1}. The strong peak of C=O stretching vibration was observed at 1602 $cm^{-1}$and C=C stretching vibration in aromatic ring at 1298 cm^{-1}. The N-H stretching vibration was observed at 3339 cm^{-1}.

The ^{1}H NMR spectrum of **TKD3** **(Figure 79**, see **Table 18)** showed two *doublet* signals of equivalent protons H-2", H-6" and H-3", H-5" at δ8.27 (2H, *d*, *J* = 8.4 Hz) and δ6.64 (2H, *d*, *J* = 8.4 Hz), respectively. Signal of *trans* protons H-1' and H-2' appeared at δ7.80 (1H, *d*, *J* = 15.3 Hz) and δ8.10 (1H, *d*, *J* = 15.3 Hz), respectively. Resonances of aromatic protons of naphthalenyl part H-1" to H-8" were shown at δ7.30 (1H, *s*), δ7.12 (1H, *d*, *J* = 7.2 Hz), δ7.40 (1H, *d*, *J* = 7.2 Hz), δ7.90 (1H, *d*, *J* = 7.2 Hz), δ7.50-7.60 (H-6, H-7, *m*) and δ8.00 (1H, *d*, *J* = 7.2 Hz), respectively. The singlet signals at δ6.19 (2H) was assigned as NH_2. These spectroscopic data confirmed that **TKD3** is (*E*)-1-(4-(aminophenyl)-3-(naphthalen-2-yl)prop-2-en-1-one.

Table 18 ^{1}H NMR of compound **TKD3**

Position	δ_H (ppm), *mult*, *J* (Hz)
NH_2	6.19, *s*
2, 6	8.27, *d*, 8.4 Hz
3, 5	6.64, *d*, 8.4 Hz
1'	7.80, *d*, 15.3 Hz
2'	8.10, *d*, 15.3 Hz
1"	7.30, *s*
3"	7.12, *d*, 7.2 Hz
4"	7.40, *d*, 7.2 Hz
5"	7.90, *d*, 7.2 Hz
6"	7.50-7.60, *m*
7"	7.50-7.60, *m*
8"	8.00, *d*, 7.2 Hz

The crystal structure and packing of **TKD3** is illustrated in **Figures 18** and **19**. The crystal and experiment data are given in **Table 19**. Bond lengths and angles are shown in **Table 20**. The X-ray study shows that the TKB3 crystallized out in non-centrosymmetric space group $P2_12_12_1$.

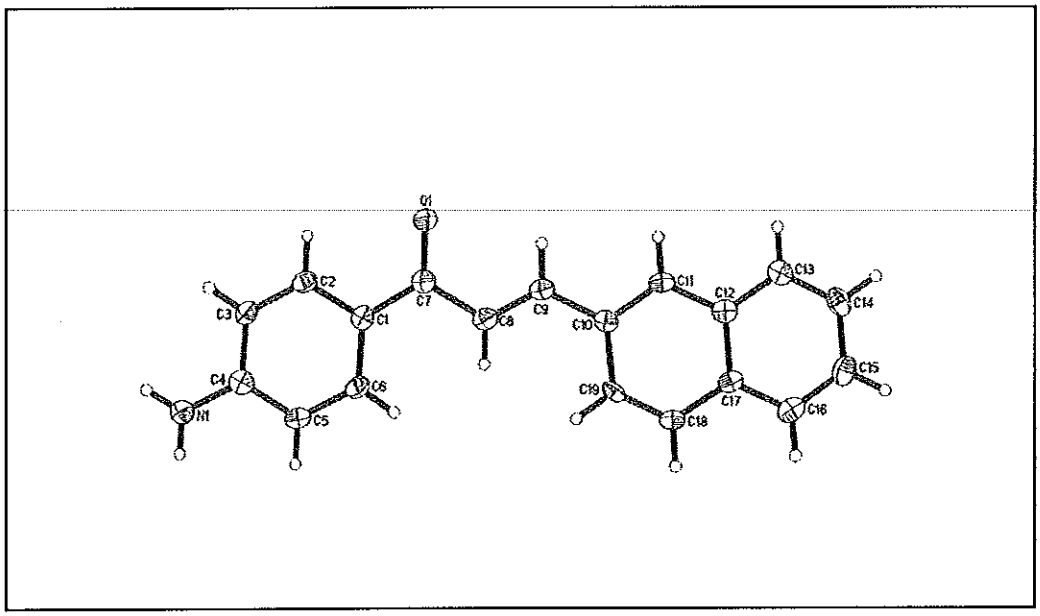

Figure 18 X-ray ORTEP diagram of the compound **TKD3**

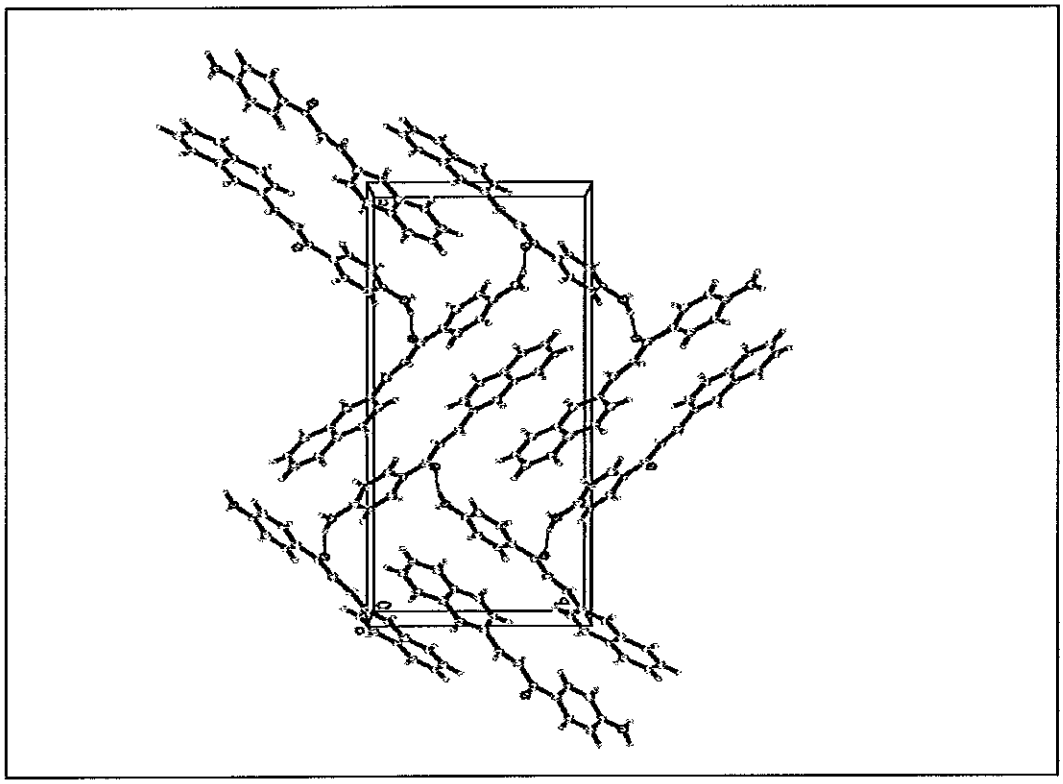

Figure 19 Packing diagram of **TKD3** viewed down the *a* axis with H-bonds shown as dashed lines.

Table 19 Crystal data and structure refinement for **TKD3**

.

Identification code	**TKD3**
Empirical formula	$C_{19}H_{15}NO$
Formula weight	273.32
Temperature	100.0(1) K
Wavelength	0.71073 Å
Crystal system, space group	Orthorhombic, $P2_12_12_1$
Unit cell dimensions	a = 5.7422(6) Å α = (90) ° b = 9.8022(10) Å β = (90) ° c = 25.504(3) Å γ = (90) °
Volume	1435.5(3) $Å^3$
Z, Calculated density	4, 1.265 Mg/m^3
Absorption coefficient	0.078 mm^{-1}
F(000)	576
Crystal size	0.32 x 0.28 x 0.07 mm
Theta range for data collection	2.23 to 27.50 deg.
Limiting indices	-6<=h<=7, -9<=k<=12, -32<=l<=33
Reflections collected / unique	8109 / 3285 [R(int) = 0.0373]
Completeness to theta = 27.50	99.7 %
Max. and min. transmission	0.9943 and 0.9755
Refinement method	Full-matrix least-squares on F^2
Data / restraints / parameters	3285 / 0 / 198
Goodness-of-fit on F^2	1.152
Final R indices [I>2σ(I)]	R1 = 0.0591, wR2 = 0.1144
R indices (all data)	R1 = 0.0764, wR2 = 0.1205
Largest diff. peak and hole	0.283, -0.250 $e.A^{-3}$

Table 20 Bond lengths [Å] and angles [°] for **TKD3**

O1-C7	1.238(3)	N1-C4	1.357(3)
N1-H2N1	0.85(3)	N1-H1N1	0.90(3)
C1-C2	1.401(3)	C1-C6	1.411(4)
C1-C7	1.480(3)	C2-C3	1.375(4)
C2-H2A	0.9300	C3-C4	1.411(4)
C3-H3A	0.9300	C4-C5	1.402(3)
C5-C6	1.374(4)	C5-H5A	0.9300
C6-H6A	0.9300	C7-C8	1.480(4)
C8-C9	1.328(3)	C8-H8A	0.9300
C9-C10	1.461(3)	C9-H9A	0.9300
C10-C11	1.389(3)	C10-C19	1.425(4)
C11-C12	1.413(3)	C11-H11A	0.9300
C12-C13	1.421(3)	C12-C17	1.430(4)
C13-C14	1.362(4)	C13-H13A	0.9300
C14-C15	1.412(4)	C14-H14A	0.9300
C15-C16	1.367(4)	C15-H15A	0.9300
C16-C17	1.413(4)	C16-H16A	0.9300
C17-C18	1.419(3)	C18-C19	1.354(3)
C18-H18A	0.9300	C19-H19A	0.9300
C4-N1-H2N1	119(2)	C4-N1-H1N1	123.2(19)
H2N1-N1-H1N1	118(3)	C2-C1-C6	117.4(2)
C2-C1-C7	119.1(2)	C6-C1-C7	123.5(2)
C3-C2-C1	121.7(3)	C3-C2-H2A	119.2
C1-C2-H2A	119.2	C2-C3-C4	120.6(2)
C2-C3-H3A	119.7	C4-C3-H3A	119.7
N1-C4-C5	121.5(3)	N1-C4-C3	120.6(2)
C5-C4-C3	117.9(2)	C6-C5-C4	121.2(2)
C6-C5-H5A	119.4	C4-C5-H5A	119.4
C5-C6-C1	121.2(2)	C5-C6-H6A	119.4
C1-C6-H6A	119.4	O1-C7-C1	121.1(2)

Table 20 Bond lengths [Å] and angles [°] for **TKD3** (continued)

O1-C7-C8	119.6(2)	C1-C7-C8	119.4(2)
C9-C8-C7	121.7(2)	C9-C8-H8A	119.2
C7-C8-H8A	119.2	C8-C9-C10	126.6(2)
C8-C9-H9A	116.7	C10-C9-H9A	116.7
C11-C10-C19	118.0(2)	C11-C10-C9	119.7(2)
C19-C10-C9	122.3(2)	C10-C11-C12	122.0(2)
C10-C11-H11A	119.0	C12-C11-H11A	119.0
C11-C12-C13	122.7(2)	C11-C12-C17	118.9(2)
C13-C12-C17	118.4(2)	C14-C13-C12	120.9(3)
C14-C13-H13A	119.6	C12-C13-H13A	119.6
C13-C14-C15	120.5(3)	C13-C14-H14A	119.7
C15-C14-H14A	119.7	C16-C15-C14	120.3(3)
C16-C15-H15A	119.8	C14-C15-H15A	119.8
C15-C16-C17	120.7(3)	C15-C16-H16A	119.6
C17-C16-H16A	119.6	C16-C17-C18	122.8(2)
C16-C17-C12	119.1(2)	C18-C17-C12	118.1(2)
C19-C18-C17	121.7(2)	C19-C18-H18A	119.2
C17-C18-H18A	119.2	C18-C19-C10	121.4(2)
C18-C19-H19A	119.3	C10-C19-H19A	119.3

3.1.12 (*E*)-1-(4-(aminophenyl)-3-(thiophen-2-yl)prop-2-en-1-one (TKD6)

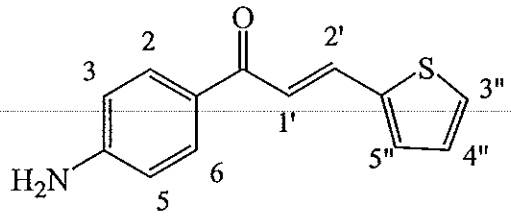

(TKD6)

Compound **TKD6** was obtained as a yellow solid (84% yield), mp. 105-106°C. The UV-Vis absorption bands (**Figure 84**) were shown at 244.58 and 360.81 nm. The FT-IR spectrum of **TKD6** (**Figure 83**) revealed the stretching vibration of aromatic C-H at 2400 cm^{-1}. The strong peak of C=O stretching vibration was observed at 1597 $cm^{-1}$and C=C stretching vibration in aromatic ring at 1437 cm^{-1}. The N-H stretching vibration was observed at 3342 cm^{-1} and C-H *trans* bending was observed at 1021 cm^{-1}.

The ^{1}H NMR spectrum of **TKD6** (**Figure 82**, see **Table 21**) showed two *doublet* signals of equivalent protons H-2, H-6 and H-3, H-5 at δ7.67 (2H, *d*, *J* = 8.1 Hz) and δ6.50 (2H, *d*, *J* = 8.1 Hz), respectively. Signal of *trans* protons H-1' and H-2' appeared at δ7.20 (1H, *d*, *J* = 15.3 Hz) and δ7.65 (1H, *d*, *J* = 15.3 Hz), respectively. The doublet signal at δ7.23 (1H, *d*, *J* = 8.7 Hz) and δ7.12 (1H, *d*, *J* = 8.7 Hz) were assigned as H-3" and H-5", respectively. The *triplet* signal at δ6.90 (1H, *t*, *J* = 8.7 Hz) was H-4". The *singlet* signal of NH_2 was observed at δ6.19 (2H, *s*). These spectroscopic data confirmed that **TKD6** is (*E*)-1-(4-(aminophenyl)-3-(thiophen-2-yl)prop-2-en-1-one.

Table 21 ^{1}H NMR of compound **TKD6**

Position	δ_H (ppm), *mult*, *J* (Hz)
NH_2	5.00, *s*
2, 6	7.67, *d*, 8.1 Hz
3, 5	6.50, *d*, 8.1 Hz
1'	7.20, *d*, 15.3 Hz
2'	7.65, *d*, 15.3 Hz
3"	7.23, *d*, 8.7 Hz
4"	6.90, *t*, 8.7 Hz
5"	7.12, *d*, 8.7 Hz

The molecule of the heteroaryl chalcone (**Figure 20**) exists in an *E* configuration with respect to the C8=C9 double bond [1.346 (3) Å], with C7—C8—C9—C10 torsion angle of 179.1 (2)°. The molecule is essentially planar as indicated by the dihedral angle between thiophene (C10–C13/S1) and 4-aminophenyl rings of 3.1 (2)°. Bond distances and angles show normal values and are comparable with those observed in closely related structures (Fun *et al.*, 2009; Suwunwong *et al.*, 2009). In the crystal, molecules are linked into chains along the *b* axis through N—H···O hydrogen bonds (**Figure 21 and Table 24**). The chains are interlinked via N—H···π interactions (**Table 24**) involving the C10-C13/S1 ring.

The thiophene ring of the chalcone is disordered over two orientations with occupancies of 0.842 (3) and 0.158 (3). The same anisotropic displacement parameters were used for atoms pairs C12A/C11, C11A/C12 and C13A/C13. Atoms S1A, C11A, C12A, C13A and C10 were restrained to be coplanar. The ethanol solvent molecule is also disordered over two positions across a center of symmetry. Their occupanicies were initially refined to 0.248 (5) and 0.242 (5) and later both were fixed at 0.25. Both disorder components were refined isotropically. The C—O, C—C and O···C distances were restrained to 1.42 (1), 1.51 (1) and 2.43 (1) Å, respectively. All H atoms were placed in calculated positions, with N-H = 0.86 Å, C-

H = 0.93-0.97 Å. The *U*iso values were constrained to be 1.5*U*eq of the carrier atom for methyl and hydroxyl H atoms and 1.2*U*eq(C) for the remaining H atoms. A rotating group model was used for the methyl groups. The highest residual electron density peak is located at 0.96 Å from H2B and the deepest hole is located at 0.30 Å from H14B. The final difference density features indicate that the solvent molecule may be disordered over multiple sites.

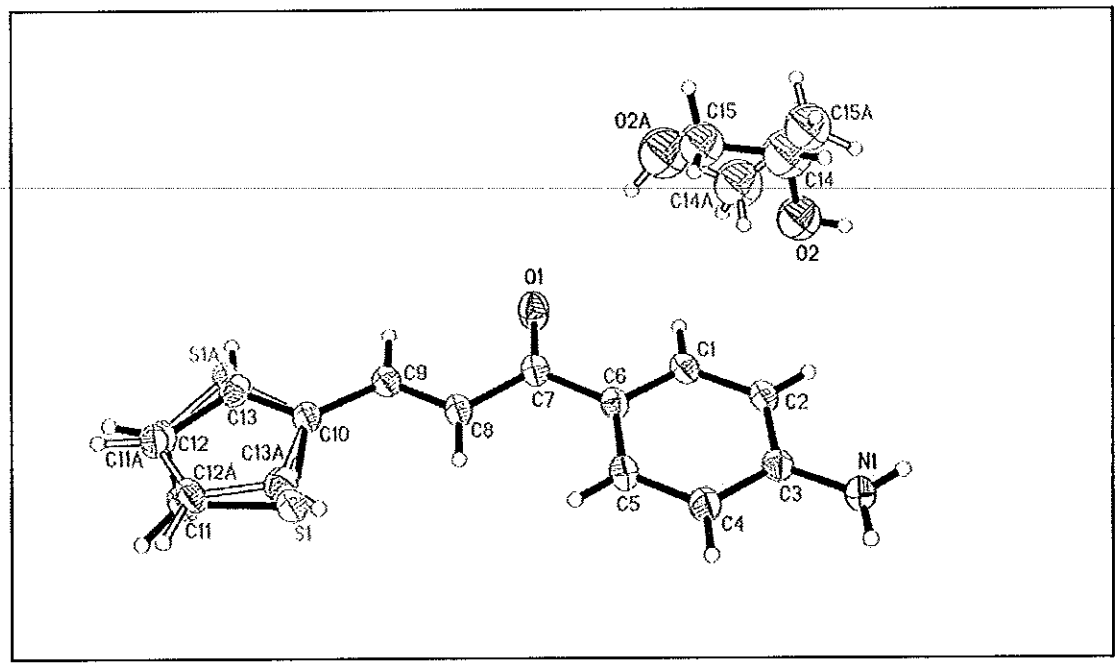

Figure 20 X-ray ORTEP diagram of the compound **TKD6**

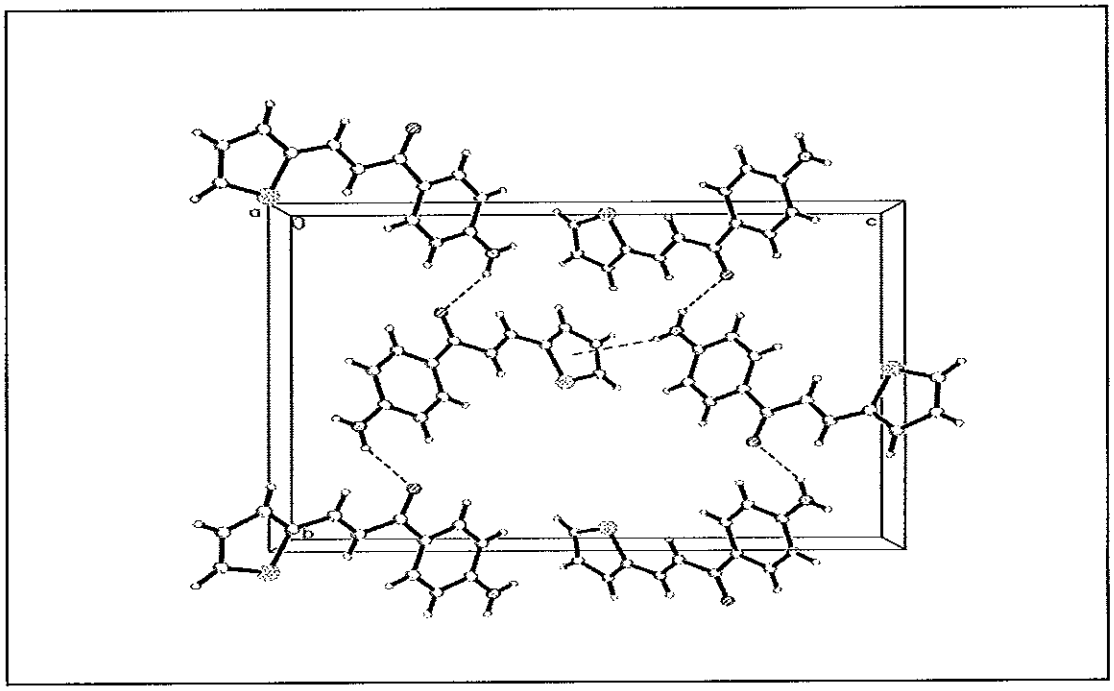

Figure 21 Packing diagram of **TKD6** viewed down the *a* axis with H-bonds shown as dashed lines.

Table 22 Crystal data and structure refinement for **TKD6**.

Identification code	**TKD6**
Empirical formula	$C_{13}H_{11}NOS$
Formula weight	252.32
Temperature	100.0(1) K
Wavelength	0.71073 Å
Crystal system, space group	Orthorhombic, $P2_12_12_1$
Unit cell dimensions	a = 5.14130(10) Å α = (90)° b = 13.9754(2) Å β = (90) ° c = 18.2647(2) Å γ = (90)°
Volume	1312.35(3) $Å^3$
Z, Calculated density	4, 1.277 Mg/m^3
Absorption coefficient	0.235 mm^{-1}
F(000)	532
Crystal size	0.56 x 0.22 x 0.17 mm
Theta range for data collection	1.83 to 31.08 deg.
Limiting indices	-7<=h<=7, -20<=k<=15, -26<=l<=24
Reflections collected / unique	22258 / 4225 [R(int) = 0.0264]
Completeness to theta = 31.02	99.9 %
Max. and min. transmission	0.9610 and 0.8794
Refinement method	Full-matrix least-squares on F^2
Data / restraints / parameters	4225 / 136 / 197
Goodness-of-fit on F^2	1.088
Final R indices [I>2σ(I)]	R1 = 0.0593, wR2 = 0.1947
R indices (all data)	R1 = 0.0633, wR2 = 0.2002
Largest diff. peak and hole	1.045, -0.286e.A^{-3}

Table 23 Bond lengths [Å] and angles [°] for **TKD6**

O1-C7	1.243(3)	N1-C3	1.364(3)
N1-H1B	0.8600	N1-H1C	0.8600
C1-C2	1.386(3)	C1-C6	1.398(3)
C1-H1A	0.9300	C2-C3	1.410(3)
C2-H2A	0.9300	C3-C4	1.406(3)
C4-C5	1.387(3)	C4-H4A	0.9300
C5-C6	1.406(3)	C5-H5A	0.9300
C6-C7	1.475(3)	C7-C8	1.475(3)
C8-C9	1.346(3)	C8-H8A	0.9300
C9-C10	1.444(3)	C9-H9A	0.9300
C10-C13	1.362(5)	C10-C13X	1.377(16)
C10-S1X	1.709(7)	C10-S1	1.723(2)
S1-C11	1.711(4)	C11-C12	1.384(5)
C11-H11A	0.9300	C12-C13	1.415(8)
C12-H12A	0.9300	C13-H13A	0.9300
S1X-C11X	1.699(19)	C11X-C12X	1.384(16)
C11X-H11B	0.9300	C12X-C13X	1.399(19)
C12X-H12B	0.9300	C13X-H13B	0.9300
O2-C14	1.358(9)	O2-H2B	0.8200
O2-H15D	1.0087	C14-C15	1.510(9)
C14-H14A	0.9700	C14-H14B	0.9700
C14-H14C	1.0303	C14-H14D	1.5472
C14-H15D	1.1079	C15-H15A	0.9600
C15-H15B	0.9600	C15-H15C	0.9600
C15-H2AA	1.3075	C15-H14C	0.6487
C15-H14D	1.2498	O2A-C14A	1.368(9)
O2A-C15A	1.40(2)	O2A-H2AA	0.8216
C14A-C15A	1.52(2)	C14A-C15A	1.532(9)
C14A-H14C	0.9601	C14A-H14D	0.9600

Table 23 Bond lengths [Å] and angles [°] for **TKD6** (continued)

C15A-O2A	1.40(2)	C15A-C14A	1.52(2)
C15A-H15D	0.9600	C15A-H15E	0.9601
C15A-H15F	0.9600	C3-N1-H1B	120.0
C3-N1-H1C	120.0	H1B-N1-H1C	120.0
C2-C1-C6	121.89(19)	C2-C1-H1A	119.1
C6-C1-H1A	119.1	C1-C2-C3	120.06(19)
C1-C2-H2A	120.0	C3-C2-H2A	120.0
N1-C3-C4	120.9(2)	N1-C3-C2	120.7(2)
C4-C3-C2	118.3(2)	C5-C4-C3	121.0(2)
C5-C4-H4A	119.5	C3-C4-H4A	119.5
C4-C5-C6	120.8(2)	C4-C5-H5A	119.6
C6-C5-H5A	119.6	C1-C6-C5	118.0(2)
C1-C6-C7	118.46(19)	C5-C6-C7	123.58(19)
O1-C7-C8	120.24(19)	O1-C7-C6	120.41(19)
C8-C7-C6	119.34(18)	C9-C8-C7	121.8(2)
C9-C8-H8A	119.1	C7-C8-H8A	119.1
C8-C9-C10	125.1(2)	C8-C9-H9A	117.5
C10-C9-H9A	117.5	C13-C10-C13X	101.6(10)
C13-C10-C9	128.0(3)	C13X-C10-C9	129.6(9)
C13-C10-S1X	9.2(4)	C13X-C10-S1X	110.2(9)
C9-C10-S1X	119.9(3)	C13-C10-S1	110.4(3)
C13X-C10-S1	11.5(12)	C9-C10-S1	121.64(16)
S1X-C10-S1	118.4(3)	C11-S1-C10	92.06(19)
C12-C11-S1	112.3(4)	C12-C11-H11A	123.9
S1-C11-H11A	123.9	C11-C12-C13	110.5(4)
C11-C12-H12A	124.7	C13-C12-H12A	124.7
C10-C13-C12	114.8(4)	C10-C13-H13A	122.6
C12-C13-H13A	122.6	C11X-S1X-C10	92.9(9)

Table 23 Bond lengths [Å] and angles [°] for **TKD6** (continued)

C12X-C11X-S1X	111.3(16)	C12X-C11X-H11B	124.4
S1X-C11X-H11B	124.4	C11X-C12X-C13X	111.8(18)
C11X-C12X-H12B	124.1	C13X-C12X-H12B	124.1
C10-C13X-C12X	113.8(15)	C10-C13X-H13B	123.1
C12X-C13X-H13B	123.1	C14-O2-H2B	109.5
C14-O2-H15D	53.4	H2B-O2-H15D	56.8
O2-C14-C15	153.9(19)	O2-C14-H14A	98.0
C15-C14-H14A	98.0	O2-C14-H14B	98.0
C15-C14-H14B	98.0	H14A-C14-H14B	103.7
O2-C14-H14C	139.2	C15-C14-H14C	20.1
H14A-C14-H14C	91.5	H14B-C14-H14C	118.1
O2-C14-H14D	140.3	C15-C14-H14D	48.2
H14A-C14-H14D	111.0	H14B-C14-H14D	50.1
H14C-C14-H14D	68.4	O2-C14-H15D4	7.0
C15-C14-H15D	157.3	H14A-C14-H15D	79.9
H14B-C14-H15D	61.1	H(4C-C14-H15D	170.7
H14D-C14-H15D	111.1	C14-C15-H2AA	167.0
H15A-C15-H2AA	81.0	H15B-C15-H2AA	58.7
H15C-C15-H2AA	72.6	C14-C15-H14C	33.2
H15A-C15-H14C	106.1	H15B-C15-H14C	136.6
H15C-C15-H14C	80.4	H2AA-C15-H14C	152.9
C14-C15-H14D	67.4	H15A-C15-H14D	100.5
H15B-C15-H14D	49.3	H15C-C15-H14D	148.6
H2AA-C15-H14D	103.8	H14C-C15-H14D	100.5
C14A-O2A-C15A	66.7(11)	C14A-O2A-H2AA	118.5
C15A-O2A-H2AA	158.8	O2A-C14A-C15A	57.7(10)
O2A-C14A-C15A	166.8(19)	C15A-C14A-C15A	114.6(12)

Table 23 Bond lengths [Å] and angles [°] for **TKD6** (continued)

O2A-C14A-H14C	90.4	C15A-C14A-H14C	140.2
C15A-C14A-H14C	91.2	O2A-C14A-H14D	94.9
C15A-C14A-H14D	102.3	C15A-C14A-H14D	97.4
H14C-C14A-H14D	103.7	O2A-C15A-C14A	55.6(8)
O2A-C15A-C14A	124.8(14)	C14A-C15A-C14A	178.4(14)
O2A-C15A-H15D	111.4	C14A-C15A-H15D	65.4
C14A-C15A-H15D	115.2	O2A-C15A-H	79.5
C14A-C15A-H15E	68.6	C14A-C15A-H15E	109.8
H15D-C15A-H15E	109.5	O2A-C15A-H15F	31.8
C14A-C15A-H15F	77.9	C14A-C15A-H15F	103.2
H15D-C15A-H15F	109.5	H15E-C15A-H15F	109.5

Table 24 Hydrogen-bond geometry (Å,°)

D—H···*A*	D—H	H···*A*	D···*A*	D—H···*A*
N1—H1A···O1^{i}	0.86	2.16	2.931 (3)	149
N1—H1B···Cg1^{ii}	0.86	2.80	3.597 (3)	156
Symmetry codes: (i) $-x+1/2, y+1/2, z-1/2$; (ii) $x, y-1, z$.				

3.1.13 (*E*)-1-(4-(aminophenyl)-3-(pyridin-3-yl)prop-2-en-1-one (TKD8)

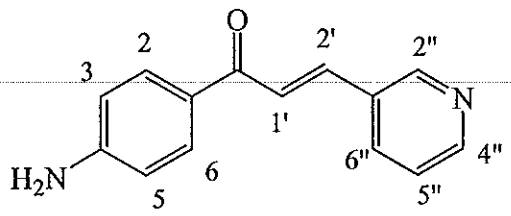

(TKD8)

Compound **TKD8** was obtained as a yellow solid (68% yield), mp. 180-181 °C. The UV-Vis absorption bands **(Figure 87)** were shown at 244.58 and 335.97 nm. The FT-IR spectrum of **TKD8 (Figure 86)** revealed the stretching vibration of aromatic C-H at 2367 cm^{-1}. The strong peak of C=O stretching vibration was observed at 1605 $cm^{-1}$and C=N stretching vibration in aromatic ring at 1416 cm^{-1}. The N-H stretching vibration was observed at 3345 cm^{-1}. The strong peak C=C stretching was appeared at 1235 cm^{-1}.

The ^{1}H NMR spectrum of **TKD8 (Figure 85**, see **Table 25)** showed two *doublet* signals of equivalent protons H-2, H-6 and H-3, H-5 at δ7.90 (2H, *d*, *J* = 8.1 Hz) and δ6.63 (2H, *d*, *J* = 8.1 Hz), respectively. Signal of *trans* protons H-1' and H-2' appeared at δ7.62 (1H, *d*, *J* = 15.9 Hz) and δ8.01 (1H, *d*, *J* = 15.9 Hz), respectively. The signal at δ7.95 (1H, *bd*, *J* = 1.0 Hz), δ8.59 (1H, *d*, *J* = 8.7 Hz) and δ8.30 (1H, *d*, *J* = 8.7 Hz) were assigned as H-2", H-4" and H-6", respectively. The doublet of doublet signal at δ7.48 (1H, *dd*, *J* = 8.7, 2.3 Hz) was H-5". The *singlet* signal of NH_2 was observed at δ6.19 (2H, *s*). These spectroscopic data confirmed that **TKD8** is (*E*)-1-(4-(aminophenyl)-3-(pyridin-3-yl)prop-2-en-1-one.

Table 25 ^{1}H NMR of compound **TKD8**

Position	δ_H (ppm), *mult*, *J* (Hz)
NH_2	6.20, *s*
2, 6	7.95, *d*, 8.1 Hz
3, 5	6.63, *d*, 8.1 Hz
1'	7.62, *d*, 15.9 Hz
2'	8.01, *d*, 15.9 Hz
2"	7.95, *bd*, 1.0 Hz
4"	8.59, *d*, 8.7 Hz
5"	7.48, *dd*, 8.7, 2.3 Hz
6"	8.30, *d*, 8.7 Hz

The crystal structure and packing of **TKD8** is illustrated in **Figures 22** and **23**. The crystal and experiment data are given in **Table 26**. Bond lengths and angles were shown in **Table 27**. Compound TKD8 crystallizes in the *Pbca* space group with z = 8.

The molecule of the heteroaryl chalcone (**Figure 22**) exists in an *E* configuration with respect to the C8=C9 double bond [1.334 (19) Å], with C7—C8—C9—C10 torsion angle of -176.57(12)°. The amino twisted with the phenyl ring in which aminogroup is indicated by tosion angles C(3)-N(1)-H(1N1) = 118.9(13) and C(3)-N(1)-H(2N1) = 118.5(12). Bond distances and angles show normal values and are comparable with those observed in closely related structures (Fun *et al.*, 2010; Kobkeatthawin *et al.*, 2009). In the crystal packing as shown in **Figure 23**, molecules are linked into chains through N—H···O hydrogen bonds (**Figure 23**). The chains are crosslinked via N—H···π interactions involving the pyridine ring.

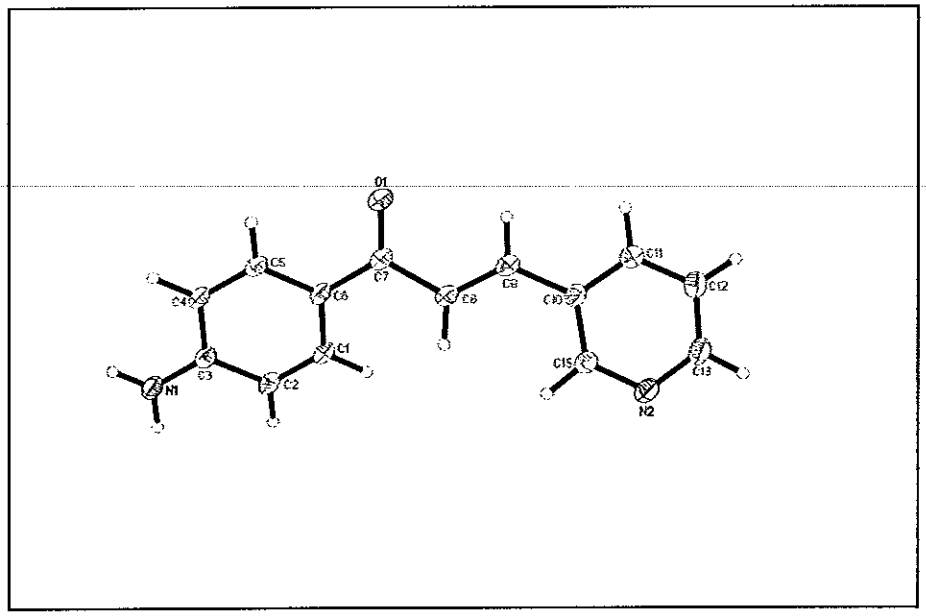

Figure 22 X-ray ORTEP diagram of the compound **TKD8**

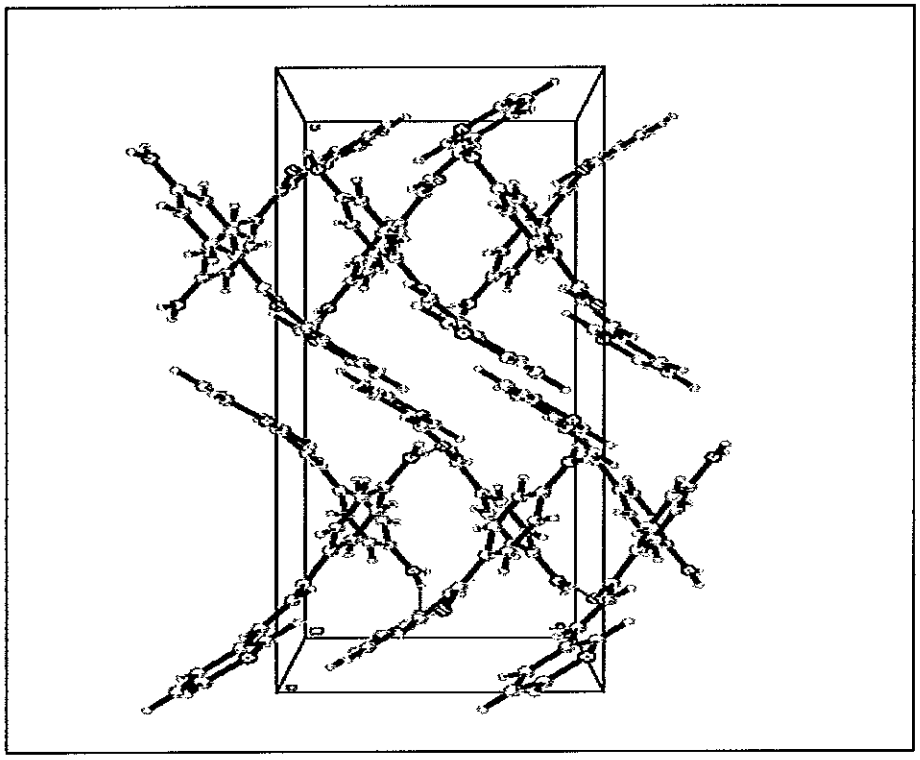

Figure 23 Packing diagram of **TKD8** viewed down the *a* axis with H-bonds shown as dashed lines.

Table 26 Crystal data and structure refinement for **TKD8**

Identification code	**TKD8**
Empirical formula	$C_{14}H_{12}N_2O$
Formula weight	224.26
Temperature	100.0(1) K
Wavelength	0.71073 Å
Crystal system, space group	Orthorhombic, *Pbca*
Unit cell dimensions	a = 12.0046(12) Å α = (90)° b = 7.9329(9) Å β = (90)° c = 22.925(3) Å γ = (90)°
Volume	2183.2(4) $Å^3$
Z, Calculated density	8, 1.365 Mg/m^3
Absorption coefficient	0.088 mm^{-1}
F(000)	944
Crystal size	0.52 x 0.32 x 0.18 mm
Theta range for data collection	2.46 to 31.28 deg.
Limiting indices	-17<=h<=15, -11<=k<=10, -33<=l<=23
Reflections collected / unique	13815 / 3553 [R(int) = 0.0454]
Completeness to theta = 31.28	99.7 %
Max. and min. transmission	0.9847 and 0.9560
Refinement method	Full-matrix least-squares on F^2
Data / restraints / parameters	3553 / 0 / 202
Goodness-of-fit on F^2	1.036
Final R indices [I>2σ(I)]	R1 = 0.0503, wR2 = 0.1260
R indices (all data)	R1 = 0.0712, wR2 = 0.1405
Largest diff. peak and hole	0.412, -0.205e.A^{-3}

Table 27 Bond lengths [Å] and angles [°] for **TKD8**

O1-C7	1.2385(15)	C10-C11	1.3927(19)
C10-C15	1.3980(18)	C10-C9	1.4665(16)
C7-C6	1.4672(18)	C7-C8	1.4901(16)
C6-C1	1.4011(17)	C6-C5	1.4094(16)
C1-C2	1.3761(18)	C1-H1A	0.997(17)
N1-C3	1.3652(17)	N1-H1N1	0.88(2)
N1-H2N1	0.92(2)	C9-C8	1.3345(19)
C9-H9A	0.993(18)	N2-C13	1.340(2)
N2-C15	1.3406(17)	C8-H8A	1.01(2)
C3-C2	1.4090(16)	C3-C4	1.4128(17)
C2-H2A	0.98(2)	C5-C4	1.3769(18)
C5-H5A	0.965(16)	C15-H15A	1.01(2)
C4-H4A	0.995(17)	C11-C12	1.3867(18)
C11-H11A	1.034(17)	C12-C13	1.379(2)
C12-H12A	0.97(2)	C13-H13A	0.989(19)
C11-C10-C15	116.88(11)	C11-C10-C9	119.88(11)
C15-C10-C9	123.24(12)	O1-C7-C6	121.70(10)
O1-C7-C8	119.70(11)	C6-C7-C8	118.60(10)
C1-C6-C5	117.42(11)	C1-C6-C7	122.55(10)
C5-C6-C7	120.03(11)	C2-C1-C6	121.88(11)
C2-C1-H1A	119.0(9)	C6-C1-H1A	119.0(9)
C3-N1-H1N1	118.9(13)	C3-N1-H2N1	118.5(12)
H1N1-N1-H2N1	121.4(18)	C8-C9-C10	127.02(11)
C8-C9-H9A	117.0(10)	C10-C9-H9A	115.9(10)
C13-N2-C15	117.16(12)	C9-C8-C7	121.19(11)
C9-C8-H8A	121.2(11)	C7-C8-H8A	117.7(11)
N1-C3-C2	120.58(11)	N1-C3-C4	121.26(11)
C2-C3-C4	118.16(12)	C1-C2-C3	120.49(11)
C1-C2-H2A	121.0(12)	C3-C2-H2A	118.5(12)

Table 27 Bond lengths [Å] and angles [°] for **TKD8** (continued)

C4-C5-C6	121.50(11)	C4-C5-H5A	118.9(9)
C6-C5-H5A	119.6(9)	N2-C15-C10	123.90(13)
N2-C15-H15A	114.7(10)	C10-C15-H15A	121.4(10)
C5-C4-C3	120.54(11)	C5-C4-H4A	120.6(10)
C3-C4-H4A	118.8(10)	C12-C11-C10	120.19(12)
C12-C11-H11A	121.3(10)	C10-C11-H11A	118.5(10)
C13-C12-C11	117.91(13)	C13-C12-H12A	120.8(11)
C11-C12-H12A	121.3(11)	N2-C13-C12	123.92(12)
N2-C13-H13A	115.2(11)	C12-C13-H13A	120.9(11)
N2-C15-C10	123.90(13)	N2-C15-H15A	114.7(10)
C10-C15-H15A	121.4(10)	C5-C4-C3	120.54(11)
C5-C4-H4A	120.6(10)	C3-C4-H4A	118.8(10)
C12-C11-C10	120.19(12)	C12-C11-H11A	121.3(10)
C10-C11-H11A	118.5(10)	C13-C12-C11	117.91(13)
C13-C12-H12A	120.8(11)	C11-C12-H12A	121.3(11)
N2-C13-C12	123.92(12)	N2-C13-H13A	115.2(11)
C12-C13-H13A	120.9(11)		

3.1.14 (*E*)-1-(4-(aminophenyl)-3-(pyridin-4-yl)prop-2-en-1-one (TKD9)

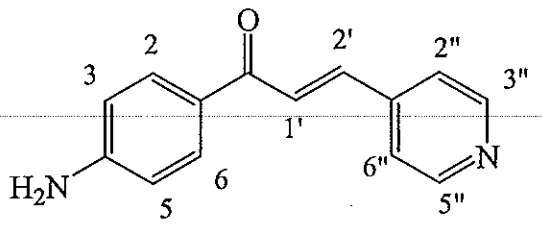

(TKD9)

Compound **TKD9** was obtained as a yellow solid (70% yield), mp. 213-214 °C. The UV-Vis absorption bands **(Figure 90)** were shown at 262.90 and 340.94 nm. The FT-IR spectrum of **TKD9** **(Figure 89)** revealed the stretching vibration of aromatic C-H at 2400 cm^{-1}. The strong peak of C=O stretching vibration was observed at 1588 $cm^{-1}$and C=C stretching vibration in aromatic ring at 1346 cm^{-1}. The N-H stretching vibration was observed at 3152 cm^{-1}.

The ^{1}H NMR spectrum of **TKD9** **(Figure 88**, see **Table 28)** showed two *doublet* signals of equivalent protons H-2, H-6 and H-3, H-5 at δ7.90 (2H, *d*, *J* = 8.7 Hz) and δ6.70 (2H, *d*, *J* = 8.7 Hz), respectively. Signal of *trans* protons H-1' and H-2' appeared at δ7.60 (1H, *d*, *J* = 15.6 Hz) and δ7.80 (1H, *d*, *J* = 15.6 Hz), respectively. Equivalent protons of 4-pyridyl unit appeared as two *doublet* signals at δ8.65 (2H, *d*, *J* = 5.7 Hz) and δ7.55 (2H, *d*, *J* = 5.7 Hz). The *singlet* signal of NH_2 was observed at δ5.45 (2H, *s*). These spectroscopic data confirmed that **TKD9** is (*E*)-1-(4-(aminophenyl)-3-(pyridin-4-yl)prop-2-en-1-one.

Table 28 ^{1}H NMR of compound **TKD9**

Position	**δ_H (ppm), *mult*, *J* (Hz)**
NH_2	5.45, *s*
2, 6	7.90, *d*, 8.7 Hz
3, 5	6.70, *d*, 8.7 Hz
1'	7.60, *d*, 15.6 Hz
2'	7.80, *d*, 15.6 Hz
2", 6"	7.55, *d*, 5.7 Hz
3", 5"	8.65, *d*, 5.7 Hz

3.1.15 (*E*)-1-(4-(aminophenyl)-3-(quinolin-4-yl)prop-2-en-1-one (TKD10)

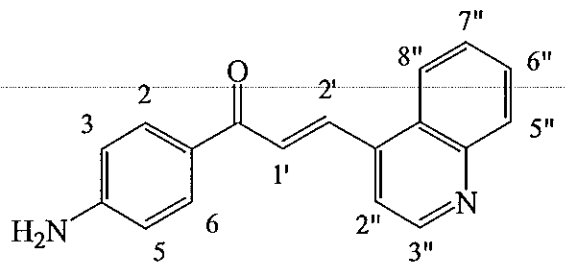

(TKD10)

Compound **TKD10** was obtained as an Orange solid (59% yield), mp. 235-236 °C. The UV-Vis absorption bands **(Figure 93)** were shown at 244.58 and 331.00 nm. The FT-IR spectrum of **TKD10 (Figure 92)** revealed the stretching vibration of aromatic C-H at 2363 cm^{-1}. The strong peak of C=O stretching vibration was observed at 1572 $cm^{-1}$and C=C stretching vibration in aromatic ring at 1340 cm^{-1}. The N-H stretching vibration was observed at 3394 cm^{-1}.

The ^{1}H NMR spectrum of **TKD10 (Figure 91,** see **Table 29)** showed two *doublet* signals of equivalent protons H-2, H-6 and H-3, H-5 at δ7.98 (2H, *d*, *J* = 8.5 Hz) and δ6.65 (2H, *d*, *J* = 8.5 Hz), respectively. Signal of *trans* protons H-1' and H-2' appeared at δ8.12 (1H, *d*, *J* = 15.6 Hz) and δ8.35 (1H, *d*, *J* = 15.6 Hz), respectively. Protons of quinoline part H-2" to H-8" were shown at δ8.28 (1H, *d*, *J* = 9.0 Hz), δ8.05-8.15 (2H, *m*, H-3", H-8"), δ8.97 (1H, *d*, *J* = 7.2 Hz), δ7.69 (1H, *t*, *J* = 7.2 Hz), δ7.83 (1H, *t*, *J* = 7.2 Hz). The *singlet* signal of NH_2 was observed at δ6.30 (2H, *s*). These spectroscopic data confirmed that **TKD10** is (*E*)-1-(4-(aminophenyl)-3-(quinolin-4-yl)prop-2-en-1-one.

Table 29 ^{1}H NMR of compound **TKD10**

Position	**δ_H (ppm), *mult*, *J* (Hz)**
NH_2	6.30, *s*
2, 6	7.98, *d*, 8.5 Hz
3, 5	6.55, *d*, 8.5 Hz
1'	8.12, *d*, 15.6 Hz
2'	8.35, *d*, 15.6 Hz
2"	8.28, *d*, 9.0 Hz
3"	8.05-8.15, *m*
5"	8.97, *d*, 7.2 Hz
6"	7.69, *t*, 7.2 Hz
7"	7.83, *t*,7.2 Hz
8"	8.05-8.15, *m*

3.1.16 (*E*)-1-(4-(aminophenyl)-3-(2,4,5-trimethoxyphenyl)prop-2-en-1-one (TKD19)

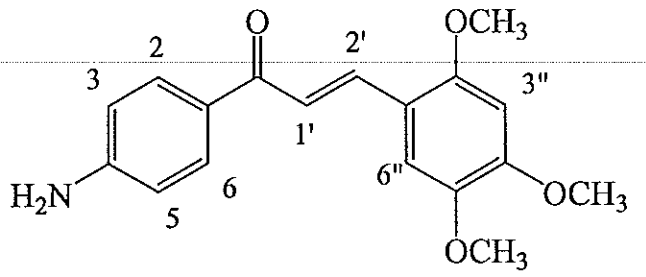

TKD19

Compound **TKD19** was obtained as an Orange solid (63% yield), mp. 207-208 °C. The UV-Vis absorption bands **(Figure 96)** were shown at 244.58, 322.71 and 379.83 nm. The FT-IR spectrum of **TKD19 (Figure 95)** revealed the stretching vibration of aromatic C-H at 2366 cm^{-1}. The strong peak of C=O stretching vibration was observed at 1600 $cm^{-1}$and C=C stretching vibration in aromatic ring at 1457 cm^{-1}. The N-H stretching vibration was observed at 3350 cm^{-1}.

The ^{1}H NMR spectrum of **TKD19 (Figure 94,** see **Table 30)** showed two *doublet* signals of equivalent protons H-2, H-6 and H-3, H-5 at δ7.90 (2H, *d*, *J* = 8.1 Hz) and δ6.67 (2H, *d*, *J* = 8.1 Hz), respectively. Signal of *trans* protons H-1' and H-2' appeared at δ7.68 (1H, *d*, *J* = 15.6 Hz) and δ7.95 (1H, *d*, *J* = 15.6 Hz), respectively. Two *singlet* signals of H-1" and H-2" were assigned as δ7.68 (1H, *s*) and δ7.45 (1H, *s*). Methoxy protons appeared at δ3.80 (3H, *s*), δ3.84 (3H, *s*) and δ3.87 (3H, *s*), respectively. The *singlet* signal of NH_2 was observed at δ6.10 (2H, *s*).These spectroscopic data confirmed that **TKD19** is (*E*)-1-(4-(aminophenyl)-3-(2,4,5-trimethoxyphenyl)prop-2-en-1-one.

Table 30 ^{1}H NMR of compound **TKD19**

Position	δ_H (ppm), *mult*, *J* (Hz)
NH_2	6.10, *s*
O-CH_3	3.80, *s*
O-CH_3	3.84, *s*
O-CH_3	3.87, *s*
2, 6	7.90, *d*, 8.1 Hz
3, 5	6.67, *d*, 8.1 Hz
1'	7.68, *d*, 15.6 Hz
2'	7.95, *d*, 15.6 Hz
1''	6.70, *s*
2''	7.45, *s*

The crystal structure and packing of **TKD19** is illustrated in **Figures 24** and **25**. The crystal and experiment data are given in **Table 31**. Bond lengths and angles were shown in **Table 32**. The Hydrogen-bond geometry was shown in **Table 33**.

Molecules of the title aminochalcone, $C_{18}H_{19}NO_4$, are twisted, with a dihedral angle of 11.26(6)° between the 4-aminophenyl and 2,4,5-trimethoxyphenyl rings. The conformations of the three methoxy groups with respect to the benzene ring are slightly different. Two methoxy groups are almost coplanar with the attached benzene ring [C—O—C—C torsion angles of —1.45 (19) and 1.5 (2)°], while the third is (—)-synclinal with the attached benzene ring [C—O—C—C = —81.36 (17)°]. In the crystal structure, molecules are stacked into columns along the b axis and molecules in adjacent columns are linked by N—H ···O hydrogen bonds into V-shaped double columns. Weak π– π interactions are also observed, with a centroidcentroid distance of 3.7532 (8) A°.

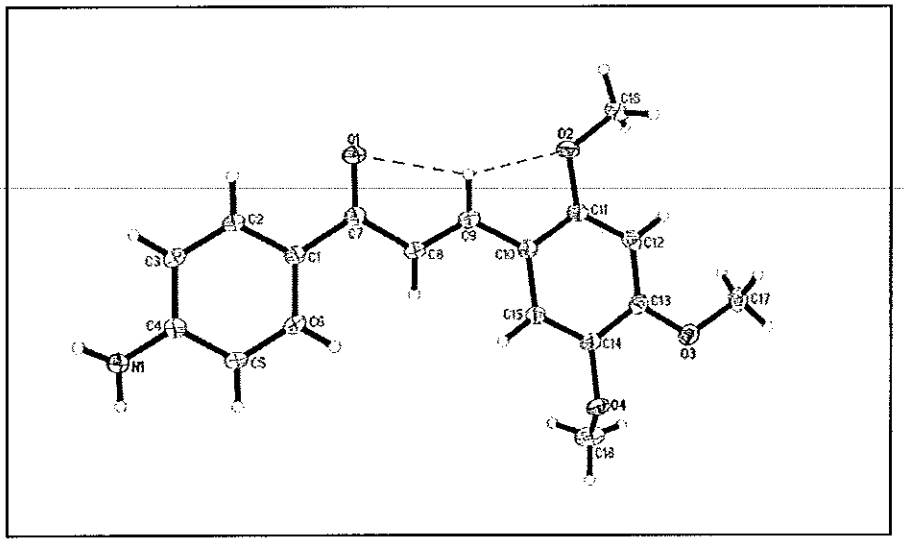

Figure 24 X-ray ORTEP diagram of the compound **TKD19**

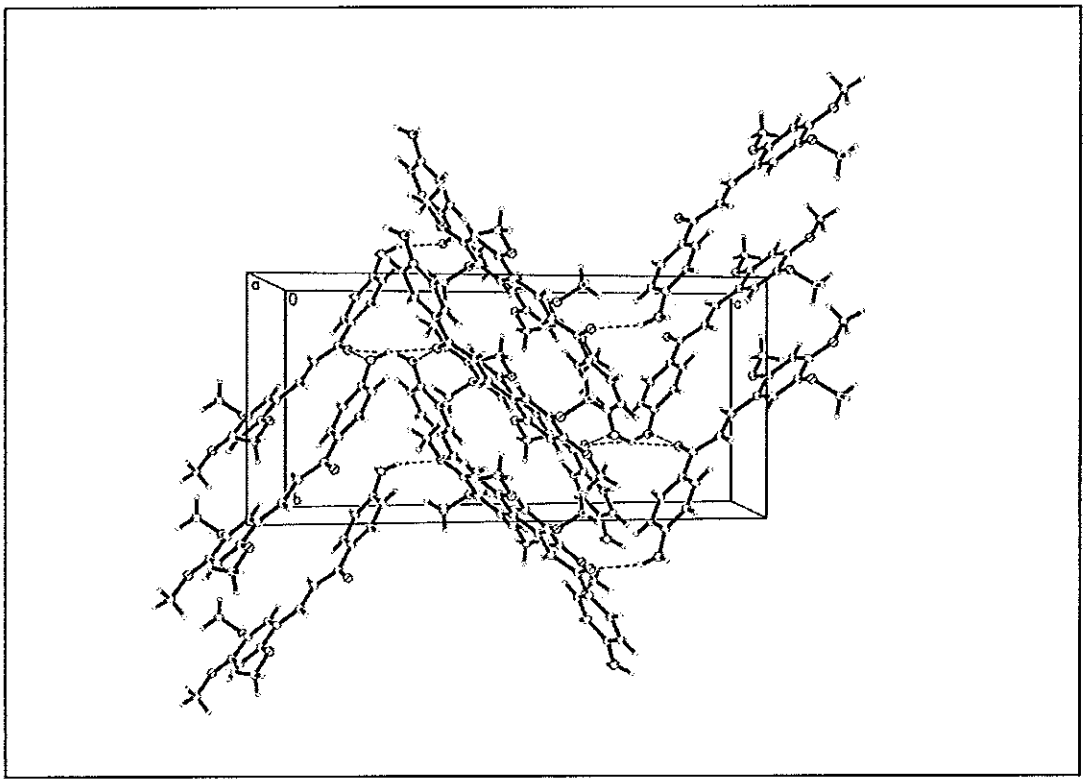

Figure 25 Packing diagram of **TKD19** viewed down the *a* axis with H-bonds shown as dashed lines.

Table 31 Crystal data and structure refinement for **TKD19**

Identification code	**TKD19**
Empirical formula	$C_{18}H_{19}N\ O_4$
Formula weight	313.34
Temperature	100.0(1) K
Wavelength	0.71073 Å
Crystal system, space group	Monoclinic, *C2/c*
Unit cell dimensions	a = 13.6117(2) Å α = (90) ° b = 10.3540(2) Å β = 100.8790(10) ° c = 22.3920(4) Å γ = (90) °
Volume	3099.11(9) $Å^3$
Z, Calculated density	8, 1.343 Mg/m^3
Absorption coefficient	0.095 mm^{-1}
F(000)	1328
Crystal size	0.38 x 0.32 x 0.10 mm
Theta range for data collection	1.85 to 30.00 deg.
Limiting indices	-19<=h<=19, -14<=k<=12, -31<=l<=31
Reflections collected / unique	19818 / 4506 [R(int) = 0.0289]
Completeness to theta = 30.00	99.9 %
Max. and min. transmission	0.9910 and 0.9647
Refinement method	Full-matrix least-squares on F^2
Data / restraints / parameters	4506 / 0 / 219
Goodness-of-fit on F^2	1.048
Final R indices [I>2σ(I)]	R1 = 0.0512, wR2 = 0.1205
R indices (all data)	R1 = 0.0676, wR2 = 0.1307
Largest diff. peak and hole	0.426, -0.228 $e.A^{-3}$

Table 32 Bond lengths [Å] and angles [°] for **TKD19**

O1-C7	1.2400(16)	O2-C11	1.3666(15)
O2-C16	1.4293(17)	O3-C13	1.3557(16)
O3-C17	1.4329(17)	O4-C14	1.3859(15)
O4-C18	1.4228(19)	N1-C4	1.3704(18)
N1-H1N1	0.862(19)	N1-H2N1	0.88(2)
C1-C6	1.4060(18)		

Table 33 Hydrogen-bond geometry (Å,°)

D—H···*A*	D—H	H···*A*	D···*A*	D—H···*A*
N1—H1A···O1^{i}	0.86(2)	2.12(2)	2.9692 (16)	170.4(17)
N1—H1B···Cg1^{ii}	0.88(2)	2.21(2)	3.0176 (17)	153.4(19)
Symmetry codes: (i) $-x+1/2, y+1/2, z-1/2$; (ii) $x, y-1, z$.				

3.1.17 (*E*)-1-(4-(aminophenyl)-3-(2,4,6-trimethoxyphenyl)prop-2-en-1-one (TKD20)

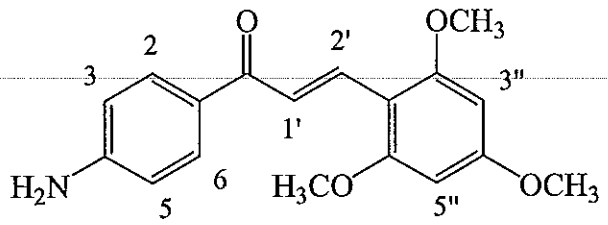

(TKD20)

Compound **TKD20** was obtained as a yellow solid (79% yield), mp. 228-229 °C. The UV-Vis absorption bands (**Figure 99**) were shown at 253.74 and 356.67 nm. The FT-IR spectrum of **TKD20** (**Figure 98**) revealed the stretching vibration of aromatic C-H at 2486 cm^{-1}. The strong peak of C=O stretching vibration was observed at 1584 $cm^{-1}$and C=C stretching vibration in aromatic ring at 1282 cm^{-1}. The N-H stretching vibration was observed at 3361 cm^{-1}.

The ^{1}H NMR spectrum of **TKD20** (**Figure 97**, see **Table 33**) showed three signals of equivalent protons H-2, H-6, H-3, H-5 and H-3", H-5" at δ7.72 (2H, *d*, *J* = 8.7 Hz), δ6.62 (2H, *d*, *J* = 8.7 Hz) and δ8.29 (2H, *s*), respectively. Signal of *trans* protons H-1' and H-2' appeared at δ7.83 (1H, *d*, *J* = 15.9 Hz) and δ7.95 (1H, *d*, *J* = 15.9 Hz), respectively. Methoxy protons appeared at δ3.90 (6H, *s*) and δ3.86 (3H, *s*). The *singlet* signal of NH_2 was observed at δ6.30 (2H, *s*).These spectroscopic data confirmed that **TKD20** is (*E*)-1-(4-(aminophenyl)-3-(2,4,6-trimethoxyphenyl)prop-2-en-1-one.

Table 34 ^{1}H NMR of compound **TKD20**

Position	**δ_H (ppm), *mult*, *J* (Hz)**
NH_2	6.30, *s*
2(O-CH_3)	3.90, *s*
O-CH_3	3.86, *s*
2, 6	7.72, *d*, 8.7 Hz
3, 5	6.62, *d*, 8.7 Hz
1'	7.83, *d*, 15.9 Hz
2'	7.95, *d*, 15.9 Hz
3", 5"	8.29, *s*

3.1.18 (*E*)-1-(4-(aminophenyl)-3-(3,4,5-trimethoxyphenyl)prop-2-en-1-one (TKD21)

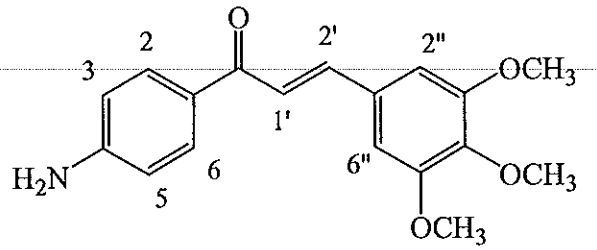

(TKD21)

Compound **TKD21** was obtained as a pale yellow solid (67% yield), mp.240-241°C. The UV-Vis absorption bands (**Figure 102**) were shown at 253.78 and 354.67 nm. The FT-IR spectrum of **TKD21** (**Figure 101**) revealed the stretching vibration of aromatic C-H at 2939 cm^{-1}. The strong peak of C=O stretching vibration was observed at 1584 $cm^{-1}$and C=C stretching vibration in aromatic ring at 1503 cm^{-1}. The N-H stretching vibration was observed at 3358 cm^{-1}.

The ^{1}H NMR spectrum of **TKD21** (**Figure 100**, see **Table 33**) showed three signals of equivalent protons H-2, H-6, H-3, H-5 and H-2", H-6" at δ7.94 (2H, *d*, *J* = 9.0 Hz), δ6.62 (2H, *d*, *J* = 9.0 Hz) and δ7.20 (2H, *s*), respectively. Signal of *trans* protons H-1' and H-2' appeared at δ7.55 (1H, *d*, *J* = 15.6 Hz) and δ7.80 (1H, *d*, *J* = 15.6 Hz), respectively. Methoxy protons appeared at δ3.69 (3H, *s*) and δ3.85 (6H, *s*). The *singlet* signal of NH_2 was observed at δ6.13 (2H, *s*).These spectroscopic data confirmed that **TKD21** is (*E*)-1-(4-(aminophenyl)-3-(3,4,5-trimethoxyphenyl)prop-2-en-1-one.

Table 35 ^{1}H NMR of compound **TKD21**

Position	**δ_H (ppm), *mult*, *J* (Hz)**
NH_2	6.13, *s*
O-CH_3	3.69, *s*
2(O-CH_3)	3.85, *s*
2, 6	7.94, *d*, 9.0 Hz
3, 5	6.62, *d*, 9.0 Hz
1'	7.55, *d*, 15.6 Hz
2'	7.80, *d*, 15.6 Hz
2", 6"	7.20, *s*

3.2 Absorption spectra and fluorescence properties of chalcones and heteroaryl chalcone derivatives

3.2.1 Absorption spectra of chalcones and heteroaryl chalcone derivatives

Absorption spectra of chalcones and heteroaryl chalcones shown in **Figures 51 (TKB1), 54 (TKB2), 57 (TKB3), 60 (TKB4), 63 (TKB5), 66, (TKB6), 69 (TKB7), 72 (TKB8), 75 (TKB9), 78 (TKD2), 81 (TKD3), 84 (TKD6), 87 (TKD8), 90 (TKD9), 93 (TKD10), 96 (TKD19), 99 (TKD20)** and **102 (TKD21)**. The summarized of absorption wavelength maxima (λ_{max}) of chalcones and heteroaryl chalcone derivatives were showed in **Table 34**. The absorption spectra of compounds have been recorded in chloroform solution with the concentration of 2.5 μM. Several absorption peaks could be observed in the wavelength range of 200-430 nm. It can be seen that the spectral shapes are similar due to their similar structures.

Table 36 Absorption spectra of chalcones and heteroaryl chalcone derivatives

Compound	Absorption maxima, λ_{max} (nm)
TKB1	258.71, 418.48
TKB2	264.68, 417.82
TKB3	274.54, 429.35
TKB4	278.70, 414.51
TKB5	254.20, 406.55
TKB6	263.73, 428.52
TKB7	278.70, 425.23
TKB8	281.19, 422.75
TKB9	276.21, 407.08
TKD2	252.91, 358.33
TKD3	246.25, 285.35, 340.94
TKD6	244.58, 360.81
TKD8	244.58, 335.97
TKD9	262.90, 340.94
TKD10	244.58, 331
TKD19	244.58, 322.71, 379.83
TKD20	253.74, 356.67
TKD21	253.78, 354.67

3.2.2 Excitation and emission spectra of chalcones and heteroaryl chalcone derivatives

In the preliminary method to study the fluorescent properties of all the synthesized compound, the pre-scan mode in fluorescence determination was selected to find the compounds which show the considerable fluorescent properties.

3.2.2.1 (*E*)-3-(4-diethylamino)phenyl)-1-phenylprop-2-en-1-one (TKB1)

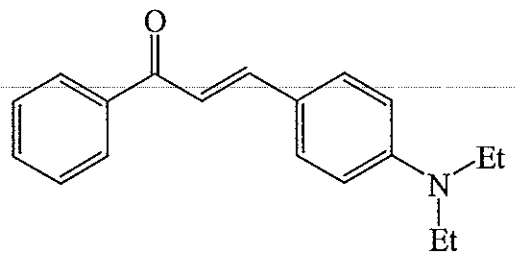

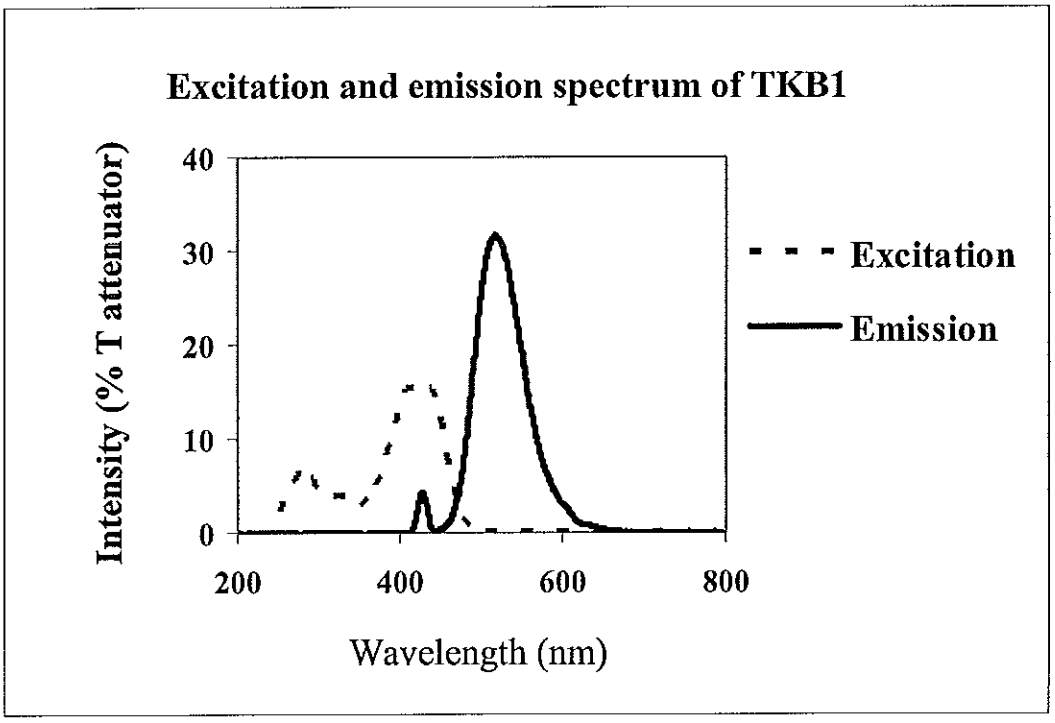

Figure 26 Excitation and emission spectrum of 2.5 μM **TKB1** in $CHCl_3$ solution at room temperature in %T attenuator mode and slit 5:10.

The pre-scan of excitation and emission fluorescence spectrum of **TKB1** was shown in **Figure 26**. Compound **TKB1** shows the fluorescent property which clearly seen in the appearance of fluorescence emission spectrum. The emission spectrum of **TKB1** was observed in the range of 450-650 nm. It was found that, in chloroform solution, **TKB1** exhibits fluorescence with the maximum emission at 513 nm when was excited at 430 nm.

3.2.2.2 (*E*)-1-(4-fluorophenyl)-3-(4-(diethylamino)phenyl)prop-2-en-1-one (TKB2)

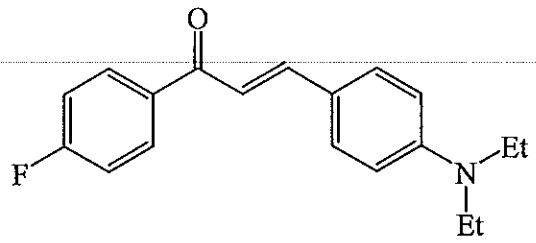

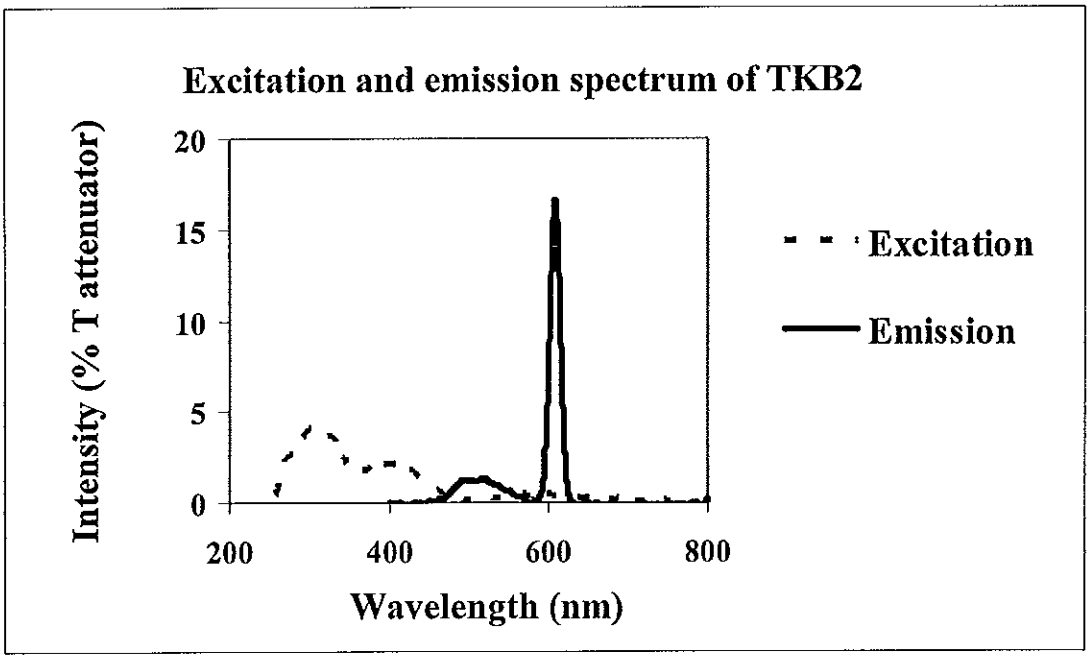

Figure 27 Excitation and emission spectrum of 2.5 μM **TKB2** in $CHCl_3$ solution at room temperature in %T attenuator mode and slit 5:10.

The pre-scan of excitation and emission fluorescence spectrum of **TKB2** was shown in **Figure 27**. Compound **TKB2** shows the fluorescent property which seen in the appearance of fluorescence emission spectrum. The emission spectrum of **TKB2** was observed in the range of 450-600 nm. It was found that, in chloroform solution, **TKB2** exhibits fluorescence with the maximum emission at 502 nm when was excited at 440 nm.

3.2.2.3 (*E*)-1-(4-chlorophenyl)-3-(4-(diethylamino)phenyl)prop-2-en-1-one (TKB3)

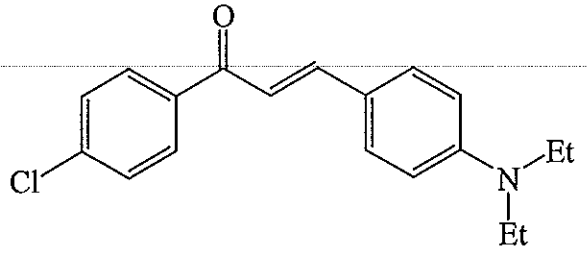

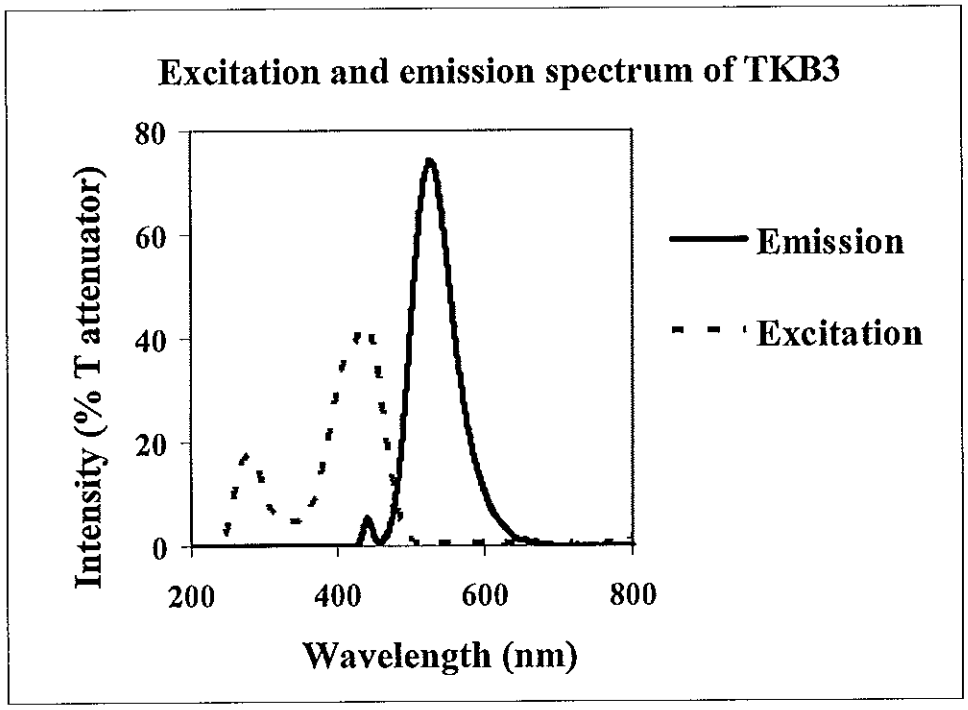

Figure 28 Excitation and emission spectrum of 2.5 μM **TKB3** in $CHCl_3$ solution at room temperature in %T attenuator mode and slit 5:10.

The pre-scan of excitation and emission fluorescence spectrum of **TKB3** was shown in **Figure 28**. Compound **TKB3** shows the fluorescent property which clearly seen in the appearance of fluorescence emission spectrum. The emission spectrum of **TKB3** was observed in the range of 460-700 nm. It was found that, in chloroform solution, **TKB3** exhibits fluorescence with the maximum emission at 527 nm when was excited at 440 nm.

3.2.2.4 (*E*)-1-(4-bromophenyl)-3-(4-(diethylamino)phenyl)prop-2-en-1-one (TKB4)

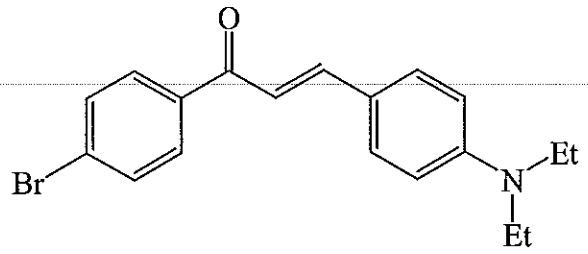

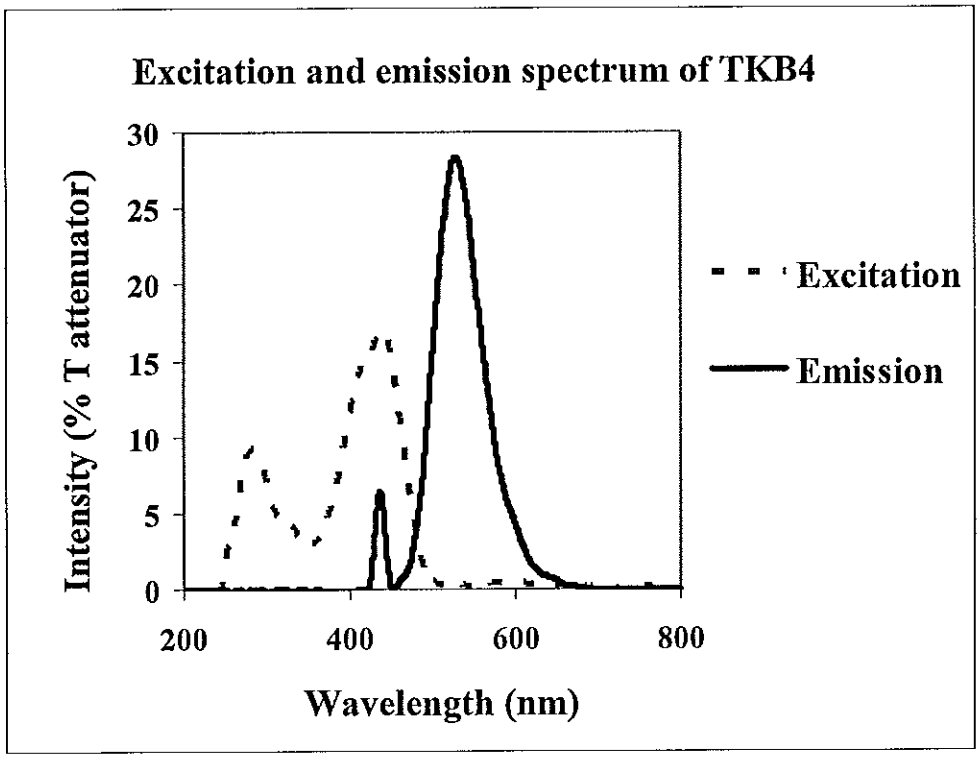

Figure 29 Excitation and emission spectrum of 2.5 μM **TKB4** in $CHCl_3$ solution at room temperature in %T attenuator mode and slit 5:10.

The pre-scan of excitation and emission fluorescence spectrum of **TKB4** was shown in **Figure 29**. Compound **TKB4** shows the fluorescent property which clearly seen in the appearance of fluorescence emission spectrum. The emission spectrum of **TKB4** was observed in the range of 460-700 nm. It was found, in chloroform solution, **TKB4** exhibits fluorescence with the maximum emission at 529 nm when was excited at 440 nm.

3.2.2.5 (*E*)-3-(4-(diethylamino)phenyl)-1-(naphthalen-1-yl)prop-2-en-1-one (TKB5)

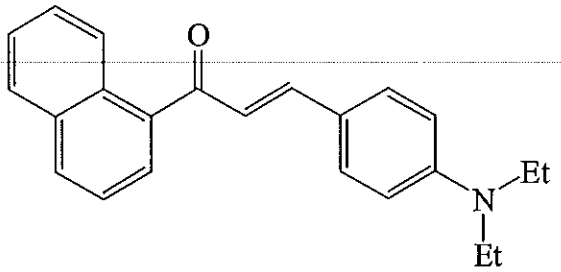

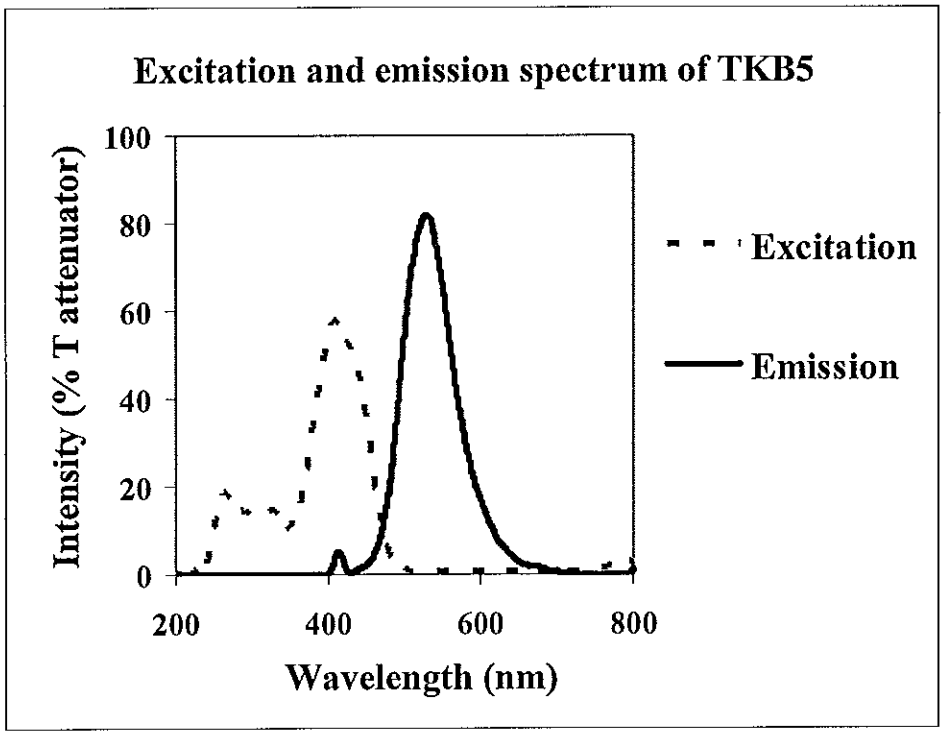

Figure 30 Excitation and emission spectrum of 2.5 μM **TKB5** in $CHCl_3$ solution at room temperature in %T attenuator mode and slit 5:10.

The pre-scan of excitation and emission fluorescence spectrum of **TKB5** was shown in **Figure 30**. Compound **TKB5** shows the fluorescent property which clearly seen in the appearance of fluorescence emission spectrum. The emission spectrum of **TKB5** was observed in the range of 460-700 nm. It was found that, in chloroform solution, **TKB5** exhibits fluorescence with the maximum emission at 528 nm when was excited at 410 nm.

3.2.2.6 (*E*)-3-(4-(diethylamino)phenyl)-1-(naphthalen-2-yl)prop-2-en-1-one (TKB6)

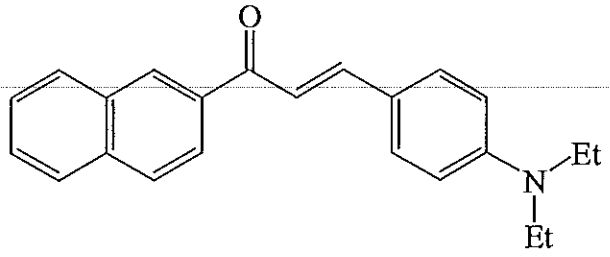

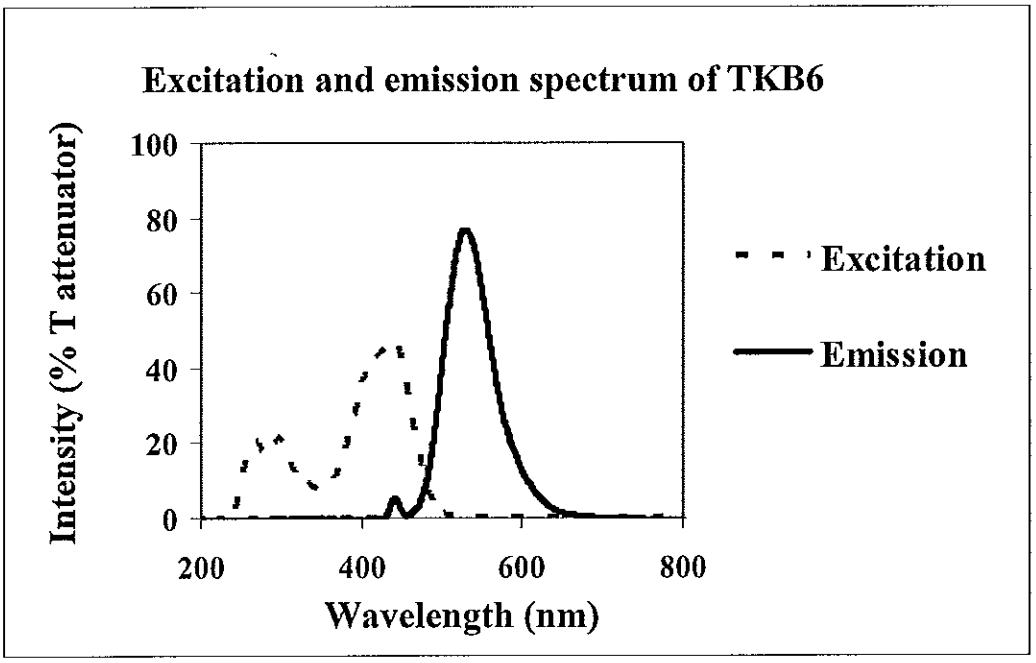

Figure 31 Excitation and emission spectrum of 2.5 μM **TKB6** in $CHCl_3$ solution at room temperature in %T attenuator mode and slit 5:10.

The pre-scan of excitation and emission fluorescence spectrum of **TKB6** was shown in **Figure 31**. Compound **TKB6** shows the fluorescent property which clearly seen in the appearance of fluorescence emission spectrum. The emission spectrum of **TKB6** was observed in the range of 460-700 nm. It was found that, in chloroform solution, **TKB6** exhibits fluorescence with the maximum emission at 530 nm when was excited at 440 nm.

3.2.2.7 (*E*)-3-(4-(diethylamino)phenyl)-1-(2-methoxyphenyl)prop-2-en-1-one (TKB7)

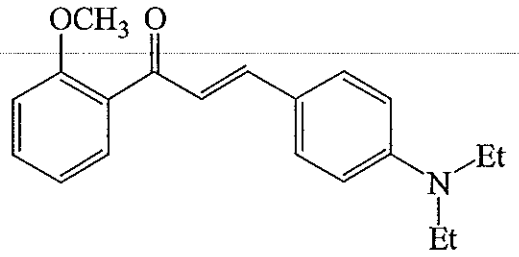

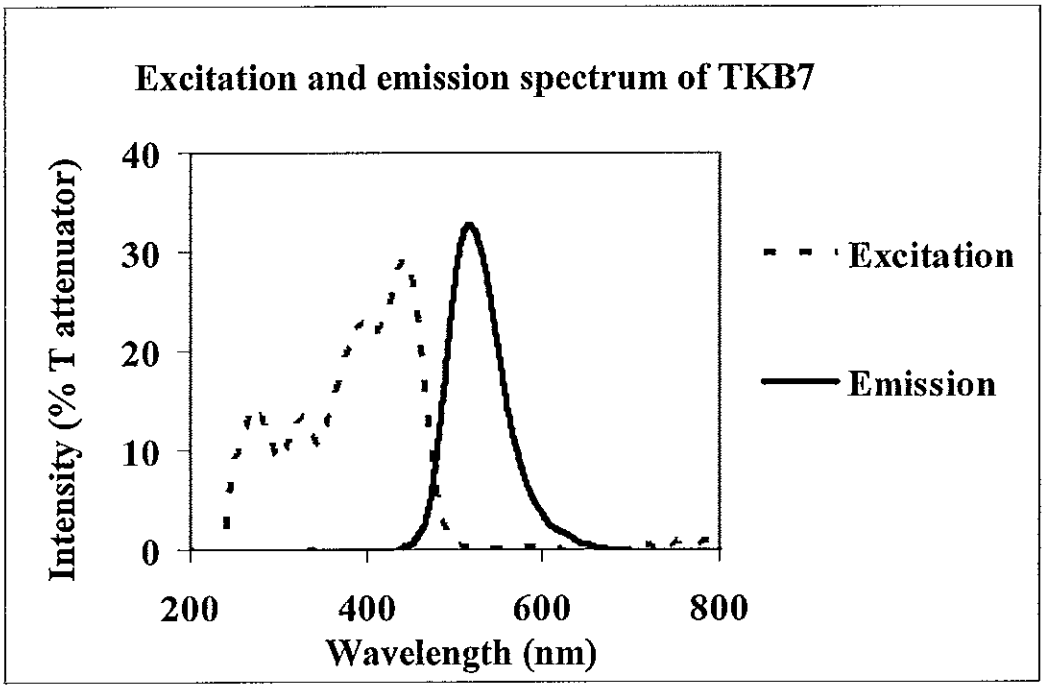

Figure 32 Excitation and emission spectrum of 2.5 μM **TKB7** in $CHCl_3$ solution at room temperature in %T attenuator mode and slit 5:10.

The pre-scan of excitation and emission fluorescence spectrum of **TKB7** was shown in **Figure 32.** Compound **TKB7** shows the fluorescent property which clearly seen in the appearance of fluorescence emission spectrum. The emission spectrum of **TKB7** was observed in the range of 450-700 nm. It was found that, in chloroform solution, **TKB7** exhibits fluorescence with the maximum emission at 517 nm when was excited at 440 nm.

3.2.2.8 (*E*)-3-(4-(diethylamino)phenyl)-1-(3-methoxyphenyl)prop-2-en-1-one (TKB8)

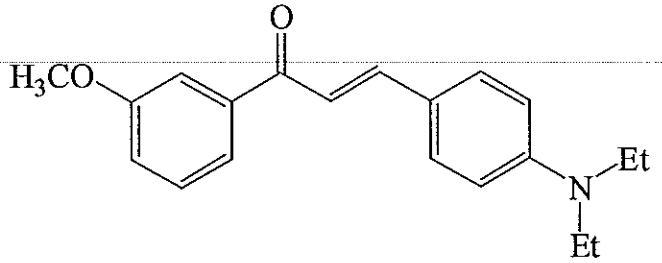

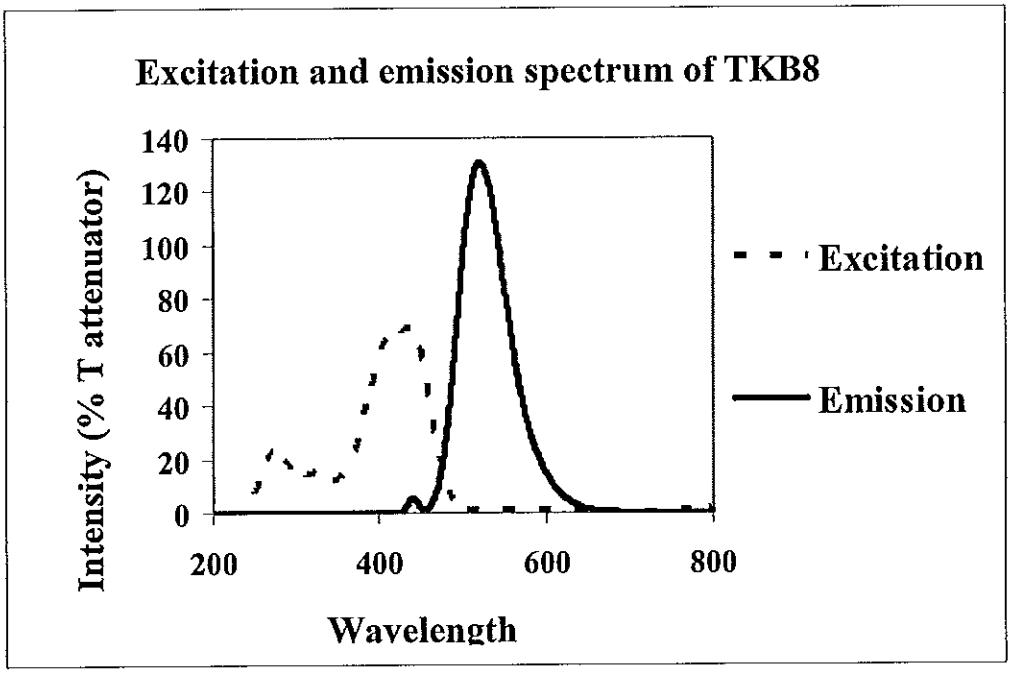

Figure 33 Excitation and emission spectrum of 2.5 μM **TKB8** in $CHCl_3$ solution at room temperature in %T attenuator mode and slit 5:10.

The pre-scan of excitation and emission fluorescence spectrum of **TKB8** was shown in **Figure 33**. Compound **TKB8** shows the fluorescent property which clearly seen in the appearance of fluorescence emission spectrum. The emission spectrum of **TKB8** was observed in the range of 450-700 nm. It was found that, in chloroform solution, **TKB8** exhibits fluorescence with the maximum emission at 521 nm when excited at 440 nm.

3.2.2.9 (*E*)-3-(4-(diethylamino)phenyl)-1-(4-methoxyphenyl)prop-2-en-1-one (TKB9)

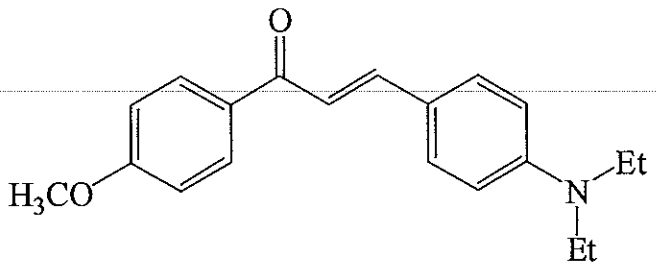

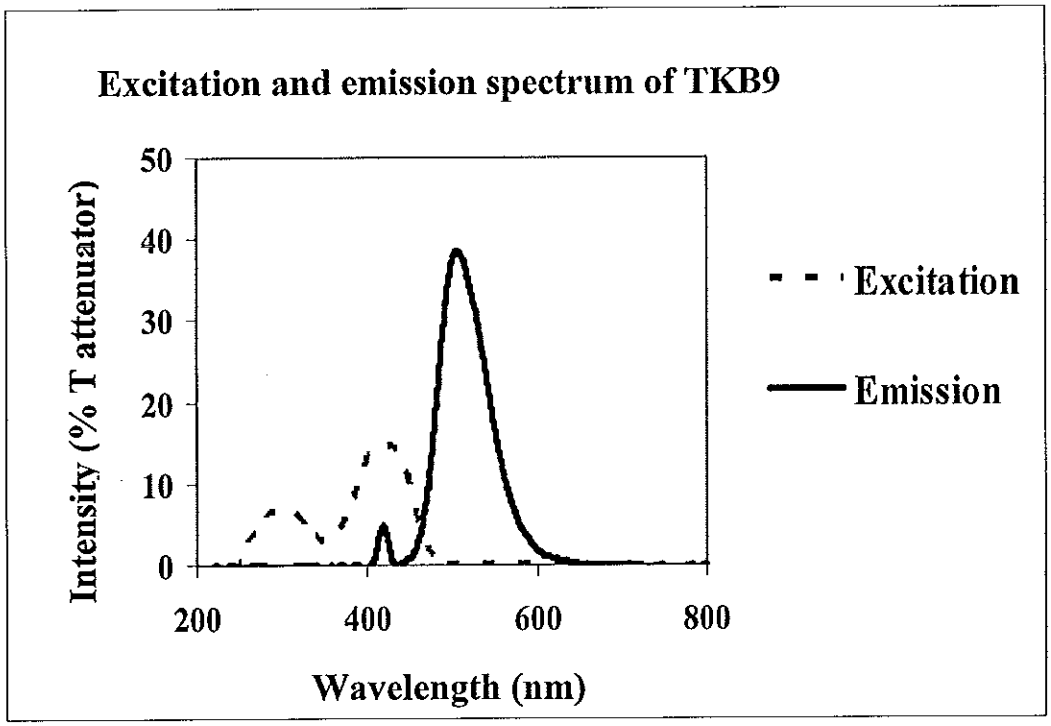

Figure 34 Excitation and emission spectrum of 2.5 μM **TKB9** in $CHCl_3$ solution at room temperature in %T attenuator mode and slit 5:10.

The pre-scan of excitation and emission fluorescence spectrum of **TKB9** was shown in **Figure 34**. Compound **TKB9** shows the fluorescent property which clearly seen in the appearance of fluorescence emission spectrum. The emission spectrum of **TKB9** was observed in the range of 450-650 nm. It was found that,in chloroform solution, **TKB9** exhibits fluorescence with the maximum emission at 507 nm when excited at 415 nm.

3.2.2.10 (*E*)-1-(4-(aminophenyl)-3-(naphthalen-1-yl)prop-2-en-1-one (TKD2)

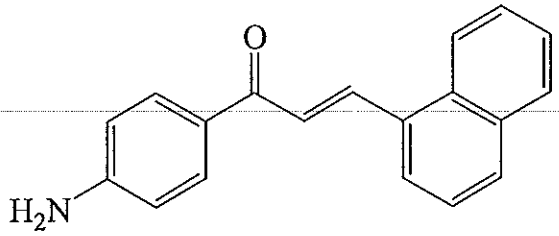

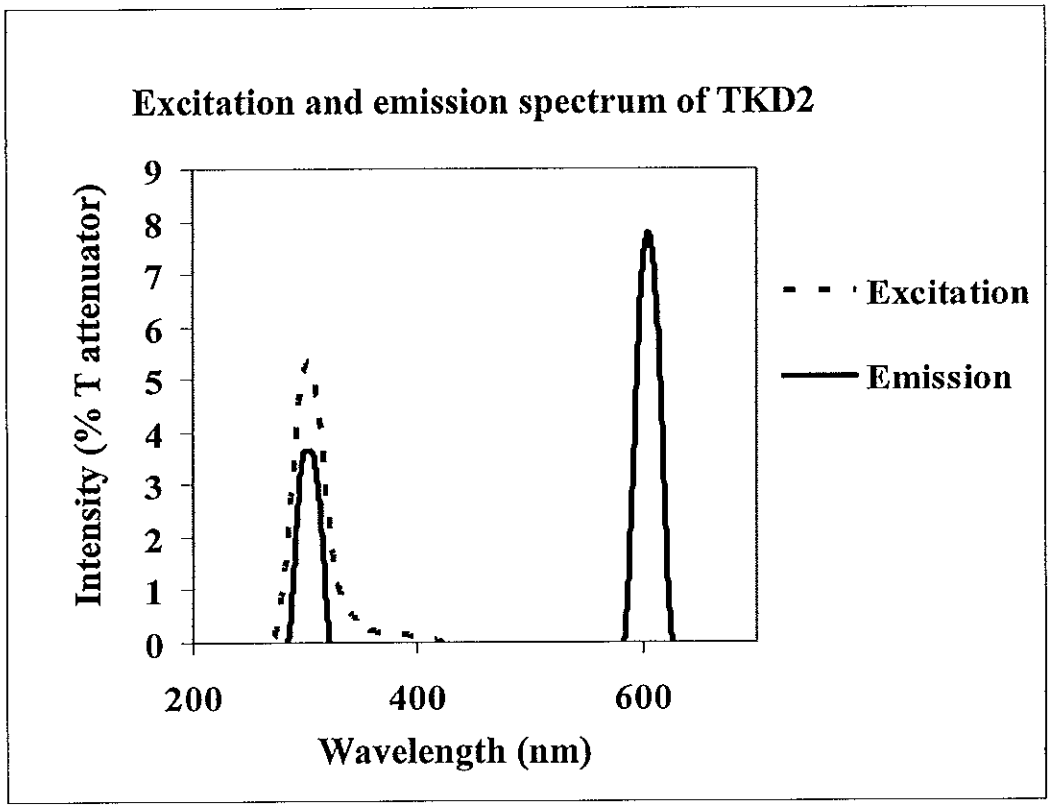

Figure 35 Excitation and emission spectrum of 2.5 μM **TKD2** in $CHCl_3$ solution at room temperature in %T attenuator mode and slit 5:10.

The pre-scan of excitation and emission fluorescence spectrum of **TKD2** was shown in **Figure 35**. Compound **TKD2** do not show the fluorescent property which could see in the absence of fluorescence emission spectrum peak. The scattering peak appeared at 306 nm and the second order scattering peak at 605 nm were not taking into account.

3.2.2.11 (*E*)-1-(4-(aminophenyl)-3-(naphthalen-2-yl)prop-2-en-1-one (TKD3)

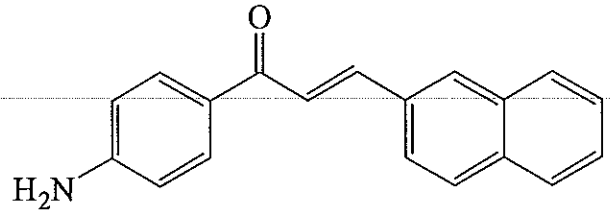

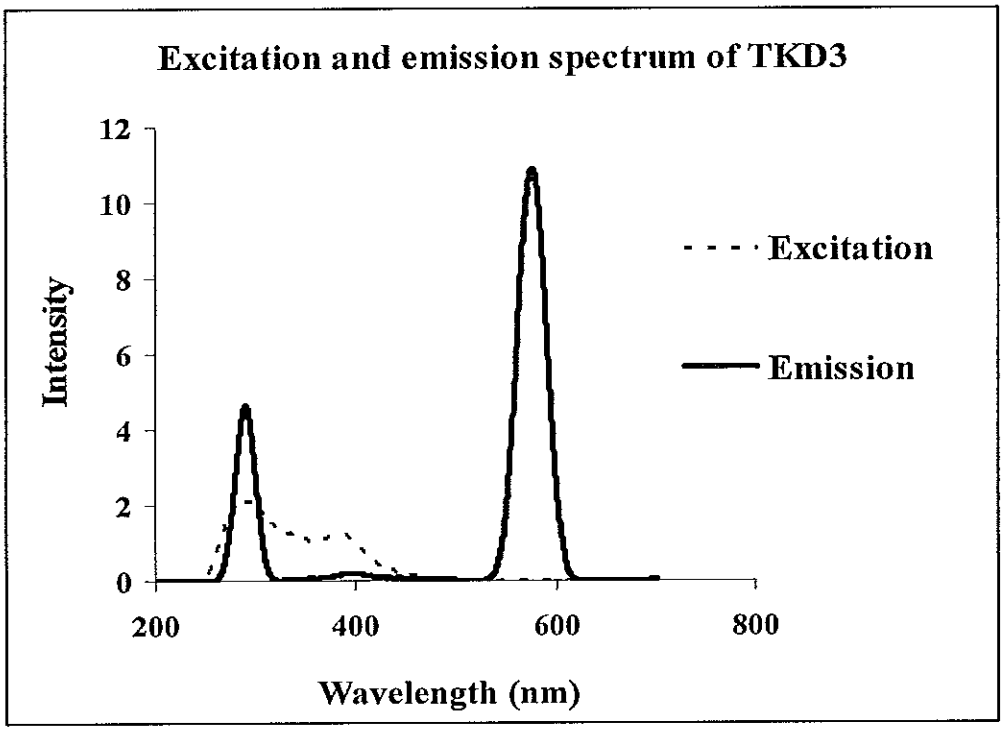

Figure 36 Excitation and emission spectrum of 2.5 μM **TKD3** in $CHCl_3$ solution at room temperature in %T attenuator mode and slit 5:10.

The pre-scan of excitation and emission fluorescence spectrum of **TKD3** was shown in **Figure 36**. Compound **TKD3** shows the fluorescent property which clearly seen in the appearance of fluorescence emission spectrum. The emission spectrum of **TKD3** was observed in the range of 400-550 nm. It was found that, in chloroform solution, **TKD3** exhibits weak fluorescence with the maximum emission at 437 nm when was excited at 310 nm. The scattering peak appeared at 297 nm and the second order scattering peak at 600 nm were not taking into account.

3.2.2.12 (*E*)-1-(4-(aminophenyl)-3-(thiophen-2-yl)prop-2-en-1-one (TKD6)

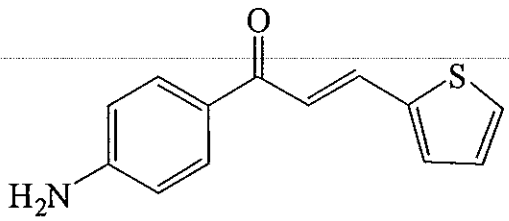

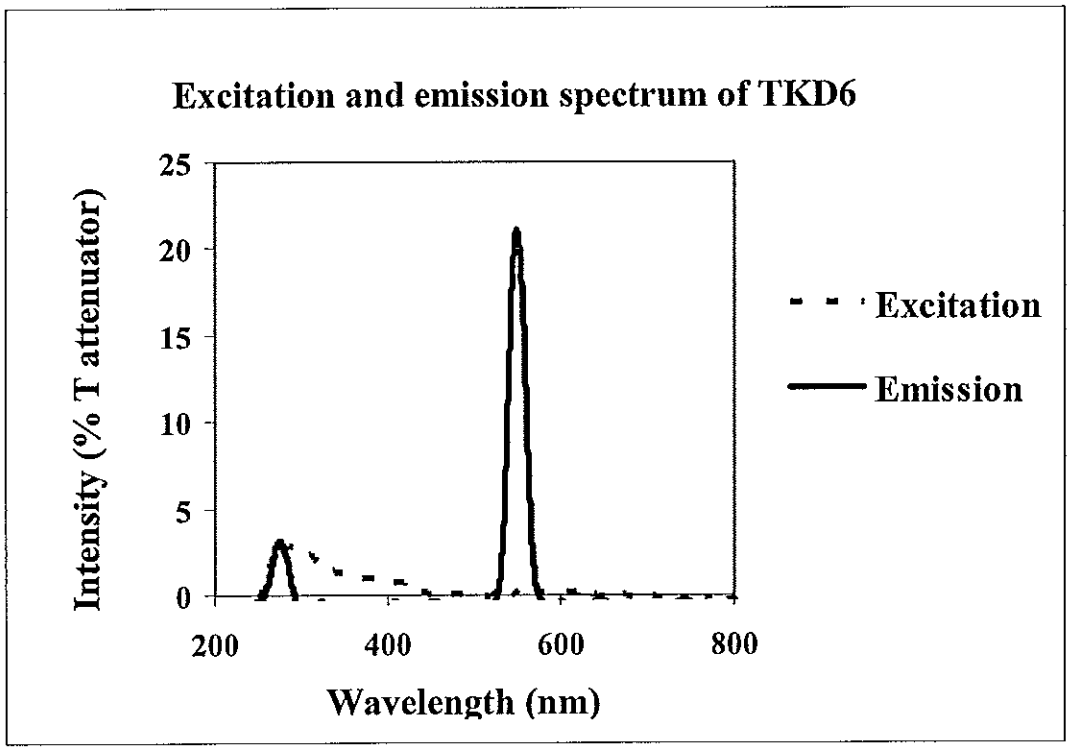

Figure 37 Excitation and emission spectrum of 2.5 μM **TKD6** in $CHCl_3$ solution at room temperature in %T attenuator mode and slit 5:10.

The pre-scan of excitation and emission fluorescence spectrum of **TKD6** was shown in **Figure 37**. Compound **TKD6** do not show the fluorescent property which could see in the absence of fluorescence emission spectrum peak. The scattering peak appeared at 277 nm and the second order scattering peak at 551 nm were not taking into account.

3.2.2.13 (*E*)-1-(4-(aminophenyl)-3-(pyridin-3-yl)prop-2-en-1-one (TKD8)

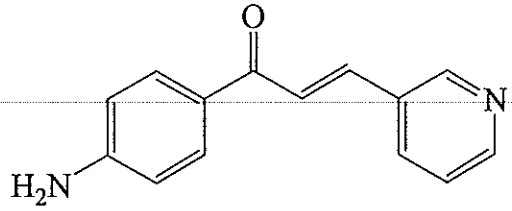

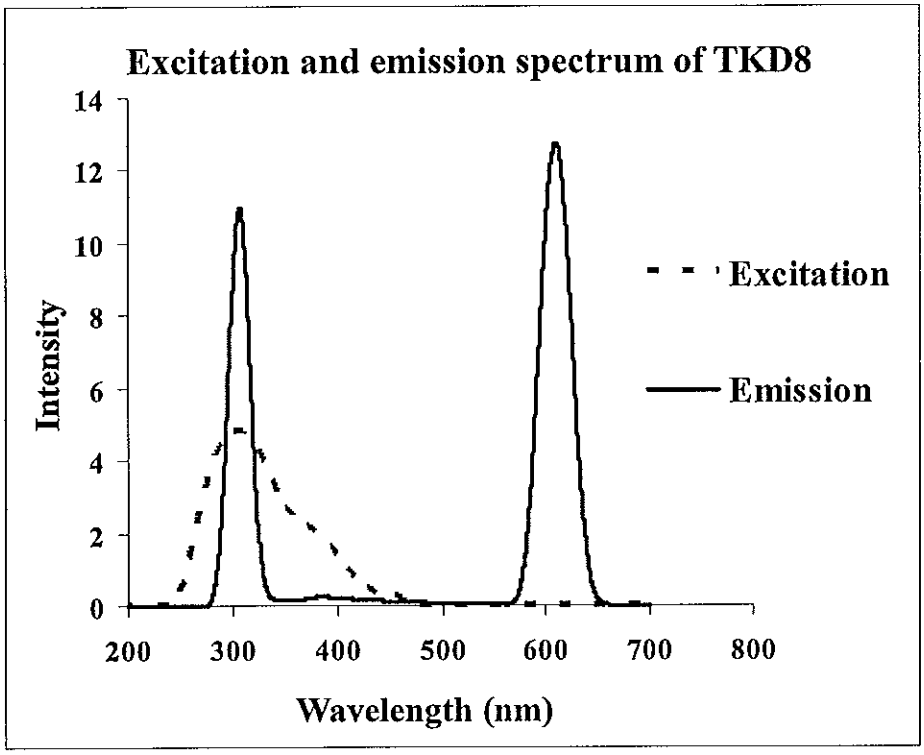

Figure 38 Excitation and emission spectrum of 2.5 μM **TKD8** in $CHCl_3$ solution at room temperature in %T attenuator mode and slit 5:10.

The pre-scan of excitation and emission fluorescence spectrum of **TKD8** was shown in **Figure 38**. Compound **TKD8** shows the fluorescent property which clearly seen in the appearance of fluorescence emission spectrum. The emission spectrum of **TKD8** was observed in the range of 400-600 nm. It was found that, in chloroform solution, **TKD8** exhibits fluorescence with the maximum emission at 437 nm when was excited at 310 nm. The scattering peak appeared at 303 nm and the second order scattering peak at 611 nm were not taking into account.

3.2.2.14 (*E*)-1-(4-(aminophenyl)-3-(pyridin-4-yl)prop-2-en-1-one (TKD9)

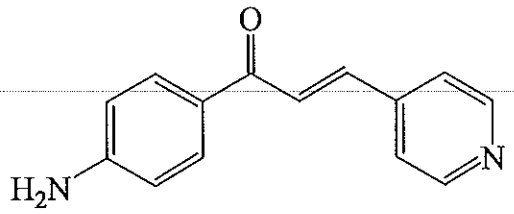

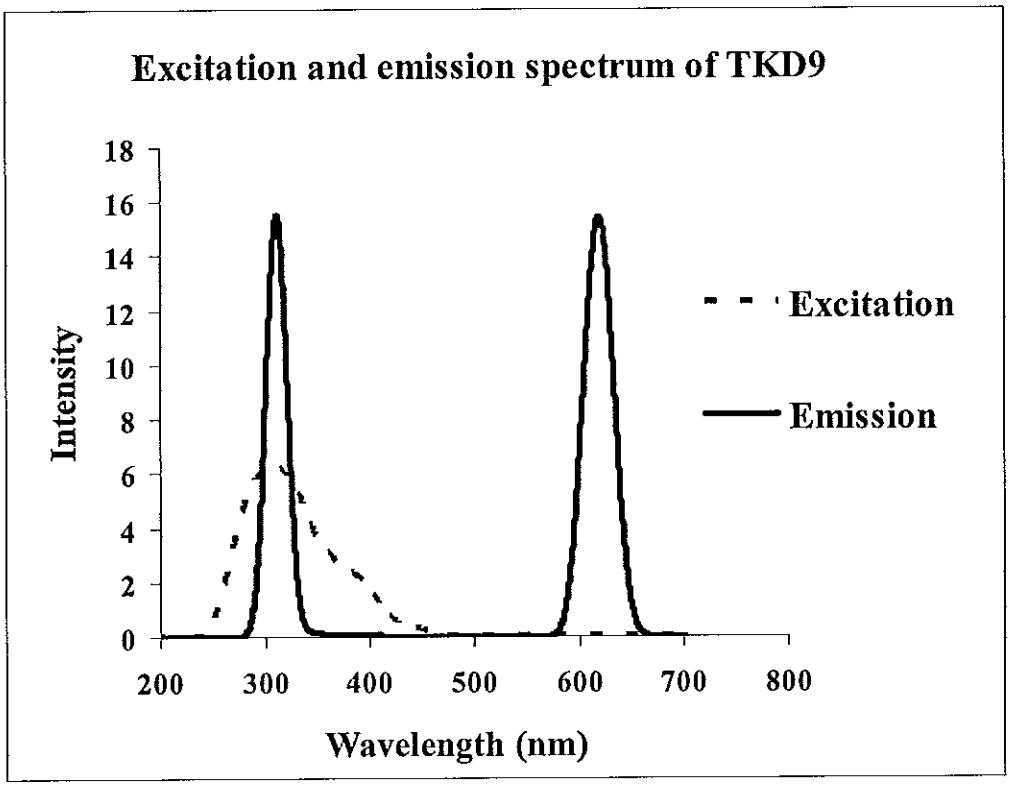

Figure 39 Excitation and emission spectrum of 2.5 μM **TKD9** in $CHCl_3$ solution at room temperature in %T attenuator mode and slit 5:10.

The pre-scan of excitation and emission fluorescence spectrum of **TKD9** was shown in **Figure 39**. Compound **TKD9** do not show the fluorescent property which could see in the absence of fluorescence emission spectrum peak. The scattering peak appeared at 319 nm and the second order scattering peak at 632 nm were not taking into account.

3.2.2.15(*E*)-1-(4-(aminophenyl)-3-(quinolin-4-yl)prop-2-en-1-one (TKD10)

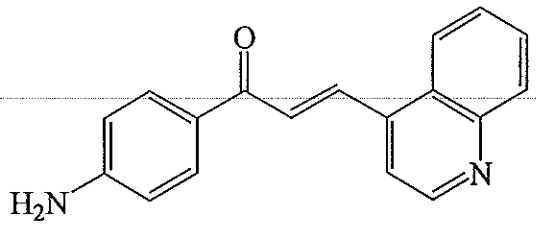

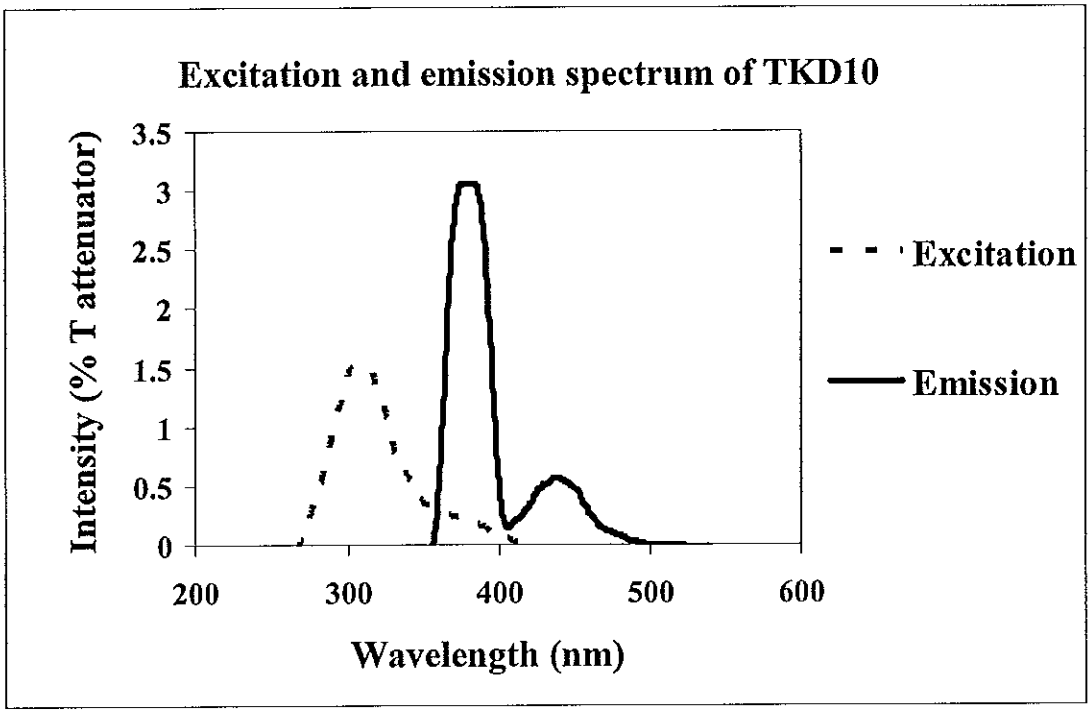

Figure 40 Excitation and emission spectrum of 2.5 μM **TKD10** in $CHCl_3$ solution at room temperature in %T attenuator mode and slit 5:10.

The pre-scan of excitation and emission fluorescence spectrum of **TKD10** was shown in **Figure 40**. Compound **TKD10** shows the fluorescent propery which clearly seen in the appearance of fluorescence emission spectrum. The emission spectrum of **TKD10** was observed in the range of 400-500 nm. It was found that, in chloroform solution, **TKD10** exhibits fluorescence with the maximum emission at 439 nm when was excited at 315 nm. The scattering peaks appeared at 383 nm was not taking into account.

3.2.2.16 (*E*)-1-(4-(aminophenyl)-3-(2,4,5-trimethoxyphenyl)prop-2-en-1-one (TKD19)

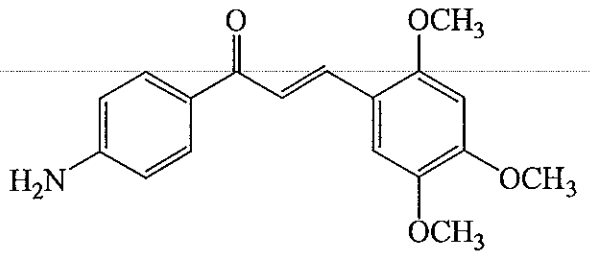

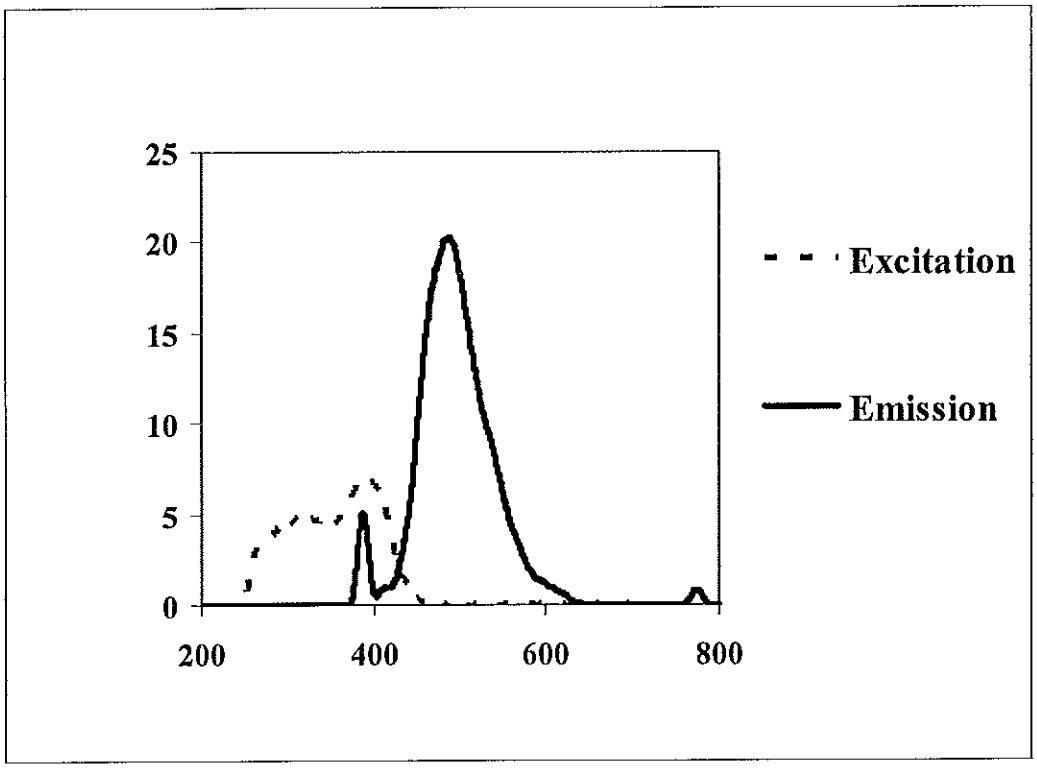

Figure 41 Excitation and emission spectrum of 2.5 μM **TKD19** in $CHCl_3$ solution at room temperature in %T attenuator mode and slit 5:10.

The pre-scan of excitation and emission fluorescence spectrum of **TKD19** was shown in **Figure 41**. Compound **TKD19** shows the fluorescent property which clearly seen in the appearance of fluorescence emission spectrum. The emission spectrum of **TKD19** was observed in the range of 450-650 nm. It was found that, in chloroform solution, **TKD19** exhibits fluorescence with the maximum emission at 488 nm when was excited at 436 nm.

3.2.2.17 (*E*)-1-(4-(aminophenyl)-3-(2,4,6-trimethoxyphenyl)prop-2-en-1-one (TKD20)

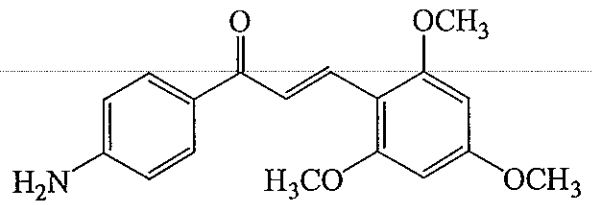

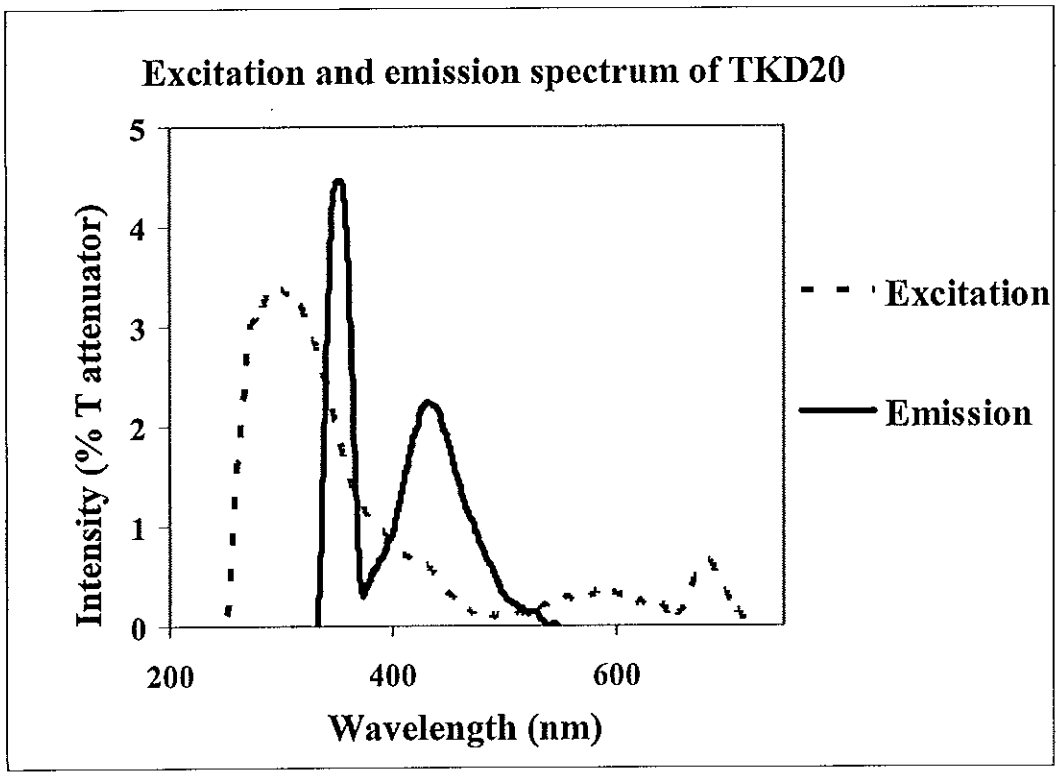

Figure 42 Excitation and emission spectrum of 2.5 μM **TKD20** in $CHCl_3$ solution at room temperature in %T attenuator mode and slit 5:10.

The pre-scan of excitation and emission fluorescence spectrum of **TKD20** was shown in **Figure 42**. Compound **TKD20** shows the fluorescent properties which clearly seen in the appearance of fluorescence emission spectrum. The emission spectrum of **TKD20** was observed in the range of 350-550 nm. It was found that, in chloroform solution, **TKD20** exhibits fluorescence with the maximum emission at 432 nm when was excited at 350 nm. The scattering peaks appeared at 355 nm was not taking into account.

3.2.2.18 (*E*)-1-(4-(aminophenyl)-3-(3,4,5-trimethoxyphenyl)prop-2-en-1-one (TKD21)

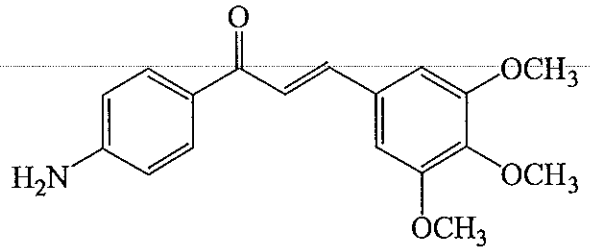

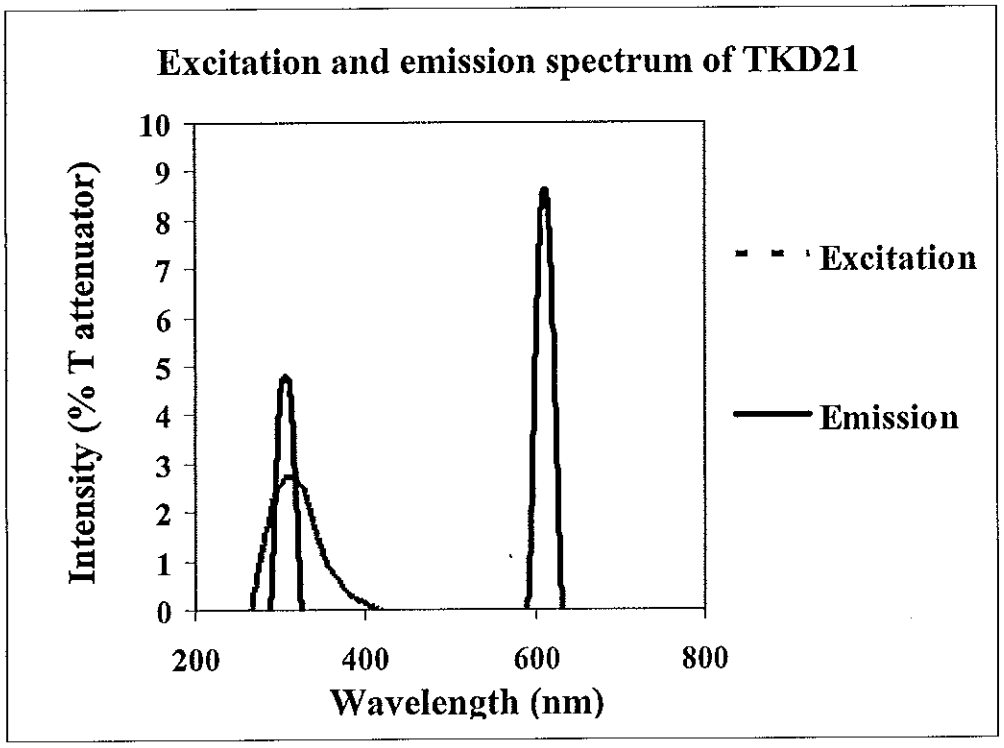

Figure 43 Excitation and emission spectrum of 2.5 μM **TKD21** in $CHCl_3$ solution at room temperature in %T attenuator mode and slit 5:10.

The pre-scan of excitation and emission fluorescence spectrum of **TKD21** was shown in **Figure 43**. Compound **TKD21** do not show the fluorescent properties which could see in the absence of fluorescence emission spectrum peak. The scattering peak appeared at 310 nm and the second order scattering peak at 613 nm were not taking into account.

It was found that compounds **TKB1, TKB2, TKB3, TKB4, TKB5, TKB6, TKB7, TKB8, TKB9, TKD3, TKD8, TKD10, TKD19** and **TKD20** show the fluorescence properties.

3.2.3 Comparison of the fluorescent spectra

The emission spectra of compounds (**TKB1-TKB9**) in chloroform solution (2.5 μM) are shown in **Figure 44**. Compounds show the maxima wavelength at 516.0, 502.0, 527.5, 529.0, 529.5, 530.0, 517.5, 521.5 and 506.5 nm, respectively. The emission wavelength of these compounds arise around 500-530 nm (yellow-green region). It was found that **TKB7** which contains methoxy moiety showed the highest fluorescent emission intensity. In addition, compounds **TKB5** and **TKB6** which posses π conjugate have red-shift phenomenon compared with the others.

The excitation spectra of compounds **TKB1-TKB9** in chloroform solution (2.5 μM) are shown in **Figure 45**. **TKB1-TKB9** show the maxima wavelength at 430.0, 411.0, 438.5, 414.0, 409.5, 437.5, 416.0, 444.0 and 434.0 nm. The highest intense was observed for **TKB8**. Moreover, the Stoke shift of **TKB5** was larger than that of the other compounds which shown in **Table 35.**

The emission spectra of compounds **TKD3, TKD8, TKD10, TKD19** and **TKD21** in chloroform solution (2.5 μM) (in **Figure 46** and **47**) show the maxima wavelength at 398.0, 388.0, 439.0, 488.5 and 432.0 nm, respectively. It can be observed that compounds **TKD19** have red-shift phenomenon compared with others. In addition, it was found that **TKD19** which contains methoxy moiety showed the highest fluorescent emission intensity.

The excitation spectra of compounds **TKD2-TKD21** in chloroform solution (2.5 μM) are shown in **Figure 48**. **TKD2-TKD21** show the maxima wavelength at 304.0, 287.0, 280.5, 306.5, 310.0, 307.0, 315.0, 309.0 and 313.0 nm, respectively. The highest intensity was observed for **TKD19.** Moreover, the Stoke shift of **TKD8** was larger than the other compounds which shown in **Table 36**

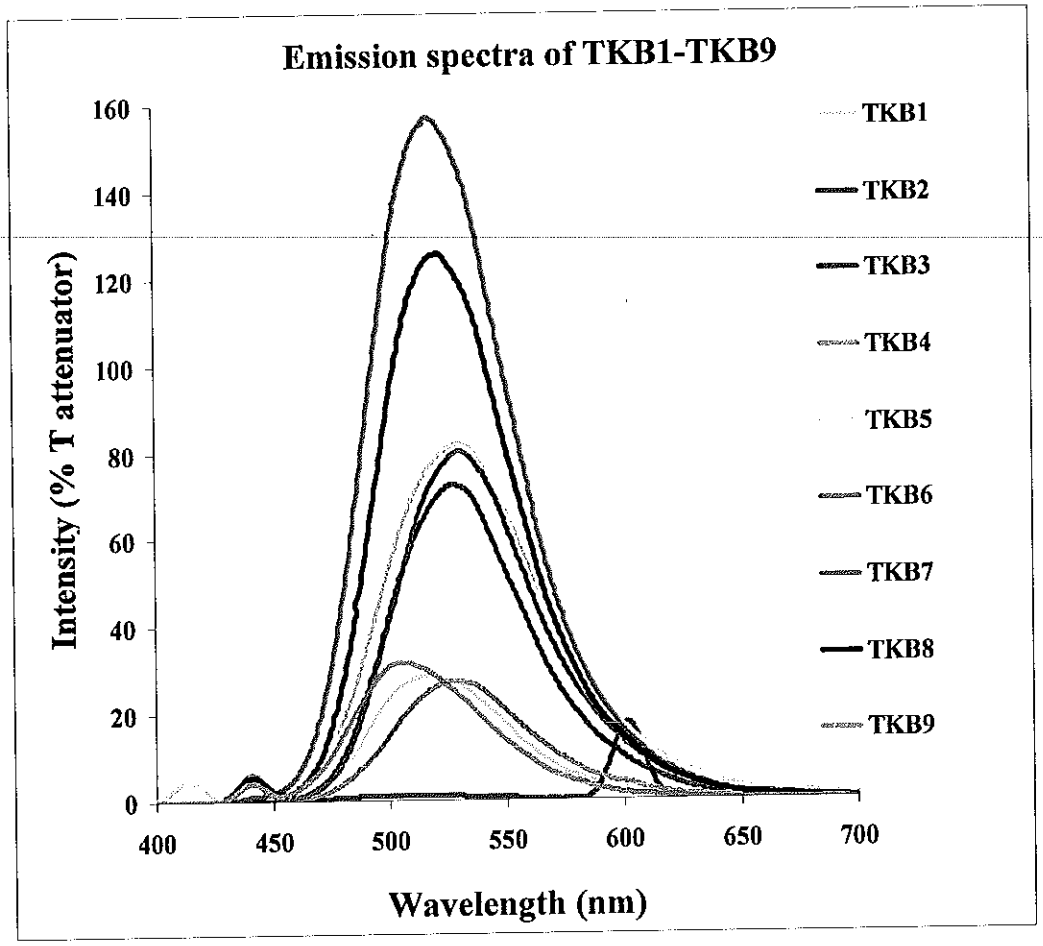

Figure 44 Emission spectra (excited at 440 nm) of 2.5μM of **TKB1**, **TKB2**, **TKB3**, **TKB4**, **TKB5**, **TKB6**, **TKB7**, **TKB8** and **TKB9** in $CHCl_3$ solution at room temperature (slit 5:10).

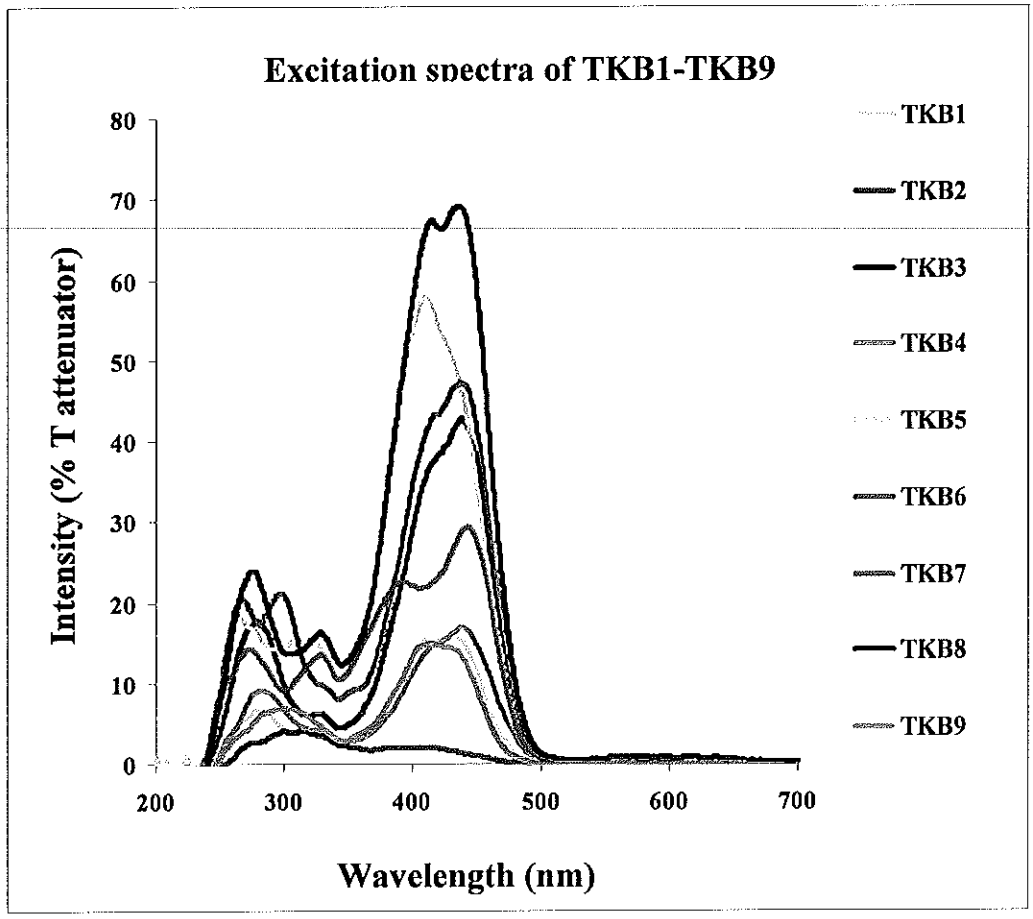

Figure 45 Excitation spectra (emitted at 520 nm) of 2.5μM of **TKB1**, **TKB2**, **TKB3**, **TKB4**, **TKB5**, **TKB6**, **TKB7**, **TKB8** and **TKB9** in $CHCl_3$ solution at room temperature (slit 5:10).

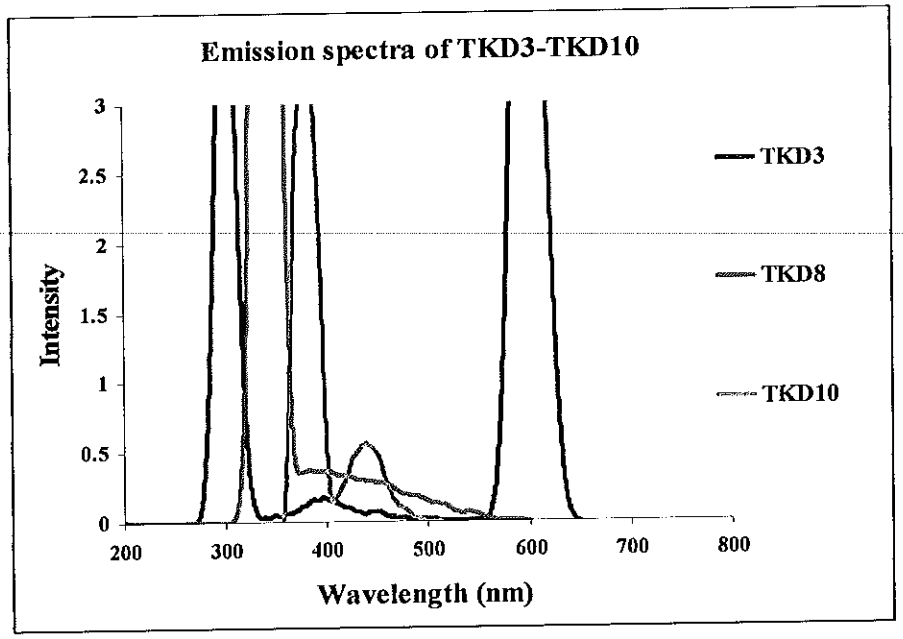

Figure 46 Emission spectra (excited at 310 nm) of 2.5μM of **TKD3**, **TKD8** and **TKD10** in $CHCl_3$ solution at room temperature (slit 5:10).

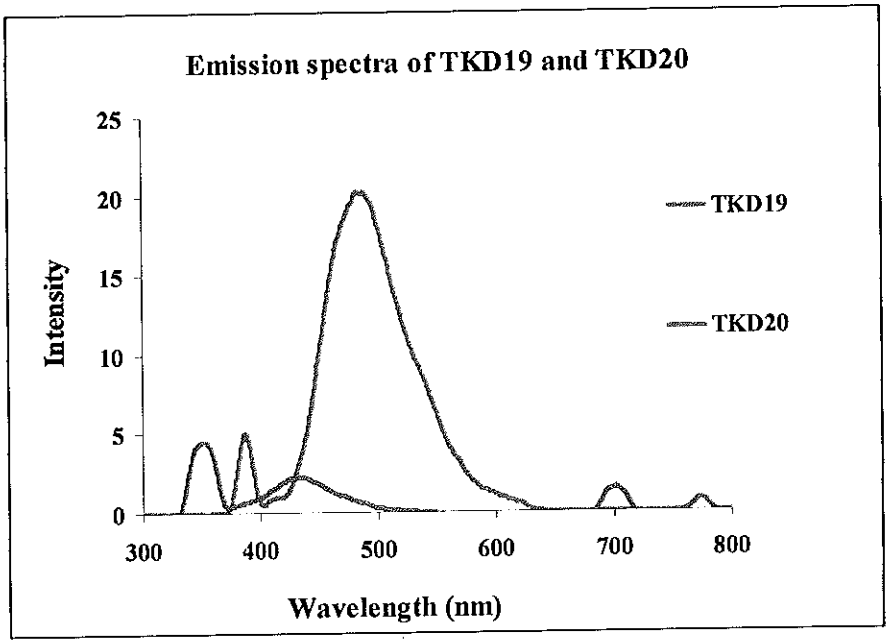

Figure 47 Emission spectra (excited at 310 nm) of 2.5μM of **TKD19** and **TKD20** in $CHCl_3$ solution at room temperature (slit 5:10).

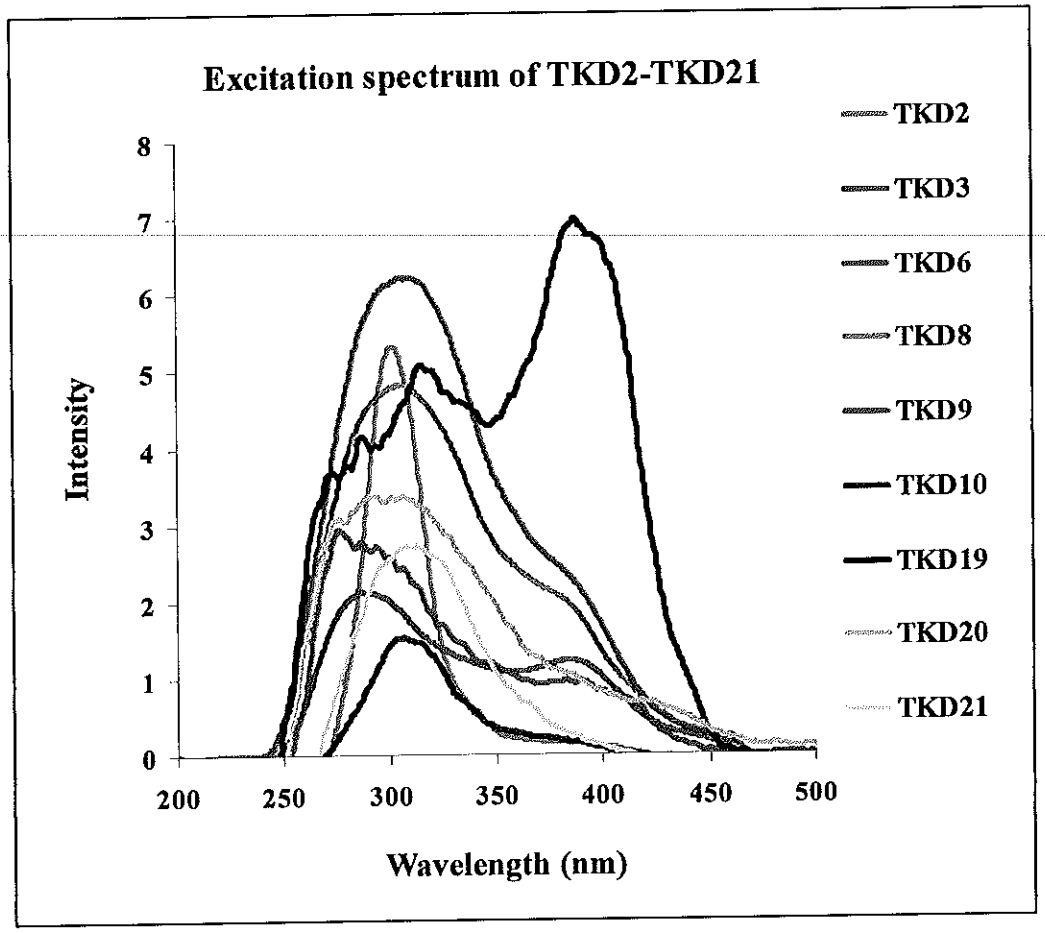

Figure 48 Excitation spectra (emitted at 430 nm) of 2.5μM of **TKD2, TKD3, TKD6, TKD8, TKD9, TKD10, TKD19, TKD20** and **TKD21** in $CHCl_3$ solution at room temperature (slit 5:10).

Table 37 Fluorescence spectra data and stokes shift of chalcones and heteroaryl chalcone derivatives (**TKB1-TKB9**) in chloroform.

Compound	Absorption maxima, λ_{ex} (nm)	Emission maxima, λ_{em} (nm)	Stoke shift (nm)
TKB1	418.4	516.0	97.6
TKB2	417.8	502.0	84.2
TKB3	429.3	527.5	98.2
TKB4	414.5	529.0	99.6
TKB5	406.5	529.5	123.0
TKB6	428.5	530.0	101.5
TKB7	425.2	517.5	92.3
TKB8	422.7	521.5	99.8
TKB9	407.0	506.5	99.5

Table 38 Fluorescence spectra data and stokes shift of chalcones and heteroaryl chalcone derivatives (**TKD2-TKD21**) in chloroform.

Compound	Absorption maxima, λ_{ex} (nm)	Emission maxima, λ_{em} (nm)	Stoke shift (nm)
TKD2	302.5	-	-
TKD3	340.9	430.0	89.1
TKD6	360.8	-	-
TKD8	335.9	437.0	101.1
TKD9	335.9	-	-
TKD10	331.0	439.0	108.0
TKD19	379.8	488.5	108.7
TKD20	356.6	432.0	75.4
TKD21	354.6	-	-

3.2.4 Fluorescence quantum yields

Table 39 Fluorescence quantum yield of chalcones (**TKB1-TKB9**) in chloroform using coumarin 7 ($\Phi_f = 0.49$ in CH_3CN) as the standard sample

Compound	Fluorescent quantum yield (Φ_f)
TKB1	0.068
TKB2	0.060
TKB3	0.091
TKB4	0.094
TKB5	0.124
TKB6	0.152
TKB7	0.233
TKB8	0.204
TKB9	0.078

From Table **39**, it can be summarized that the fluorescent quantum yields of these compounds were lower than that of coumarin 7 which is fluorescent standard. Compound **TKB7** indicated the highest fluorescent quantum yield value (Φ_f = 0.233) when compared with the other compounds in these series. Nevertheless, the fluorescent quantum yield value of compound **TKB7** is about 2-time-lower than that of coumarin 7.

Noteworthy, compounds **TKB7** and **TKB8** which contained methoxy group show higher fluorescent quantum yields value than the other compounds. Among the compounds containing electron donating groups (ortho-methoxy in **TKB7**, meta-methoxy in **TKB8** and para-methoxy in **TKB9**), compound **TKB7** shows the most fluorescence quantum yield value. These results can be explained by the different π electron delocalization ability of the compounds, in which the better π electron delocalization contributes to the better fluorescent quantum yield. The result suggested that ortho-methoxy group can bring about the best π electron delocalization when compared which meta-methoxy and para-methoxy groups.

In addition, the above results imply that the longer π-conjugated structure may be increased in fluorescence quantum yield. So, compounds **TKB5** and **TKB6** which containing π-conjugate show higher fluorescence quantum yields value than **TKB1**.

For compounds containing electron withdrawing groups, compound **TKB2** indicated the lowest fluorescence quantum yield value (Φ_f = 0.060) when compared with the other compounds (**TKB3** and **TKB4**). The result may be due to the effect of strong electron withdrawing group.

Table 40 Fluorescence quantum yield of chalcones and heteroaryl chalcone derivatives in chloroform using coumarin 1 (Φ_f = 0.73 in EtOH) as the standard sample

Compound	**Fluorescent quantum yield (Φ_f)**
TKD2	-
TKD3	0.008
TKD6	-
TKD8	0.003
TKD9	-
TKD10	0.005
TKD19	0.039
TKD20	0.012
TKD21	-

It can be seen from this table that the fluorescent quantum yields of these compounds were lower than that of coumarin 1 which is fluorescent standard. Compound **TKD19** which show the highest fluorescent quantum yields value (Φ_f = 0.039) when compared with the other compounds in these series. In addition, the fluorescent quantum yield value of compound **TKD19** is about 18-times-lower than that of coumarin 1.

Compound **TKD19** which is the compound containing 2,4,5-trimethoxy group show higher fluorescent quantum yields value than the other compounds (compounds containing 2,4,6- and 3,4,5-trimethoxy groups). The highest fluorescent quantum yields of **TKD19** may be affected by the good π electrons donating ability from two methoxy groups at 2 (*ortho*) and 4 (*para*) positions.

For compounds containing 2,4,6-trimethoxyphenyl (**TKD20**), the barrier between 2- and 6-methoxy groups in *ortho* positions bring about the steric effect that causes the low quantum yield values ($\Phi_f = 0.012$) of compounds in series

Whereas the compounds containing 3,4,5-trimethoxyphenyl (**TKD21**) don't show the fluorescence properties. Because the less π electron donating ability of two methoxy groups at 3 and 5 (both *meta*) positions which results the less π electron delocalization compare to 2 and 4 positions.

For compound **TKD3** which is the compound containing 2-nahpthaldehyde show higher fluorescence quantum yield value than the other compounds (compound containing 1-nahpthaldehyde and 4-quinoline carboxaldehyde). These result may be effect of planarity of molecule. For heteroaryl chalcone derivatives (**TKD6**) show weak fluorescence quantum yield.

Noteworthy, the different substituents on the benzene ring have a remarkable effect on the fluorescence properties. However, besides the π electron delocalization ability, the planarity of molecule and π-conjugate system also play an important role on the fluorescent property of compounds.

CHAPTER 4
CONCLUSION

Eighteen new chalcones and heteroaryl chalcone derivatives were successfully synthesized. Their structures were elucidated by spectroscopic techniques. The eighteen compounds are

(*E*)-3-(4-diethylamino) phenyl)-1-phenylprop-2-en-1-one (**TKB1**),

(*E*)-1-(4-fluorophenyl)-3-(4-(diethylamino)phenyl)prop-2-en-1-one (**TKB2**),

(*E*)-1-(4-chlorophenyl)-3-(4-(diethylamino)phenyl)prop-2-en-1-one (**TKB3**),

(*E*)-1-(4-bromophenyl)-3-(4-(diethylamino)phenyl)prop-2-en-1-one (**TKB4**),

(*E*)-3-(4-(diethylamino)phenyl)-1-(naphthalen-1-yl)prop-2-en-1-one (**TKB5**),

(*E*)-3-(4-(diethylamino)phenyl)-1-(naphthalen-2-yl)prop-2-en-1-one (**TKB6**),

(*E*)-3-(4-(diethylamino)phenyl)-1-(2-methoxyphenyl)prop-2-en-1-one (**TKB7**),

(*E*)-3-(4-(diethylamino)phenyl)-1-(3-methoxyphenyl)prop-2-en-1-one (**TKB8**),

(*E*)-3-(4-(diethylamino)phenyl)-1-(4-methoxyphenyl)prop-2-en-1-one (**TKB9**),

(*E*)-1-(4-(aminophenyl)-3-(naphthalen-1-yl)prop-2-en-1-one (**TKD2**),

(*E*)-1-(4-(aminophenyl)-3-(naphthalen-2-yl)prop-2-en-1-one (**TKD3**),

(*E*)-1-(4-(aminophenyl)-3-(thiophen-2-yl)prop-2-en-1-one (**TKD6**),

(*E*)-1-(4-(aminophenyl)-3-(□yridine-3-yl)prop-2-en-1-one (**TKD8**),

(*E*)-1-(4-(aminophenyl)-3-(pyridin-4-yl)prop-2-en-1-one (**TKD9**),

(*E*)-1-(4-(aminophenyl)-3-(quinolin-4-yl)prop-2-en-1-one (**TKD10**),

(*E*)-1-(4-(aminophenyl)-3-(2,4,5-trimethoxyphenyl)prop-2-en-1-one (**TKD19**),

(*E*)-1-(4-(aminophenyl)-3-(2,4,6-trimethoxyphenyl)prop-2-en-1-one(T**KD20**),

(*E*)-1-(4-(aminophenyl)-3-(3,4,5-trimethoxyphenyl)prop-2-en-1-one (**TKD21**)

Their fluorescence properties were studied in chloroform solution at room temperature. It was found that the fourteen compounds in both **TKB** and **TKD** series, which are **TKB1**, **TKB2**, **TKB3**, **TKB4**, **TKB5**, **TKB6**, **TKB7**, **TKB8**, **TKB9**, **TKD3**, **TKD8**, **TKD10**, **TKD19** and **TKD20**, exhibited fluorescence properties. Their emission spectra pattern are similar and present maxima wavelength in the range of 430-.530 nm. It was found that, the fluorescence quantum yield valves of **TKB1**, **TKB2**, **TKB3**, **TKB4**, **TKB5**, **TKB6**, **TKB7**, **TKB8**, **TKB9**, **TKD3**,

TKD8, TKD10, TKD19 and **TKD20** are 0.068, 0.060, 0.091, 0.094, 0.124, 0.152, 0.233, 0.204, 0.078, 0.008, 0.003, 0.005, 0.039 and 0.012, respectively. However, the fluorescent quantum yields of these compounds are lower than that of coumarin 7 and 1 which are fluorescent standards in this study. Compounds which contain methoxy group and π-conjugate show higher fluorescent quantum yield value than that of the other compounds. Moreover, six structures of the compounds namely :

(*E*)-1-(4-chlorophenyl)-3-(4-(diethylamino)phenyl)prop-2-en-1-one (**TKB3**),

(*E*)-1-(4-bromophenyl)-3-(4-(diethylamino)phenyl)prop-2-en-1-one (**TKB4**),

(*E*)-1-(4-(aminophenyl)-3-(naphthalen-2-yl)prop-2-en-1-one (**TKD3**),

(*E*)-1-(4-(aminophenyl)-3-(thiophen-2-yl)prop-2-en-1-one (**TKD6**),

(*E*)-1-(4-(aminophenyl)-3-(pyridin-3-yl)prop-2-en-1-one (**TKD8**) and

(*E*)-1-(4-(aminophenyl)-3-(2,4,5-trimethoxyphenyl)prop-2-en-1-one (**TKD19**)

were also determined by single crystal X-ray diffraction. Compounds **TKB3** and **TKB4** crystallized out in the $P2_1/c$ space group while compounds **TKD3** and **TKD6** crystallized out in the $P2_12_12_1$ space group. Whereas, compounds **TKD8** and **TKD19** were crystallized out in *Pbca* and *C2/c* space group, respectively, which indicate that TKD6 also exhibits the second order NLO property since it crystallizes in non-centrosymmetric space group.

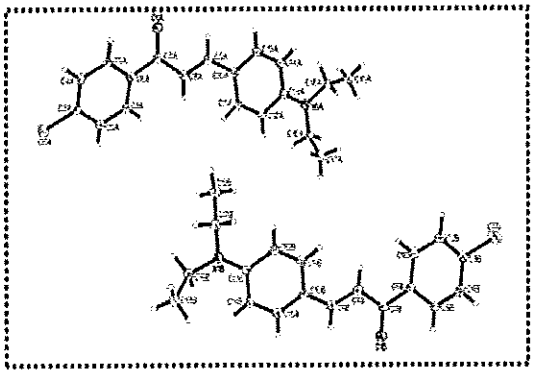

TKB3

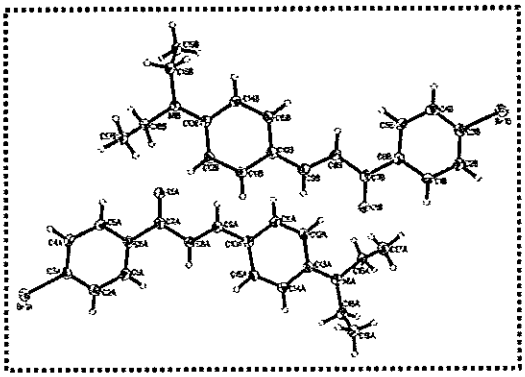

TKB4

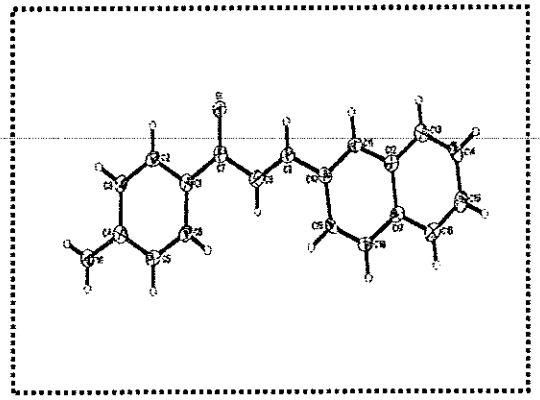

TKD3

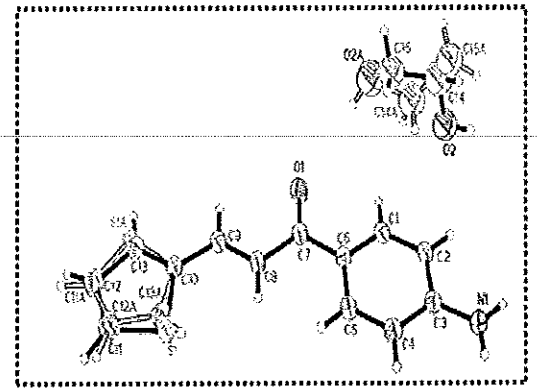

TKD6

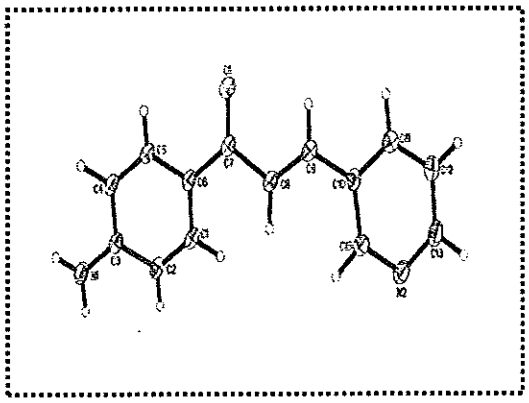

TKD8

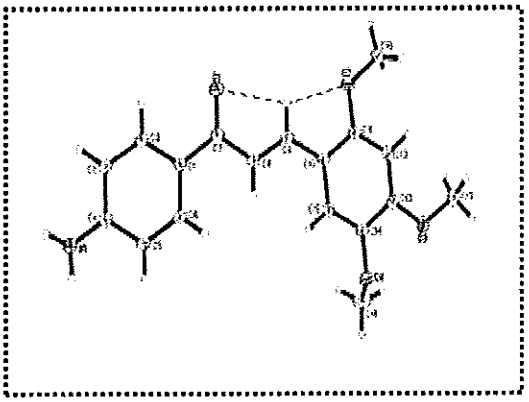

TKD19

REFERENCES

Aneta, M., Catherine, P., Geetha, A., Nancy, E.D., Peng, H. (2006) "Anticancer activities of novel chalcone and bis-chalcone derivatives", *Bioorg. Med. Chem.*, **14**, 3491-3495.

Ashutosh, S., tephen, G.S. (1999) "Introduction to Fluorescence Spectroscopy", University of Florida, USA.

Barik, A., Priyadarsini, K. I. & Mohan, H. (2003) "Photophysical studies on binding of curcumin to bovine serum albumin", *Photochem. Photobiol.*, **77**, 597–603.

Batovska, D., Parushev, St., Slavova, A., Bankova, V., Tsvetkova, I., Nonova, M. and Najdenski, H. (2007) "Study on the substituents' effects of a series of synthetic chalcones against the yeast Candida albicans", *Eur.J. Med.Chem.*, **42**, 87-92.

Bruker 2005. *APEX2*, *SAINT* and *SADABS*. Bruker AXS Inc., Madison, Wisconsin, USA.

Dhami, S., de Mello, A. J., Rumbles, G., Bishop, S. M., Phillips D. & Beeby, A. (1995) "Phthalocyanine fluorescence at high concentration: dimers or reabsorption effect?", *Photochem. Photobiol.*, **61**, 341-346.

Dong, M. S., Kyoung, H. J., Ji, H. M., Dong, M. S. (2002) "Photochemistry of chalcone and the application of chalcone-derivatives in photo-alignment layer of liquid crystal display", *Opt. Mater.*, **21**, 667-671.

Fayed, T. A. & Awad, M. K. (2004) "Dual emission of chalcone-analogue dyes emitting in the red region", *Chem. Phys.*, **303**, 317-326.

Gaber, M., El-Daly, S.A. & El-Sayed, Y.S. (2008) "Spectral properties and inclusion of 3-(4′-dimethylaminophenyl)-1-(2-furanyl)prop-2-en-1-one in organized media of micellar solutions, β-cyclodextrin and viscous medium", *Colloids Surf., B*, **66**, 103–109

Jen-Hao, C., Chi-Feng, H., Shyh-Chyun, Y., Jih-Pyang, W., Shen-Jeu, W. and Chun-Nan, L. (2008) " Synthesis and cytotoxic, anti-inflammatory, and anti-oxidant activities of 2',5'- dialkoxychalcones as cancer chemopreventive agents", *Bioorg. Med. Chem.*, **16**, 7270-7276.

Jung, Y. J., Son, K. I., Oh, Y. E. and Noh, D. Y. (2008) "Ferrocenyl chalcones containing anthracenyl group: Synthesis, X-ray crystal structures and electrochemical properties", *Polyhedron*, **27**, 861-867.

Knut, R., Marina, L. D., Julia, L. B. and Ute, R.-G. and Wolfgang R. (1999) "Quantum yield switching of fluorescence by selectively bridging single and double bonds in chalcones: involvement of two different types of conical intersections", *J. Phy. Chem. A*, **103**, 9626-9635.

Lakowicz, J.R. (1999) "Principles of Fluorescence Spectroscopy (2nd ed^{n})", Kluwer Academic/Plenum Publishers, New York, London, Moscow, Dordrecht.

Lewis, G. N. and Calvin, M. (1939), *J. Chem. Phys*, **7**, 536.

Mashraqui, S.H., Khan T., Sundaram, S. and Ghadigaonkar, S. (2008) "Phenothiazine-pyridyl chalcone: an easily accessible colorimetric and fluoimetric 'on-off' dual sensing probe for Cu^{2+}", Tetrahedron Lett, **49**, 3739-3743.

Nishida, J., Gao, H., Kawabata, J. (2007). *Bioorg. Med. Chem.*, **15**, 2396-2402.

Nurettin, Y., Osman, U., Ebru, A., Ahmet, Y., Cemalettin, B., Nuri, Y., Murat. (2005) "Stereoselective photochemistry of heteroaryl chalcones in solution and the antioxidant activities", *J. Photochem. Photobiol. A*, **169**, 229-134.

Niu, C. G., Guan, A. L., Zeng, G. M., Liu, Y. G. and Li, Z. W. (2006) " Fluorescence water sensor based on covalent immobilization of chalcone derivative", *Anal. Chim. Acta*, **577**, 264-270.

Patil, C., Mahajan, S.K. and Kitti, A. (2009) " Chalcone: A versatile molecule", *J. Pharm. Sci. & Res*, **3**, 11-22.

Prakriti, R. B., Saswati, L., Samiran, K. and Sankar, C. (1996) "Vibronic interaction and photophysics of chalcone derivertives", *J. Lumin*, **69**, 49-56.

Prasad, Y. R., Rao A. L. & Rambabu, R. (2007) "Synthesis and Antimicrobial Activity of Some Chalcone Derivatives", *E-J. Chem.*, **5**, 461-466.

Ravindra, H. J., Kiran, A. J., Dharmaprakash, S. M., Rai, N. S., Chandrasekharan, K., Kalluraya, B. and Kotermund, F. (2008) "Growth and characterization of an efficient nonlinear optical D-π-A-π-D type chalcone single crystal", *J. Crys. Growth*, **310**, 4169-4176.

Romagnoli, R., Baraldi, P. G., Carrion, M. D., Cara, C. L., Cruz-Lopez, O., Preti, D., Tolomeo, M., Grimaudo, Stefania., Cristina, A. D., Zonta, N., Balzarini, J., Brancale, A., Sarkare, T. and Hamele, E. (2008) " Design, synthesis, and biological evaluation of thiophene analogues of chalcones", *Bioorg. Med. Chem*, **16**, 5367-5376.

Rtishchev, N. I., Nosava, G. I., Solovskaya, N. A., Luk'yashina, V. A., Galaktionova, E. F. and Kudryavtsev, V. V. (2000) "Spectral properties and photochemical activity of Chalcone derivatives", *Russ. J. Gen. Chem.*, **71**, 1272-1281.

Rtishchev, N.I., Nosova, G.I., Solovskaya, N.A., Luk'yashina, V.A., Galaktionova, E.F. and Kudryavtsev, V.V. (2001) "Spectral properties and photochemical activity of chalcone derivatives", *Russ. J. Gen. Chem.*, **71**, 1345-1355.

Rurack, K., Bricks, J. L., Reck, G., Radeglia, R. and Resh-Genger, U. (2000) "Chalcone-analogue dyes emitting in the near-infared (NIR): Influence of donor-acceptor substitution and cation complexation on their spectroscopic properties and X-ray structure", *J. Phys. Chem. A*, **104**, 3087-3109.

Sabir, H.M., Tabrez, K., Subramanian, S. and Shailesh, G. (2008) "Phenothiazine-pyridyl chalcone: an easily accessible colorimetric and fluorimetric 'on-off' dual sensing probe for Cu^{2+}", *Tetrahedron Lett*, **49**, 3739-3743.

Samiran, K., Sanjukta, A., Samita, B. and Saswati, L. (1999) "Intramolecular charge transfer in Naphthalene analogues of Chalcone", *Res. Chem. Intermed*, **25**, 903-913.

Sens, R. and Drexhage, K. H. (1981) "Fluorescence quantum yield of oxazine and carbazine laser dyes", *J. Lumin*, **24-25**, 709-712.

Sun, Y. F. and Cui, Y. P. (2008) "The synthesis, characterization and properties of coumarin-based chromophores containing a chalcone moiety", *Dyes Pigm*, **780**, 65-76.

Tarek, A. F. (2006) "A novel chalcone-analogue as an optical sensor based on ground and excited states intramolecular charge transfer: A combined experimental and theoretical study", *Chem. Phys*, **324**, 631-638.

Tomar, V., Bhattacharjee, G., Kamaluddin, S., Kumkum, S. (2010) "Synthesis of new chalcone derivatives containing acridinyl moiety with potential antimalarial activity", *Eur. J. Med.l Chem*, **45**, 745-751.

Tomeckova, V., Perjesi, P., Guzy, J., Kusnir, J. Chovanova, Z. and Marekova, M. (2004) "Comparison of effect of selected synthesic chalcone analogues on mitochondrial outer membrane determined by fluorescence spectroscopy", *J. Biochem. Bioph. Methods*, **61**, 135-141.

Valeur, B. (2002) "Molecular Fluorescence: Principles and Applications", Wiley-VCH,Weinheim.

Venkataraya, S., Patila, S., Naveenb, S.M., Dharmaprakasha, M.A., Sridharb, J., Shashidhara P. (2006) "Crystal growth and characterization of new nonlinear optical chalcone derivative: 1-(4-Methoxyphenyl)-3-(3,4-dimethylphrnyl)-2-propen-1-one" *J. Crys. Growth*, **295**, 44–49.

West, W. (1956) " Chemical Applications of Spectroscopy", Technique of organic chemistry.

Williams, A. T. R., Winfield, S. A. & Miller, J. N. (1983) "Relative fluorescence quantum yields using a computer controlled luminescence spectrometer", *Analyst*, **108**, 1067.

Zhang, J., Xu, Z., Wei, Y., Shuang, S. & Dong, C. (2008) "Spectral properties of intramolecular charge transfer fluorescence probe 1-keto-2-(*p*-dimethylaminobenzal)-tetrahydronaphthalene", *Spectrochim. Acta, Part A*, **70**, 888-891.

Zhicheng, X., Guan, B. and Chuan, D. (2005) "Studies on interaction of an Intramolecular charge transfer fluorescence probe: 4'-Dimethylamino-2,5-dihydroxychalcone with DNA", *Bioorg. Med. Chem*, **13**, 5694-5699.

APPENDIX

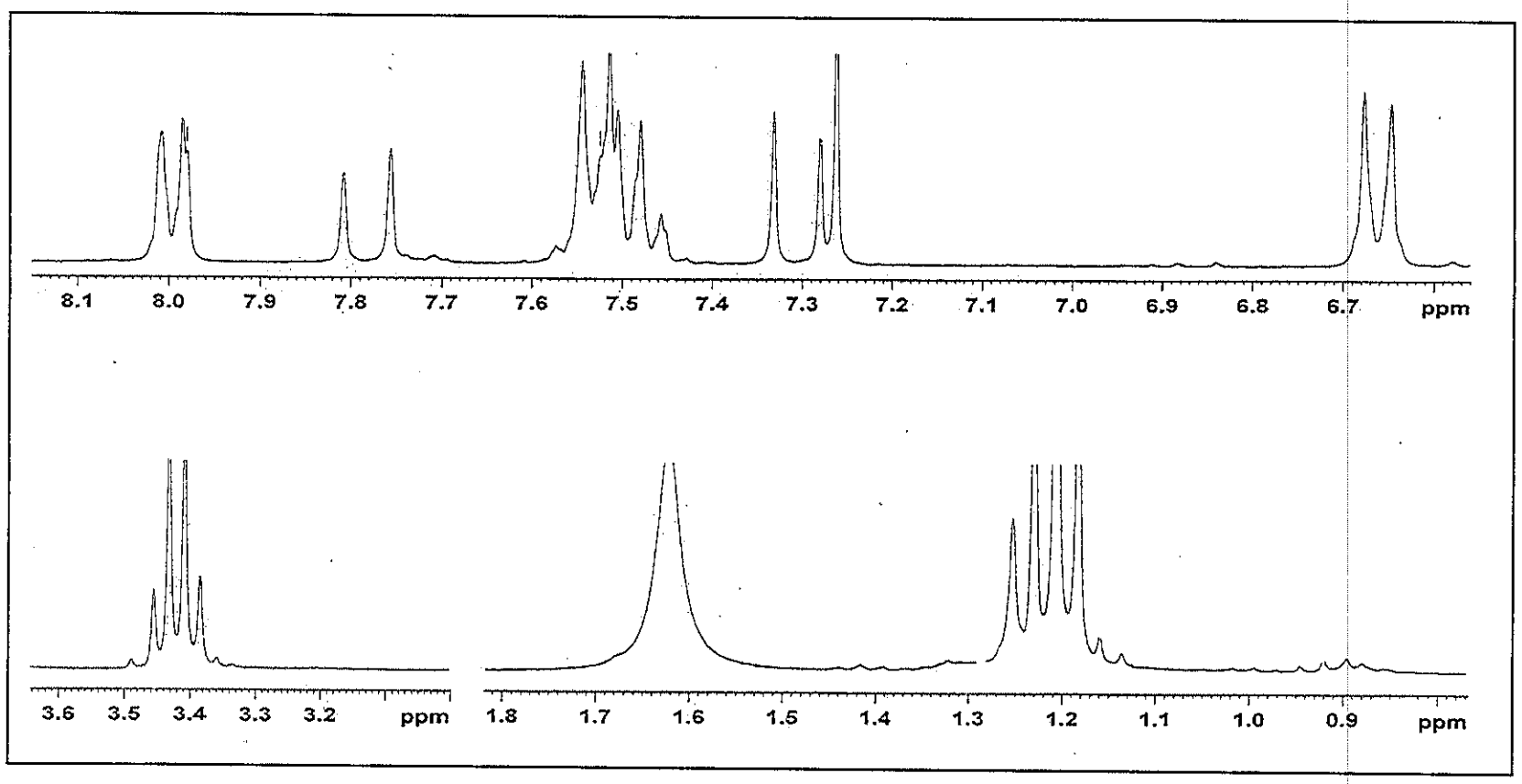

Figure 49 ^{1}H NMR (300 MHz, $CDCl_3$) spectrum of compound **TKB1**

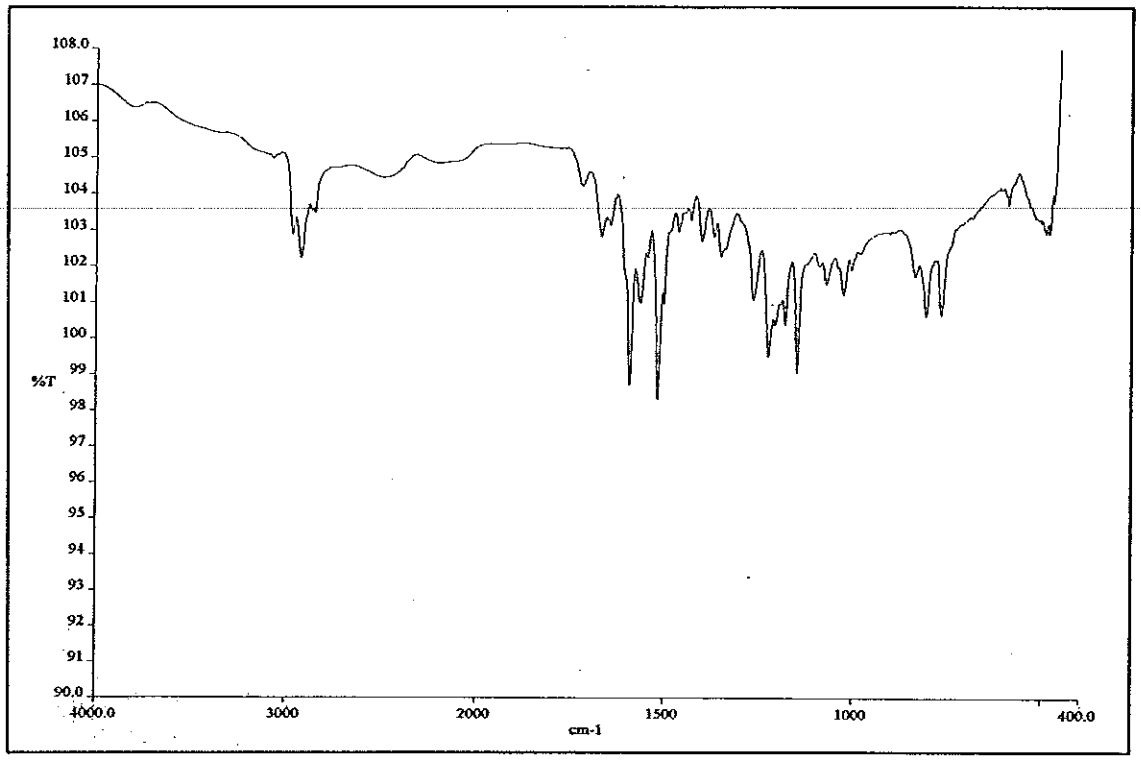

Figure 50 FT-IR (neat) spectrum of compound **TKB1**

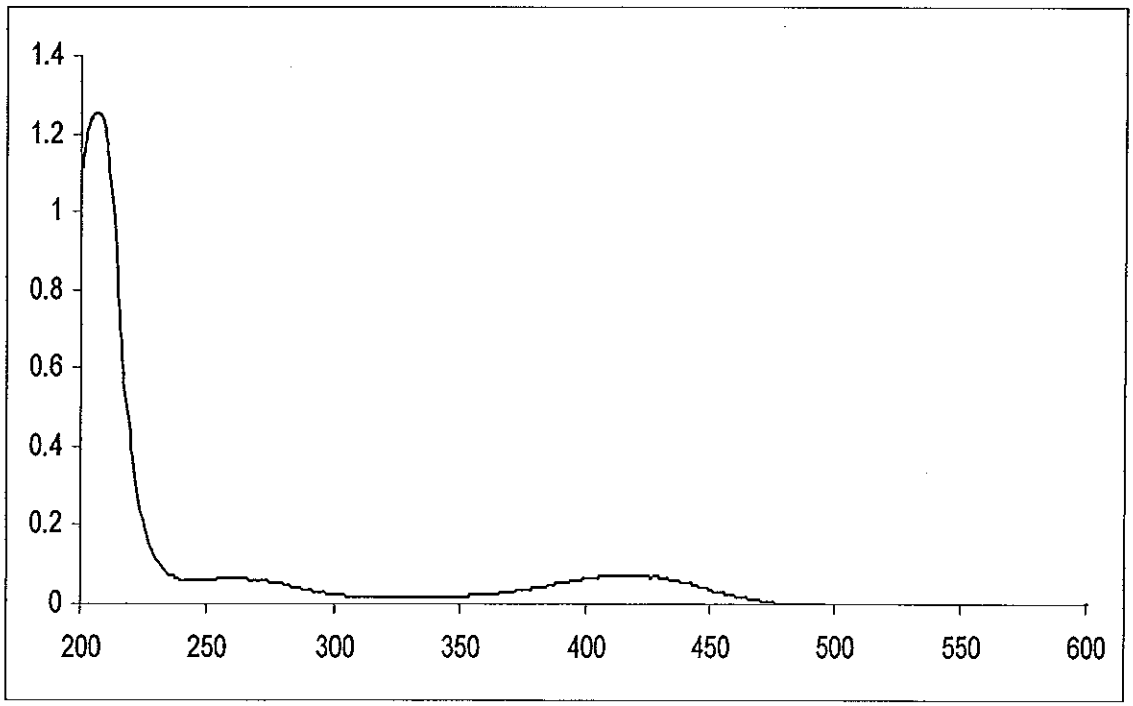

Figure 51 UV-Vis spectrum of compound **TKB1**

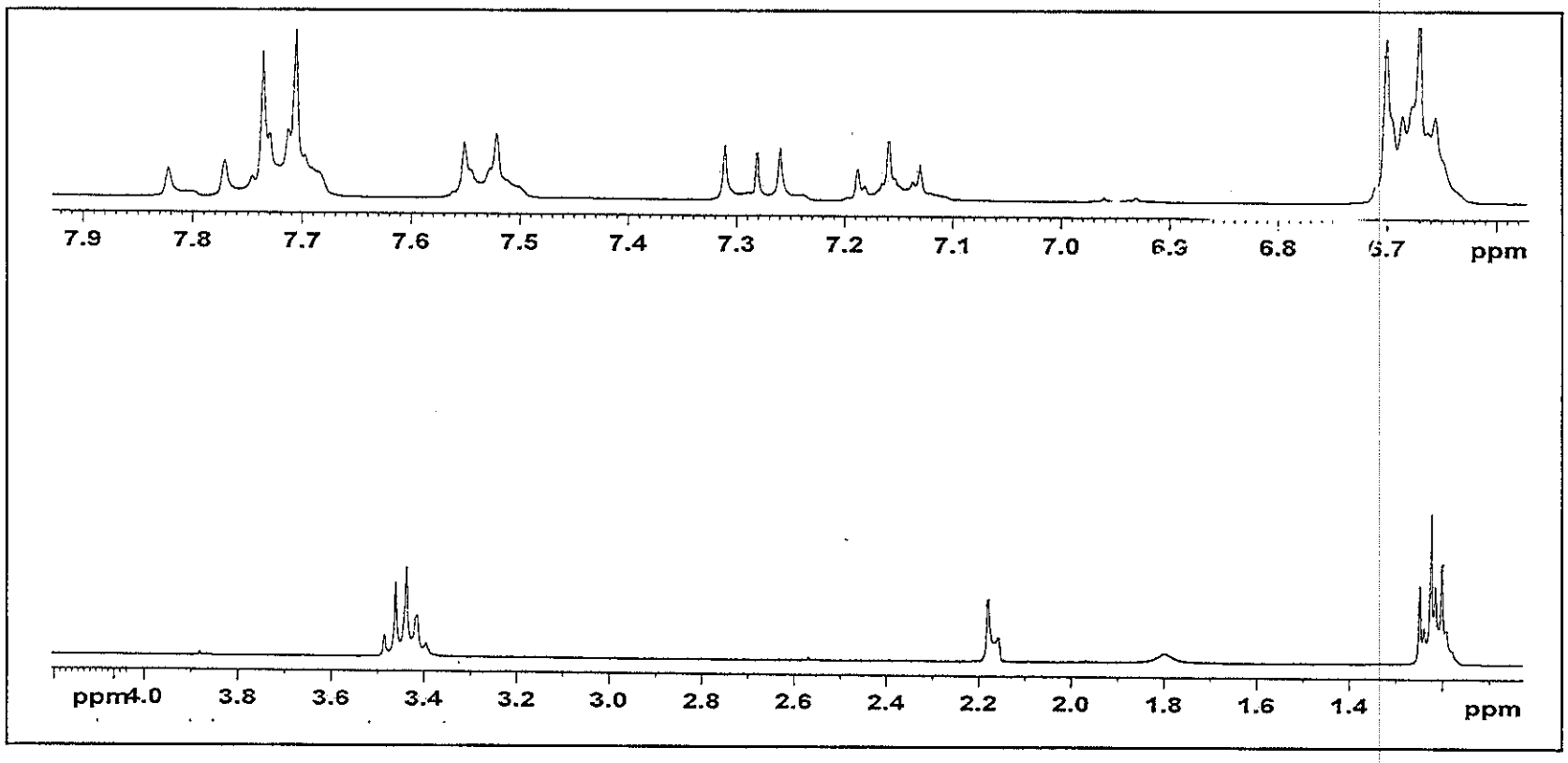

Figure 52 ^{1}H NMR (300 MHz, $CDCl_3$) spectrum of compound **TKB2**

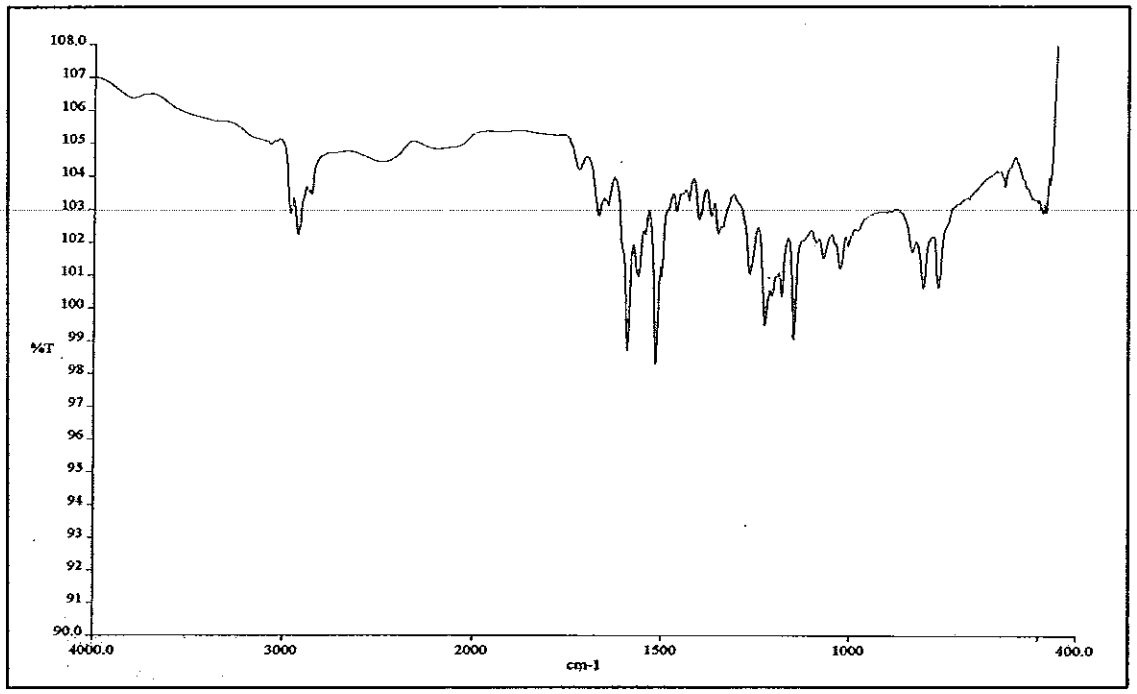

Figure 53 FT-IR (neat) spectrum of compound **TKB2**

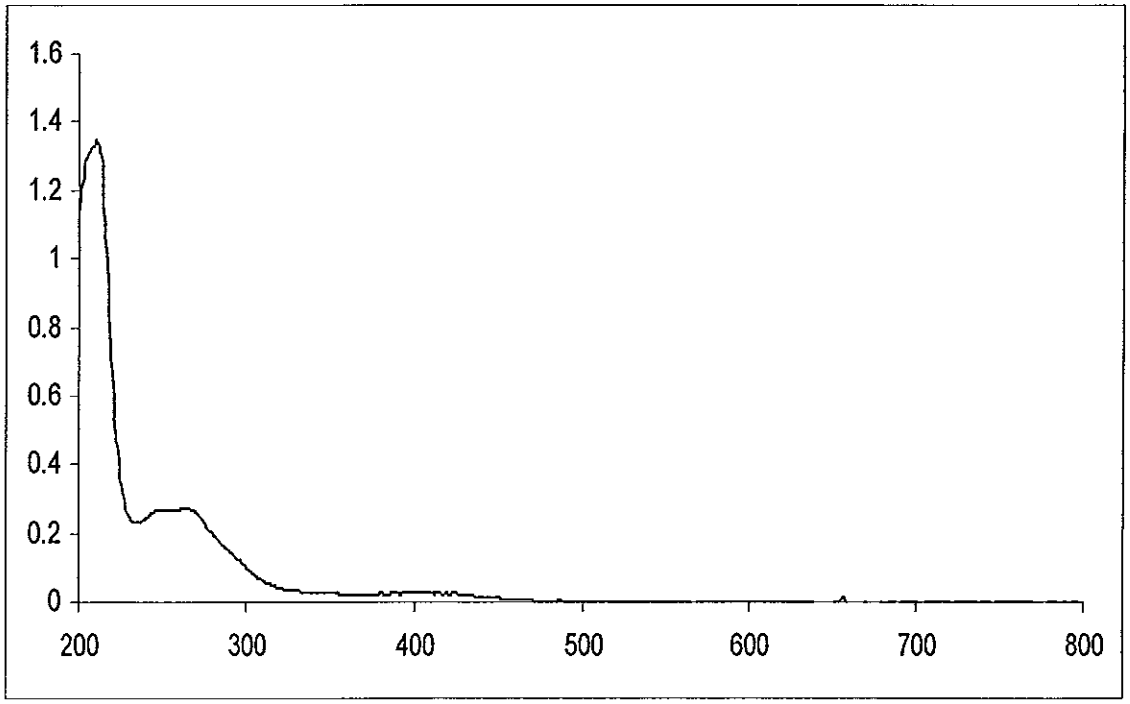

Figure 54 UV-Vis spectrum of compound **TKB2**

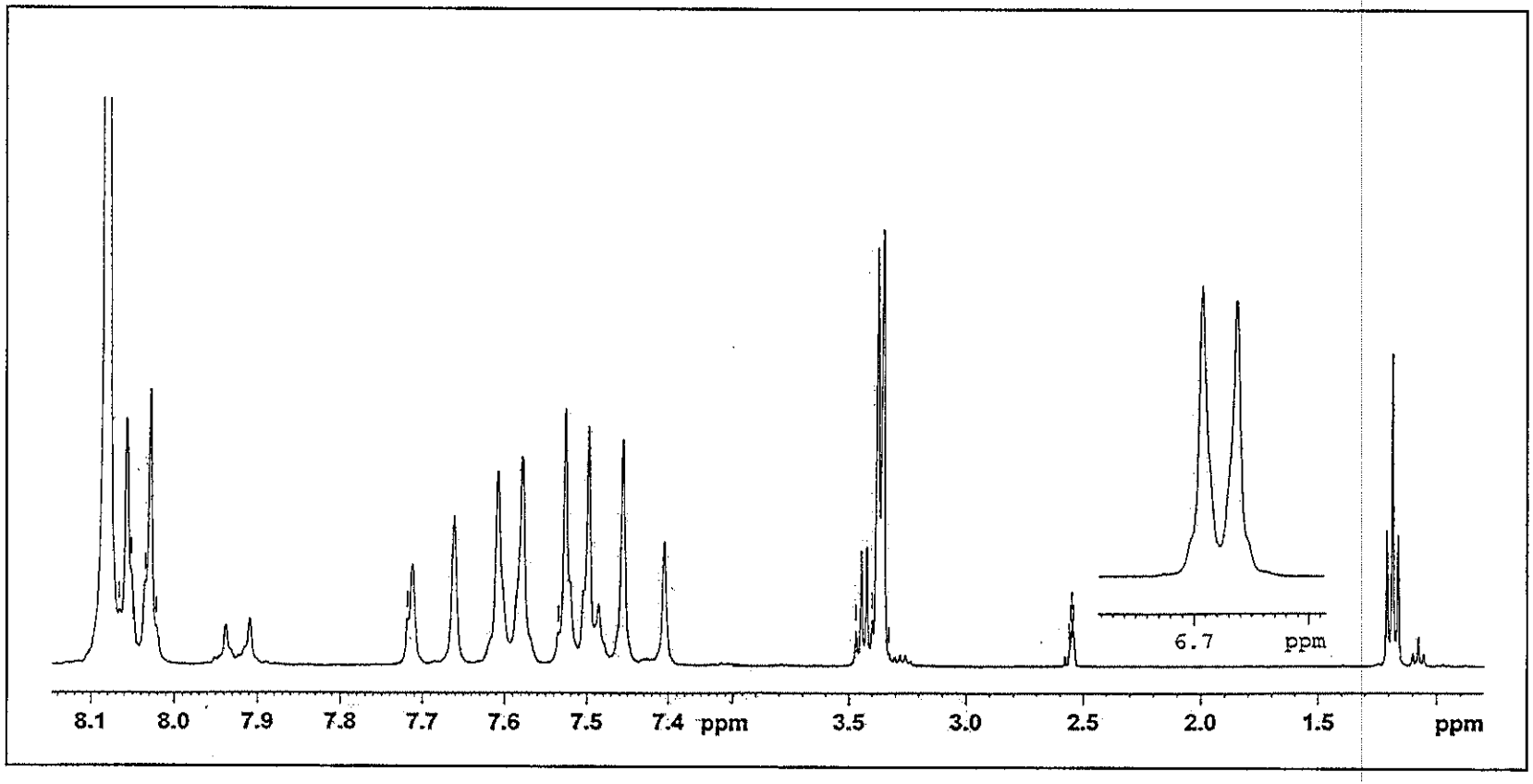

Figure 55 ^{1}H NMR (300 MHz, $CDCl_3$) spectrum of compound **TKB3**

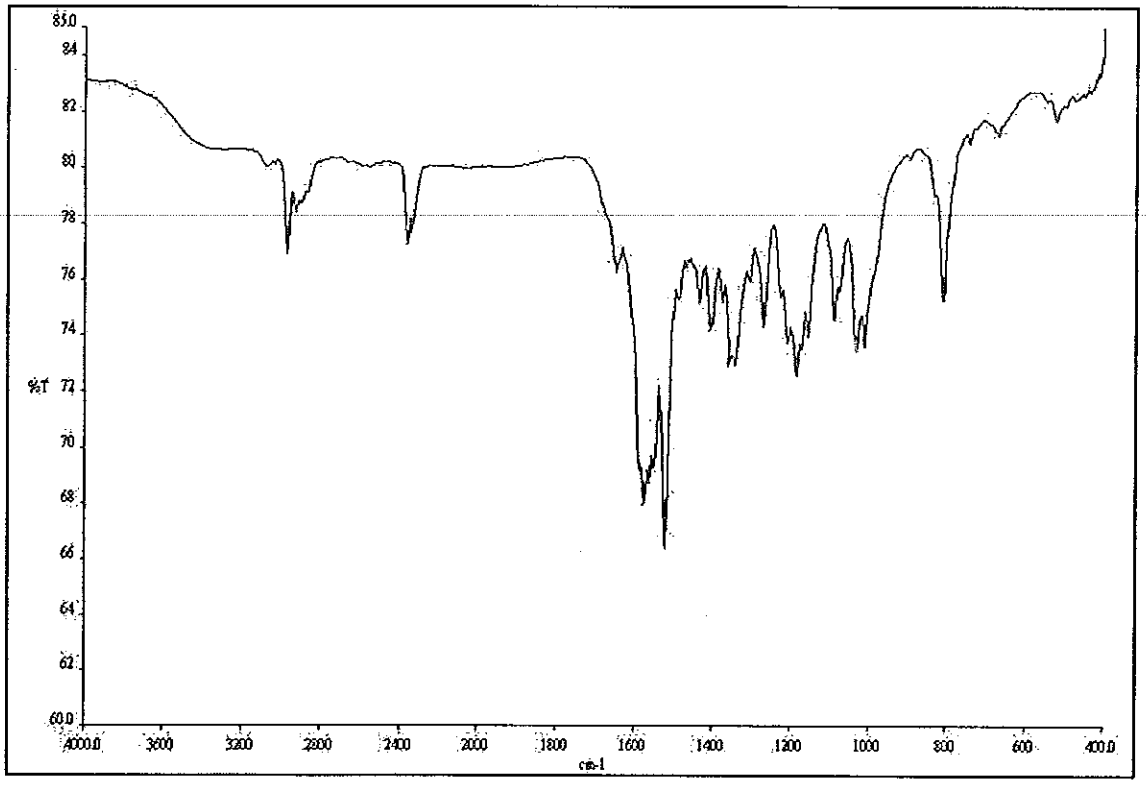

Figure 56 FT-IR (KBr) spectrum of compound **TKB3**

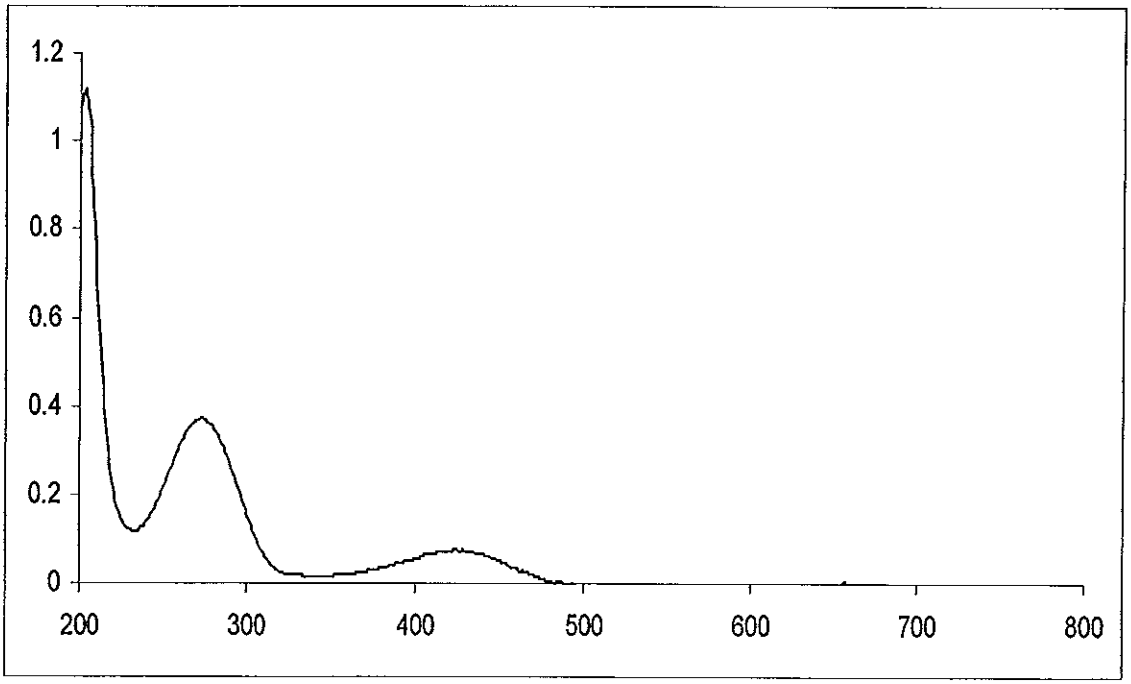

Figure 57 UV-Vis spectrum of compound **TKB3**

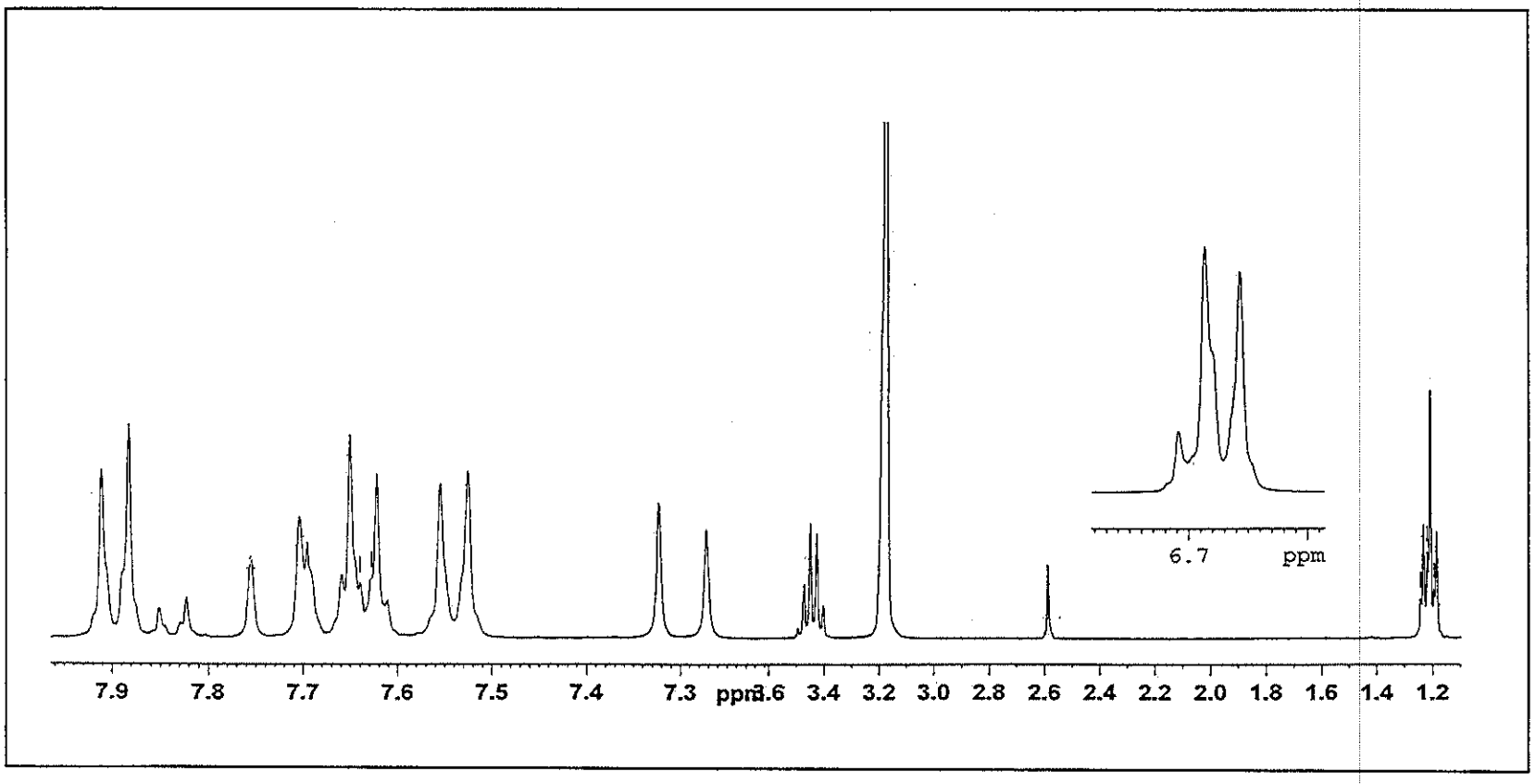

Figure 58 ^{1}H NMR (300 MHz, $CDCl_3$) spectrum of compound **TKB4**

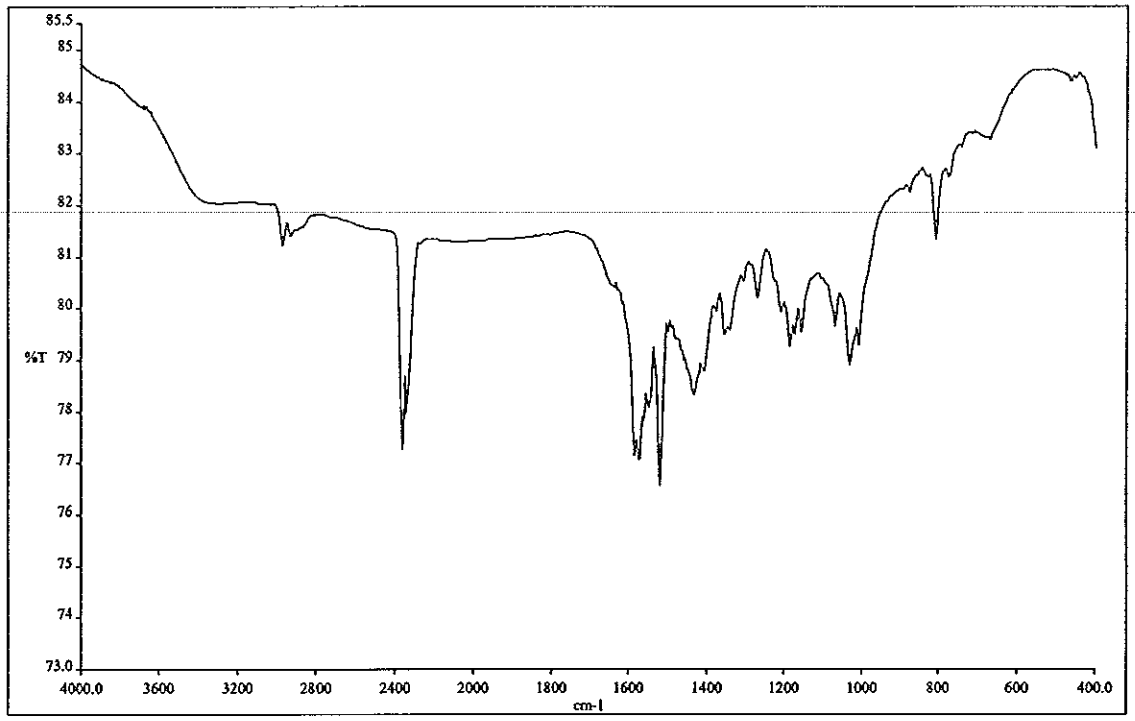

Figure 59 FT-IR (KBr) spectrum of compound **TKB4**

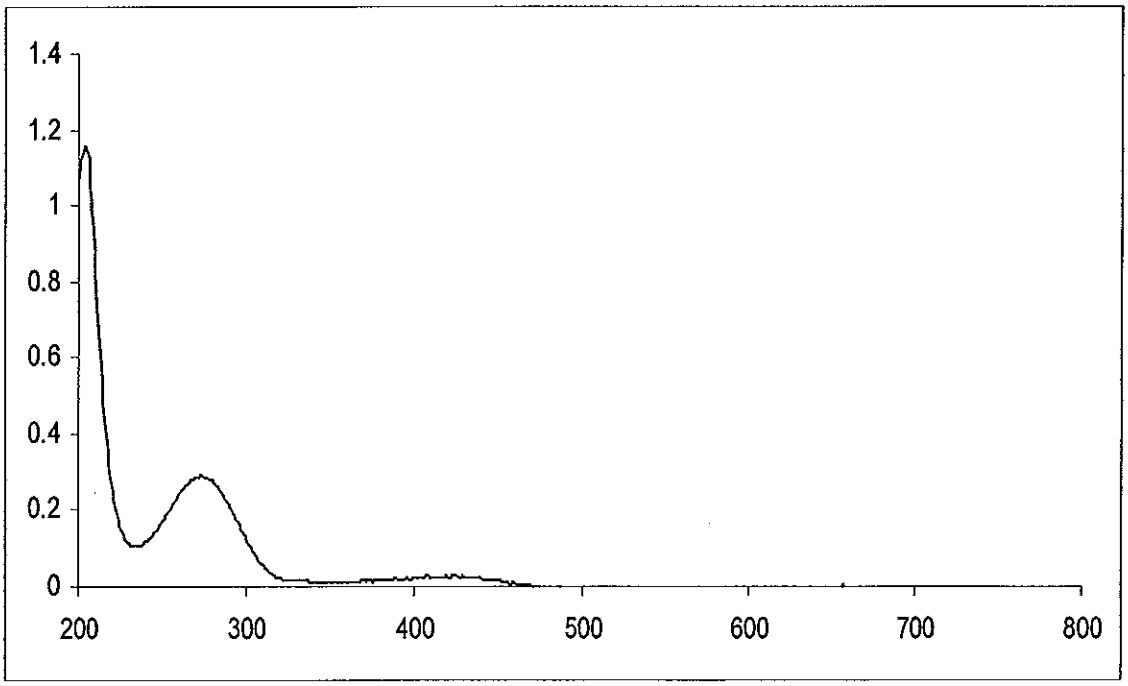

Figure 60 UV-Vis spectrum of compound **TKB4**

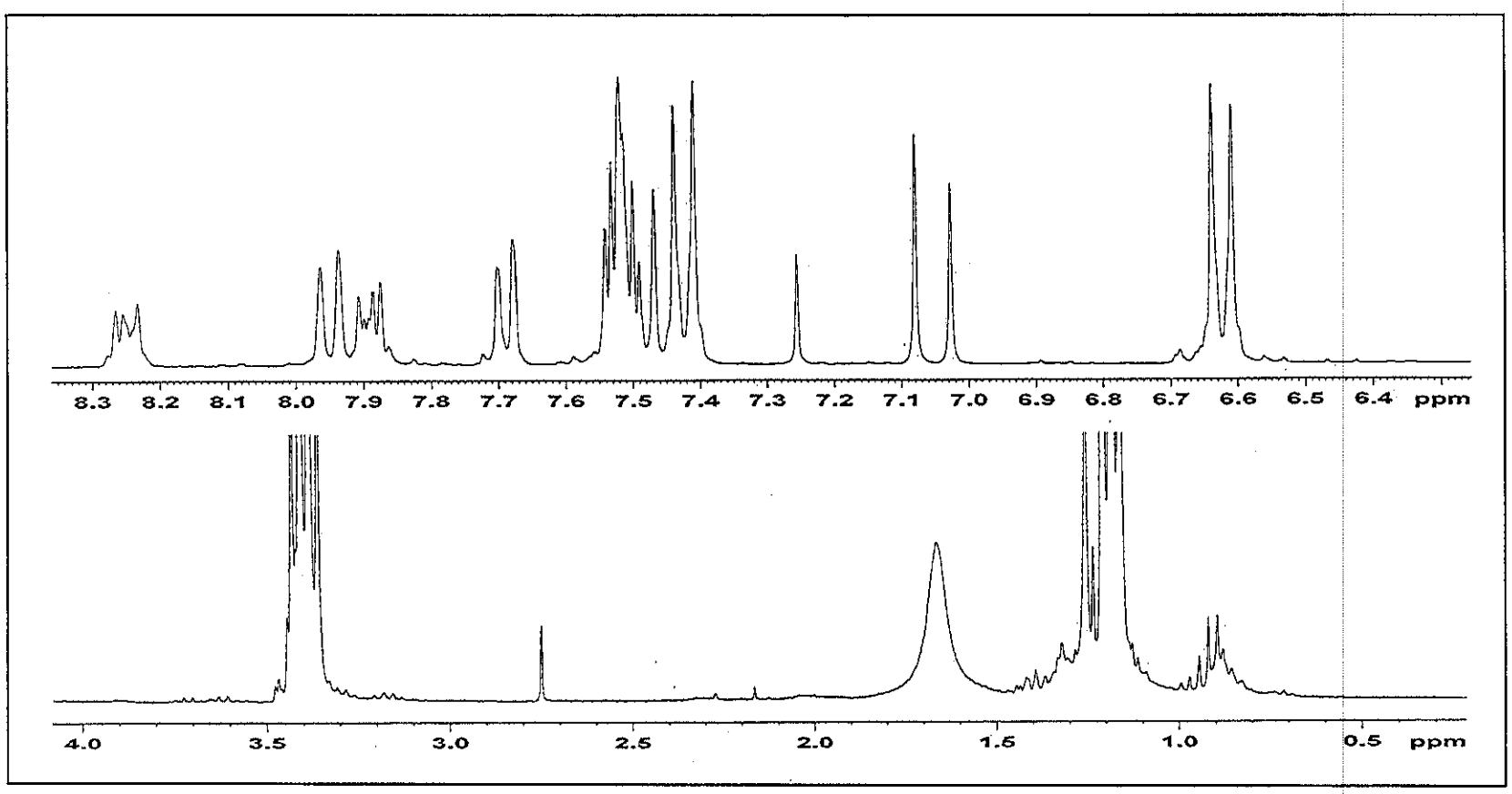

Figure 61 ^{1}H NMR (300 MHz, $CDCl_3$) spectrum of compound **TKB5**

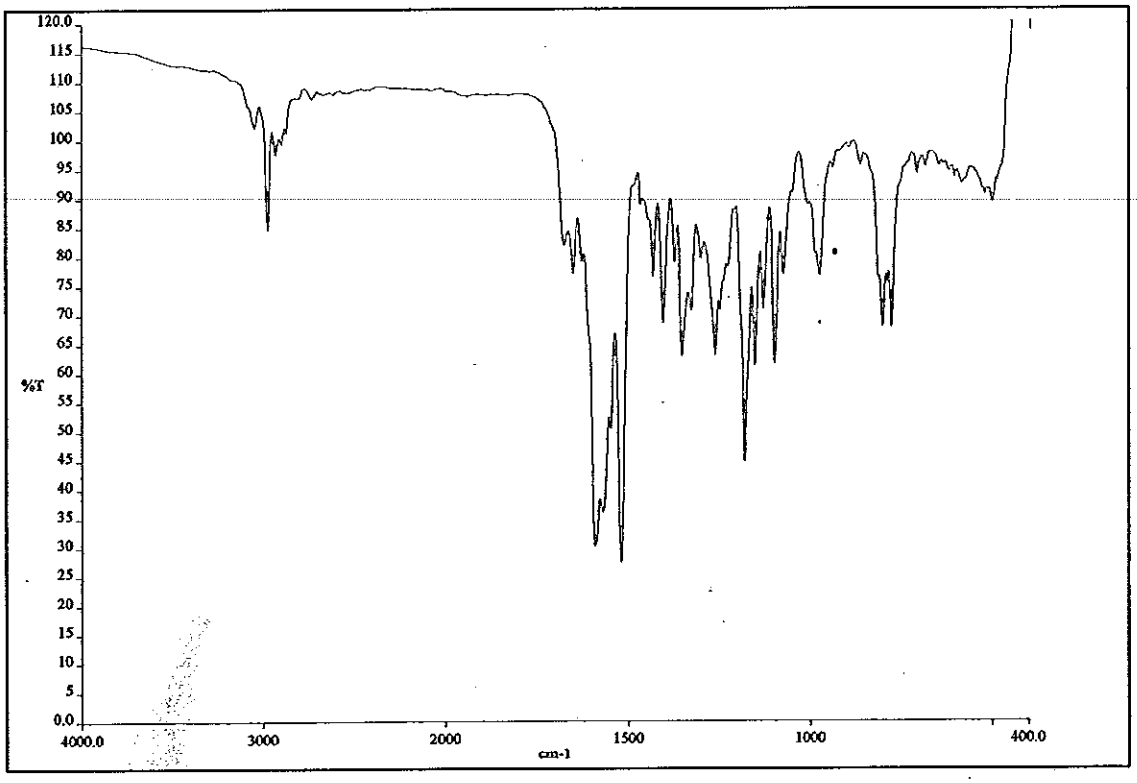

Figure 62 FT-IR (neat) spectrum of compound **TKB5**

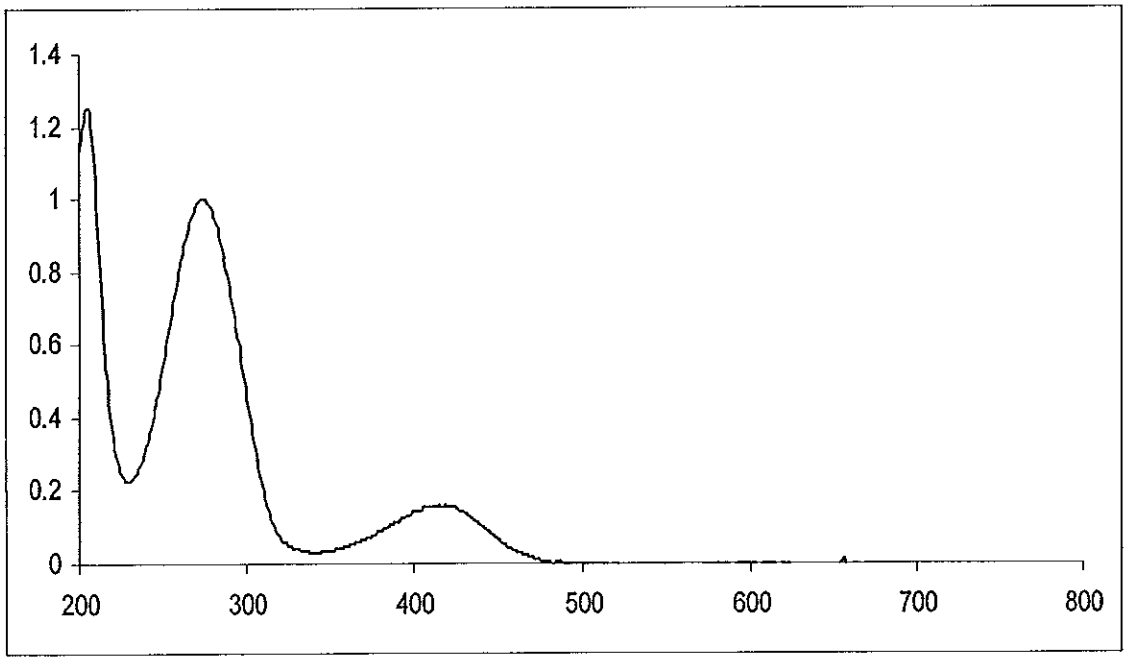

Figure 63 UV-Vis spectrum of compound **TKB5**

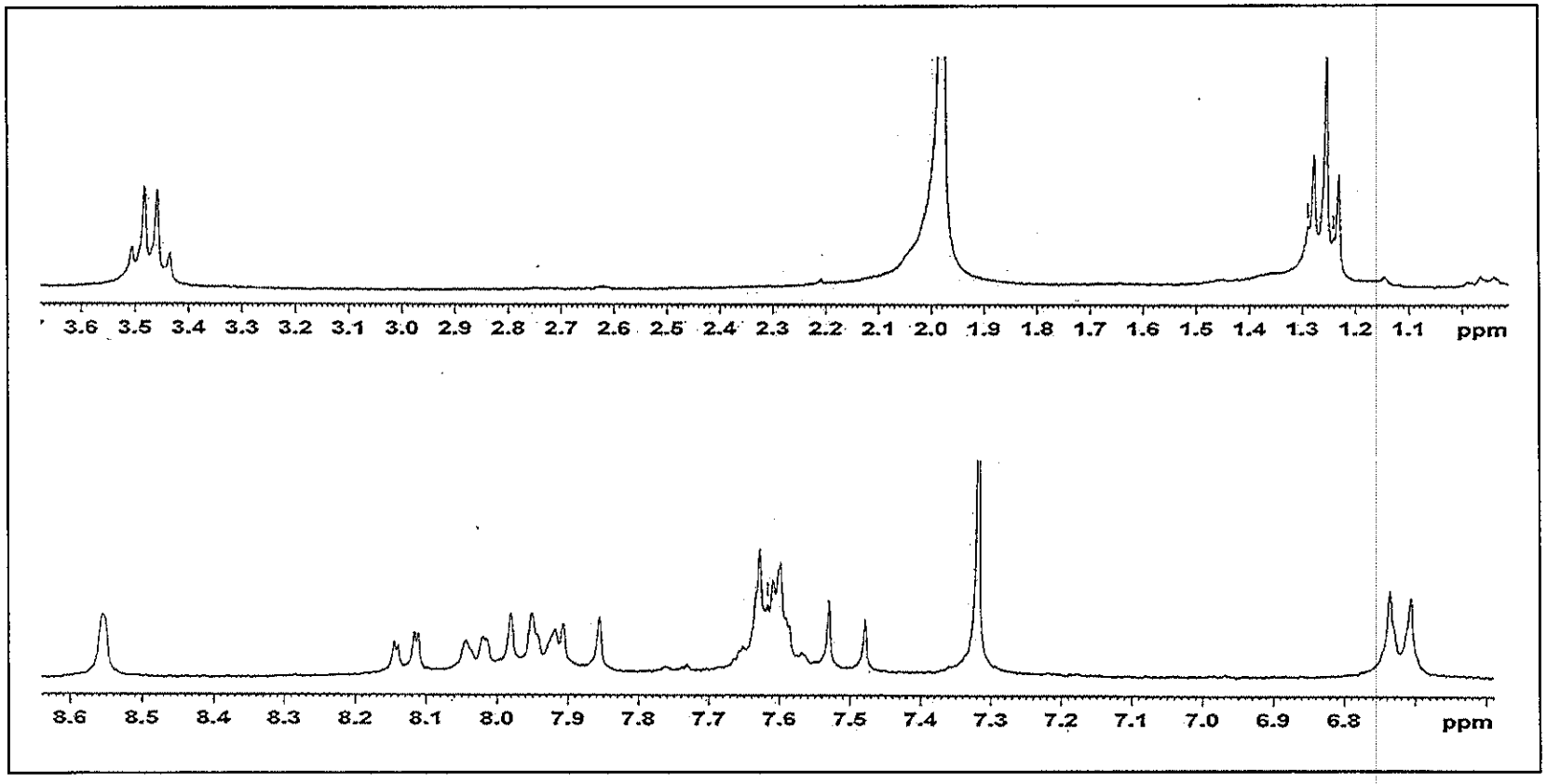

Figure 64 ^{1}H NMR (300 MHz, $CDCl_3$) spectrum of compound **TKB6**

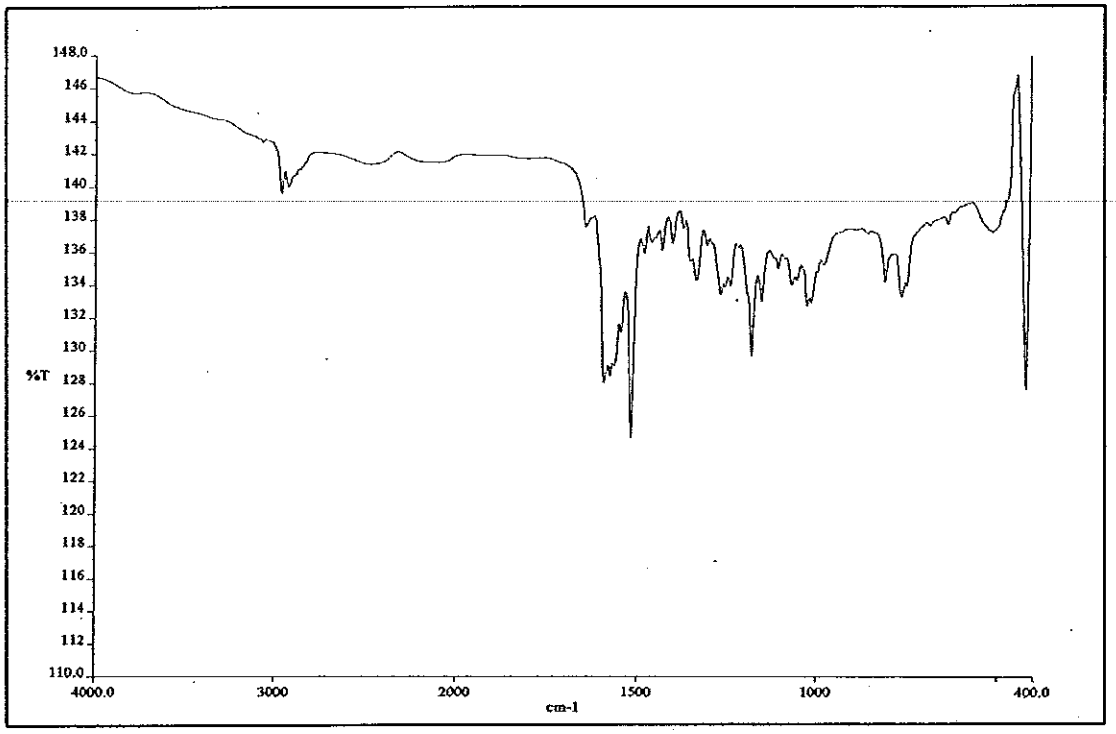

Figure 65 FT-IR (neat) spectrum of compound **TKB6**

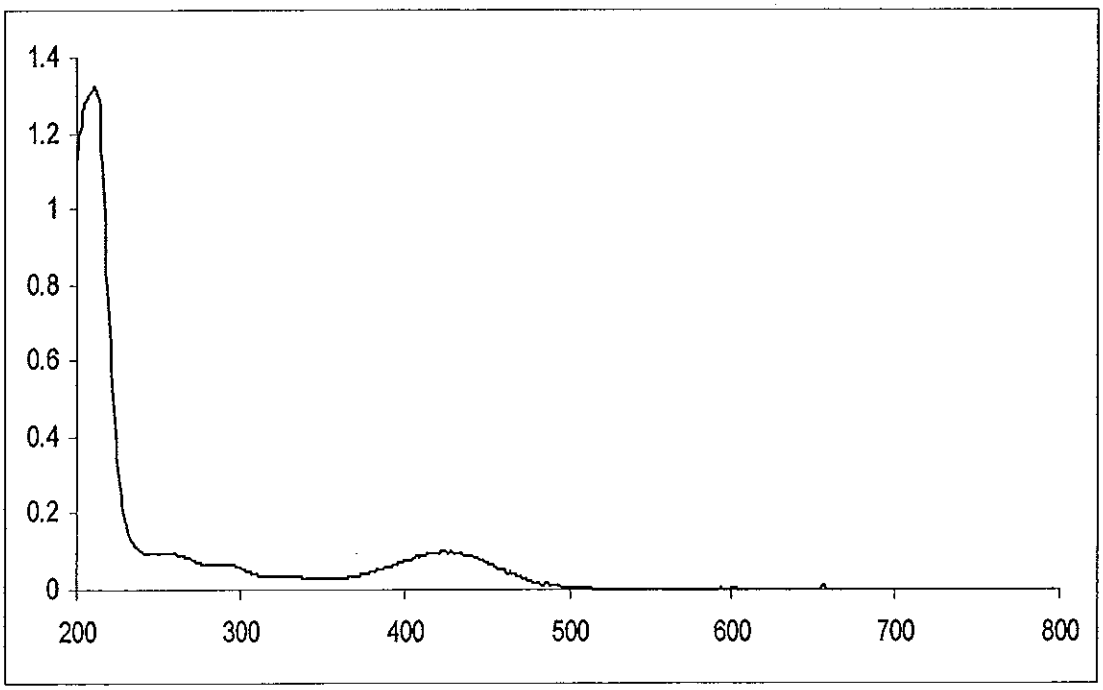

Figure 66 UV-Vis spectrum of compound **TKB6**

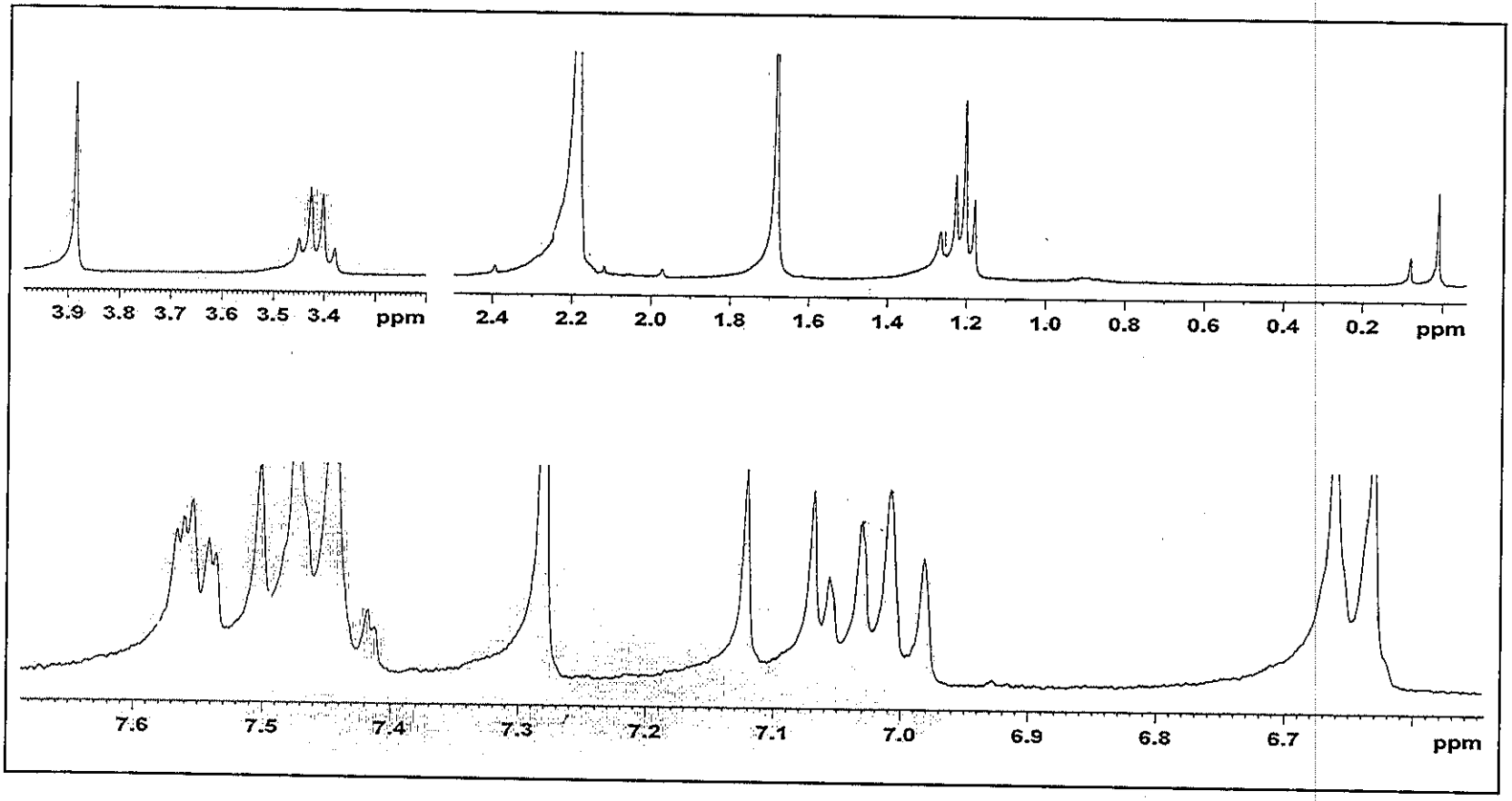

Figure 67 ^{1}H NMR (300 MHz, $CDCl_3$) spectrum of compound **TKB7**

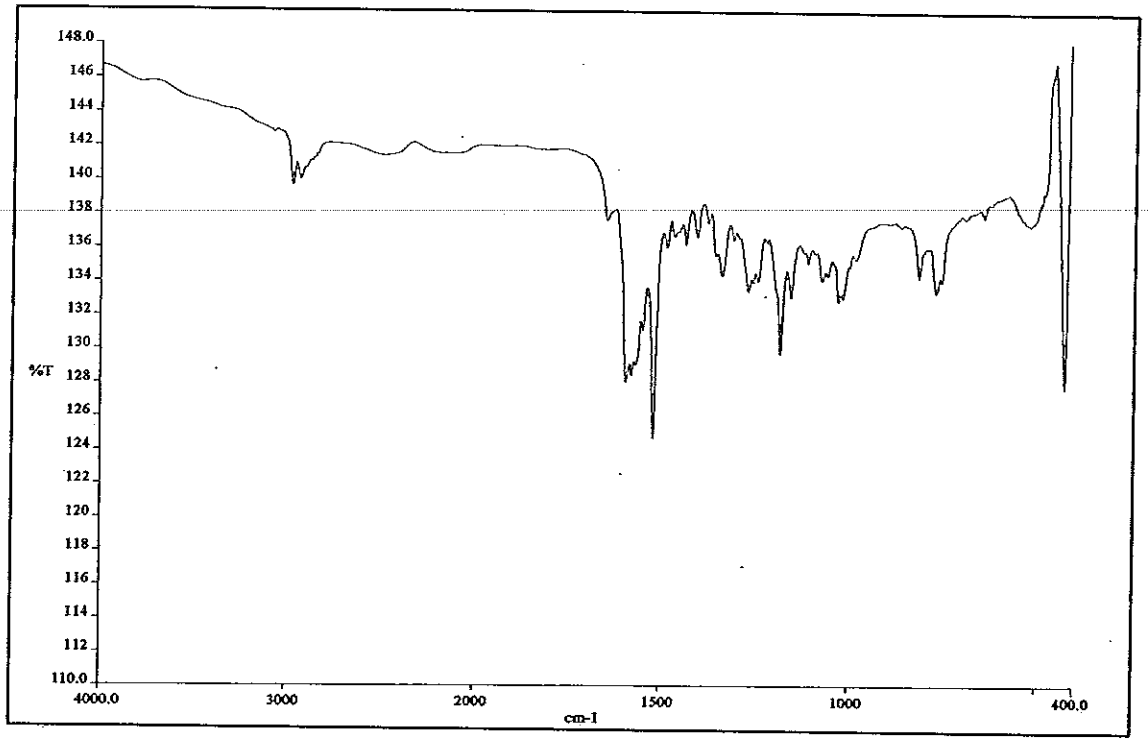

Figure 68 FT-IR (neat) spectrum of compound **TKB7**

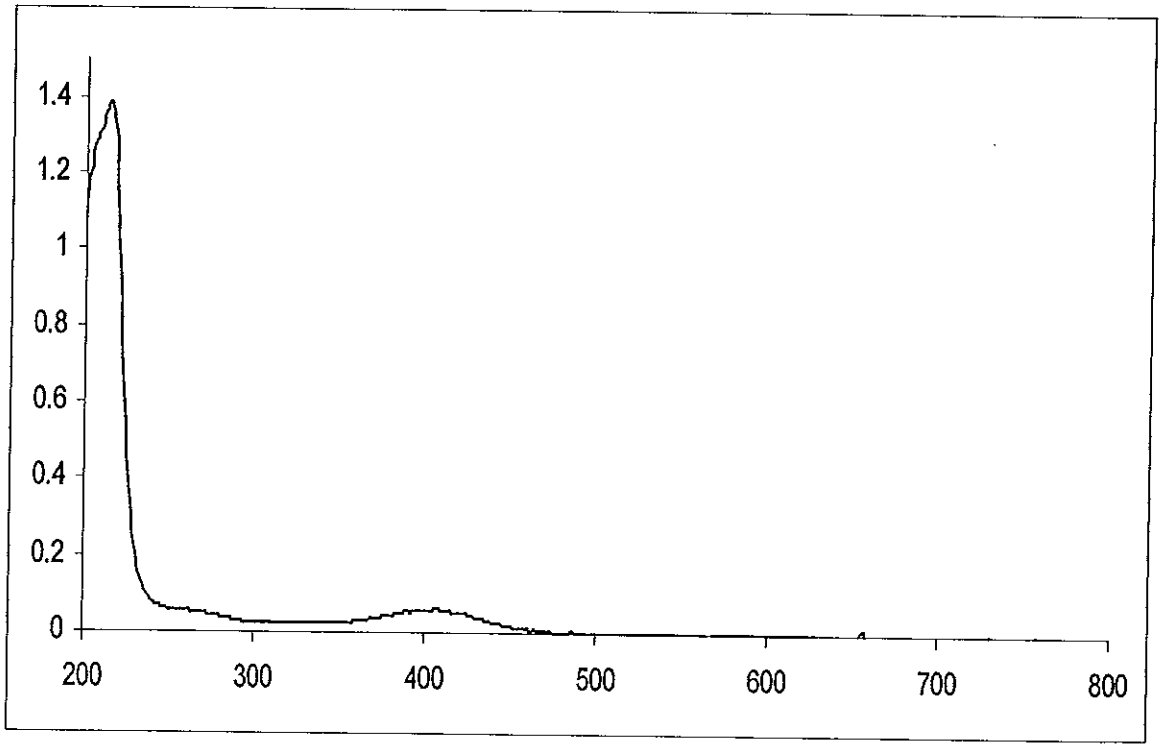

Figure 69 UV-Vis spectrum of compound **TKB7**

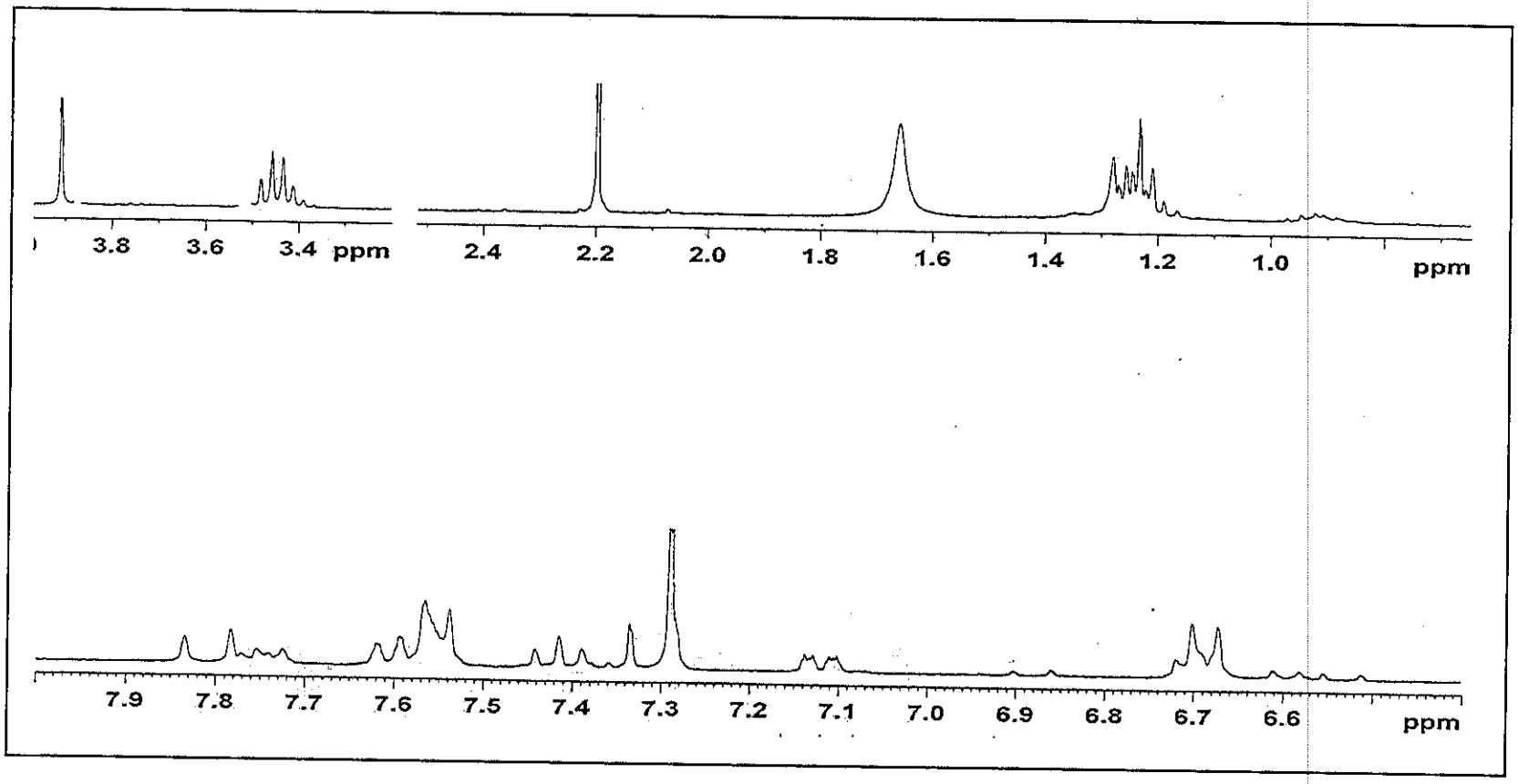

Figure 70 ^{1}H NMR (300 MHz, $CDCl_3$) spectrum of compound **TKB8**

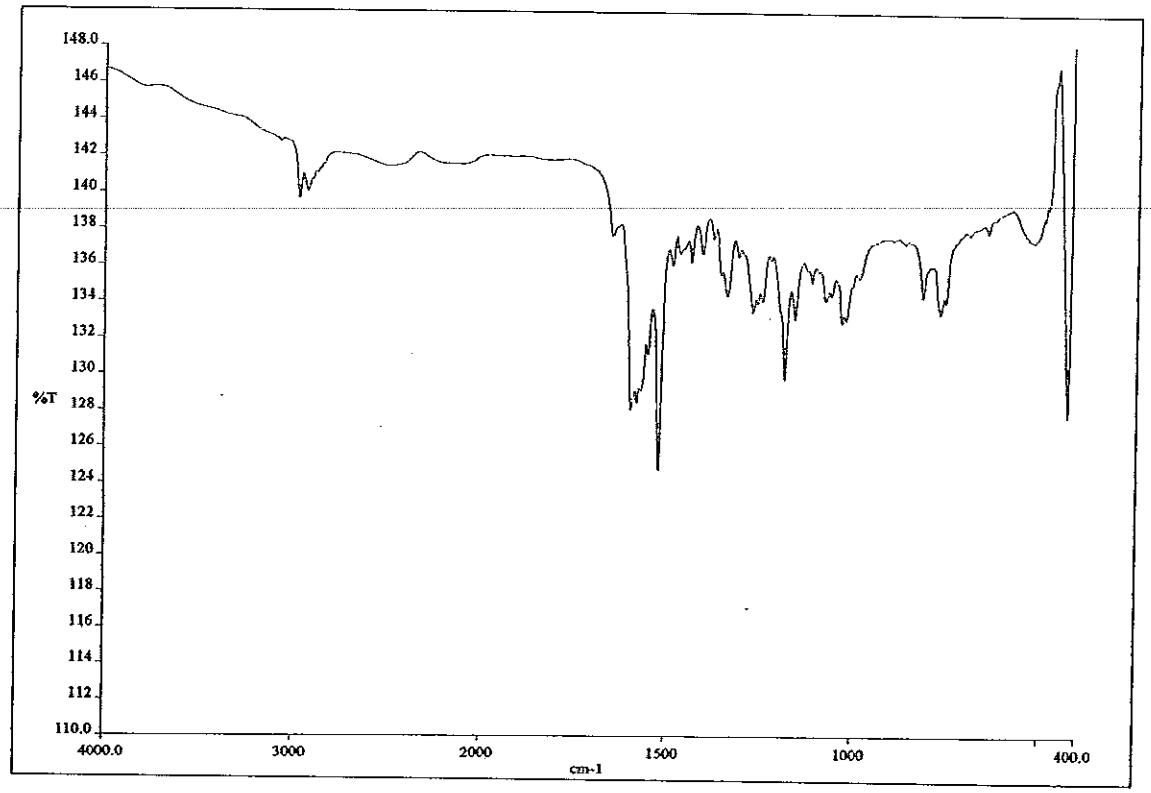

Figure 71 FT-IR (neat) spectrum of compound **TKB8**

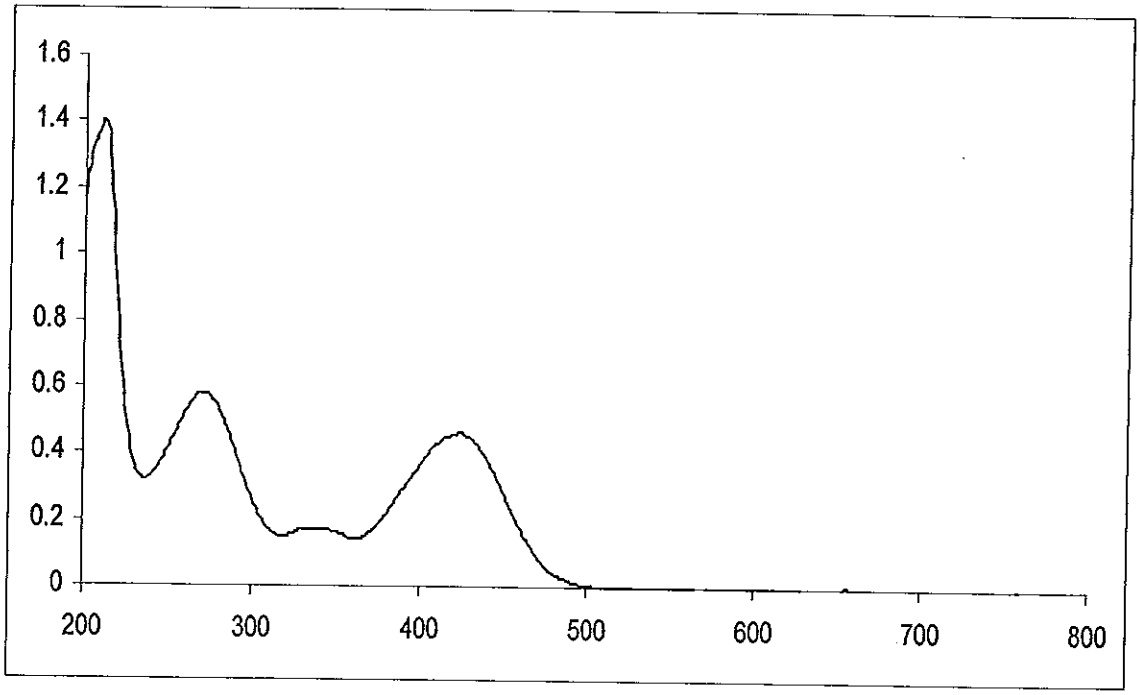

Figure 72 UV-Vis spectrum of compound **TKB8**

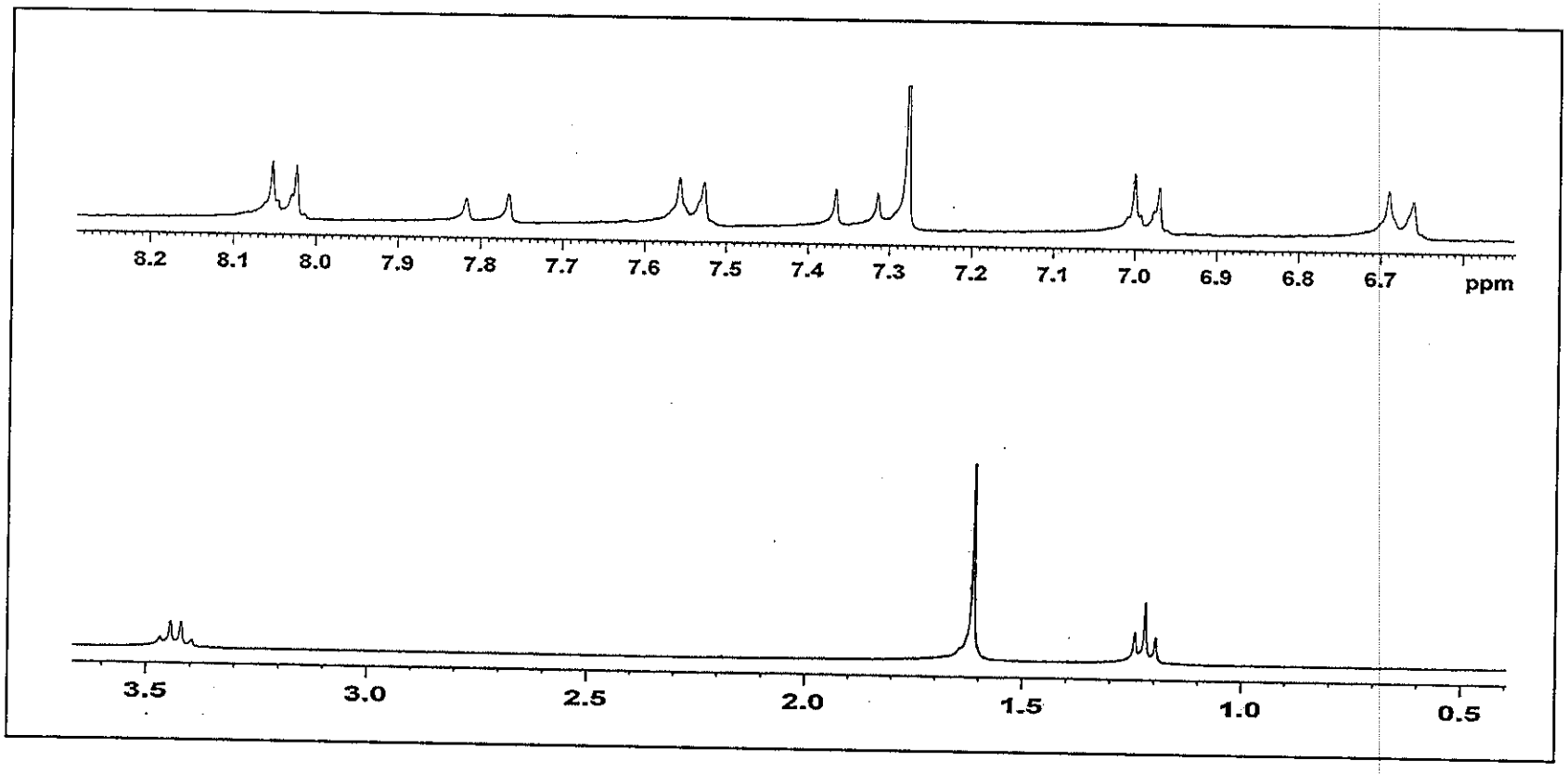

Figure 73 ^{1}H NMR (300 MHz, $CDCl_3$) spectrum of compound **TKB9**

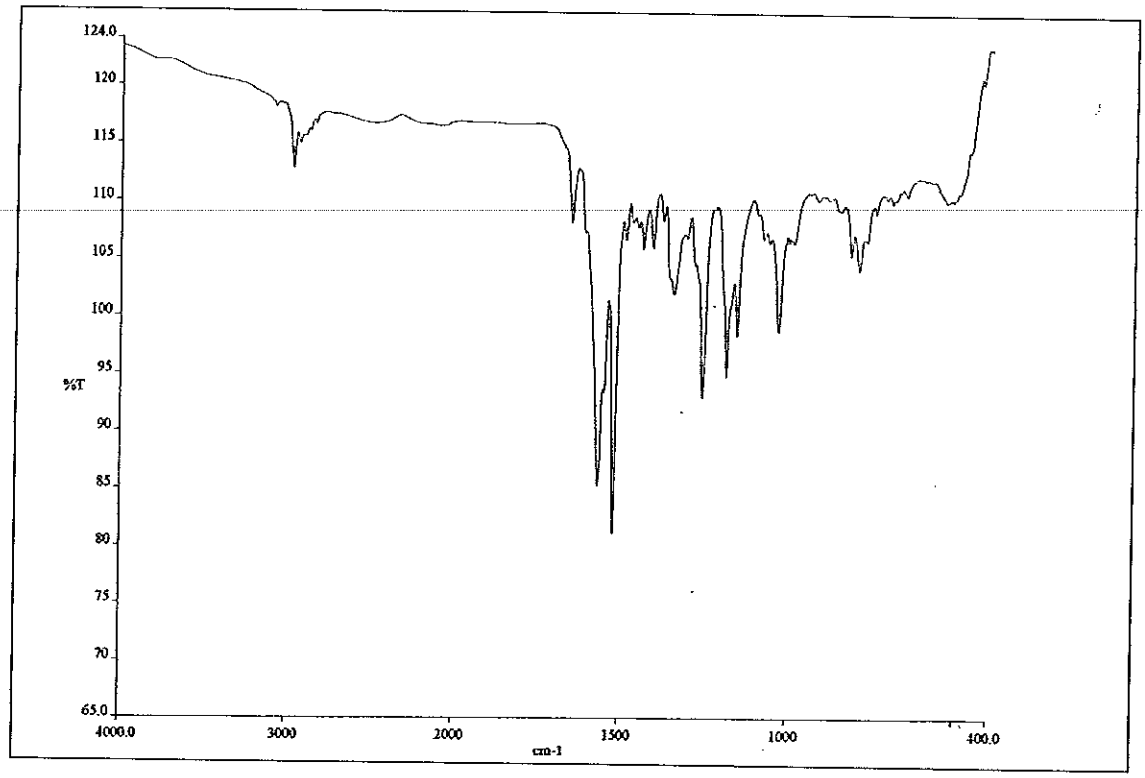

Figure 74 FT-IR (neat) spectrum of compound **TKB9**

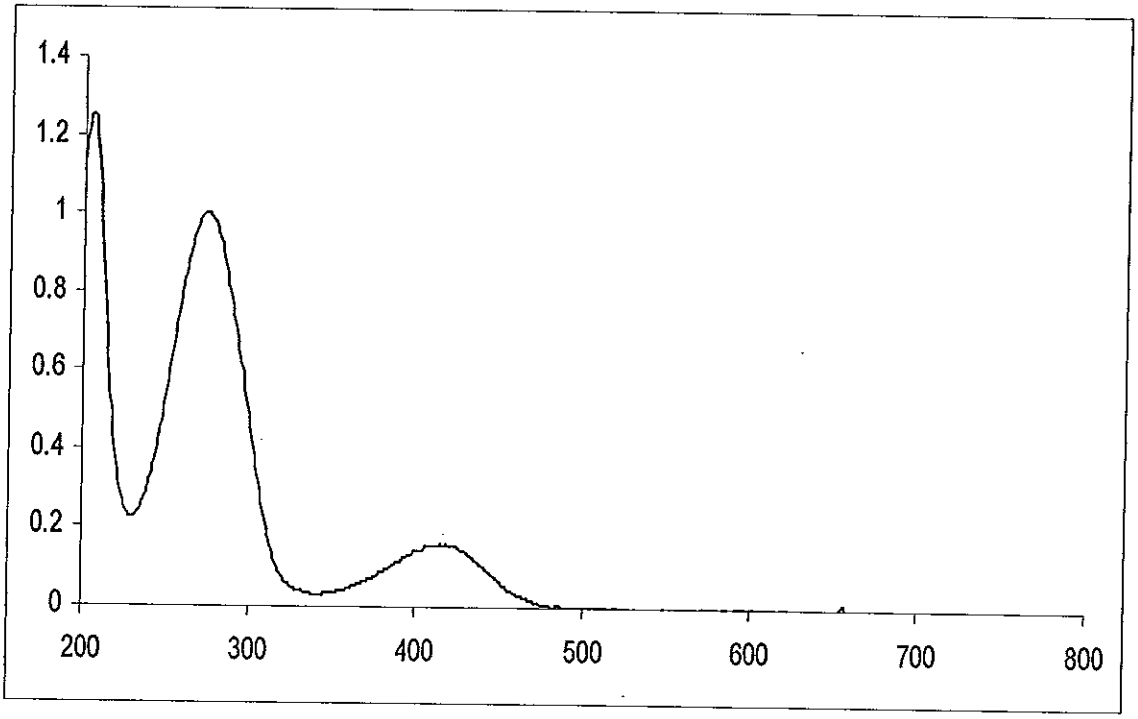

Figure 75 UV-Vis spectrum of compound **TKB9**

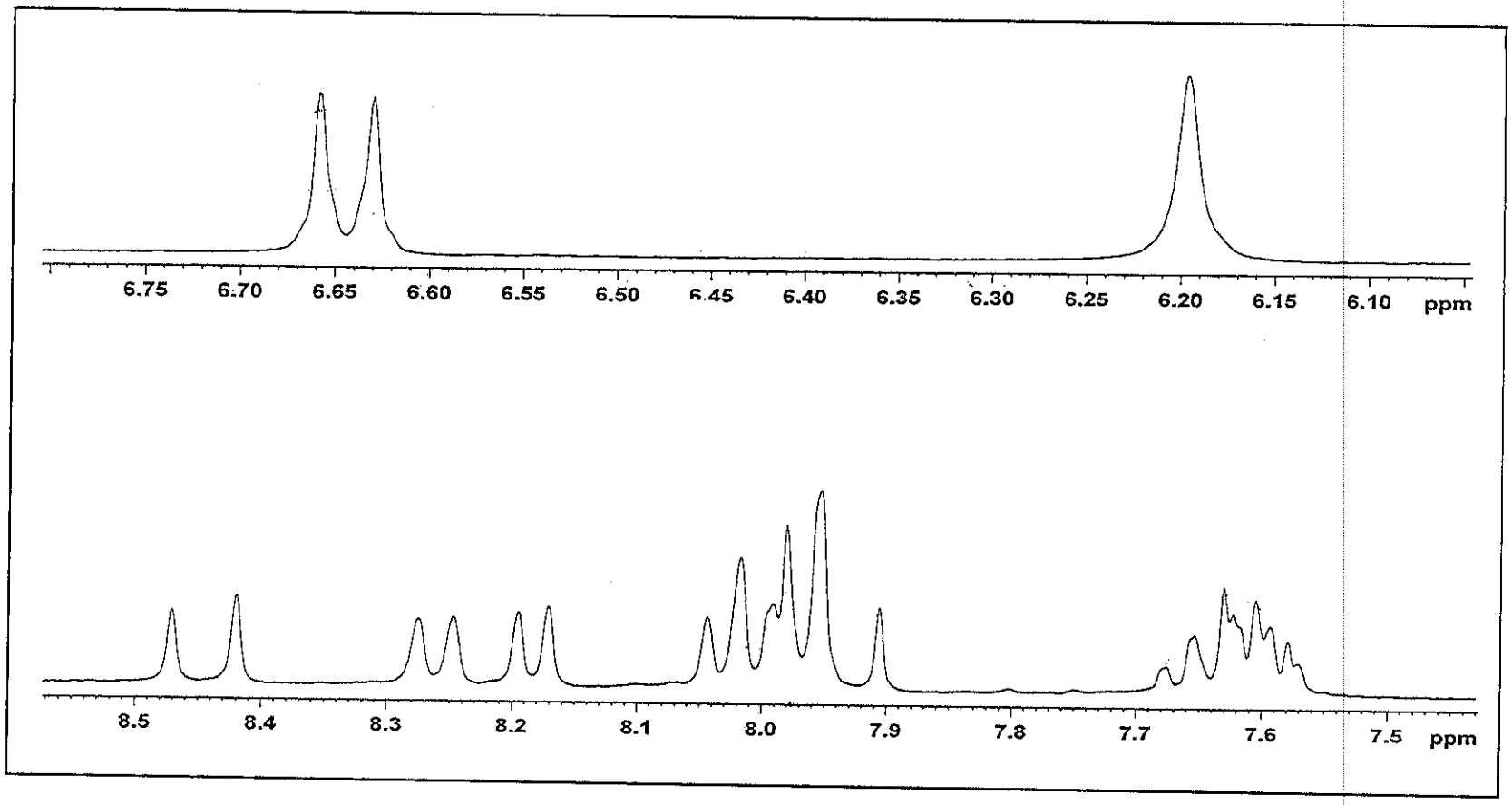

Figure 76 ^{1}H NMR (300 MHz, $CDCl_3$) spectrum of compound **TKD2**

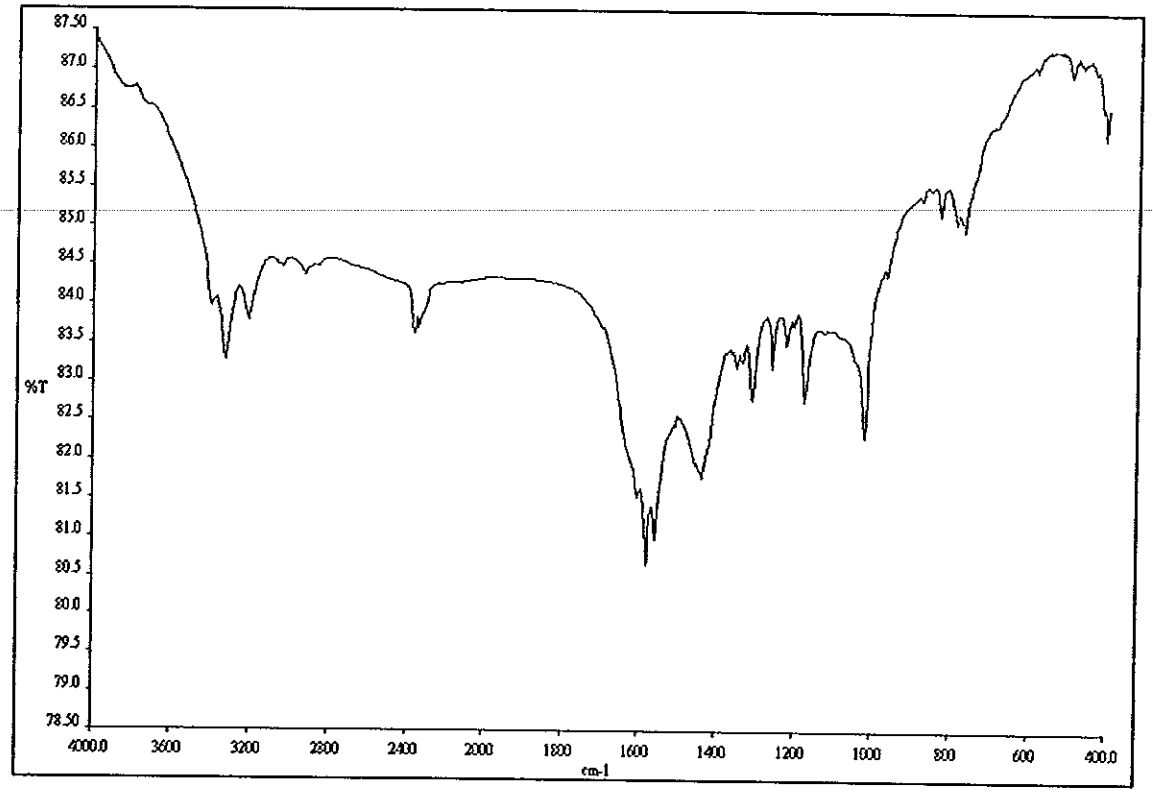

Figure 77 FT-IR (KBr) spectrum of compound **TKD2**

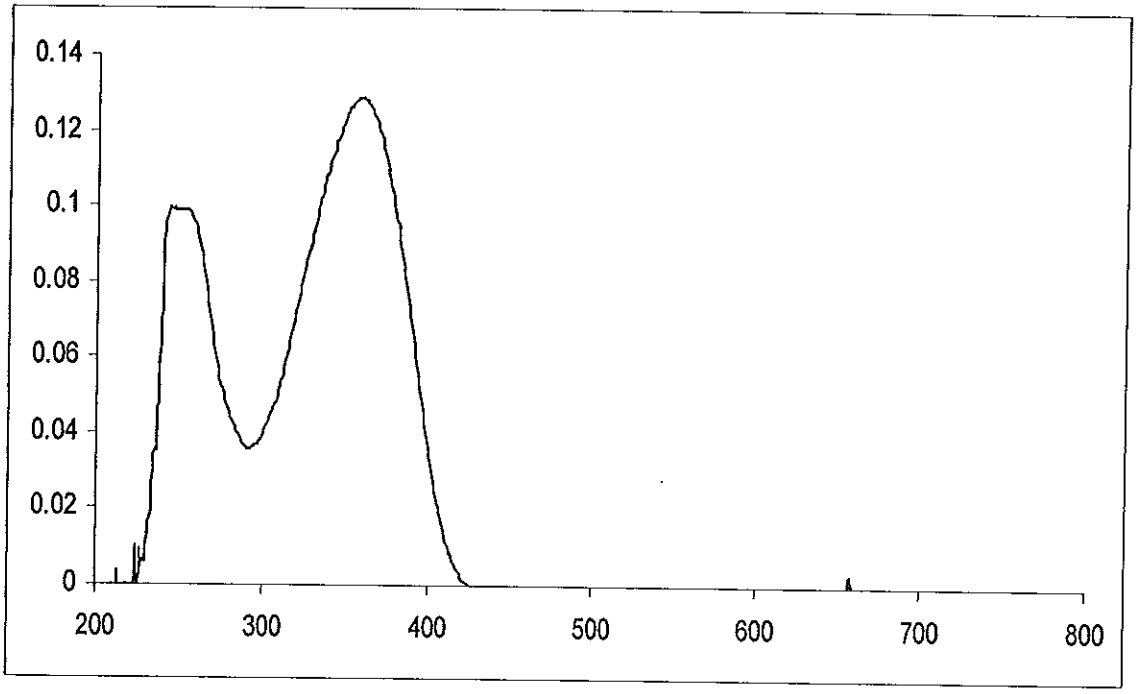

Figure 78 UV-Vis spectrum of compound **TKD2**

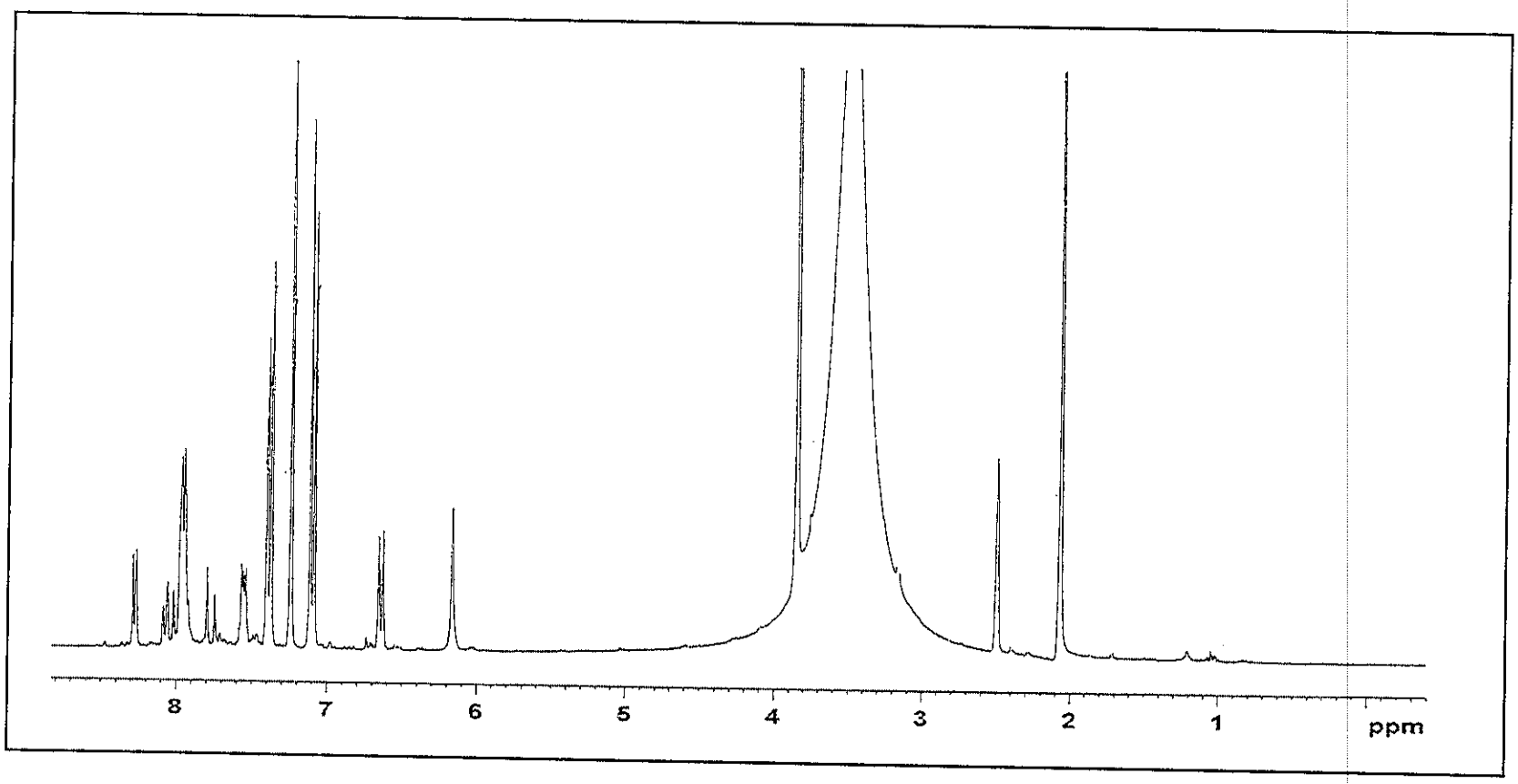

Figure 79 ^{1}H NMR (300 MHz, $CDCl_3$) spectrum of compound **TKD3**

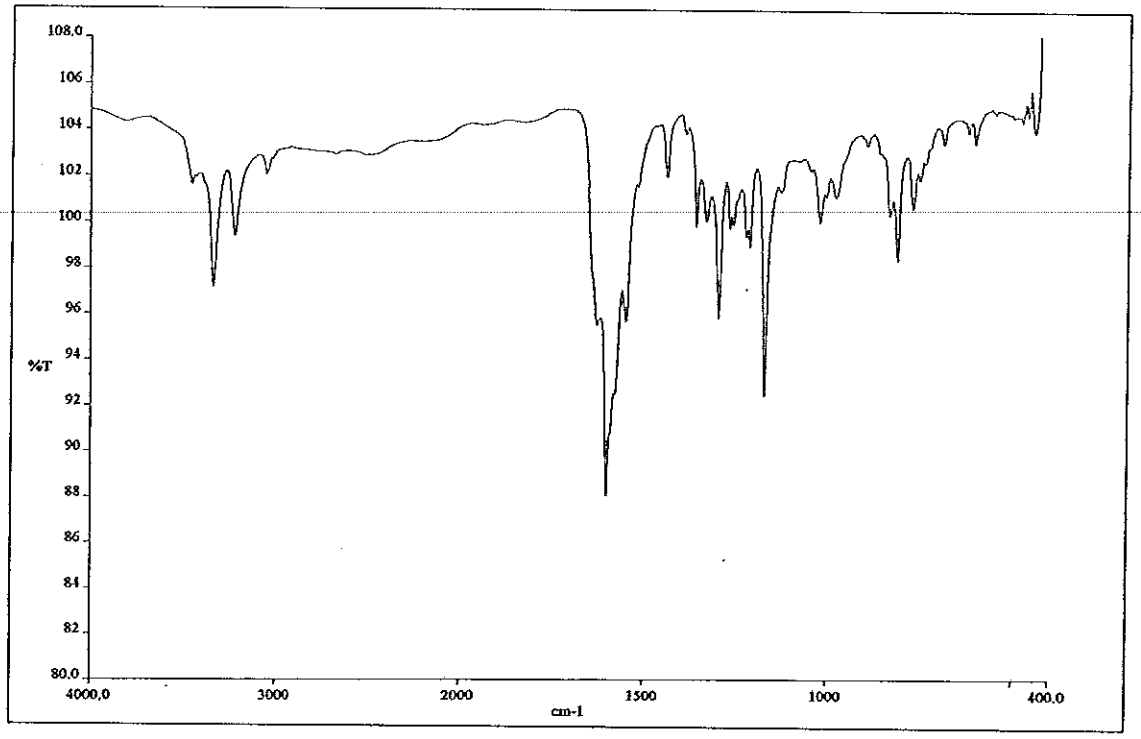

Figure 80 FT-IR (KBr) spectrum of compound **TKD3**

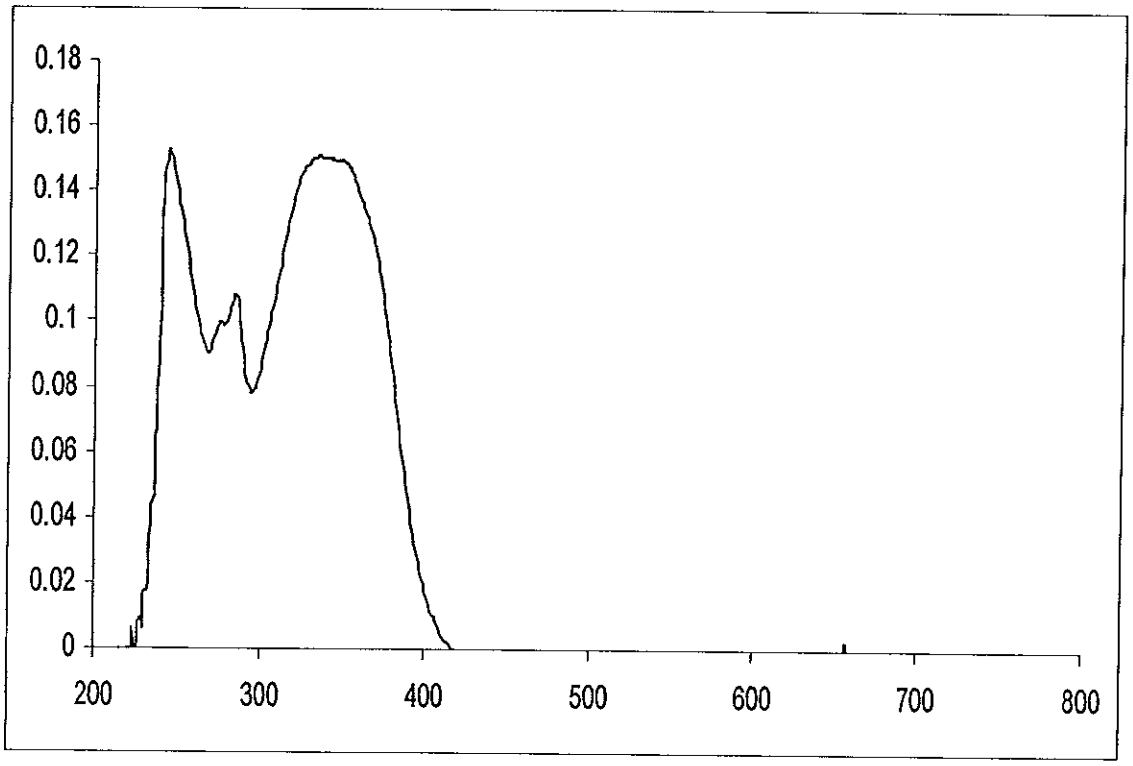

Figure 81 UV-Vis spectrum of compound **TKD3**

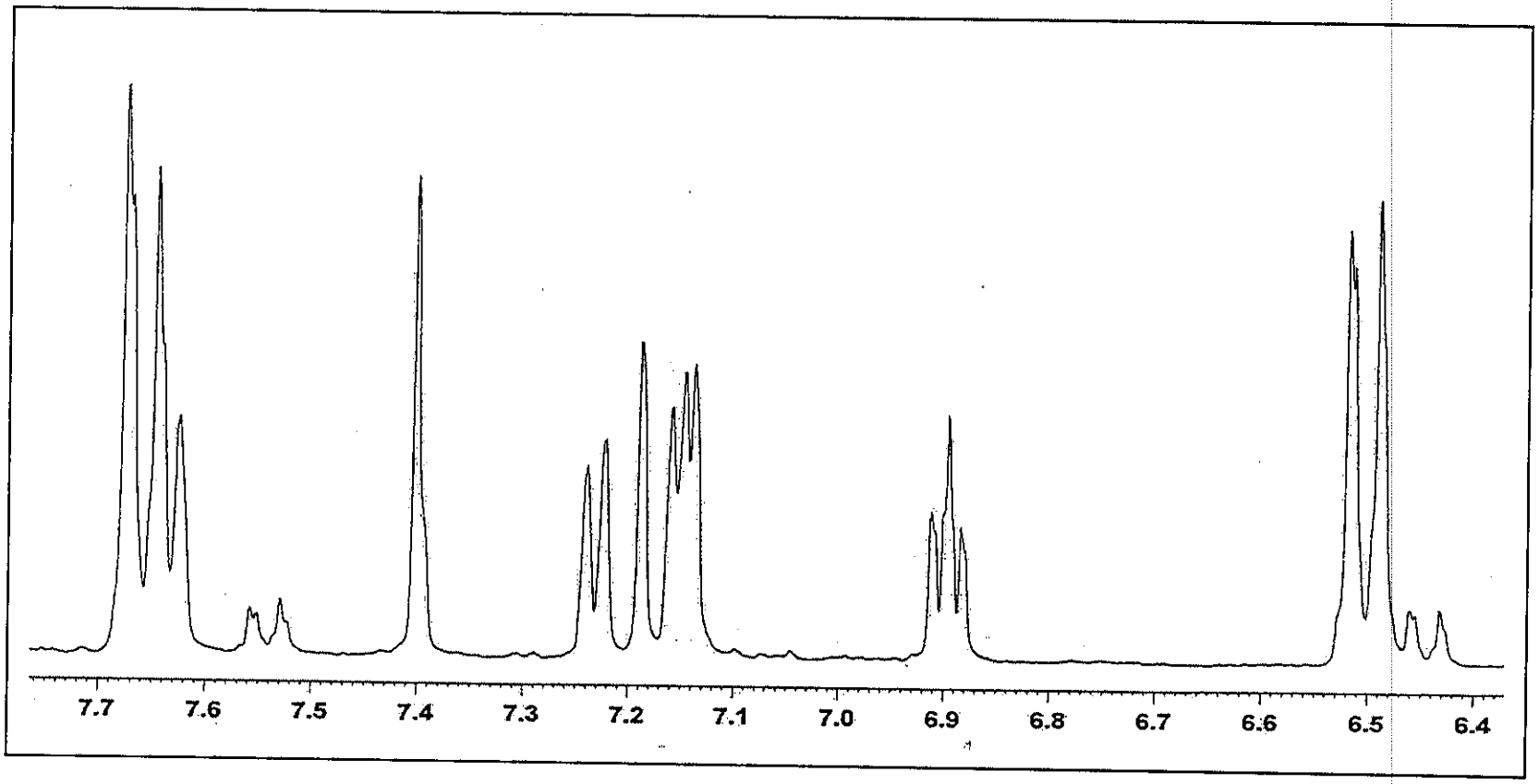

Figure 82 ^{1}H NMR (300 MHz, $CDCl_3$) spectrum of compound **TKD6**

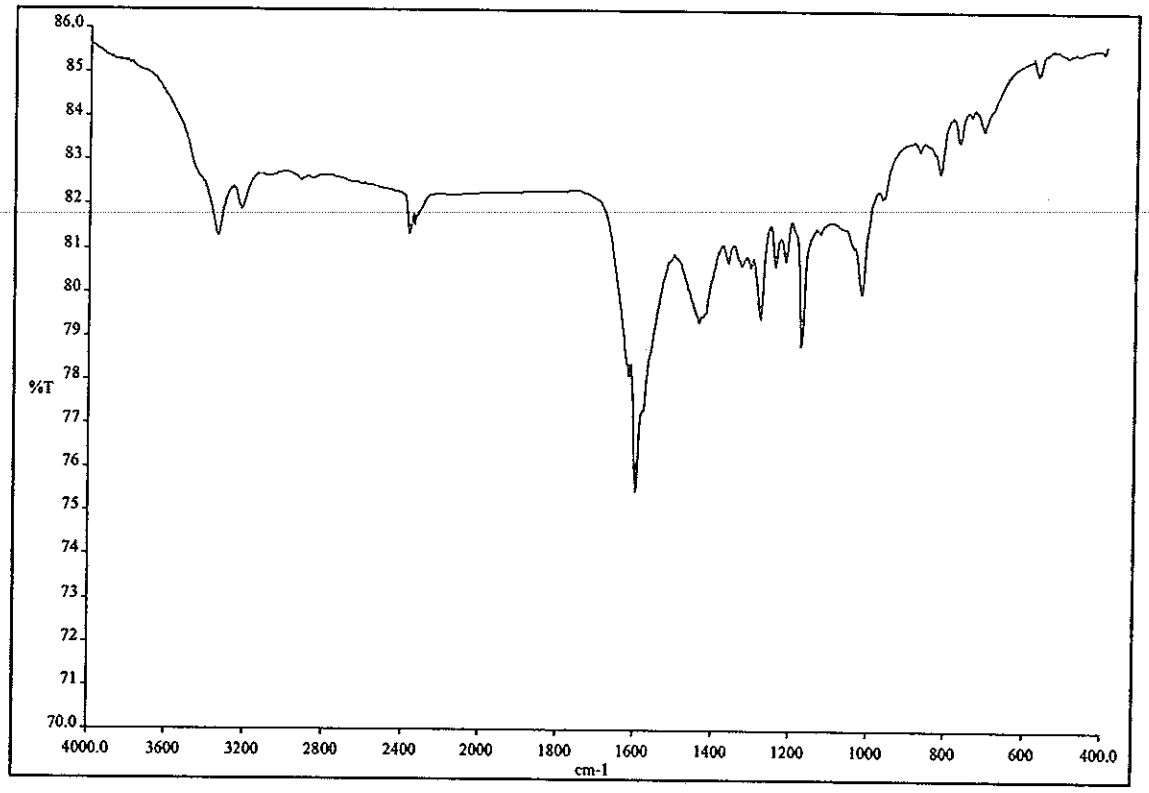

Figure 83 FT-IR (KBr) spectrum of compound **TKD6**

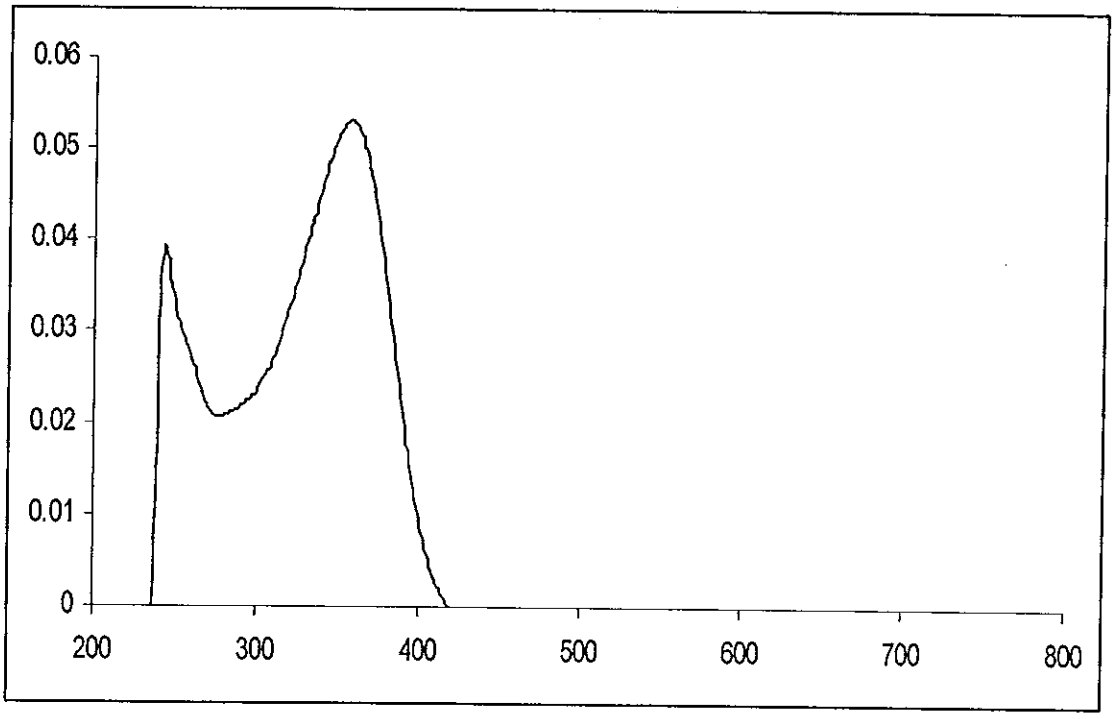

Figure 84 UV-Vis spectrum of compound **TKD6**

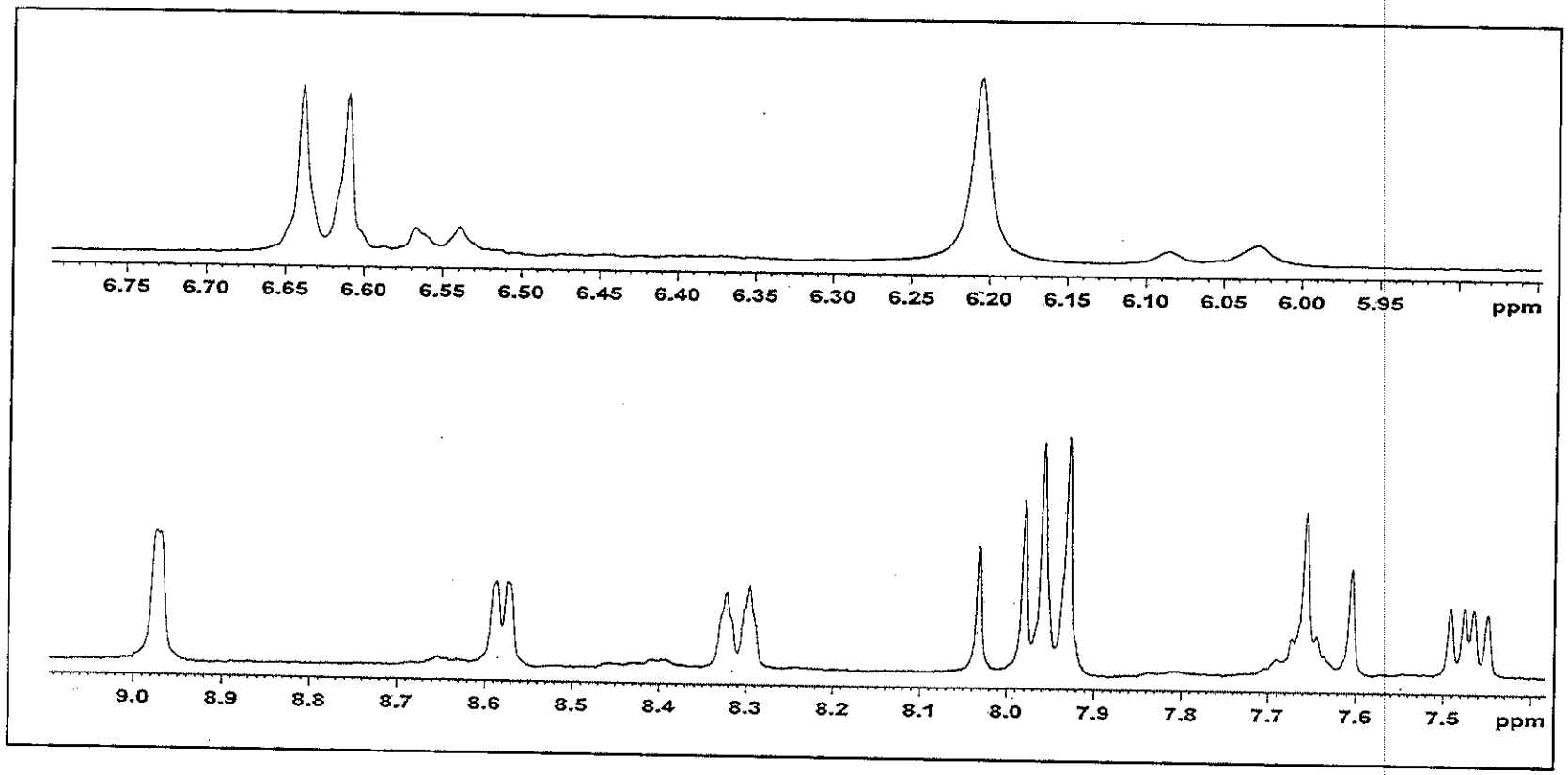

Figure 85 ^{1}H NMR (300 MHz, $CDCl_3$) spectrum of compound **TKD8**

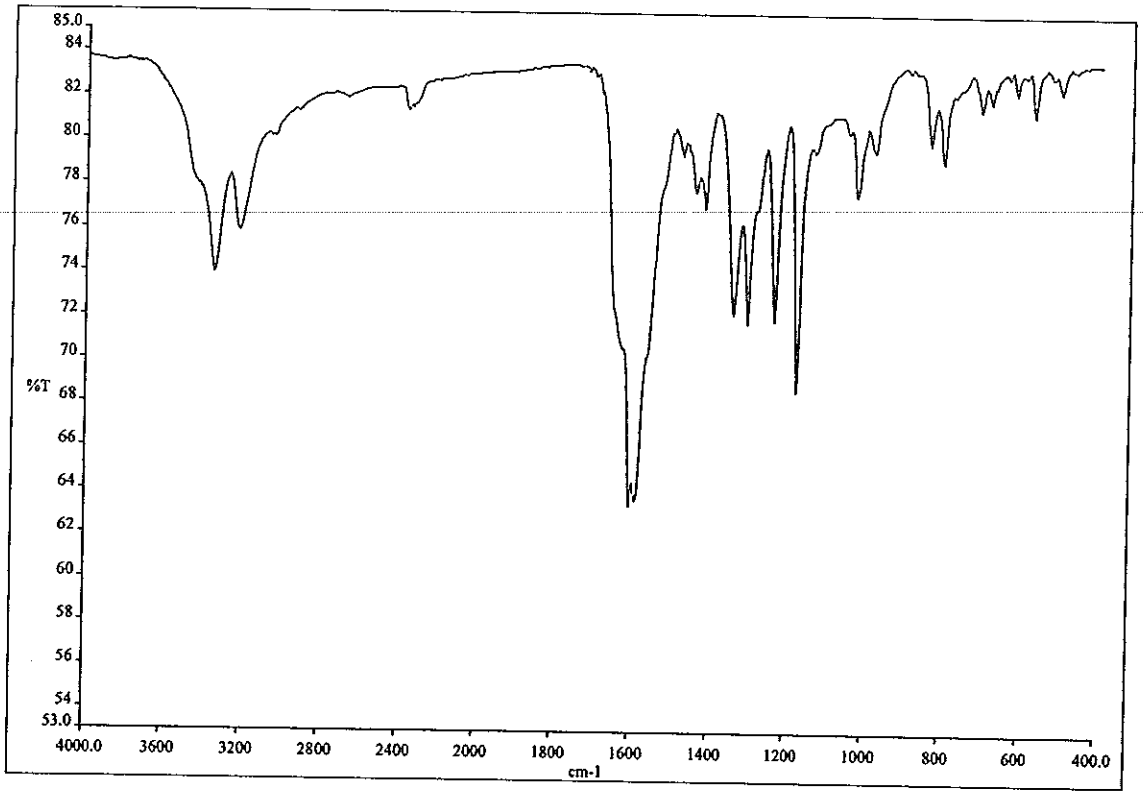

Figure 86 FT-IR (KBr) spectrum of compound **TKD8**

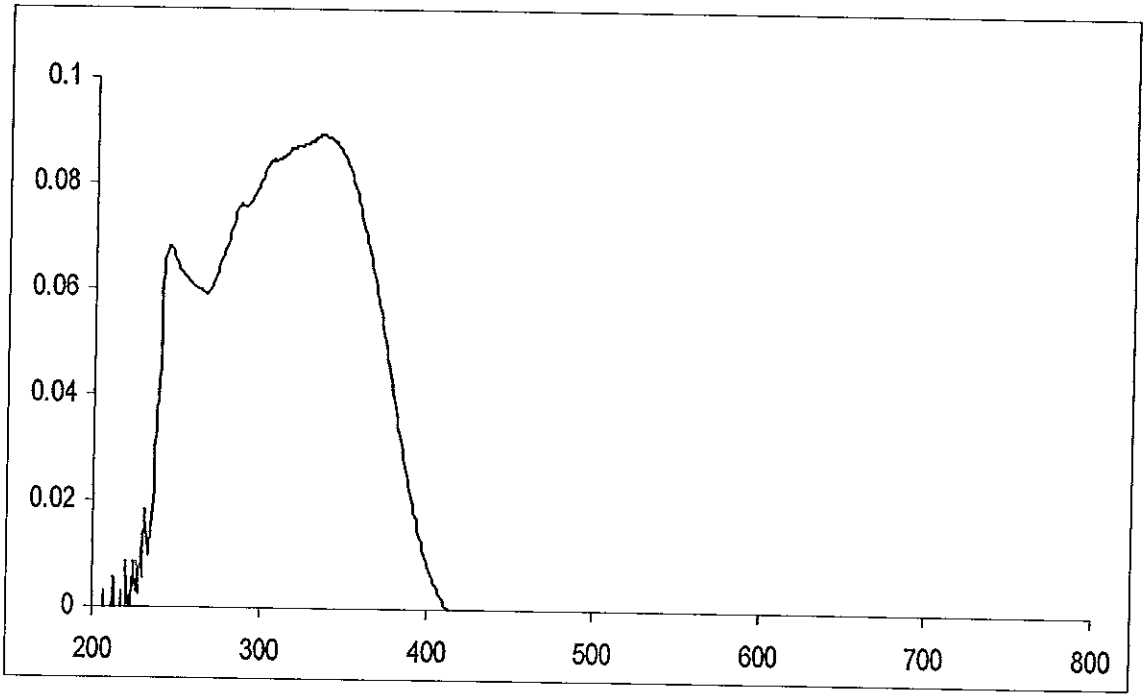

Figure 87 UV-Vis spectrum of compound **TKD8**

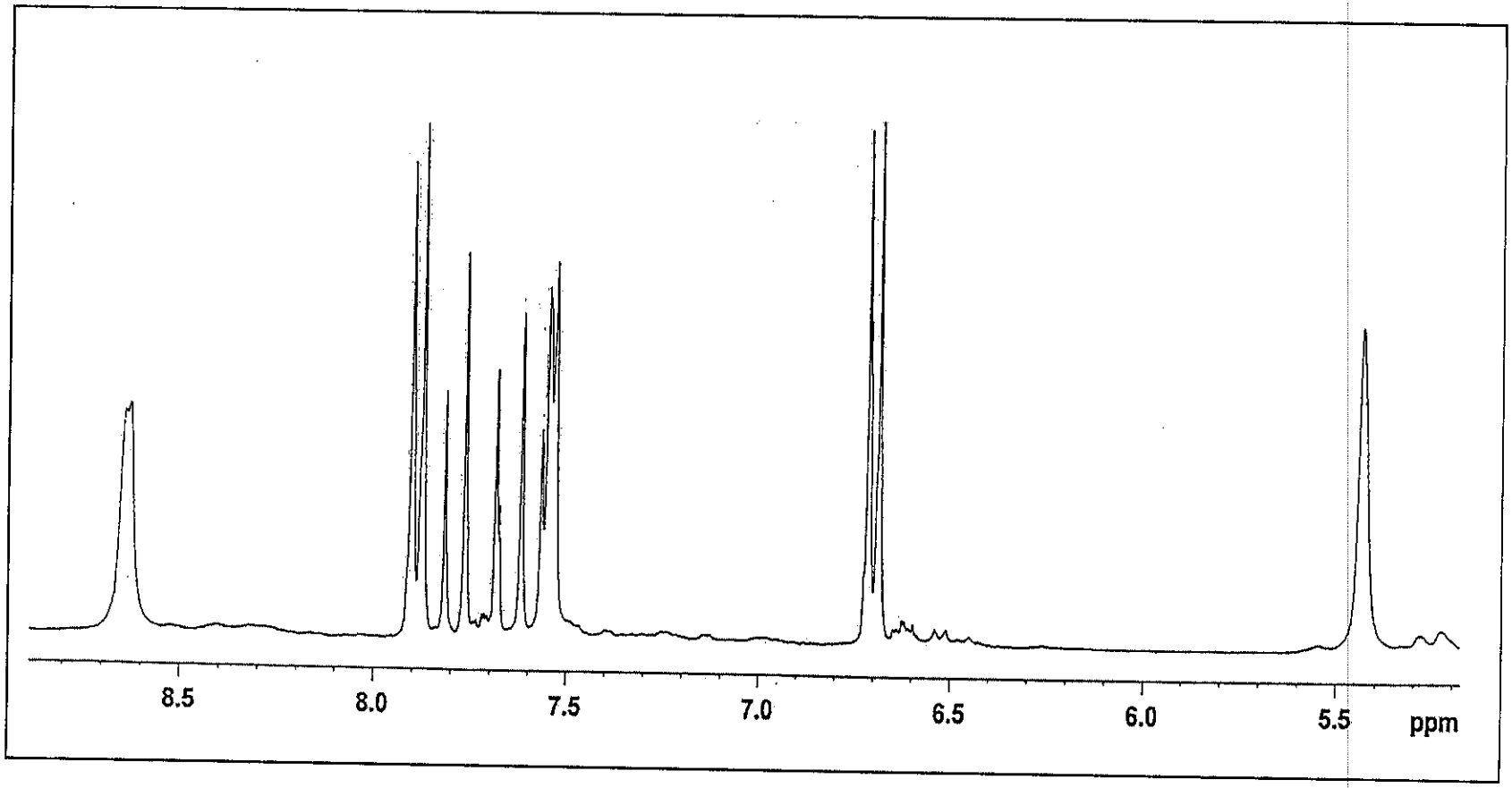

Figure 88 ^{1}H NMR (300 MHz, $CDCl_3$) spectrum of compound **TKD9**

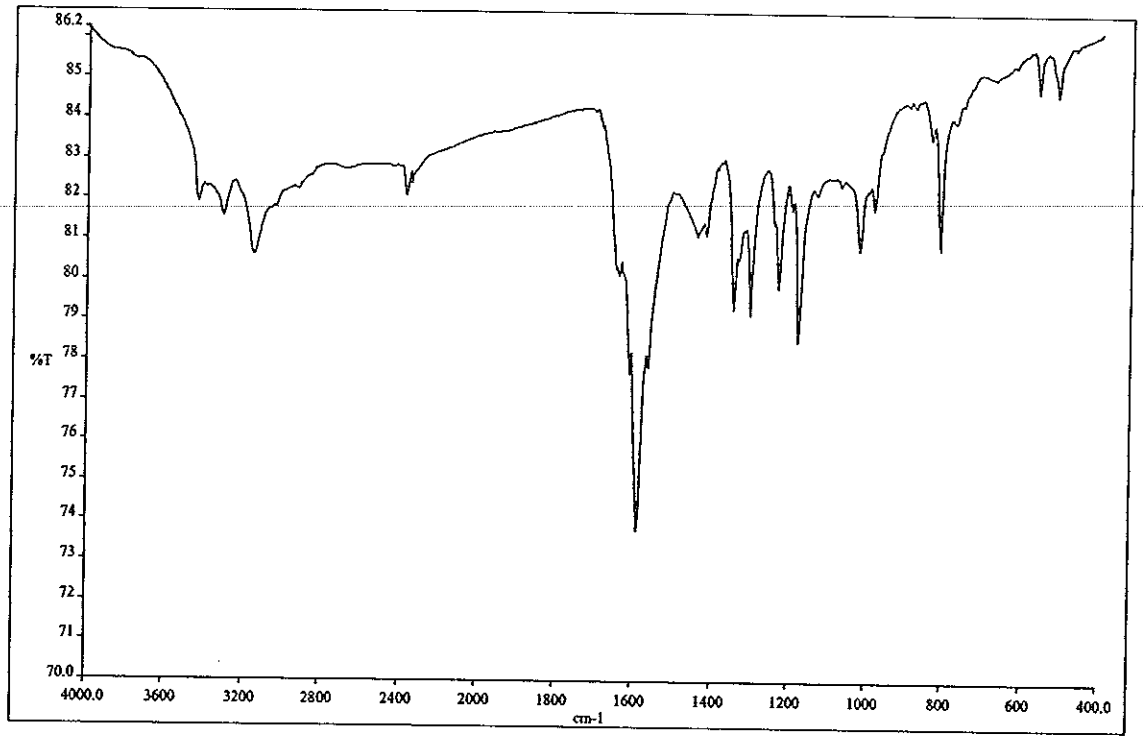

Figure 89 FT-IR (KBr) spectrum of compound **TKD9**

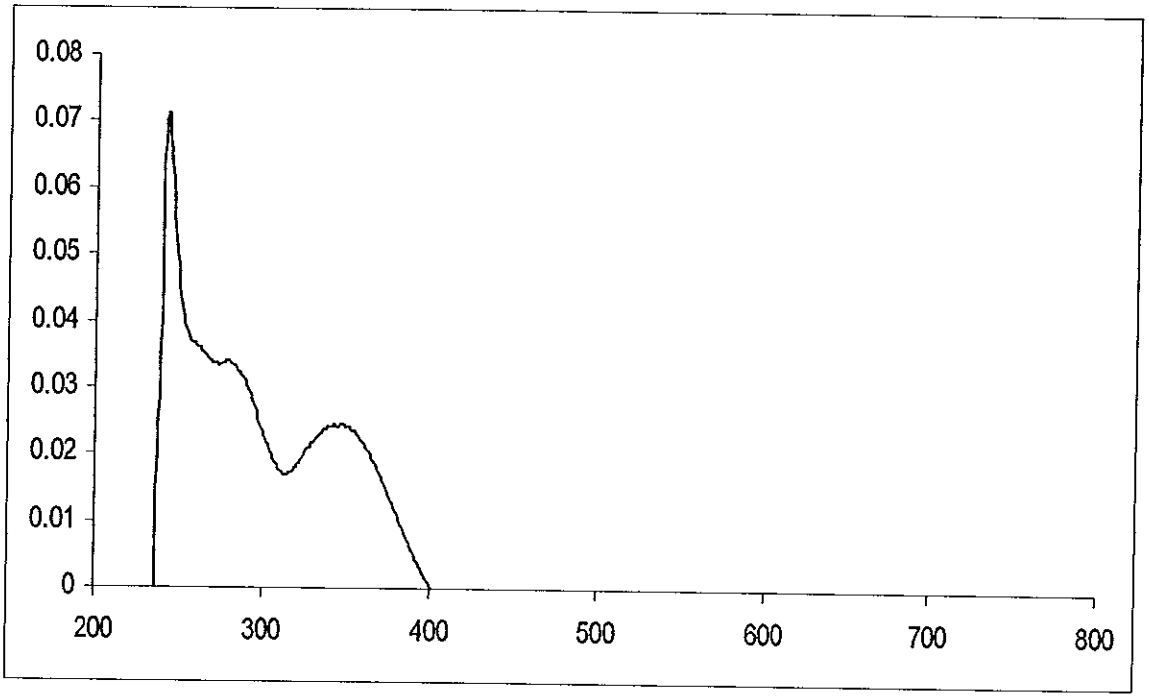

Figure 90 UV-Vis spectrum of compound **TKD9**

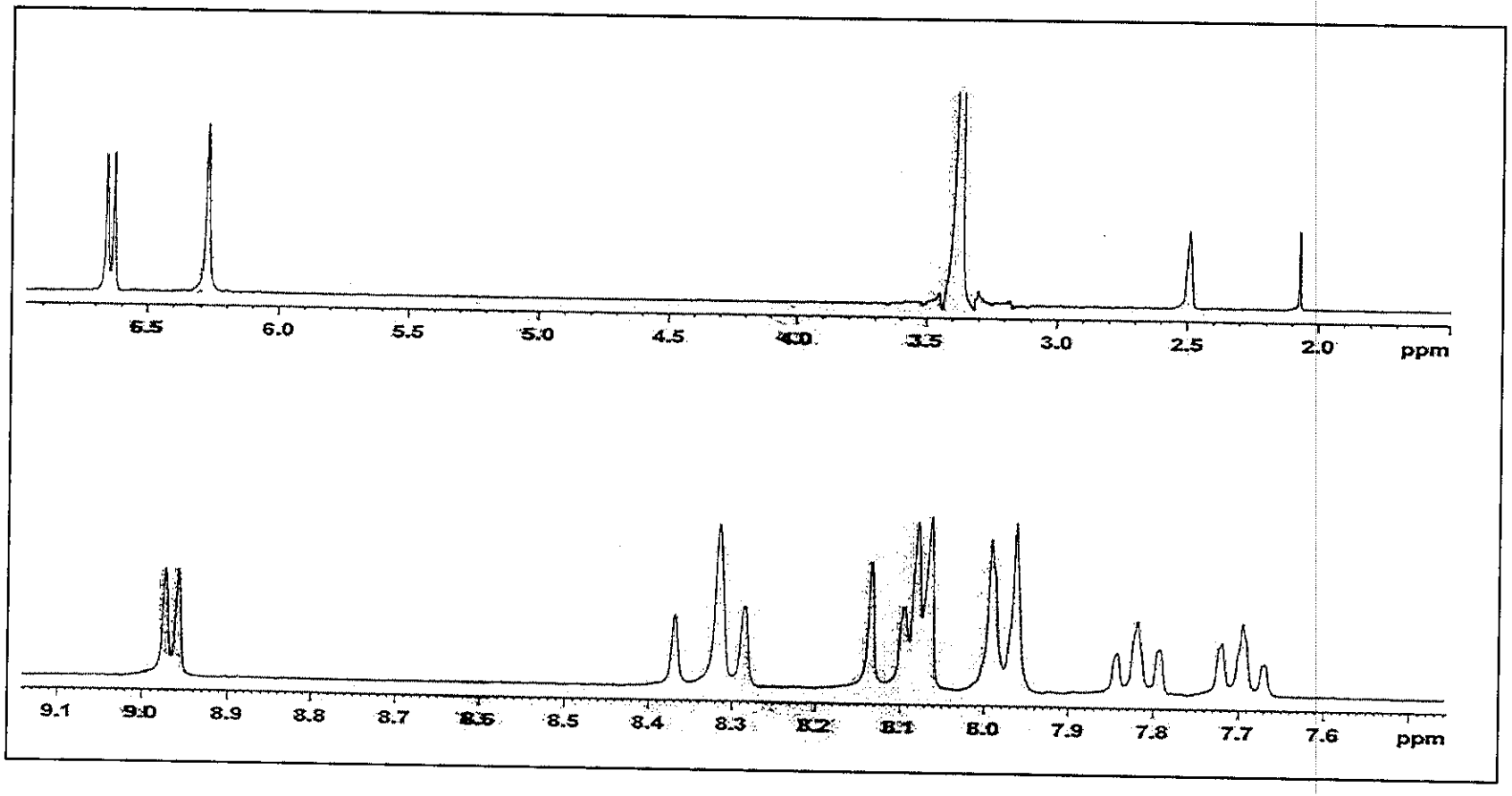

Figure 91 ^{1}H NMR (300 MHz, $CDCl_3$) spectrum of compound **TKD10**

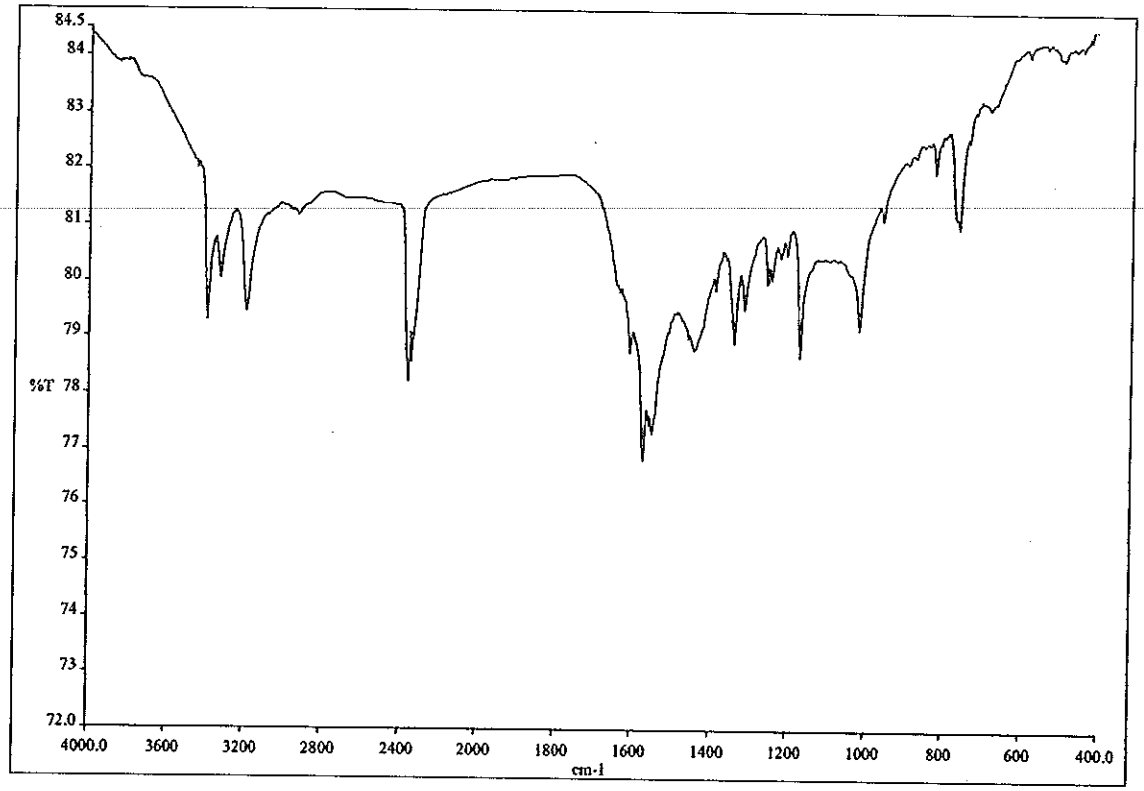

Figure 92 FT-IR (KBr) spectrum of compound **TKD10**

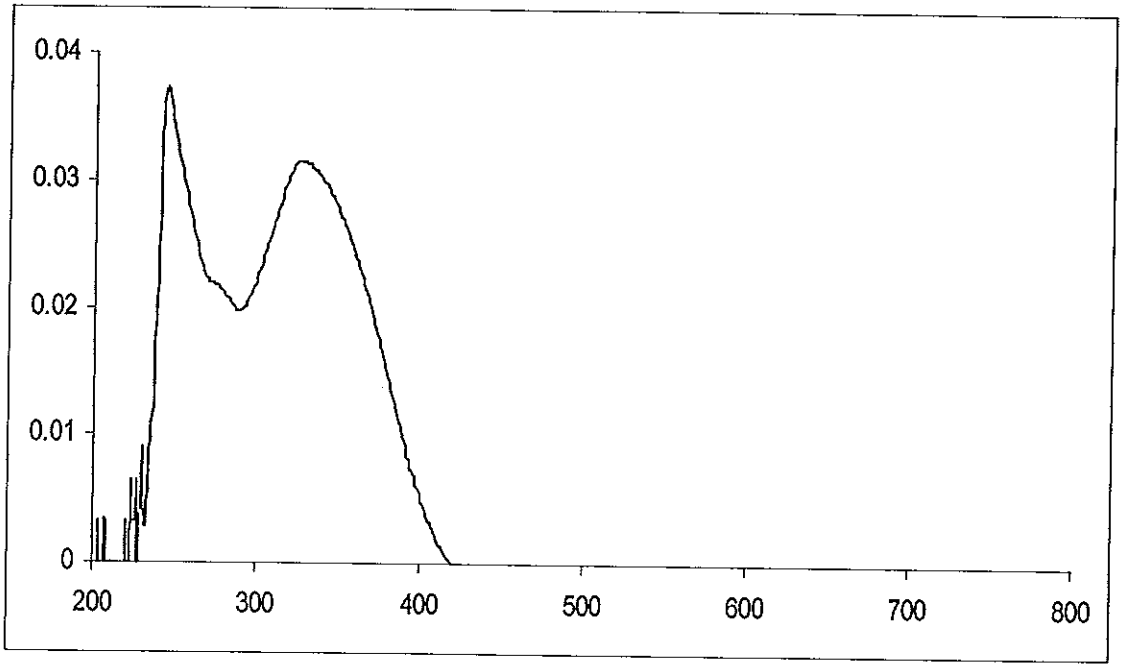

Figure 93 UV-Vis spectrum of compound **TKD10**

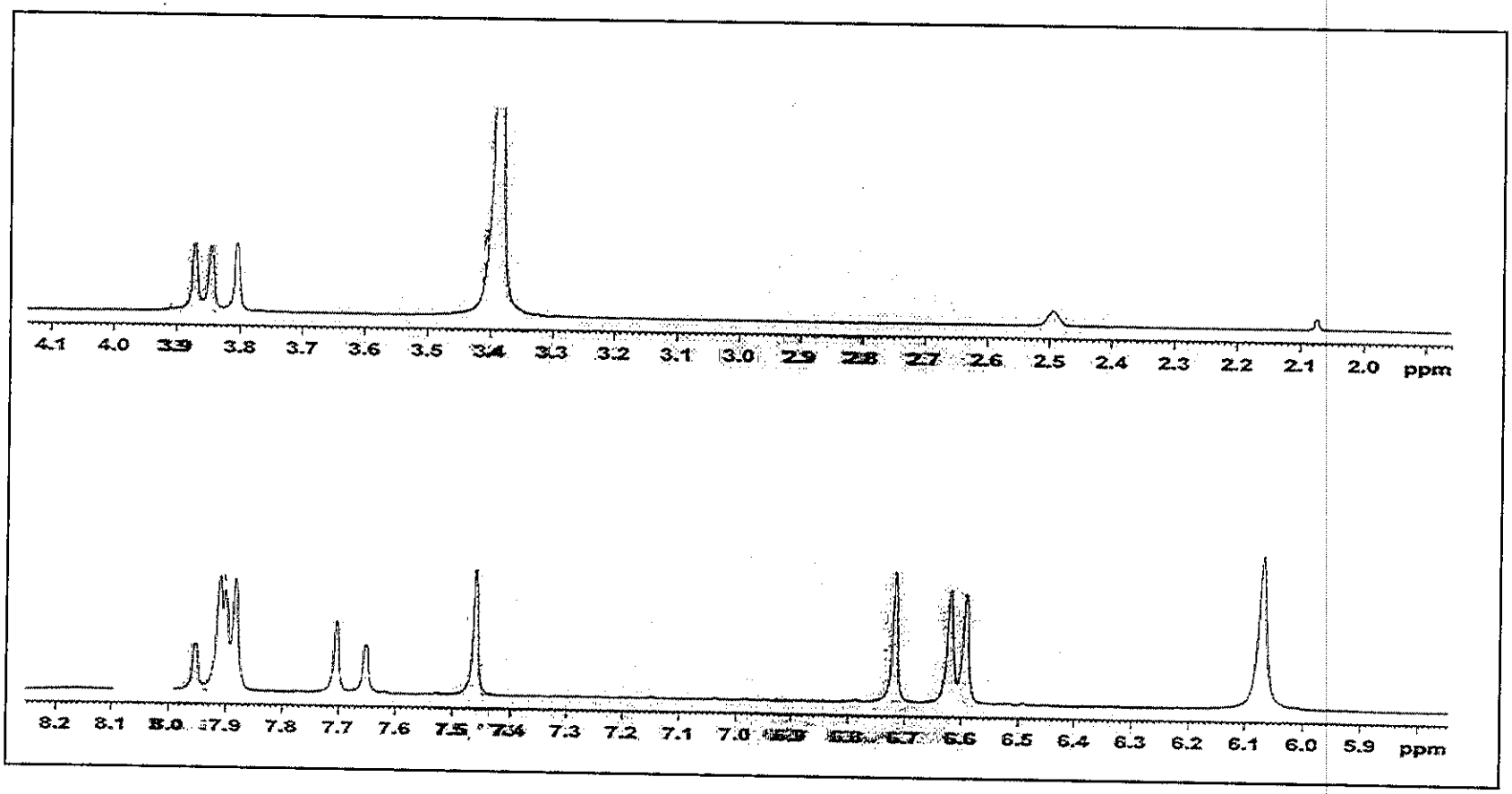

Figure 94 ^{1}H NMR (300 MHz, $CDCl_3$) spectrum of compound **TKD19**

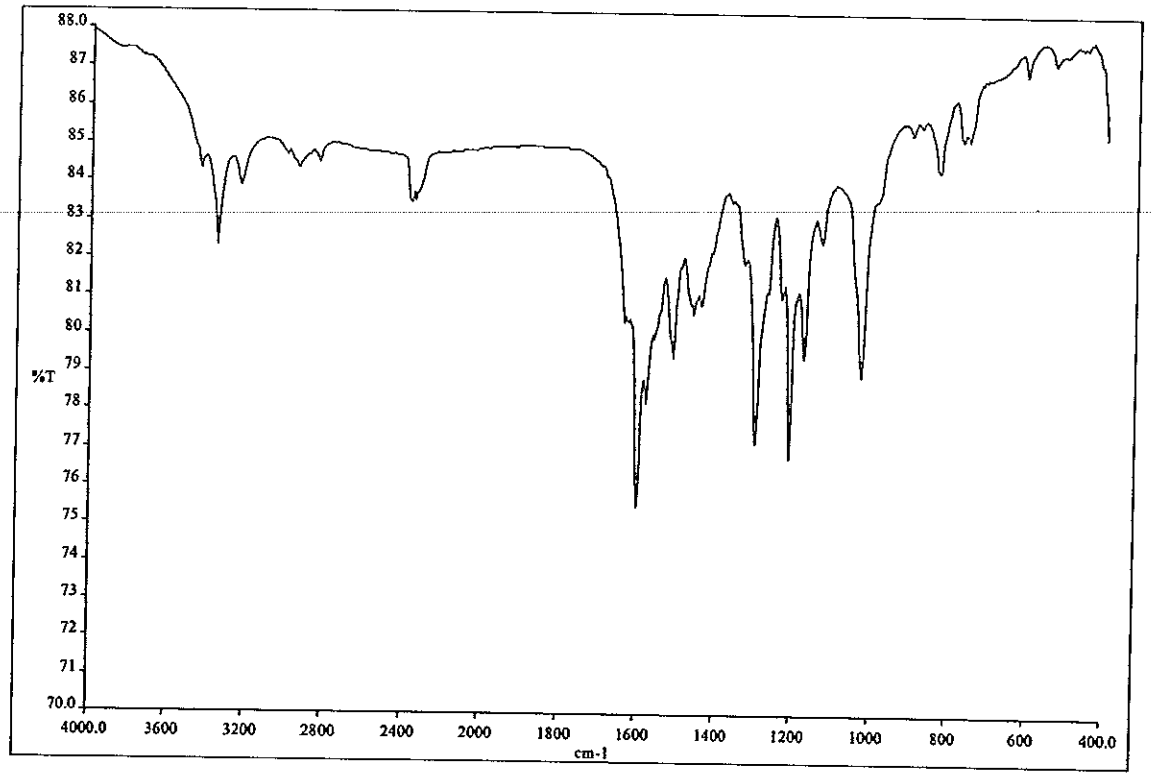

Figure 95 FT-IR (KBr) spectrum of compound **TKD19**

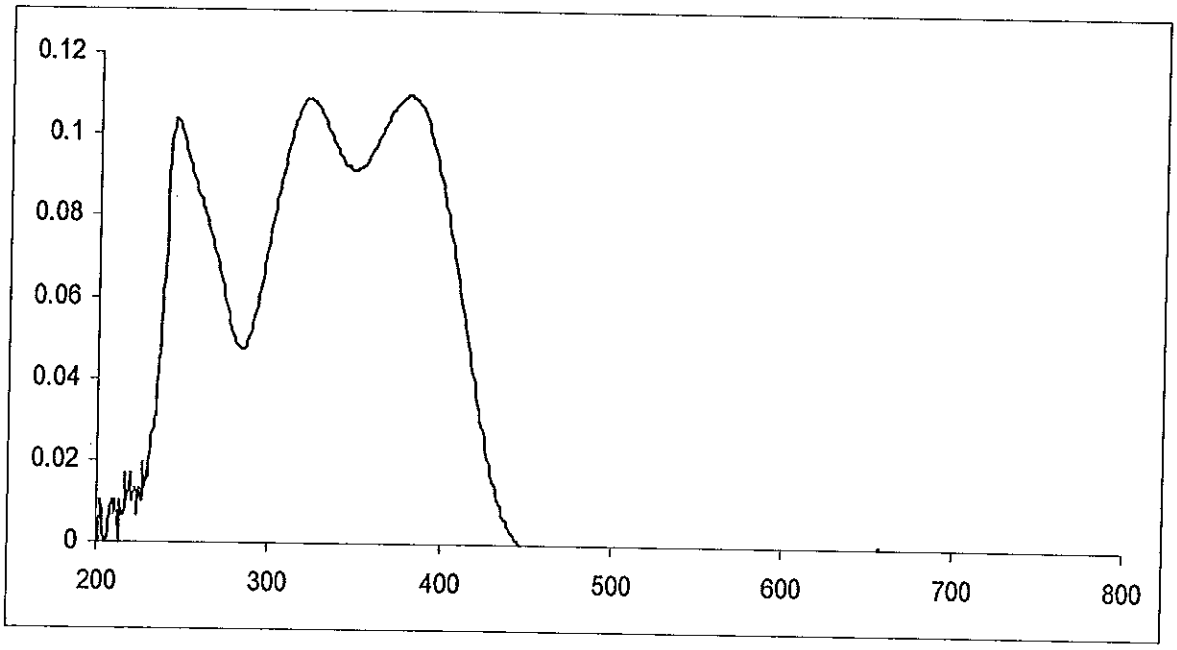

Figure 96 UV-Vis spectrum of compound **TKD19**

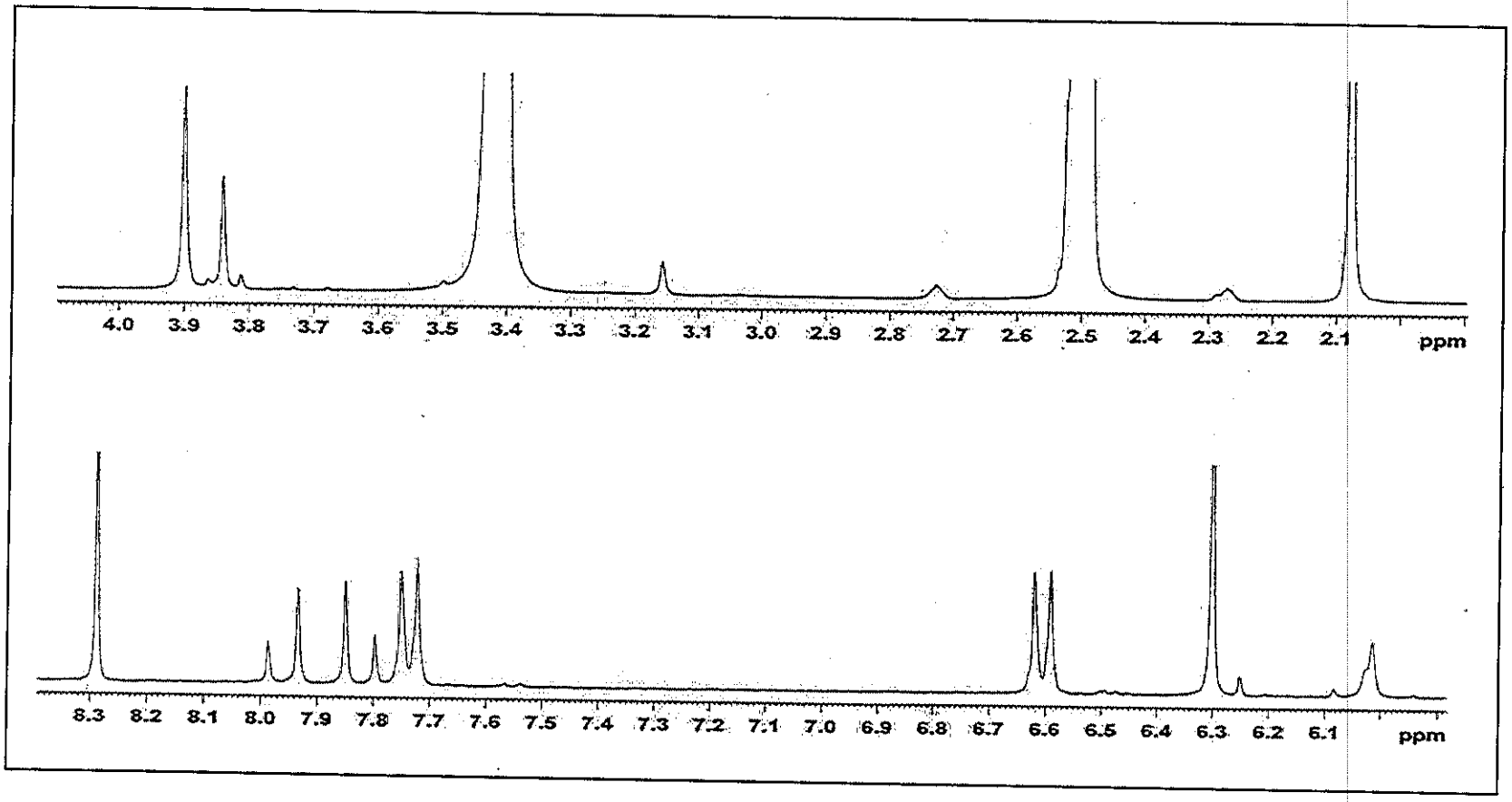

Figure 97 ^{1}H NMR (300 MHz, $CDCl_3$) spectrum of compound **TKD20**

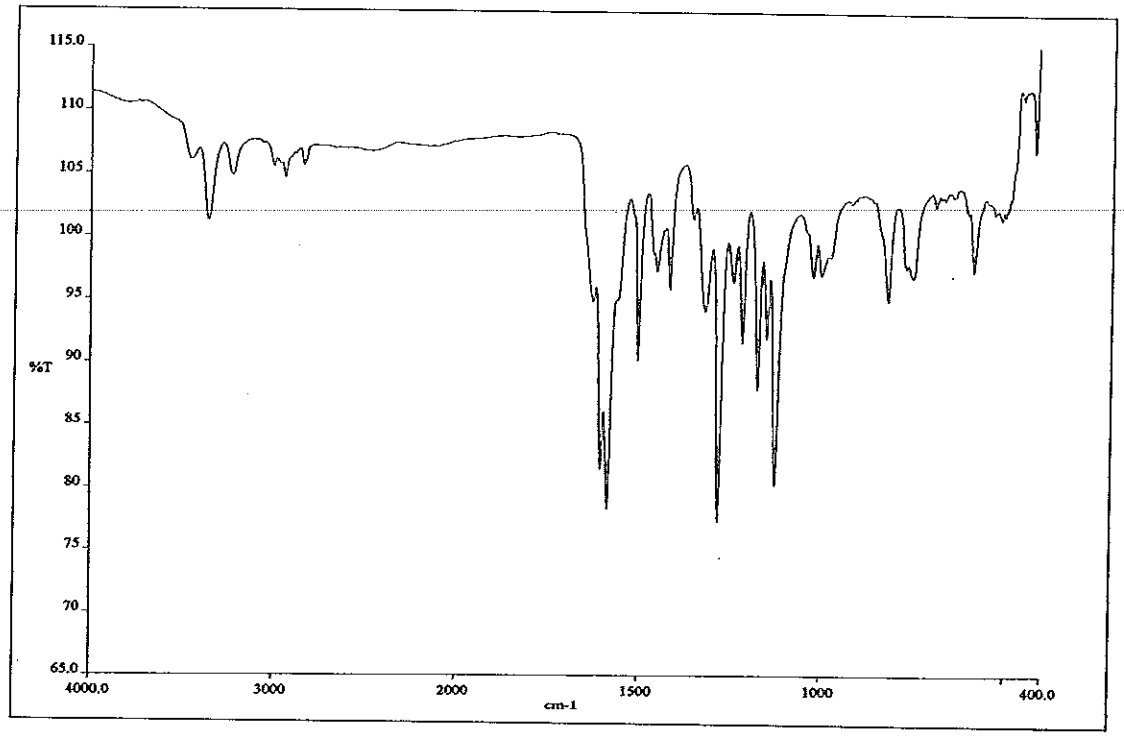

Figure 98 FT-IR (KBr) spectrum of compound **TKD20**

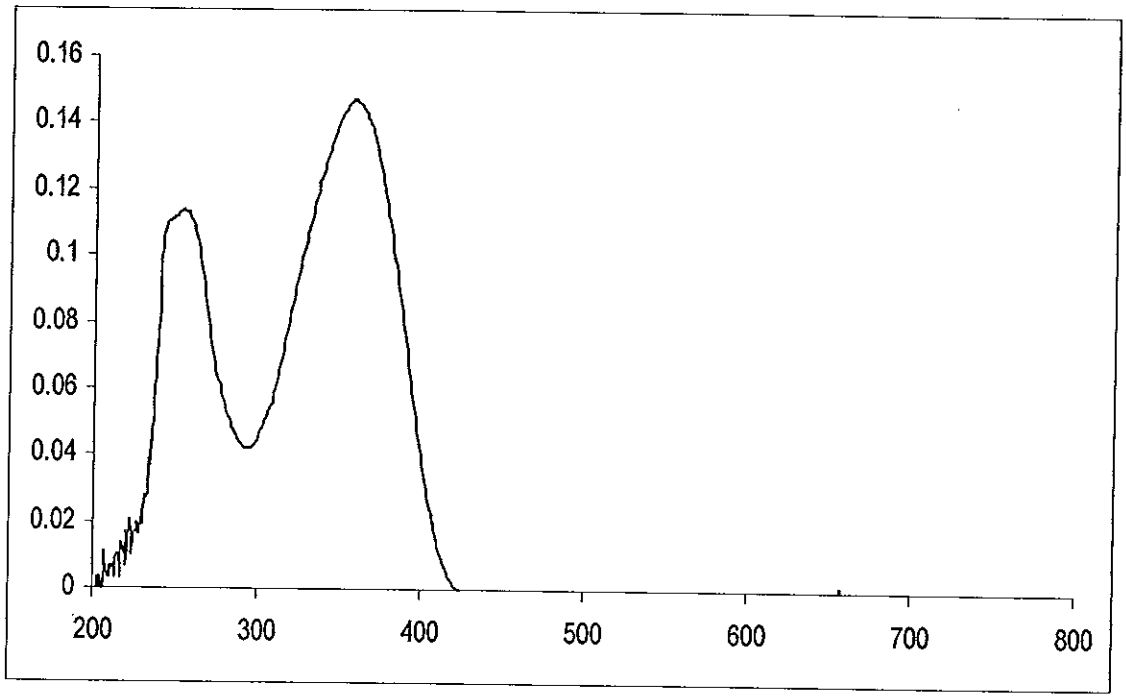

Figure 99 UV-Vis spectrum of compound **TKD20**

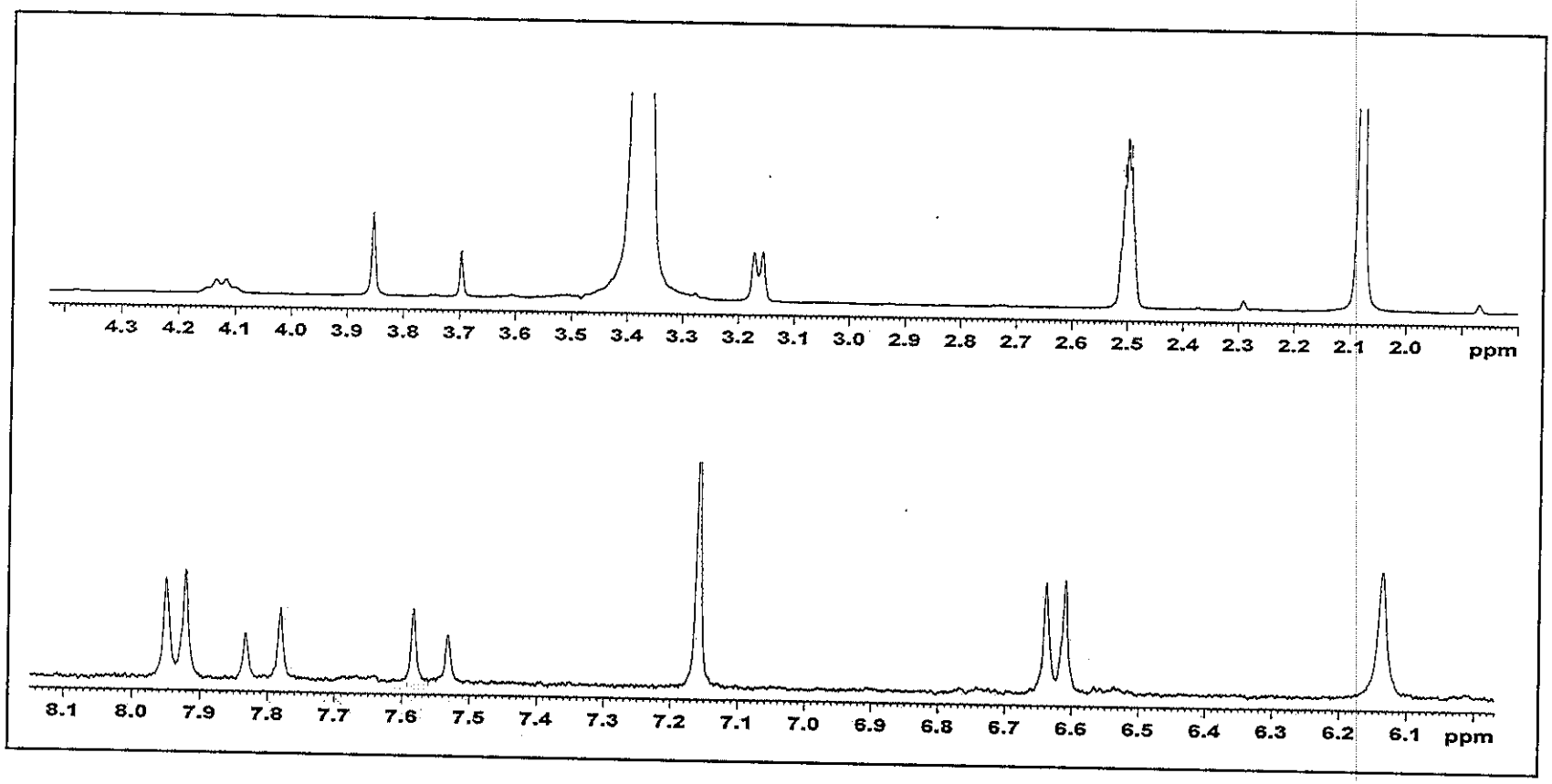

Figure 100 ^{1}H NMR (300 MHz, $CDCl_3$) spectrum of compound **TKD21**

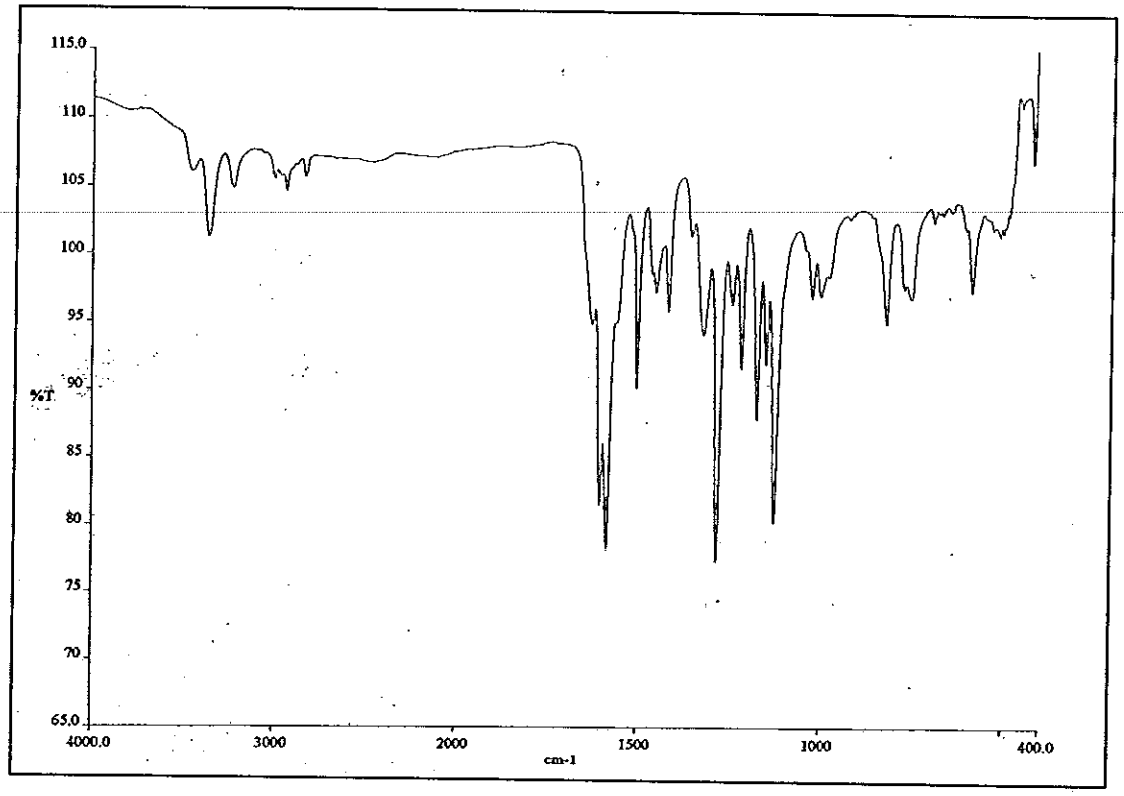

Figure 101 FT-IR (KBr) spectrum of compound **TKD21**

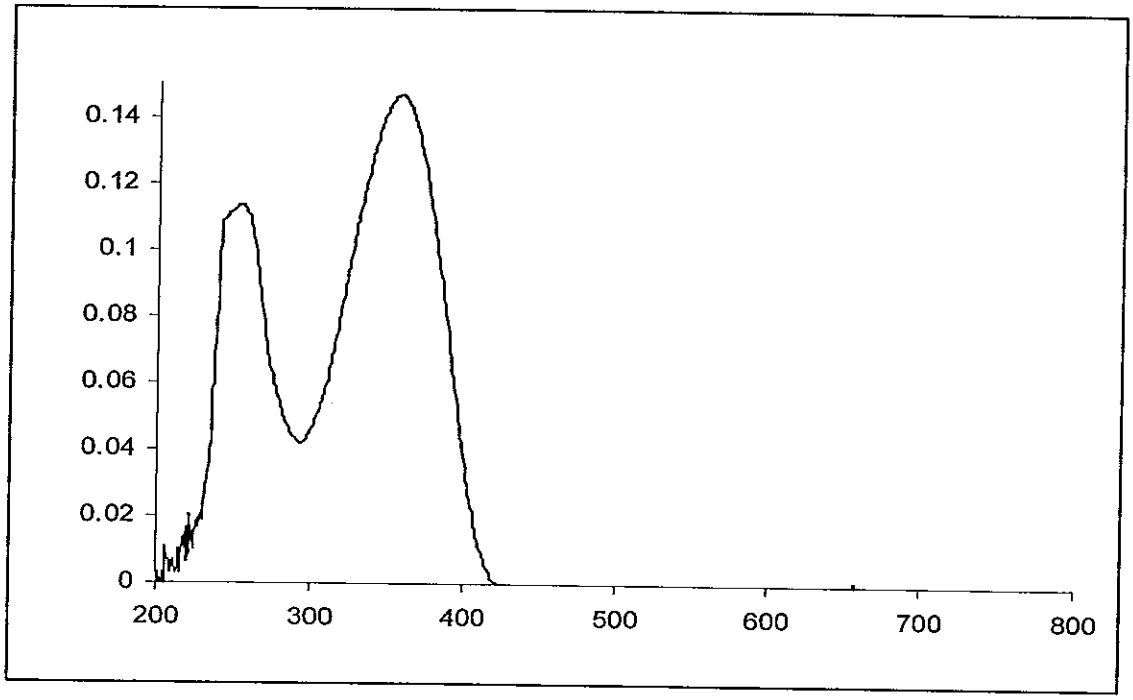

Figure 102 UV-Vis spectrum of compound **TKD21**

VITAE

Name Miss Thawanrat Kobkeatthawin

Student ID 5110220129

Educational Attainment

Degree	Name of Institution	Year of Graduation
B.Sc. (Chemistry)	Prince of Songkla University	2007

Scholarship Awards during Enrolment

Scholarship was awarded by the Center of Excellence for Innovation in Chemistry (PERCH-CIC), Commission on Higher Education, Ministry of Education, the Crystal Materials Research Unit (CMRU) and Prince of Songkla University.

List of Publications and Proceedings

Publications

1. Kobkeatthawin, T.; Chantrapromma, S.; Fun, H.-K. (2009). "2-[(*E*)-2-(1H-Indol-3-yl)etenyl]-1-methylpyridinium 4-chlorobenzenesulfonate", *Acta Cryst.*, **E65**, o2045-o2046.
2. Chantrapromma, S.; Kobkeatthawin, T.; Fun, H.-K. (2009). "2-[(*E*)-2-(1H-Indol-3-yl)etenyl]-1-methylpyridinium 4-bromobenzenesulfonate", *Acta Cryst.*, **E65**, o950-o951.
3. Fun, H.-K.; Kobkeatthawin, T.; Chantrapromma, S. (2009). "(2*E*)-1-(4-Aminophenyl)-3-(2-thienyl)-prop-2-en-1-one ethanol hemisolvate", *Acta Cryst.*, **E65**, o2532-o2533.
4. Fun, H.-K.; Kobkeatthawin, T.; Chantrapromma, S. (2009). "(*E*)-1-(4-Chlorophenyl)-3-[4-(diethylamino)phenyl]prop-2-en-1-one1", *Acta Cryst.*, **E66**, o254-o255.
5. Fun, H.-K.; Kobkeatthawin, T.; Chantrapromma, S. (2009). "1-Methyl-2-[(E)-2-(2-thienyl)ethenyl]-quinolinium 4-bromobenzenesulfonate", *Acta Cryst.*, **E66**, o1053-o1054.

6. Ruanwas, P.; Kobkeatthawin, T.; Chantrapromma, S.; Fun, H.-K.; Philip, R.; Padaki, M.; Isloor, A. (2010). "Synthesis, characterization and nonlinear optical properties of 2-[(*E*)-2-(4-ethoxyphenyl)ethenyl]-1-methylquinolinium 4-substituted benzenesulfonate compounds", *Acta Cryst.*, **E65**, o819-o824.
7. Fun, H.-K.; Chanawanno, K.; Kobkeatthawin, T.; Chantrapromma, S. (2010). "2-[(*E*)-2-(4-Ethoxyphenyl)ethenyl]-1-methylquinolinium iodide dihydrate", *Acta Cryst.*, **E65**, o938–o939.
8. Fun, H.-K.; Chantrapromma, S.; Kobkeatthawin, T.; Padaki, M.; Isloor, A. (2010). "6-(4-Aminophenyl)-2-ethoxy-4-(2-thienyl)nicotinonitrile", *Acta Cryst.*, **E66**, o1811–o1812.
9. Fun, H.-K.; Kobkeatthawin, T.; Ruanwas, P.; Chantrapromma, S. (2010) "(*E*)-1-(4-Aminophenyl)-3-(2,4,5-trimethoxyphenyl)prop-2-en-1-one", *Acta Cryst.*, **E66**, o1973–o1974.
10. Joothamongkhon, J.; Chantrapromma, S.; Kobkeatthawin, T.; Fun, H.-K. (2010) "(*Z*)-3-(Anthracen-9-yl)-1-(2-ethoxyphenyl)prop-2-en-1-one", *Acta Cryst.*, **E66**, o2669–o2670.
11. Fun, H.-K.; Kobkeatthawin, T.; Joothamongkhon, J.; Chantrapromma, S. (2010) "(*E*)-3-(Anthracen-9-yl)-1-(2-bromophenyl)prop-2-en-1-one", *Acta Cryst.*, **E66**, o3312–o3313.

Proceedings

1. Kobkeatthawin, T.; Chantrapromma, S.; Fun, H.-K. "Synthesis, crystal structure, and fluorescence property of chalcone derivatives", The 10th Conference of the Asian Crystallographic Association, Busan Exhibition and Convention Center, Busan, Korea. 31th October–3rd November 2010. (Poster).
2. Kobkeatthawin, T.; Chantrapromma, S.; Fun, H.-K. "Synthesis, Characterizations, and Fluorescence Properties of Chalcone Derivatives", The international congress for innovation in chemistry (PERCH-CIC), Jomtien Palm Beach Hotel & Resort, Pattaya, Thailand. 4th-7th May 2011. (Best presentation Poster Award).